

A STABLE ISOTOPE AND HYDROCHEMICAL APPROACH TO
EXAMINING DENITRIFICATION ALONG A SHALLOW
GROUNDWATER – SURFACE WATER CONTINUUM IN AN
AGRICULTURALLY-IMPACTED CATCHMENT

BY

NICHOLAS LIAM GARRARD

JANUARY 2019

A thesis submitted to the School of Environmental Sciences of the University of East
Anglia in partial fulfilment of the degree of Doctor of Philosophy

© This copy of the thesis has been supplied on condition that anyone who consults it is
understood to recognise that its copyright rests with the author and that use of any
information derived therefrom must be in accordance with current UK Copyright Law. In
addition, any quotation or extract must include full attribution

Abstract

The global population is steadily increasing and subsequently, so is food production. Over the past century, the global pool of reactive nitrogen has doubled. Whilst improving crop production, this has detrimental effects on human and environmental health. Therefore, it is important to understand the consequential forcing of the nitrogen cycle and the natural attenuation processes within, namely denitrification.

The main aim of this research was to determine the spatial distribution and significance of denitrification in an agriculturally-impacted catchment in Norfolk, UK. The stable isotopes of nitrate ($^{15}\text{N}_{\text{NO}_3}$ and $^{18}\text{O}_{\text{NO}_3}$) were measured alongside hydrochemical characteristics of field drains (representing the soil zone), stream water, benthic sediment pore water, boreholes and the hyporheic zone (HZ) (beneath and to the sides of the stream bed). The HZ was sampled from a series of nested in-stream piezometers along a 1.6 km reach. A mass balance approach was then used to assess the magnitude of denitrification within the study catchment.

The results show evidence for denitrification within the soil zone, demonstrated by dual fractionation of nitrate isotopes and negative correlation between nitrate concentration and $\delta^{15}\text{N}_{\text{NO}_3}$ and $\delta^{18}\text{O}_{\text{NO}_3}$ values. Soil type influenced denitrification, showing a positive correlation between percentage clay and $\delta^{15}\text{N}_{\text{NO}_3}$ and $\delta^{18}\text{O}_{\text{NO}_3}$ values. Tillage regime was also suggested to influence denitrification. In-stream denitrification was also detected, though there was no associated reduction in dissolved nitrate concentration with nitrate isotope enrichment. Tentative isotopic evidence for benthic pore water denitrification is also presented. There was no isotopic evidence for HZ denitrification, suggesting that management approaches should not focus on this zone. Mass balance calculations indicate catchment-wide denitrification rate of $0.023 - 0.044 \text{ kg N ha d}^{-1}$, equating to 27 – 42% of nitrogen in soil leachate.

Acknowledgements

I first thank Kevin Hiscock for his continued support, patience and encouragement throughout my PhD. His enthusiasm, good humour and insight have been central to the progress of this project.

I also thank Alina Marca for her tireless effort in providing support and advice from the simplest concept to the most complex process, no question was too simple. I thank Tim Jickells for his input as a late addition to the project, his good natured approach was refreshing and provided encouragement, and a different perspective identified many interesting nuances in the data.

The technical support has been outstanding, and Liz Rix and Alina Mihailova are thanked for their expertise and understanding of an often-difficult analysis campaign. My special thanks go to Sarah Wexler, without whom I am confident that no isotope data would have been generated and therefore my gratitude to Sarah is immense. Outside of the isotope work Sarah's friendship and advice have had a profound impact on my PhD experience. Sarah's involvement has been crucial.

I am grateful to Steve Dugdale, Simon Ellis, Jenny Stevenson, Gilla Sünnerberg, Richard Cooper and Zanist Hama-Aziz for welcoming me into the Wensum Demonstration Test Catchment group and for the enjoyable fieldwork days. Gilla is thanked in particular for her help with GIS, and Richard is also thanked for his input in the mass balance work.

I thank Lewis Dunham for his assistance in installing the piezometers and collecting subsurface sediments, and for the endless discussions around ale and home brew.

I thank my family for offering support without hesitation throughout my PhD. They have shared my excitement and provided support in periods of despair, and of my family my appreciation is limitless.

Finally, I thank my long-suffering partner Lisa Hobson, who has lived through every moment of my academic pursuits over the last nine years, never once complaining and always understanding.

Table of Contents

List of figures	7
List of tables	10
Chapter 1 Introduction	12
1.1 Rationale and motivations	12
1.2 Primary research aim.....	15
1.3 Main research objectives.....	15
1.4 Thesis structure.....	16
Chapter 2 Use of stable isotopes in the investigation of nitrogen cycling, stable isotope theory and study site background	18
2.1 Nitrate in agricultural systems: examining the soil-surface water-groundwater continuum.....	18
2.1.1 Denitrification within the hyporheic zone	21
2.1.2 Mass balance and nitrogen budgets	26
2.1.3 The fate of reactive nitrogen following incorporation into agricultural soils	27
2.2 Stable isotope concepts and definitions.....	30
2.2.1 Stable isotope fractionation.....	30
2.2.2 Kinetic fractionation.....	31
2.2.3 Equilibrium fractionation.....	31
2.2.4 Isotope fractionation within the nitrogen cycle.....	32
2.2.4.1 Fixation	34
2.2.4.2 Assimilation.....	35
2.3 Dual isotope technique for nitrogen cycling studies	42
2.4 Study site background.....	44
2.4.1 Geology of the Blackwater sub-catchment	49
2.4.2 Soil physicochemical characteristics of the Blackwater sub-catchment.....	54
2.4.3 Hyporheic zone sediments and piezometer infiltration rates	59
2.4.4 Hydrology of the Blackwater sub-catchment.....	65
2.4.5 Hydrogeology of the Wensum Catchment.....	66
2.4.6 Hydrochemistry of the Blackwater sub-catchment.....	67
2.4.7 Topography and land use in the Blackwater sub-catchment.....	67
2.4.8 Climate in East Anglia and the Wensum.....	68
2.4.9 Selection of study fields	68
2.5 Summary	69
Chapter 3 Research methods.....	71

3.1 Experimental design	71
3.2 Field sampling	74
3.2.1 Piezometer installation and sampling	74
3.2.3 Subsurface sediment sampling	76
3.2.4 Stream and field drain sampling	77
3.2.5 Borehole sampling	78
3.2.6 Diffuse Equilibrium in Thin Films probe deployment and sample processing.....	79
3.2.7 Sediment particle size distribution	80
3.3 Laboratory techniques	80
3.3.1 Major ions and dissolved organic carbon.....	80
3.3.4 Nitrate stable isotopes.....	82
3.3.5 Water isotope analysis	90
3.4 Statistical analysis.....	91
Chapter 4 Soil zone denitrification: evidence from field drain hydrochemical and isotope data.....	92
4.1 Introduction	92
4.2 Results.....	94
4.2.1 Results of field measurements and overview of hydrochemical data.....	95
4.2.2 Nitrate	99
4.2.3 Chloride	101
4.2.4 Sulphate	102
4.2.5 Bicarbonate	103
4.2.6 Calcium.....	104
4.2.7 Magnesium	105
4.2.8 Potassium.....	106
4.2.9 Sodium	107
4.3.10 Dissolved organic carbon	108
4.2.11 Nitrite and ammonium	109
4.2.12 Stable isotopic composition of nitrate	110
4.3 Discussion of Denitrification in the soil zone.....	112
4.3.1 The influence of soil physical characteristics on denitrification.....	115
4.3.2 Soil water hydrochemistry and stoichiometry	122
4.5 Summary	133
Chapter 5 Evidence for denitrification in the stream – hyporheic zone continuum.....	134
5.1 Introduction	134
5.2 Results.....	138

5.2.1 Overview of field measurement and major ion data	139
5.2.2 Field measurements	143
5.2.3 Nitrate	144
5.2.4 Nitrite and ammonium	146
5.2.5 Chloride	147
5.2.6 Sulphate	149
5.2.7 Bicarbonate	150
5.2.8 Calcium	151
5.2.9 Potassium	152
5.2.10 Magnesium	153
5.2.11 Sodium	154
5.2.12 Dissolved organic carbon	155
5.2.13 Piezometer hydraulic head measurements and hydraulic gradients	156
5.2.14 Stable isotopes of nitrate along the stream - hyporheic zone continuum	157
5.2.15 $\delta^{18}\text{O}_{\text{H}_2\text{O}}$ and $\delta^2\text{H}_{\text{H}_2\text{O}}$ values of stream and piezometer samples	159
5.3 Discussion	165
5.3.1 Isotopic evidence for denitrification in the stream, benthic sediment and hyporheic zone	165
5.3.2 Transfer of water across the groundwater - surface water interface	171
5.3.3 Nitrogen cycling in the stream	174
5.3.4 Nitrogen cycling in the hyporheic zone	182
5.4 Summary	186
Chapter 6 Catchment nitrogen mass balance	188
6.1 Introduction	188
6.2 Setting up the nitrogen mass balance model	194
6.2.1 Delineation of nutrient budget boundary	194
6.2.2 Nitrogen Export Coefficients	196
6.2.3 Nitrogen inputs to the study area	198
6.2.4 Riverine nitrogen flux	203
6.3 Results of the nitrogen mass balance	203
6.4 Discussion	205
6.4.1 Assumptions in the mass balance	205
6.4.2 Denitrification in the study catchment	207
6.4.3 Catchment conceptual model	209
6.5 Summary	211
Chapter 7 Conclusions, policy implications and recommendations for further work	212

7.1 Conclusions.....	212
7.2 Policy implications.....	217
7.3 Recommendations for further work	219
References.....	221
Appendix 1 - Field measurements.....	235
Appendix 2 – Stable isotope data	244
Appendix 3 – Major ion data.....	252
Appendix 4 – Mass balance data	261

List of figures

Figure 2.1 Cross-sectional lateral schematic showing gradients of water movement in the hyporheic zone. Adapted from Boulton et al. (1998).	26
Figure 2.2 Ranges of $\delta^{15}\text{N}_{\text{NO}_3}$ and $\delta^{18}\text{O}_{\text{NO}_3}$ associated with agricultural sources of nitrate. Adapted from Kendall et al. (2007)	34
Figure 2.3 Simplified schematic of soil nitrogen cycling from atmospheric nitrogen, through the soil zone and returning to the atmosphere showing both aerobic and anaerobic processes	41
Figure 2.4 Map of the Wensum catchment and within it, the Blackwater sub-catchment. From Hama-Aziz (2016).	44
Figure 2.5 Location of the boreholes described in Section 3.2.5.....	51
Figure 2.6 Geological map of the study site showing bedrock formation	52
Figure 2.7 Soil fraction distribution throughout the fields surrounding the study reach. Adapted from Hama-Aziz (2016)	54
Figure 2.8 Map of the fields surrounding the study reach with soil sampling locations highlighted.	56
Figure 2.9 Particle size distributions from soil samples taken at the 0-30cm horizon in Dunkirk, Swanhills and Gatehouse. Adapted from Hama-Aziz (2016).....	57
Figure 2.10 Particle size distributions from soil samples taken at the 30-60cm horizon in Dunkirk, Swanhills and Gatehouse. Adapted from Hama-Aziz (2016)	57
Figure 2.11 Particle size distributions from soil samples taken at the 60-90cm horizon in Dunkirk, Swanhills and Gatehouse. Adapted from Hama-Aziz (2016)	58
Figure 2.12 Ternary plot showing particle size distributions of subsurface sediments at 0.5 and 1.0m depth across all sampling sites.....	60
Figure 2.13 . Sites 1-4 piezometer recharge rates between April 2016 and January 2017	61
Figure 2.14 Recharge rates for piezometers at Site 5 between November 2016 and January 2017.	61
Figure 3.1 Images and locations of the five sampling at which the piezometers were installed ..	72
Figure 3.2 Schematic showing the process by which the bailer is used to collect a sample from a piezometer following purging and refilling of the piezometer	75
Figure 3.3 Bailer and tubing used to collect piezometer samples.....	75
Figure 3.4 Cofferdam installed next to piezometers prior to bailing	76
Figure 3.5 Cofferdam empty following bailing, ready for augering.....	77
Figure 3.6 Dual height cover dam for use in deeper water	77
Figure 3.7 Schematic showing N ₂ O extraction and purification using the Geo 20:20. From Wexler (2010).....	86

Figure 3.8 Example of calibration curve for $\delta^{18}\text{O}_{\text{N}_2\text{O}}$ (relative to reference gas) against the accepted $\delta^{18}\text{O}_{\text{NO}_3}$ values of the international standards.	89
Figure 3.9 Example of calibration curve for $\delta^{15}\text{N}_{\text{N}_2\text{O}}$ (relative to reference gas) against the accepted $\delta^{15}\text{N}_{\text{NO}_3}$ values of the international standards	89
Figure 4.1 Locations of the sampling sites at which piezometer, stream and field drain water samples were collected.	94
Figure 4.2 Box and whisker diagram showing intra-site comparison of median nitrate concentrations between spring/summer and autumn/winter.....	100
Figure 4.3 Box and whisker diagram showing intra-site comparison of median chloride concentrations between spring/summer and autumn/winter.....	101
Figure 4.4 Box and whisker diagram showing intra-site comparison of median sulphate concentrations between spring/summer and autumn/winter.....	102
Figure 4.5 Box and whisker diagram showing intra-site comparison of median bicarbonate concentrations between spring/summer and autumn/winter.....	103
Figure 4.6 . Box and whisker diagram showing intra-site comparison of median calcium concentrations between spring/summer and autumn/winter.....	104
Figure 4.7 Box and whisker diagram showing intra-site comparison of median magnesium concentrations between spring/summer and autumn/winter. T	105
Figure 4.8 Box and whisker diagram showing intra-site comparison of median potassium concentrations between spring/summer and autumn/winter.....	106
Figure 4.9 Box and whisker diagram showing intra-site comparison of median sodium concentrations between spring/summer and autumn/winter.....	107
Figure 4.10 Box and whisker diagram comparing autumn/winter and spring/summer $\delta^{15}\text{N}_{\text{NO}_3}$ values at each site.	111
Figure 4.11 Box and whisker diagram comparing autumn/winter and spring/summer $\delta^{18}\text{O}_{\text{NO}_3}$ values at each site.	111
Figure 4.12 Cross-plot of $\delta^{15}\text{N}_{\text{NO}_3}$ and $\delta^{18}\text{O}_{\text{NO}_3}$ values of samples from all sites collected between November 2015 and January 2017.	113
Figure 4.13 Nitrate concentration plotted with $\delta^{15}\text{N}_{\text{NO}_3}$ values of samples collected between November 2015 and January 2017.	114
Figure 4.14 Nitrate concentration plotted with $\delta^{18}\text{O}_{\text{NO}_3}$ values of samples collected between November 2015 and January 2017	114
Figure 4.15 $\delta^{15}\text{N}_{\text{NO}_3}$ and $\delta^{18}\text{O}_{\text{NO}_3}$ values for sites 1-4 plotted with average clay content (%) across 0-90 cm depth for corresponding fields.....	118
Figure 4.16 Relationship between pH and major ions in field drain samples	123
Figure 4.17 Relationship between DOC and NO_3^- concentrations in all field drain samples....	127
Figure 4.18 . Relationship between SO_4^{2-} and NO_3^- concentrations in all field drain samples....	128
Figure 4.19 Relationship between measured NO_3^- and calculated HCO_3^- concentrations in all field drain samples collected between November 2015 and January 2017	129
Figure 5.1 Locations of the sampling sites at which piezometer samples were collected.	139
Figure 5.2 Depth profile of nitrate concentrations from the stream to 1.5m below the streambed from spring/summer,	145
Figure 5.3 Stream sediment pore water nitrate concentration depth profile from 2.5cm to 15.0cm beneath the stream bed from DET probe deployments.....	146
Figure 5.4 Depth profile of chloride concentrations from the stream to 1.5m below the streambed from spring/summer and autumn/winter samples.....	148
Figure 5.5 Stream sediment pore water chloride concentration depth profile from 2.5cm to 15.0cm beneath the stream bed from DET probe deployments.....	148
Figure 5.6 Depth profile of sulphate concentrations from the stream to 1.5m below the streambed from spring/summer and autumn/winter samples.....	149

Figure 5.7 Stream sediment pore water sulphate concentration depth profile from 2.5cm to 15.0cm beneath the stream bed from DET probe deployments.....	150
Figure 5.8 Depth profile of bicarbonate concentrations calculated from ion balance from the stream to 1.5m below the streambed from spring/summer and autumn/winter samples	151
Figure 5.9 Depth profile of calcium concentrations from the stream to 1.5m below the streambed from spring/summer and autumn/winter samples.....	152
Figure 5.10 Depth profile of potassium concentrations from the stream to 1.5m below the streambed from spring/summer and autumn/winter samples collected between.....	153
Figure 5.11 Depth profile of potassium concentrations from the stream to 1.5m below the streambed from spring/summer and autumn/winter samples	154
Figure 5.12 Depth profile of sodium concentrations from the stream to 1.5m below the streambed from spring/summer and autumn/winter samples	155
Figure 5.13 Depth profile of DOC concentrations from the stream to 1.5m below the streambed collected along a 1.6 km study reach.....	156
Figure 5.14 Shallow sediment pore water $\delta^{15}\text{N}_{\text{NO}_3}$ and $\delta^{18}\text{O}_{\text{NO}_3}$ values along a 2.5 – 15.0 cm profile.....	158
Figure 5.15 Stream, 0.5m, 1.0m and 1.5m piezometer $\delta^{15}\text{N}_{\text{NO}_3}$ and $\delta^{18}\text{O}_{\text{NO}_3}$ values in samples collected from five locations along the study reach.	159
Figure 5.16 Boxplots comparing $\delta^{18}\text{O}_{\text{H}_2\text{O}}$ values along the stream - 1.5m depth profile by season in samples collected between November 2015 and January 2017.....	160
Figure 5.17 Boxplots comparing seasonal $\delta^{18}\text{O}_{\text{H}_2\text{O}}$ values by depth along the stream - 1.5m continuum in samples collected between November 2015 and January 2017.....	160
Figure 5.18 $\delta^{18}\text{O}_{\text{H}_2\text{O}}$ and $\delta^2\text{H}_{\text{H}_2\text{O}}$ values for stream samples.....	161
Figure 5.19 $\delta^{18}\text{O}_{\text{H}_2\text{O}}$ and $\delta^2\text{H}_{\text{H}_2\text{O}}$ values for 0.5 m piezometer samples	162
Figure 5.20 $\delta^{18}\text{O}_{\text{H}_2\text{O}}$ and $\delta^2\text{H}_{\text{H}_2\text{O}}$ values for 1.0 m piezometer samples	162
Figure 5.21 $\delta^{18}\text{O}_{\text{H}_2\text{O}}$ and $\delta^2\text{H}_{\text{H}_2\text{O}}$ values for 1.5 m piezometer samples	163
Figure 5.22 $\delta^{18}\text{O}_{\text{H}_2\text{O}}$ and $\delta^2\text{H}_{\text{H}_2\text{O}}$ values for all stream and piezometer samples	164
Figure 5.23 Crossplot of $\delta^{18}\text{O}_{\text{NO}_3}$ vs $\delta^{15}\text{N}_{\text{NO}_3}$ values measured in stream samples separated into spring/summer and autumn/winter	166
Figure 5.24 Relationship between $\delta^{15}\text{N}_{\text{NO}_3}$ values and stream nitrate concentrations. Samples separated into spring/summer and autumn/winter	166
Figure 5.25 Relationship between $\delta^{18}\text{O}_{\text{NO}_3}$ values and stream nitrate concentrations. Samples separated into spring/summer and autumn/winter	167
Figure 5.26 Shallow sediment profile (2.5 – 15.0cm below the stream bed) of $\delta^{15}\text{N}_{\text{NO}_3}$ and $\delta^{18}\text{O}_{\text{NO}_3}$ values.....	168
Figure 5.27 Cross-plot of $\delta^{15}\text{N}_{\text{NO}_3}$ and $\delta^{18}\text{O}_{\text{NO}_3}$ values measured in 0.5 m piezometer samples separated into spring/summer and autumn/winter	170
Figure 5.28 Cross-plot of $\delta^{15}\text{N}_{\text{NO}_3}$ and $\delta^{18}\text{O}_{\text{NO}_3}$ values measured in 1.0 m piezometer samples separated into spring/summer and autumn/winter	170
Figure 5.29 Cross-plot of $\delta^{15}\text{N}_{\text{NO}_3}$ and $\delta^{18}\text{O}_{\text{NO}_3}$ values measured in 1.5 m piezometer samples separated into spring/summer and autumn/winter	171
Figure 5.30 Mean $\delta^{18}\text{O}_{\text{H}_2\text{O}}$ values from 0.5m piezometer samples plotted with daily precipitation.	173
Figure 5.31 Deriving the process responsible for fractionation of $^{15}\text{N}_{\text{NO}_3}$ by plotting $\ln[\text{NO}_3^-]$ vs $\delta^{15}\text{N}_{\text{NO}_3}$	175
Figure 5.32 Correlation between $\delta^{15}\text{N}_{\text{NO}_3}$ and $\delta^{18}\text{O}_{\text{NO}_3}$, and the natural log of the nitrate concentrations measured in stream samples	176
Figure 5.33 Relationship between DOC and nitrate concentration along the stream-1.5m continuum	181
Figure 6.1 Basic diagram of potential nutrient flows within a farm (Watson et al., 2002)	190

Figure 6.2 Map of the Blackwater sub-catchment with the area encompassed by the mass balance exercise highlighted (mini-catchments A, B and E).	194
Figure 6.3 Land use in the area covered by the nitrogen budget calculation (mini-catchments A, B and E) in 2014, 2015 and 2016.	195
Figure 6.4 Schematic diagram of the nitrogen mass balance study area showing the inputs of nitrogen from fertiliser and turkey manure, and the removal pathways	205
Figure 6.5 Conceptual model of water flow within the top 1.5 m of weathered till in the study catchment showing nitrate concentrations and isotope delta values for each component	210

List of tables

Table 2.1 Fractionation of ¹⁵ N in soils associated with the various stages of the nitrogen cycle. 41	
Table 2.2 Stratigraphic sequence of the Aylsham district.....	50
Table 2.3 Stratigraphy of the 0-50 m geological profile at location ‘A’ in Figure 2.6 within the Blackwater sub-catchment.....	53
Table 2.4 Soil chemical characteristics at 0-30, and particle size distribution at 0-30, 0-60 and 0-90 cm depth for fields associated with sampled field drains.	55
Table 2.5 Particle size distribution for sediments collected at 0.5 and 1.0 m beneath the stream bed at each sampling site	60
Table 2.6 Porosity, bulk density (BD) and hydraulic conductivity of sediments at each of the piezometer locations.	63
Table 2.7 Observations made at each of the sites selected for piezometer installation and predictions for groundwater-surface water exchange direction explained.	64
Table 2.8 Hydrological and abstraction data for the Wensum catchment at Environment Agency gauging stations..	66
Table 3.1 GPS coordinates and elevation of the top of each piezometer above Ordinance Datum for each of the 15 piezometers.....	73
Table 3.2 Borehole diameter, length of screened section and volume of water removed prior to sampling.....	78
Table 3.3 Precision and limit of detection (LOD) for each of the analytes measured in stream, field drain, piezometer and borehole samples.	81
Table 3.4 Isotopic composition of international nitrate standards	84
Table 4.1 Field measurements of field drain samples collected between March-August 2016....	96
Table 4.2 Field measurements of field drain samples collected between September-February 2016/17	96
Table 4.3 Major ion concentrations in field drain samples collected between March-August 2016	97
Table 4.4 Major ion concentrations in field drain samples collected between November 2015 – February 2016 / September 2016 – January 2017	98
Table 4.5 Atmospheric deposition of major ion molecules across the three study fields Dunkirk, Swanhills and Gatehouse.....	99
Table 4.6 Field drain DOC concentrations (mg L ⁻¹) across all sites during spring/summer and autumn/winter sampling periods covering March – August and September-February respectively.	108
Table 4.7 Nitrite and ammonium concentrations in field drain samples collected from all sites	109
Table 5.1 Field measurements of samples collected from stream, 0.5m, 1.0m and 1.5m piezometers.....	140

Table 5.2 Major ion concentrations (mg L ⁻¹) in stream, 0.5m, 1.0m and 1.5m piezometer samples.	141
Table 5.3 Major ion concentrations (mg L ⁻¹) in stream, 0.5m, 1.0m and 1.5m piezometer samples.	142
Table 5.4 Nitrite and ammonium concentrations for all stream and piezometer samples	147
Table 6.1 Crops grown in the study site during the timeframe covered by the nutrient budget and their corresponding nitrogen export coefficients.	197
Table 6.2 Nitrogen product applied to fields with corresponding percentage nitrogen	198
Table 6.3 Calculation of uncertainty of turkey manure available nitrogen content from three analyses of turkey manure samples	199
Table 6.4 Rates of ammonia volatilisation from poultry manure under varying precipitation and temperature scenarios.	202
Table 6.5 Results of the nitrogen mass balance for mini-catchments A, B and E	204

Chapter 1 Introduction

1.1 Rationale and motivations

Nitrogen is crucial for the survival of the human population. To support an ever-increasing human population, agriculture has been intensified through the development of the Haber-Bosch process which ‘fixes’ atmospheric nitrogen gas (N_2), converting it to ammonium, a bioavailable form of nitrogen which is then applied to fields as agricultural fertilisers. Globally, nitrogen fixed by the Haber-Bosch process ($\sim 120 \text{ Tg N yr}^{-1}$) in 2010 was double that of natural terrestrial sources (63 Tg N yr^{-1}) (Fowler *et al.*, 2013).

Additionally, unintentional fixation of nitrogen occurs through the combustion of fossil fuels and electricity production, with an increase of $< 1 \text{ Tg N yr}^{-1}$ being produced in 1860 to $\sim 25 \text{ Tg N yr}^{-1}$ in 1910, as a result of the industrial revolution (Galloway *et al.*, 2003).

The global cycling of nitrogen has doubled over the last century with an estimated 210 Tg N yr^{-1} from all anthropogenic sources and 203 Tg N yr^{-1} from combined natural sources (Fowler *et al.*, 2013), this equates to $1.04 \text{ Tg N yr}^{-1}$ being produced synthetically for every 1 Tg N yr^{-1} fixed naturally. This dramatic increase in the global nitrogen budget has revolutionised the production of food and vastly improved global food security, however it is not without detrimental impacts to the environment and to human health including, but not limited to:

- Acute respiratory problems, cancer and heart disease in humans through the production of harmful aerosols, and methaemoglobinemia (blue baby syndrome) in infants (Wolfe and Patz, 2002).
- Fluctuations in forest and grassland productivity occur wherever this productivity is enhanced by increases in atmospheric nitrogen deposition, and curtailed when critical thresholds are exceeded. Biodiversity is probably decreased by such fluctuations in many habitats (Aber *et al.*, 1995).
- The acidification of lakes and streams and subsequent loss of biodiversity (Kopáček *et al.*, 2013).
- As alluded to previously, an increase in global reactive nitrogen contributes to global climate change through the release of N_2O gas into the atmosphere, a greenhouse gas roughly 300 times the potency of carbon dioxide (CO_2) (Ming *et al.*, 2016).

Perhaps most pertinent to this thesis however, is the impact that elevated levels of reactive nitrogen in the environment has on aquatic ecosystems. Reactive nitrogen causes eutrophication, hypoxia events, loss of biodiversity and habitat degradation in coastal and freshwater ecosystems, and is now considered the largest issue in relation to pollution in coastal waters (Rabalais, 2002). In England and Wales alone, the estimated annual cost associated with such eutrophication is around £75 - £114 million due to loss of amenity value and the costs of water treatment (Pretty *et al.*, 2008). Additionally, Sutton *et al.* (2011) estimated that the annual cost of nitrogen pollution to the EU is in the range of €70 - €320 billion.

It is clear that the economic and ecological impacts of a vastly increased global reactive nitrogen budget are as profound as the intended benefits to food security and quality of life. Green *et al.* (2004) examined preindustrial and modern global nitrogen loading. It was estimated that since the industrial revolution, total nitrogen loading in Europe has increased from 4.5 to 26.2 Tg yr⁻¹. Europe, alongside Asia and North America saw the largest increase in reactive nitrogen transfer to rivers from preindustrial levels. This is a significant perturbation in the global nitrogen cycle, however the mean global export of terrestrial nitrogen to rivers was estimated at just 18%, suggesting that the river system itself has the potential for high rates of nitrogen transformation, storage and removal.

Natural attenuation of nitrogen through denitrification is crucial in mitigating the above consequences. Denitrification is a key stage of the nitrogen cycle as it represents the removal of nitrogen from terrestrial and aquatic ecosystems through reduction of nitrate (NO₃⁻) to gaseous nitrogen species (N₂O, N₂). Denitrification requires low oxygen conditions and a ready supply of carbon (acting as an electron donor), and of course nitrate. The hyporheic zone, located directly beneath and to the sides of the stream bed is typically considered as containing the requisite conditions as it represents the interface between surface water and groundwater, where exchange of nutrients and organic matter is high, and anoxic conditions are common (but not in all cases) (Boulton *et al.*, 1998). The stable isotopes of nitrate can be measured and the rate and extent of denitrification delineated through $\delta^{15}\text{N}_{\text{NO}_3}$ and $\delta^{18}\text{O}_{\text{NO}_3}$ values of the remaining nitrate pool (following partial denitrification).

In agricultural systems, the use of nitrate fertilisers is considered non-point source, or diffuse (Ray and Member, 1999). Nitrogen compounds in fertilisers are oxidised in soils to nitrate, a highly soluble and therefore mobile form of nitrogen. Surface water nitrogen is then leached below the root zone and into groundwater (and eventually discharged into surface water bodies), or is incorporated into surface water directly by runoff. In areas where the water table is shallow and the aquifer is unconfined, this infiltration of nitrogen to groundwater is of great concern. The diffuse nature of agricultural nitrogen pollution (that is, where there is no single source as nitrogen fertilisers are applied over large areas) makes it difficult to manage, and represents one of the greatest challenges associated with intensive non-organic agriculture. Therefore, the need for mitigation strategies is strong and in the UK there has been a drive for EU directives and catchment research, for example the implementation of nitrate vulnerable zones (NVZs) and the adoption of the EU Water Framework Directive.

The Department for Food, Agriculture and Rural Affairs (DEFRA) introduced the Demonstration Test Catchment (DTC) project in order to tackle the problem of diffuse nitrate pollution from agriculture, designed to provide evidence of cost-effective controls on diffuse agricultural nitrate pollution without compromising yields. The DTC project currently covers four study catchments throughout England, representing ~80% of UK soil type and precipitation regime combinations, and the major farm types established in England and Wales. The four study catchments are the Eden in Cumbria, The Avon in Hampshire, The Tamar on the Devon/Cornwall border and The Wensum in Norfolk.

The study site examined in this thesis is based in the Wensum DTC, located on the Salle Farms Estate in Norfolk, UK. At the Wensum DTC, the main work is around the establishment of cover crops to mitigate soil nitrogen leaching to the groundwater and surface water reserves. To monitor the impact of the cover crops, state-of-the-art kiosks have been installed to collect high resolution stream water hydrochemical and flow data. The work presented in this thesis contributes to this monitoring through nitrate stable isotope and hydrochemical analysis of soil leachate (collected from field drains), stream water and groundwater.

A novel approach to examining catchment scale denitrification along a vertical continuum from soil water to surface water via groundwater, the hyporheic zone and benthic sediments is presented. This is achieved through measurement of the dual stable isotopes of dissolved nitrate. The significance of denitrification in these vertical strata is then examined through mass balance calculation.

1.2 Primary research aim

- To determine the presence or absence, and significance of denitrification within the soil zone and stream-subsurface continuum of a stream reach in a lowland arable catchment.

1.3 Main research objectives

- To examine integrated field scale denitrification through use of nitrate stable isotope data, addressing a knowledge gap for land users regarding losses of nitrogen via denitrification in agricultural soils across at the field scale.
- To investigate denitrification within surface stream water, and hyporheic zone and benthic sediments. This objective aims to provide new insight into the fate of nitrogen along a shallow groundwater – surface water continuum across a gradient of physicochemical conditions and at deeper depths within the hyporheic zone than is typically studied.
- To provide a nitrogen mass balance case study for the Blackwater sub-catchment, based on the findings in Chapters 4 and 5. This work will provide new primary data contributing the limited existing data regarding natural catchment scale nitrogen attenuation in an intensive arable setting, focussing on quantifying catchment scale denitrification, a component of many mass balance exercises that is often regarded as a major assumption.

1.4 Thesis structure

Relating to the motivations outlined in this chapter, the forthcoming chapters that comprise the rest of the thesis as follows:

Chapter 2 “Use of stable isotopes in the investigation of nitrogen cycling, stable isotope theory and study site background” Introduces the nitrogen cycle and outlines the key challenges in understanding the role of denitrification, discusses the role of stable isotopic measurements in the delineation of nitrogen cycling processes and describes the study site to which these isotopic techniques were applied. The purpose of this chapter is to provide the reader with the necessary background information regarding the nitrogen cycle and stable isotope theory in relation to the measurement of denitrification within a heavily agriculturally-impacted setting. The nitrogen cycle as a whole is briefly described, with greater attention paid to nitrification and denitrification. Within this, processes affecting nitrogen speciation are discussed in terms of their influence on nitrate isotope fractionation.

Chapter 3 “Research methods” Describes the range of field and laboratory techniques utilised to carry out the collection of samples and their physicochemical and isotopic analyses. Method developments of the field sampling campaign are described as well as the collection of auxiliary data.

Chapter 4 “Soil zone denitrification: evidence from field drain hydrochemical and isotope data” Presents hydrochemical and isotopic data from samples collected from field drains within the study site, acting as a proxy for nitrogen cycling within the soil zone. The evidence for denitrification from the stable isotopic analysis is discussed in the context of soil physicochemical characteristics.

Chapter 5 “Evidence for denitrification in the stream – hyporheic zone continuum”

Presents hydrochemical and isotopic data from samples collected from the stream study reach, a shallow benthic sediment profile, and piezometers installed to three depths beneath the streambed, representing the hyporheic zone. The isotopic evidence for denitrification at these vertical horizons is then discussed in relation to surface and subsurface conditions.

Chapter 6 “Catchment nitrogen budget and mass balance” Brings together the information from Chapters 4 and 5 and places it in the context of a catchment mass balance. A quantitative mass balance approach is then presented and the importance of denitrification in terms of the catchment nitrogen balance is discussed.

Chapter 7 “Conclusions, policy implications and recommendations for further work” Summarises the observations made in Chapters 4, 5 and 6 and places its relevance with a policy framework with recommendations for further work.

Chapter 2 Use of stable isotopes in the investigation of nitrogen cycling, stable isotope theory and study site background

2.1 Nitrate in agricultural systems: examining the soil-surface water-groundwater continuum

Intensive agriculture is the key driver of the human perturbation of the nitrogen cycle. Its annual contribution to fixation of atmospheric nitrogen (N_2 gas) was estimated to be 25 – 53 Tg (Galloway *et al.*, 1995; Smil, 1999). Global anthropogenic nitrogen fixation is now comparable to and is predicted to exceed natural nitrogen fixation by 2020 (Millennium Ecosystem Assessment, 2005). Given the urgency in ensuring food security for an ever-growing human population, it is crucial that a full understanding of the processes through which nitrogen is fixed, utilised by plants and microbiota, and returned to the atmosphere, is developed. Quantifying the various components of the nitrogen cycle is a formidable undertaking as each is interlinked and relies on varying conditions and other nutrient cycles (e.g. the carbon cycle). As such, this thesis will primarily examine the role of denitrification with an arable system, though not at the exclusion of other biological nitrogen cycling processes.

Roughly 75% of reactive nitrogen cycling through agricultural systems is anthropogenic in origin (Galloway *et al.*, 2004). Smil (1999) calculated that during the 1990s, ~ 170 Tg $N\ yr^{-1}$ was introduced to global agro-ecosystems, with around 70% originating from ‘new’ reactive nitrogen (that is, nitrogen in bioavailable forms, termed N_r , in the form of fertiliser and biological nitrogen fixation stimulated by cultivation) and the remaining 30% from existing N_r (atmospheric deposition, crop residues and animal manure). Smil (1999) further commented that only a small percentage of N_r that enters an agricultural system remains there ($\sim 2 - 5\%$), with roughly half being removed through crop uptake, $\sim 25\%$ emitted to the atmosphere via volatilisation and denitrification or entering aquatic systems through leaching from the soil zone ($\sim 20\%$).

Denitrification is a profoundly important stage within the nitrogen cycle, as it represents the removal of N_r from an ecosystem, returning it to the atmosphere. Without denitrification nitrogen would accumulate in terrestrial and aquatic ecosystems, vastly accelerating their decline in terms of ecosystem services. From an agricultural perspective, denitrification can represent a significant loss of nitrogen from a system (Mosier *et al.*, 2002). Rates of N_2 production via denitrification can vary significantly, depending on the conditions, discussed in further sections of this chapter. In arable wheat systems, similar to that of the study site examined in this thesis, total reduction of N_r to N_2 accounted for 2 -14% of the loss of N_r as measured in three systems under different tillage regimes by Bacon and Freney (1989). The results shown in Bacon and Freney (1989) demonstrate the influence of agricultural practice on preventing nitrate pollution, and feed into relevant policy making that may inform best management practices.

Streams, rivers, soils and wetlands represent important zones for nitrogen removal through denitrification as they are typically abundant in nitrate. Organic matter is readily available and anoxic environments (necessary for the onset of denitrification, where oxygen is sourced from nitrate during microbial anaerobic respiration, explained further in Section 2.2.4.5) are present in the form of suspended particulate microsites and benthic sediments (Galloway *et al.*, 2004). Seitzinger *et al.* (2002) developed a regression model (RivR-N) to predict the proportion of nitrogen removed from streams as a function of water residence time. This model was applied to 16 watersheds throughout the US, and it was estimated that 36 – 76% of nitrogen applied to these watersheds was removed during downstream transport. The authors explained that ~50% of nitrogen is removed in 1st to 4th order streams, representing 90% of the total stream length. The remaining 50% is removed in 5th order streams where the larger size and typically slower flow rates provide longer residence times and more anoxic microsites that generate more favourable conditions for denitrification than headwaters. A global study by Green *et al.* (2004) revealed that the combined influence of soil, reservoir, wetland and riverine systems in terms of their water residence time and temperature dynamics can account for an average of 18% of N_r loss, though the range is very high (0 - 100%), demonstrating the difficulty in scaling up of such analyses.

Increases in food production and the use of septic tanks have resulted in an increase in groundwater nitrate concentrations, a concern in many regions of the world where groundwater is relied upon as a source of drinking water. In Europe, high levels of nitrate in groundwater have been linked to agricultural activities (Howarth *et al.*, 1996).

Howarth *et al.* (1996) explained that changes in land use such as the replacement of grasslands and riparian zones with agricultural land could compromise the denitrification potential of many watersheds, therefore potentially increasing groundwater nitrate concentrations.

Early work by Strebel *et al.* (1989) showed that in the chalk aquifer in Eastern Central England, the same aquifer that supplies the study site presented in this thesis, significant nitrate contamination of groundwater occurred in the late 1970s, but has stabilised since. This stabilisation is probably due to the long residence time of the groundwater within the chalk, owing to the very high pore volume but low hydraulic conductivity. Strebel *et al.* (1989) went on to explain that nitrate leaching in Europe typically takes place during the autumn and winter and that concentrations of groundwater nitrate are highest where there are sandy soils and an arable system is in place. Strebel *et al.* (1989) suggested that to reduce the contamination of groundwater by nitrate, minimising residual root zone nitrate following harvest is crucial. Cover cropping aims to achieve this, where a cover or 'catch' crop is established following harvest of the crop. The cover crop takes up residual nitrogen in the soil zone, preventing it from leaching into the adjacent surface water or groundwater. An added benefit of establishing cover crops is that it preserves the nitrate in a biologically available form during this leaching period, where it can be reintroduced to the soil at a time when runoff potential is lower.

Removal of nitrate by denitrification in groundwater relies upon a stable supply of carbon (acting as an electron donor) (Heppel *et al.*, 2017). Where carbon is not limiting, another key control on aquifer denitrification rates is the matrix, where large pore size and high hydraulic conductivity such as sandstone are associated with the highest rates of denitrification. This is because there is enough space for communities of denitrifying bacteria to establish and proliferate, and the movement of water is such that fresh sources of carbon and nitrate are delivered to these pore spaces (Powell *et al.*, 2003). Chalk aquifers typically do not contain conditions that are favourable for denitrification. This is due to their dual porosity - where the effective porosity refers to the intergranular pore space, and fissures represent additional, much larger pore space. The effective pore space

is too small for bacteria to enter or proliferate in due to the small grain size and hence dense aggregation, leaving only the fissure space. Since fissures are associated with preferential groundwater flow paths, residence times are often too short for denitrification to occur (Powell *et al.*, 2003). Where nitrate concentrations in groundwater are low, the dual stable isotopes of nitrate can be used to determine whether this is due to its reduction by denitrification or another process.

2.1.1 Denitrification within the hyporheic zone

One region within the surface-subsurface continuum that should be discussed in detail is the surface water-groundwater interface, known as the hyporheic zone (HZ). The HZ has interdisciplinary significance to hydrologists, hydrogeologists and ecologists, who have traditionally approached its study from within their own research remit. The Water Framework Directive (2000/60/EU) requires a more integrated approach in terms of management of the hydrological system. This includes both surface water and groundwater, and the improvement of the ecological functionality of these water bodies (Environment Agency, 2007). Given the relatively recent impetus to consider all resources as connected components of a dynamic system in the form of this legislation, it is important then that the HZ be included in this, as it represents a key boundary zone between surface water and groundwater, and an understanding of the exchange of pollutants across this zone is therefore crucial.

The overall definition of the HZ is debatable depending on which discipline is describing it. For example, ecologists might describe the HZ as delineated by the presence of hypogean (subterranean) organisms as they might consider the lateral and vertical boundaries being identified through the distribution of indicator species. Hydrologists on the other hand might consider the HZ as part of the whole stream system, describing it as an area through which water might pass with the potential for geochemical reactions to influence the water chemistry. To a hydrogeologist, the HZ is typically omitted from conceptual models as it is a relatively small component on the scale usually considered within this discipline. However, the HZ is usually still considered as part of a system's groundwater reserve (Environment Agency, 2007).

Although there exist a number of definitions describing the HZ, a general description is as a “spatially fluctuating ecotone between the surface stream and the deep groundwater where important ecological processes and their requirements and products are influenced at a number of scales by water movement, permeability, substrate particle size, resident biota, and the physicochemical features of the overlying stream and adjacent aquifers” (Boulton *et al.*, 1998). Different hyporheic processes are important at different scales, ranging from sediment, to reach, to catchment.

The boundary of the HZ is difficult to define and has undergone a number of classifications throughout recent decades. Initially, delineation of the HZ was attempted based on the distribution of certain surface and subsurface indicator species, where Schwoerbel (1961) classified the HZ as the middle zone between the overlying channel waters and groundwater. Later on, Williams (1989) applied the vertical and lateral distribution of interstitial invertebrates to the definition of the HZ, though this was ineffective given the different possible hydrological characteristics (e.g. perched, losing or gaining reaches) which might influence invertebrate mobility. Triska *et al* (1989) took a hydrochemical approach, identifying the ‘surface zone’ as the region directly beneath the stream bed containing > 98% of surface water and thus chemically indistinguishable. The ‘interactive zone’ contained 10 – 98% of surface water with this depth representing the boundary between the stream and subsurface. This approach received criticism from Vervier *et al.* (1993), who considered these boundaries arbitrary in their static nature.

As a result of the difficulty in delineating the HZ, many authors consider its extent differently. For example, Harvey *et al.* (2013) examined denitrification rates in the HZ by collecting samples from 2.5 – 15 cm beneath the stream bed. On the other hand, Wexler *et al.* (2011) estimated the mean depth of the hyporheic sediments in the River Wensum to be 1.5 ± 0.5 m. In this thesis, for consistency with Wexler *et al* (2011) who studied the same geographical location, the HZ is defined as 1.5 ± 0.5 m beneath the stream bed. In reality, the extent of the HZ is probably not a fixed boundary as it responds to the hydrological conditions within the catchment (Boulton *et al.*, 1998), therefore placing a definite limit on its extent is impossible, especially where a period of study covers an entire seasonal cycle.

Granulometric features (i.e. size, shape and composition) within hyporheic sediments are key determinants of the majority of physical and chemical processes occurring in the HZ (Brunke and Gonser, 1997). Patterns of interstitial flow are co-governed by streambed porosity and hydraulic gradient. These flows are characterised by turbulence and irregularity, generating zones of rapid, low and no flow (Boulton *et al.*, 1998). Where flows are rapid, dead zones are created in sheltered areas, creating anaerobic conditions. Accordingly, an apparently well oxygenated HZ can include zones of anoxia and hypoxia. These microzones are generally associated with irregularities in sediment particle surfaces, small pore spaces and localised accumulations of organic material (Briggs *et al.*, 2015). This heterogeneity in conditions allows for the existence of a diversity of microzones, in turn facilitating a range of ecological processes on small scales. These microzones exist until some change in the system occurs, allowing for hydrological exchange to break them down (Briggs *et al.*, 2015).

As water enters the HZ, the processes of ammonification, nitrification and denitrification occur almost immediately, for example sediments within the HZ that have high cation exchange capacity will readily sorb ammonium, creating large reserves for use in nitrification. Therefore, sediments with high cation exchange capacity can indirectly increase nitrate concentrations in the pore water, providing other conditions are met. This cycling of nitrogen is controlled by oxygen availability and determines the status of the upwelling water in terms of nutrient content and can therefore influence the surface stream water processes (Holmes *et al.*, 1996). The distribution of organic material throughout sediments is of particular importance in its role as a substrate and an energy source (of carbon) for microbial respiration, and in governing the porosity and hydraulic conductivity of the sediment (Brunke and Gonser, 1997). Organic material acts as a source of inorganic nutrients following mineralisation, or as a sink for ions such as ammonium through cation exchange interactions. Small particles are key sites for biofilm production due to their high surface area to volume ratio. This results in a negative correlation between mean sediment particle size and abundance of bacteria in river sediments (Claret and Fontvieille 1997).

Low porosity sediments can influence water velocity, allowing fine particles to retain organic material, resulting in an association with high organic matter content sediments, stimulating the growth of biofilms (Boulton *et al.*, 1998). As mentioned previously, the presence of biofilms stimulates microbial activity, including denitrification. In this way,

HZs under the correct conditions can have a significant capacity for nitrate removal, especially in agricultural catchments where inorganic nitrogen inputs are high.

The reach scale is probably the best understood of all HZ processes (Briggs *et al.*, 2015). The clearest link between surface water and groundwater is through hydrological exchange facilitated by up welling and down welling regions. Such regions are created as a result of reach-scale geomorphological features such as slope, channel shape and characteristics of the stream bed and obstacles (e.g. boulders) (Boulton *et al.*, 1998). Holmes *et al.* (1996) conducted tracer experiments that revealed extremely complex flow paths and commented that these paths are subject to influence by factors such as flooding and transpiration in the riparian zone. Furthermore, Boulton *et al.* (1998) explained that geomorphological features such as the shallowness of the HZ (i.e. depth to bedrock) is also significant, adding that the ecological significance of shallow HZs could be less important to the total stream ecosystem.

Up welling and down welling through the streambed are indicated by horizontal flows of water entering and leaving the streambanks and gravel bars. Combined, these flow paths contribute to the delay in downstream water movement, occurring when water enters flow paths with lower velocity than the surface stream (also known as hydrologic retention) (Boulton *et al.*, 1998), where hydrologic exchange increases with sediment particle size (Morrice *et al.*, 1997). In systems where hydrologic exchange is high, the result is that not only has more water been exchanged between the stream and the aquifer, but also that water has remained in the subsurface for longer. In terms of nitrogen transformations, this increases overall denitrification as the residence time, and hence opportunity for denitrification is greater, which can be measured using the dissolved nitrate stable isotopic composition of water samples.

Long retention times within the HZ foster interactions between the biofilms formed on sediment particles and the macronutrients found in subsurface flow. Accordingly, patterns in physicochemical conditions such as temperature, pH, nutrient concentrations, dissolved organic carbon and dissolved oxygen within the HZ can give an indication of the surface water influx to, or the movement of water along the HZ (Boulton *et al.*, 1998). Triska *et al.* (1990) found evidence of nitrification within the HZ through showing the accumulation of nitrate along a flow path. Triska *et al.* (1990) explained that a variation in local exchange of water between the HZ and the stream channel resulted in

temporally variable gradients in dissolved oxygen, nitrate and ammonium in the subsurface waters of a small gravel-cobble bed stream. The results presented in Triska *et al.* (1990) indicated that laterally advected channel water and groundwater contributions to the HZ supplied sufficient dissolved oxygen and ammonium respectively to facilitate hyporheic nitrification. Valett *et al.* (1994) discussed that gradients such as those described in Triska *et al.* (1990) are typically associated with oxygen depletion resulting from the mineralisation of organic matter, thus highlighting the capacity of the HZ for inorganic nitrogen regeneration where the incorporation of high dissolved oxygen surface water is sufficient. The newly nitrified nitrate then becomes available to surface biota in nutrient limited conditions.

Where hyporheic hydrological exchange is active, there is evidence for ecological response to upwelling zones (Boulton *et al.*, 1998). These zones are nutrient rich and therefore create productivity 'hot spots' (described as locations where rates of microbial activity are disproportionately higher than the baseline conditions, Vidon *et al.*, 2010) within the stream. For example, Grimm (1987) explained that in some desert streams, activity in the HZ, promoted by flow conditions, can generate nitrate where primary production is normally limited. In Grimm (1987), nitrogen storage in periphyton, macroinvertebrates and fish were assessed over 24 hr cycles and it was found that benthic algae and autochthonous detritus contributed ~90% of the nitrogen stored within the HZ and proved a useful indicator of post flood successional processes. Boulton *et al.* (1998) present a useful diagram showing the movement of water (and hence nutrients and carbon) at the catchment, reach and sediment scales (Figure 2.1).

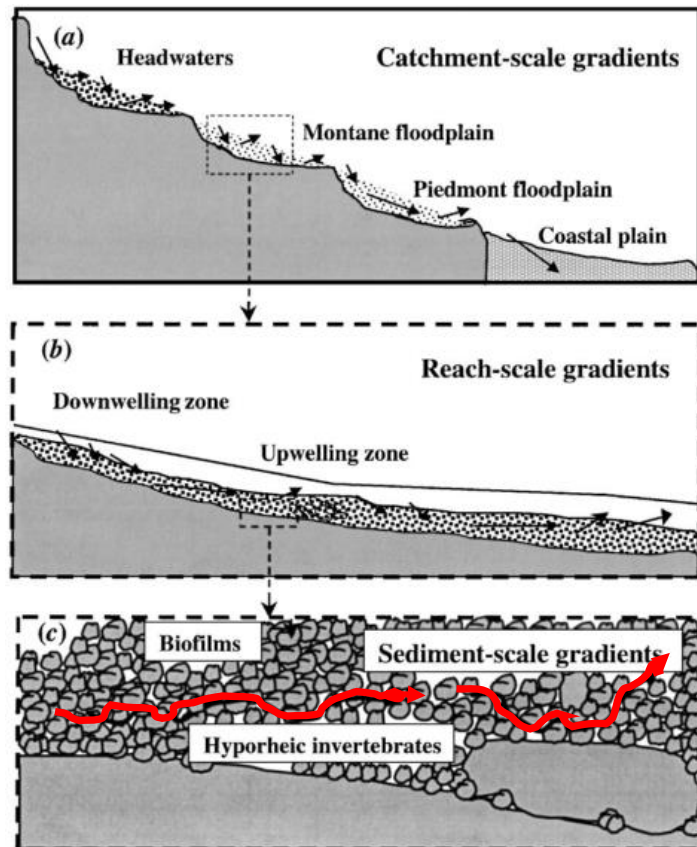


Figure 2.1 Cross-sectional lateral schematic showing gradients of water movement in the hyporheic zone at the catchment (a), reach (b) and sediment (c) scales. The etched section represents the hyporheic zone. Adapted from Boulton et al. (1998).

2.1.2 Mass balance and nitrogen budgets

Nitrogen budgeting through mass balance modelling is a useful way to describe the capacity of a system to retain and cycle nitrogen. The concept of nitrogen budgeting is a quantitative method of examining nitrogen usage within a given system. It is not a new research approach, being first introduced over a century ago in Lawes *et al.* (1882) but is still common practice today (e.g. Gentry *et al.*, 2008). At its core, a nitrogen budget relates to the conservation of mass (Meisinger and Randall, 1991) which can be simply illustrated by the following: Nitrogen in – nitrogen out = nitrogen stored within, or lost from the system (Watson *et al.*, 2002).

One major advantage of this simple method is that it allows different systems to be compared in the same way. It is not without its limitations however, in that simple budgets do not give any indication of where nitrogen is stored, for how long, or inform of any removal pathways and so often the necessary data are not available for more

comprehensive models. In Chapter 6 of this thesis, a mass balance approach is presented for Salle Farms, in which the concept of nutrient budgeting is discussed in further detail.

Excess nitrogen within a system, which might pose a threat to surrounding ecosystems, human health or natural resources, can be identified by quantifying nitrogen inputs and outputs. Nutrient budgets can be used as a tool to directly inform management approaches such as those aimed at improving soil fertility. Watson *et al.* (2002) explained that on organic farms, where manipulation of soil mineral content to maintain soil fertility is heavily restricted, the balance between inputs and outputs is all the more important. Watson *et al.* (2002) reviewed 88 nutrient budgets, with all of the nitrogen budgets reporting excess nitrogen. The efficiency of nitrogen usage was highest in arable systems (0.9, i.e. that 90% of the nitrogen applied is taken up by crops or stored in the soil). By contrast, nitrogen use efficiency was lowest in cattle livestock systems (0.2).

The purpose of the budget will typically inform the level of detail within the resulting conceptual model. Nutrient budgets are varied in their level of sophistication and are typically employed to identify gaps in scientific knowledge, identify dominant processes (such as denitrification), examine how different processes interact within a system and what conditions might affect these interactions, or simply to estimate losses of nutrients from an economic perspective (Watson *et al.*, 1999). As such, the nitrogen input information is subject to the reliability of the data. For example, nitrogen inputs from fertiliser applications are well documented, but soil processes are less well represented. Overall the impact of the accuracy of the data is relative to the purpose of the budget (Watson *et al.*, 2002).

2.1.3 The fate of reactive nitrogen following incorporation into agricultural soils

Nitrogen fertilisers are central in maintaining the ever-increasing intensification of agriculture across the globe. As such, given the ecological, economic and human health implications associated with elevated nitrogen levels in the environment discussed in Chapter 1, a key issue is the immediate post-application and long-term fate of fertiliser-derived nitrogen if such intensification is to be achieved sustainably.

Previous studies examining the long-term fate of soil nitrogen amendments have shown that applying fertiliser-derived nitrogen can deplete the soil nitrogen pool by enhancing nitrification and subsequent leaching of nitrate (Mulvaney *et al.*, 2009), and have been demonstrated to impact soil carbon stocks by stimulating decomposition of crop residues (Khan *et al.*, 2007), highlighting a crucial interaction between the nitrogen cycle and other major nutrient cycles.

^{15}N -enriched fertiliser compounds have been successfully used to track the uptake of fertiliser-derived nitrogen by crops, and its retention in soil organic matter. Overall, rapid uptake of fertiliser nitrogen by crops has been shown to account for 40 – 60% of total applied nitrogen, while the remaining fertiliser nitrogen is incorporated into microbial biomass and soil organic matter, volatilised as ammonia or leached from the soil. An important component of the nitrogen cycle relating to the application of nitrogen fertilisers is the incorporation into soil organic matter, where nitrate is formed from this soil organic nitrogen pool and lost from the soil zone through leaching and denitrification (Sebilo *et al.*, 2013 and references within).

Sebilo *et al.* (2013) investigated the long-term (1982 – 2012) fate of ^{15}N -labelled fertiliser-derived nitrate in the plant, soil and water zones in two lysimeters (referred to as Lys S and Lys W) in an arable system in France. The objectives of this study were to establish the proportion of nitrogen taken up by crops following its application as fertiliser; determine the mean residence time of nitrogen applied as fertiliser in soil organic matter; and measure the flux rate of fertiliser nitrogen into the hydrosphere over 30 years following application.

Sebilo *et al.* (2013) reported $\delta^{15}\text{N}_{\text{NO}_3}$ values of +32‰ in Lys S and +53‰ in Lys W after almost 30 years since application of ^{15}N labelled nitrate, significantly above the baseline lysimeter $\delta^{15}\text{N}_{\text{NO}_3}$ value of +2.5‰. Sebilo *et al.* (2013) attribute this continual export of the isotopically labelled tracer to long retention times within the soil-plant system. This is corroborated by the significantly enriched $^{15}\text{N}_{\text{NO}_3}$ measured in soil nitrogen after over 25 years since labelled nitrogen fertiliser application (+41.5 ‰ in Lys S and +52.2‰ in Lys W) with respect to the baseline $\delta^{15}\text{N}_{\text{NO}_3}$ values of +4.4 to +5.4‰.

The $\delta^{15}\text{N}$ value of total nitrogen in plants was 0‰ prior to application of isotopically labelled nitrogen, with the $\delta^{15}\text{N}$ value increasing to +230‰ and +340‰ in Lys S and Lys W, respectively during the first cropping season, indicating that a significant proportion

of nitrogen applied as fertiliser was taken up and removed in the first crops harvested post labelled nitrogen application. This proportion was shown to decrease dramatically by 2009, with total nitrogen $\delta^{15}\text{N}$ values of crops in Lys S and Lys W of +28‰ and +38‰, respectively. Given the baseline $\delta^{15}\text{N}$ value of total nitrogen in plants, the $\delta^{15}\text{N}$ data collected in 2009 demonstrates the persistence of isotopically labelled nitrogen almost 30 years after its application, suggesting that soil organic nitrogen persists on a decadal time scale.

The discussions in Sebiló *et al.* (2013) show that leaching, crop uptake and incorporation into soil organic matter represent significant nitrogen removal pathways from the soil and plant zones both immediately following nitrogen fertiliser application, but also over a decadal timescale due to the persistence of soil organic nitrogen in soil organic matter. In contrast to storage and release of nitrogen from soil organic matter, volatilisation of ammonia represents a potential significant loss of nitrogen under a much shorter timeframe.

Losses of fertiliser-derived nitrogen via volatilisation have been demonstrated to occur rapidly following application. Pain *et al.* (1989) combined meteorological data and ammonia concentrations in air at different heights above slurry-treated areas of grassland in The Netherlands and the UK. Losses of nitrogen to volatilisation of ammonia during spreading accounted for just 1% of total nitrogen applied, with up to 85% of total nitrogen lost to volatilisation in the 12h following application. Pain *et al.* (1989) attribute high rates of volatilisation to slurry composition, with wet pig manure slurry associated with the highest rates and dry cow manure showing losses of nitrogen of 5 – 27% of total nitrogen applied. Furthermore, volatilisation rates were positively correlated with wind speed and air temperature. In the UK, it is common practice to incorporate organic manure fertilisers into the soil subsurface within 24h of application, however given the up to 85% loss of nitrogen to volatilisation within 12h of application reported by Pain *et al.* (1989), a maximum 24h lag between manure application and incorporation may result in significant losses of nitrogen to the atmosphere. Volatilisation of ammonia is discussed further in Chapter 6.

The fate of nitrogen following its application through organic and inorganic fertilisers forms the context within which Chapters 4 and 6 are discussed. Understanding the potential pathways through which nitrogen can be lost from a system is key in creating a

mass balance for a given system, and in discussing rates of denitrification in the context of substrate sources.

2.2 Stable isotope concepts and definitions

In this study, evidence for denitrification is presented through the use of the stable isotopic composition of the nitrate contained in the collected samples. A stable isotope represents an atom of a particular element with a different number of neutrons in its nucleus, and hence a different mass. It is described as ‘stable’ because it does not undergo radioactive decay (as opposed to e.g. ^{14}C , a radioisotope). Stable isotope ratios are measured (through isotope ratio mass spectrometry (IRMS)) to quantify the ratio of the heavier, less abundant isotope to that of its lighter, more common counterpart (some elements have more than one heavy isotope - for example oxygen, which has ^{17}O and ^{18}O isotopes as well as the common ^{16}O). This ratio of heavy to light isotopes is measured relative to the same ratio of an international standard. For nitrogen, this standard is AIR, and for oxygen Vienna Standard Mean Ocean Water (V-SMOW) is used. Delta notation (δ) is used to express these ratios and are calculated as:

$$\delta(\text{‰}) = (R_{\text{sample}} - R_{\text{standard}} / R_{\text{standard}}) * 1000 \quad \text{Equation 2.1}$$

where R_{sample} and R_{standard} represent the ratio of heavy to light isotope (e.g. $^{15}\text{N}/^{14}\text{N}$) in the sample and standard, respectively (Kendall and McDonnell, 1998). A negative δ value indicates that the isotope ratio measured in the sample is lower than that of the known standard, i.e. it is depleted in the heavy isotope relative to the standard whereas a positive δ value describe a sample where the heavy isotope is enriched relative to the standard.

2.2.1 Stable isotope fractionation

The physical and chemical properties of isotopes of a given element alter very slightly owing to the differences in mass, hence these differences can generate mass-dependent isotope fractionation (Kendall and McDonnell, 1998). Because the thermodynamic properties of an atom are dependent on its mass, the identical chemical compounds, which contain different isotopes of an element (e.g. $^{15}\text{N}^{14}\text{N}$ and $^{14}\text{N}^{14}\text{N}$) are characterised by different thresholds in terms of boiling/melting points, vapour pressure etc. This is a result of their different bond vibrational frequencies when in a ground state. These differences in mass are significant enough for many chemical, biological and physical

processes to alter the relative proportions of different isotopes of the same element (i.e. produce fractionation). Bonds containing heavier isotopes have lower vibrational frequencies in relation to those containing lighter isotopes, resulting in a lower zero point energy (ZPE).

Because of this lower ZPE, heavier isotopes form slightly stronger chemical bonds than lighter isotopes, which is why microbially mediated denitrification results in an enrichment of both the ^{15}N and ^{18}O in the remaining nitrate, because less energy is required to break the chemical bonds within the nitrate molecule containing lighter isotopes. As a result of this fractionation, solutes can develop unique isotopic compositions, often referred to as ‘isotopic fingerprints’ which can then be used to trace the source of a solute, be that physically (e.g. evaporation, which enriches a water mass in ^{18}O and ^2H) or through some biological process (e.g. denitrification). There are two main types of isotopic fractionation: kinetic and equilibrium.

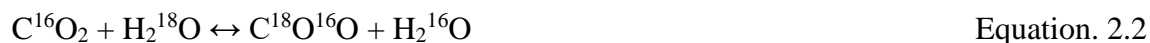
2.2.2 Kinetic fractionation

Kinetic isotopic fractionation describes incomplete and irreversible processes, where the reverse reaction is inhibited or is not occurring. Examples of such processes include evaporation, where the gas phase (water vapour) is transported away from the source liquid pool, diffusion of a solute into the surrounding matrix (e.g. diffusion of nitrate from stream water into benthic sediments), dissociation reactions and, central to this thesis, biologically-mediated processes such as denitrification (Hoefs, 2004). The size of kinetic fractionations are typically larger than those brought about through equilibrium fractionation, resulting in the lighter isotope accumulating in the product (in the case of evaporation, the gas phase would be isotopically lighter than the remaining liquid phase) (Sulzman, 2007). The magnitude of fractionation is still governed by the pathway and rate of the process, and the relative energies of the bonds being formed or broken (Mariotti *et al.*, 1981).

2.2.3 Equilibrium fractionation

The process of equilibrium fractionation alters the distribution of isotopes between reactants and products, or between phases (e.g. vapour and liquid) but only when the reaction is in equilibrium. During such processes, and unlike kinetic isotopic

fractionation, the reactants and products remain in contact. This tends to happen in well mixed, closed systems in which back reactions are allowed to progress, resulting in chemical equilibrium. A simple example of an equilibrium exchange reaction is shown in Equation 2.2, where isotopic exchange is occurring between carbon dioxide and water in a closed container (Sulzman, 2007):



in this reaction, the masses of the isotopologues of the reactants and products are different to the initial masses due to the thermodynamic variations between the heavy and light isotopes, as discussed in Section 2.2.1 (Sulzman, 2007).

Phase changes alter the distribution of heavy and light isotopes between the two phases. An example of this can be seen in cloud formation during condensation of water (an equilibrium process), where the heavier isotopes, ^{18}O and ^2H (deuterium) are concentrated in the liquid water phase, hence enriching it in ^{18}O and ^2H . The lighter isotopes (^{16}O and ^1H) persist in the water vapour phase (Kendall and McDonnell, 1998).

2.2.4 Isotope fractionation within the nitrogen cycle

The application of $\delta^{15}\text{N}_{\text{NO}_3}$ and $\delta^{18}\text{O}_{\text{NO}_3}$ values to determine the source of nitrate within a system relies on the level of isotopic fractionation during its production and cycling, under the assumption that no subsequent biogeochemical cycling takes place that might alter the original isotopic composition of the source material. In this section, the influence on nitrate isotopic composition of the different stages of the nitrogen cycle relevant to an agricultural setting are discussed.

As previously mentioned, measurement of the dual isotopic composition of nitrate allows for source partitioning and an insight into processes contributing to the cycling of nitrate within a system. The added level of information that is provided by the measurement of $\delta^{18}\text{O}_{\text{NO}_3}$ is the identification of biogeochemical processes that are not captured by the nitrogen isotopes (Sigman *et al.*, 2005). Some processes affect ^{15}N in the same way, and hence are associated with the same range or fractionation of ^{15}N , overlapping when the sources of nitrogen share a similar isotopic range. Measurement of both $\delta^{15}\text{N}_{\text{NO}_3}$ and $\delta^{18}\text{O}_{\text{NO}_3}$ values allows for the separation of such processes. An example of this is the distinction between nitrogen fixation and denitrification in a water column. During denitrification within a water column, nitrate with lighter isotopes of nitrogen and oxygen

is preferentially used, and so the residual nitrate becomes enriched in both ^{15}N and ^{18}O . The difference in the fractionation of ^{15}N and ^{18}O originates from nitrification during nitrogen fixation, where the addition of nitrate through nitrification of newly fixed nitrogen will typically lower the $\delta^{15}\text{N}_{\text{NO}_3}$ value of the existing nitrate pool because it is less enriched (nitrification adds isotopically light nitrate to the existing water column). Meanwhile, the ^{18}O remains unaffected by this as it is independent of the nitrogen source. Measurements of $\delta^{18}\text{O}_{\text{NO}_3}$ are therefore useful in identifying scenarios where nitrogen fixation has caused an underestimation of denitrification rates (Bristow, 2009).

The dual stable isotope approach is also key in identifying the sources of nitrate within a system. While some processes may overlap in terms of their impact on $\delta^{15}\text{N}_{\text{NO}_3}$ values, rendering them indistinguishable from one another without the measurement of $\delta^{18}\text{O}_{\text{NO}_3}$ values, so do some sources of nitrate. Figure 2.2 shows the typical sources of nitrate from an agricultural system, demonstrating that in many cases, a single isotopic value (i.e. that of just ^{15}N) is not sufficient to separate sources. The sources of nitrate in surface water and groundwater bodies typically have a $\delta^{15}\text{N}$ range of -10 to $\sim +30\text{‰}$, with denitrification capable of causing further enrichments, as discussed later in this chapter. There have been fewer studies carried out to measure $\delta^{18}\text{O}_{\text{NO}_3}$ values of nitrate sources and so the ranges are less constrained (Kendall *et al.*, 2007), the research presented in this thesis therefore contributes to the wider nitrate $^{18}\text{O}_{\text{NO}_3}$ database. The purpose of this research was to use stable isotopic evidence to identify the presence of denitrification in a range of locations along a vertical profile within an arable catchment. As such, an understanding of wider nitrogen cycling processes and their associated nitrate fractionation potential is necessary. The following sections describe such processes and their potential isotopic influence.

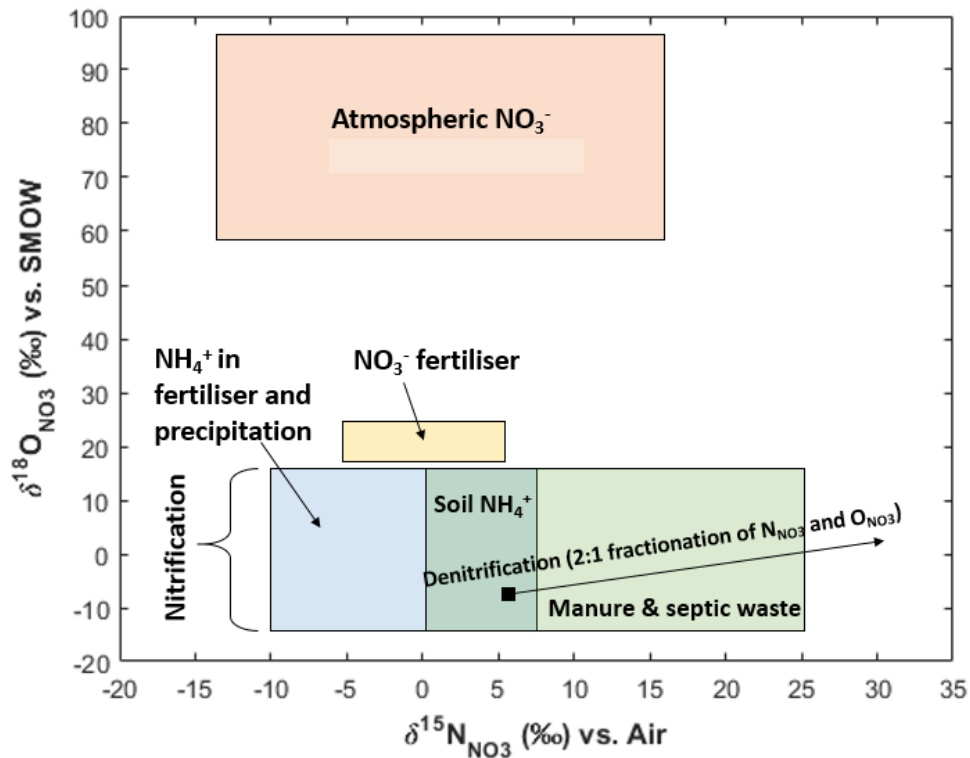


Figure 2.2 Ranges of $\delta^{15}\text{N}_{\text{NO}_3}$ and $\delta^{18}\text{O}_{\text{NO}_3}$ associated with agricultural sources of nitrate. A 2:1 N:O fractionation ratio associated with denitrification is also shown, with a slope of 0.5. Adapted from Kendall et al. (2007).

2.2.4.1 Fixation

Nitrogen fixation is a process in which unreactive N_2 from the atmosphere is converted to biologically available forms of nitrogen. This fixation is typically carried out by specialised bacteria; however a small amount of fixation occurs through lightning where the associated high temperatures separate the N_2 atoms to form atmospheric NO. This is subsequently oxidised to NO_2 , then converted to HNO_3 and removed from the atmosphere by wet and dry deposition, introducing reactive nitrogen into terrestrial and aquatic ecosystems (Galloway *et al.*, 2004). Hill *et al.* (1980) estimated the contribution to nitrogen fixation by lightning to be $\sim 14.4\text{Tg N yr}^{-1}$. Fixation of unreactive N_2 by bacteria was estimated to produce $90\text{--}130\text{Tg yr}^{-1}$ reactive nitrogen, with human activities alone surpassing this at $\sim 140\text{Tg N yr}^{-1}$ (Galloway *et al.*, 1995).

Biological fixation of atmospheric N_2 (to include fixation by legumes and alders) typically yields organic matter with a $\delta^{15}\text{N}$ value of $< 0\text{‰}$. Fogel and Cifuentes (1993) reported fractionation factors (referring to the extent of isotopic fractionation associated with an exchange reaction between two substances) ranging between -3 to $+1\text{‰}$. These

values were in agreement with early work by Hoering and Ford (1960), who examined the nitrogen isotope effects of fixation by a range of *Azobacter* species (*Azobacter agile*, *chroococcum*, *indicum* and *vinelandii*), reporting a range of -0.7 to + 3.5‰ for $\delta^{15}\text{N}$ in incubation studies ranging from 19 to 48 days.

Low $\delta^{15}\text{N}$ values in organic material are often used as indicators for fixation of N_2 , however because anthropogenic production of ammonium fertilisers relies on near full conversion of atmospheric N_2 , it produces ammonium with $\delta^{15}\text{N}$ values of around 0‰ (Bateman and Kelly, 2007), thus making it difficult to differentiate between sources of ammonium, again demonstrating the value of dual stable isotope analysis (which can be applied to nitrified soil ammonium).

2.2.4.2 Assimilation

Assimilation refers to the uptake of reactive forms of nitrogen by plants and biota. Oxidised forms of nitrogen (i.e. nitrate and nitrite) are reduced to ammonium and eventually into organic matter (Kendall and McDonnell, 1998). Like other biological processes, assimilation favours the uptake of the lighter ^{14}N over ^{15}N , and so results in a slight isotopic fractionation of the remaining material. Hübner (1986) compiled fractionation factors for soil nitrogen under microbial assimilation, citing a range of -1.6 to +1‰ whereas fractionation by vascular plants causes slightly more enrichment of ^{15}N with a range of -2.2 to 0.5‰ to that compared of soil organic matter (Mairiotti *et al.*, 1980).

In aquatic environments, the range of N fractionation through assimilation is much higher at -27 to 0‰ (Fogel and Cifuentes, 1993). This much larger degree of fractionation in comparison to soil environments demonstrates the significance of various kinetic and equilibrium effects arising from the very different environmental conditions.

Swart *et al.* (2014) investigated the fractionation of nitrate stable isotopes as the result of assimilation by marine benthic algae. Two experiments were carried out, one in which the concentration of nitrate in the substrate was allowed to reduce as assimilation progressed, and one where the nitrate concentration was kept constant. When the data were modelled it was revealed that that fractionation of nitrate as a result of assimilation was limited by nitrate concentration, with concentrations of $<2 \mu\text{M}$ yielding no fractionation. Experiments with concentrations between 2 and $10 \mu\text{M}$ (categorised as low

concentration in Swart *et al.*, 2014) showed the greatest change in fractionation between, and stabilised at 4-6‰ between 50 and 500 $\mu\text{M NO}_3^-$. These values were within the range reported in (Fogel and Cifuentes, 1993) but fall at the lower end, further demonstrating the highly variable nature of marine environments with respect to nitrogen (and in this case oxygen) isotope fractionation through assimilation.

2.2.4.3 Mineralisation

Occasionally referred to as ammonification, mineralisation is the production of ammonium from soil organic matter (SOM), and typically has a very small contribution to soil N isotopic fractionation (around 1‰ between SOM and soil ammonium, Kendall and McDonnell, 1998). It should be noted however that the term mineralisation is often used to describe the overall production of nitrate from organic material arising from several steps. This broader description of mineralisation results in a much larger range of fractionation, from -35 to ~0‰ (Delwiche and Steyn, 1970). These large fractionations arise from the nitrification of ammonium, rather than the previous step of ammonification of organic nitrogen.

2.2.4.4 Nitrification

Nitrification refers to the oxidation of ammonium to nitrate and is carried out by a number of different autotrophic bacterial species and archaea. Nitrification is classified as ‘decoupled’ because the sources of N and O can be unrelated (as opposed to ‘coupled’ processes such as denitrification where nitrate is consumed, and the N and O come from the same source – nitrate).

Nitrification progresses through two steps: oxidation of ammonium to nitrite followed by oxidation of nitrite to nitrate. The influence of nitrification on ^{15}N is dependent on which of these two steps is rate limiting. Typically, the final step, oxidation of nitrite to nitrate, is very fast and does not allow for much opportunity for fractionation to occur. The first step, oxidation of ammonium to nitrite is thus usually considered to have a more dominant influence on ^{15}N fractionation (Kendall *et al.*, 2007).

Mariotti *et al.* (1981) and Casciotti *et al.* (2003) showed large isotopic fractionations associated with ammonium oxidation in the range of -38 to -14‰. Where concentrations of ammonium are low however, the process of nitrification is limited by diffusion, with

the net result being lower fractionation of ^{15}N . Casciotti *et al.* (2003) explained that in marine environments, nitrifying bacteria have adapted to low ammonium conditions. As such, within the cell wall, the cells that are more effective at transporting ammonium do not allow for transfer of partially utilised oxidised ammonium across the cell wall. If this is the case then diffusion is one of the main processes affecting the isotopic composition of the nitrogen utilised in nitrification, which typically exhibits lower isotope effects than enzymatic processes.

Relatively recently, ammonia-oxidising archaea have been introduced into the wider research agenda associated with nitrification. Leininger *et al.* (2006) studied the abundance of ammonia monooxygenase (and the gene for which this enzyme is produced, *amoA*) in 12 pristine and agricultural soils. The results showed that crenarchaeota (Archaea) contributed up to 3000 times more *amoA* than *amoA* sourced from bacterial genes. Moreover, it was demonstrated that the *in-situ* activity of the archaea was supportive of this high abundance of archaeal *amoA*. The authors suggested that crenarchaeota could be the most abundant ammonia-oxidising organisms within the soil environment.

Jung *et al.* (2014) studied the isotopic signatures of N_2O produced in soils by ammonia-oxidising archaea. The results showed that the N_2O produced from ammonia-oxidising archaea and nitrifying bacteria were isotopically similar. Jung *et al.* (2014) commented that for this reason, in many soil production N_2O studies the isotopic effect of ammonia-oxidising archaea may have been masked as these have, only examined the isotopic effects resulting from bacterial activity.

The extent to which nitrogen undergoes isotopic fractionation during nitrification depends on the amount of available substrate (the ammonium reservoir). In systems where nitrogen availability is limited, fractionations are very small and the $\delta^{15}\text{N}$ of the nitrate produced through nitrification is comparable to that of the original substrate (Kendall and McDonnell, 1998). In agricultural systems however, where there is a large amount of available ammonium through fertiliser applications, nitrification is stimulated and the rate determining step becomes the oxidation of the ammonium within the fertiliser, which yields larger fractionations than in nitrogen limited systems (Kendall and McDonnell, 1998). Ostrom *et al.* (1998) explained that during the oxidation of fertiliser

ammonium, the initial nitrite produced has a relatively low $\delta^{15}\text{N}$ value, but this value increases as the pool of ammonium is exhausted and the rate of nitrification decreases.

Early work by Aleem *et al.* (1965) has shown that during nitrification, two oxygen atoms are derived from water and one from atmospheric O_2 . Atmospheric O_2 has a $\delta^{18}\text{O}$ value of 23.5‰ (with reference to V-SMOW), with soil water falling within the range of -20 to +5‰ depending on environmental conditions (Horibe *et al.*, 1973; Gat, 1996). Based on the assumptions outlined in Aleem *et al.* (1965), with the caveat that no subsequent fractionation has occurred, nitrate generated through nitrification in soils should have $\delta^{18}\text{O}$ values in the range of -2 to +6‰ (Durka *et al.*, 1994), where $\delta^{18}\text{O}_{\text{NO}_3} = 2/3(\delta^{18}\text{O}_{\text{H}_2\text{O}}) + 1/3(\delta^{18}\text{O}_{\text{O}_2})$.

This range for $\delta^{18}\text{O}$ values of nitrification-derived nitrate relies on not only the assumption that no fractionation has taken place but also that the $\delta^{18}\text{O}$ values of the water utilised by nitrifying bacteria (and archaea) are the same as the bulk soil values and that the $\delta^{18}\text{O}$ values of the O_2 utilised are the same as atmospheric O_2 . In aquatic systems however, there is more to consider. The $\delta^{18}\text{O}$ values of the dissolved O_2 are affected by a number of processes; mainly photosynthesis, which introduces ^{18}O -depleted O_2 into the system, and respiration which results in higher ^{18}O values in the residual O_2 (Kendall *et al.*, 2007).

Often, $\delta^{18}\text{O}$ values reported as a result of nitrification are a few ‰ higher than suggested in Durka *et al.* (1994). Buchwald and Casciotti (2010) commented that there are three factors (aside from the source composition of the H_2O and O_2) that govern the $\delta^{18}\text{O}$ value of nitrate produced through nitrification. Firstly, exchange of oxygen atoms between nitrite and water facilitated by microbial activity. Buchwald and Casciotti (2010) explained that during nitrite oxidation, an oxygen atom derived from water is bound to the enzyme nitrite oxidoreductase. This enzyme-oxygen complex goes on to bind nitrite which creates an enzyme-bound intermediate which will either progress to form nitrate or revert back to nitrite through a back reaction. If the latter occurs, then some of the oxygen atoms comprising the original nitrite are replaced by those derived from H_2O . The result of this exchange is the evolution of the $\delta^{18}\text{O}_{\text{NO}_3}$ values over time which, leads to the increased expression of $\delta^{18}\text{O}_{\text{H}_2\text{O}}$ values in the nitrite and nitrate produced through microbial activity in the system. Other ways in which $\delta^{18}\text{O}$ values are affected through nitrification are largely the result of source $\delta^{18}\text{O}$ values. For example, evaporation will

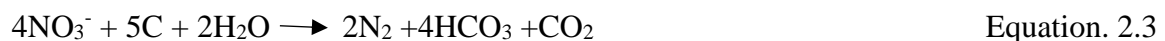
leave the source H₂O pool (from which two oxygen atoms are usually obtained) enriched in ¹⁸O (Kendall *et al.*, 2007).

2.2.4.5 Denitrification

Denitrification is the dissimilatory reduction of nitrate, resulting in N₂ (after denitrification is allowed to progress to completion), N₂O or NO intermediary gaseous N products. This process typically occurs under low oxygen conditions; however it has been demonstrated that seemingly oxic environments can contain anaerobic microsites which allow for denitrification to occur (Briggs *et al.*, 2015).

Denitrification causes a large increase in the δ¹⁵N values of residual nitrate as its concentration decreases. An example of this can be seen in the case of denitrification of ammonium nitrate fertiliser with a δ¹⁵N value of 0‰, which can produce residual nitrate with values of +15 to +30‰ (Kendall *et al.*, 2007). Meijide *et al.* (2010) conducted laboratory experiments where an arable soil was kept at 85% moisture content and treated with glucose and KNO₃ in order to obtain the isotopic composition of N₂O produced from denitrification. Results showed a high level of fractionation in the nitrogen isotope, rising from -34.4 ‰ in the bulk soil to +4.5‰ in the N₂O produced, within the range reported in Kendall *et al.* (2007). The δ¹⁸O values of residual nitrate following denitrification are also increased, hence the influence of denitrification on the stable isotopes of nitrate is considered to be coupled, as both the N and O atoms come from the same source.

In soils, *Pseudomonas denitrificans* is primarily responsible for the reduction of nitrate and simultaneous production (through respiration) of CO₂ due to its oxidation of organic material after the reaction (Kendall and McDonnell 1998):



Pseudomonas denitrificans is a facultative anaerobe, which is capable of both heterotrophic and autotrophic activity under anaerobic conditions and begins nitrate reduction at dissolved oxygen levels of around 0.5 mg/L (Hübner, 1986), with other facultative denitrifying microbiota making this transition at different levels (Kendall and McDonnell, 1998).

An example of autotrophic denitrification carried out by *Thiobascillus denitrificans*, where sulphate is the primary electron donor is:



The environmental conditions in which denitrification occurs are key to governing the degree of isotopic fractionation. Authors largely distinguish between benthic and riparian denitrification. During benthic denitrification, nitrate diffuses into anaerobic groundwater before denitrification can begin. The isotope effects resulting from benthic denitrification are typically small, as diffusion across the sediment-water interface does not usually yield much isotopic fractionation, and is the rate determining step (Sebilo *et al.*, 2003). Alkhatib *et al.* (2012) measured the $\delta^{15}\text{N}$ values of nitrate within sediment porewaters from the St. Lawrence Estuary and the Gulf of St. Lawrence, Canada. Results revealed very little isotopic fractionation of N isotopes in the porewaters of this sediment-water interface with fractionation factors of <3%.

Riparian denitrification is characterised by partial conversion of the nitrate in anaerobic groundwater (Kendall *et al.*, 2007). Sebilo *et al.* (2003) estimated the isotope fractionation associated with riparian denitrification to be around -18‰. This is because denitrification is allowed to progress within the anaerobic groundwater without being tempered by the rate-limiting diffusion of nitrate across the sediment-water boundary. It is well established that denitrification causes fractionation of N and O isotopes in a general ratio of 2:1, hence when freshwater nitrate $\delta^{15}\text{N}$ and $\delta^{18}\text{O}$ data are plotted together and the slope of the line is around 0.5, this can be confidently interpreted as a denitrification signal (Kendall *et al.*, 2007). A summary of ^{15}N isotope fractionations and associated processes, can be found in Table 2.1, and a diagram of the nitrogen cycle is shown in Figure 2.3.

Table 2.1 Fractionation of ^{15}N in soils associated with the various stages of the nitrogen cycle. Adapted from Hobbie and Ouimette (2009), original references within

Process	Fractionation (‰)	Reference
N_2 fixation	-2 to +2	Högberg (1997)
Assimilation	-1 to +1.6	Kendall and McDonnell (1998)
Mineralisation	-1 to +1	Kendall and McDonnell (1998)
Volatilisation	20 to 27	Högberg (1997)
Nitrification	12 to 35	Shearer and Kohl (1986); Högberg (1997)
Denitrification	0 to 33	Högberg (1997); Pörtl <i>et al.</i> (2007)

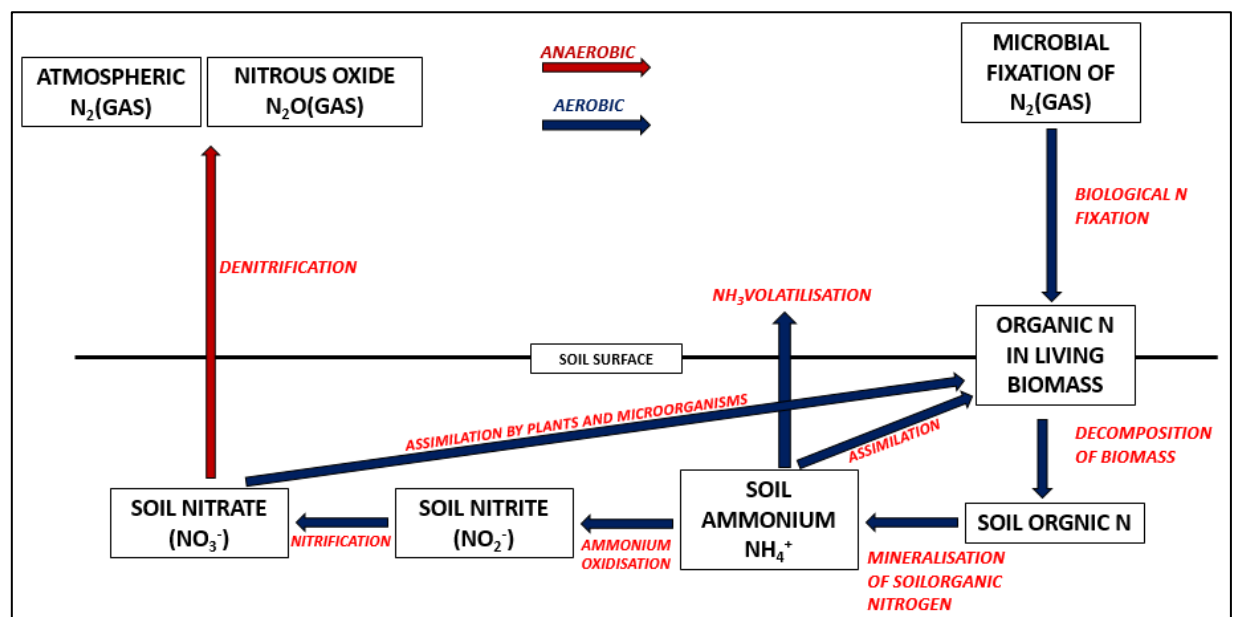


Figure 2.3 Simplified schematic of soil nitrogen cycling from atmospheric nitrogen, through the soil zone and returning to the atmosphere showing both aerobic and anaerobic processes

2.3 Dual isotope technique for nitrogen cycling studies

As discussed in the previous sections, isotopic fractionation within the nitrogen cycle leads to identifiable isotopic compositions of the resulting product or residual substrate. In denitrification, nitrate is the substrate and so studies using nitrate isotope data present $\delta^{15}\text{N}_{\text{NO}_3}$ and $\delta^{18}\text{O}_{\text{NO}_3}$ values of the nitrate remaining following partial denitrification. By measuring the stable isotopes of nitrate, one can begin to elucidate the processes by which the nitrate present in a system has been influenced. Moreover, the source of the nitrate can be identified. Previous studies utilising the dual isotopes of nitrate to achieve this have been successful in identifying key locations within systems, or processes which have significantly influenced the local nitrogen cycle.

Fukada *et al.* (2003) combined measurements of nitrate concentration and dual stable isotopes of nitrate (^{15}N and ^{18}O) to identify the process of denitrification at a river-bank infiltration site in the Torgau sand and gravel aquifer, Germany. Groundwater samples collected adjacent to the river and from directly beneath the river bed revealed low nitrate concentrations associated with high $\delta^{15}\text{N}_{\text{NO}_3}$ and $\delta^{18}\text{O}_{\text{NO}_3}$ values and vice versa, a relationship indicative of denitrification, and one that is also demonstrated in Chapter 4 of this thesis. The work presented in Fukada *et al.* (2003) demonstrates the utility of measuring both the stable isotopes of nitrate. Fukada *et al.* (2003) made use of both the relationship between $\delta^{15}\text{N}_{\text{NO}_3}$ and $\delta^{18}\text{O}_{\text{NO}_3}$ values with nitrate concentration and also the correlation between $\delta^{15}\text{N}_{\text{NO}_3}$ and $\delta^{18}\text{O}_{\text{NO}_3}$ values themselves to identify the process of denitrification

Feast *et al.* (1998) examined the sources and fate of nitrate within the chalk aquifer in the Bure catchment, Norfolk. Feast *et al.* (1998) used ^{15}N nitrate isotopic data in combination with hydrochemical data and dissolved $\text{N}_2:\text{Ar}$ ratios. The data showed that no heavy (in this study, defined as +20 to +40‰) $\delta^{15}\text{N}$ values were measured in the chalk groundwater, with the lowest nitrate concentration samples associated with the lightest isotopic signatures. The absence of heavy $\delta^{15}\text{N}$ values connected to low nitrate concentrations in the chalk indicated that the nitrate present in this aquifer was not affected by denitrification. Conflicting $\text{N}_2:\text{Ar}$ data, however, showed a higher than expected ratio than that of equilibrium with air, with an excess of N_2 typically indicative of denitrification (as N_2 is the terminal product). Feast *et al.* (1998) explained that the most probable cause of this was denitrification within the glacial deposits as the water recharges the chalk, rather than in the chalk itself.

Petitta *et al.* (2009) were able to describe the seasonal movement of nitrate from agricultural land during the winter, through to irrigation channels during the summer using dual stable isotope measurements of nitrate. Petitta *et al.* (2009) examined seasonal groundwater – surface water exchange within irrigation ditches used in agricultural land in Central Italy. Measurements of nitrate (^{15}N and ^{18}O) and water (^2H and $^{18}\text{O}_{\text{H}_2\text{O}}$) isotopes were combined with analysis of major ions, dissolved organic carbon in groundwater and surface water samples. A conceptual model was developed based on these data in which it was shown that nitrate from agricultural lands (applied as manure) was carried to the irrigation channels in runoff during early winter and spring rains also flushed out nitrate-rich shallow groundwater. The resulting water in the irrigation channels was then a mixture of these sources and contained high concentrations of nitrate. The irrigation channels were first used in the early summer, during which time discharge from nearby artesian springs was at its peak (thus acting as a third source of low nitrate water), diluting the concentration in the irrigation channels. At the end of the irrigation season, water was sourced from the high nitrate shallow groundwater again, increasing the nitrate concentration in the channel once more. This conceptual model was reinforced by the hydrologic and isotopic compositions of the water samples. Enriched $\delta^{15}\text{N}_{\text{NO}_3}$ and $\delta^{18}\text{O}_{\text{NO}_3}$ data in conjunction with high dissolved organic carbon in the shallow groundwater indicated the presence of denitrification. Petitta *et al.* (2009) presented a strong example of the value of dual stable isotopic analyses and their combination with hydrochemical data. Their study demonstrated how complex seasonal cycles can be described and how important spatiotemporal ‘hot spots’ of denitrification can be identified. Information such as this presented as a conceptual model is valuable for land managers and policy makers.

2.4 Study site background

The location of this study lies within the Wensum catchment in Norfolk, East Anglia. The catchment covers an area of 570 km² and is drained by the River Wensum, which is ~75 km long. Within the Wensum catchment is the Blackwater sub-catchment – the location of the study site for this thesis and from which hydrochemical and stable isotope data are presented in Chapters 4 and 5 (Figure 2.4). Agricultural productivity in East Anglia is among the highest in the UK. As a result, the region is highly susceptible to the issue of diffuse, or non-point source pollution caused by manure and nitrogen fertilisers which are transferred to the water course through runoff and baseflow (Wexler, 2010).

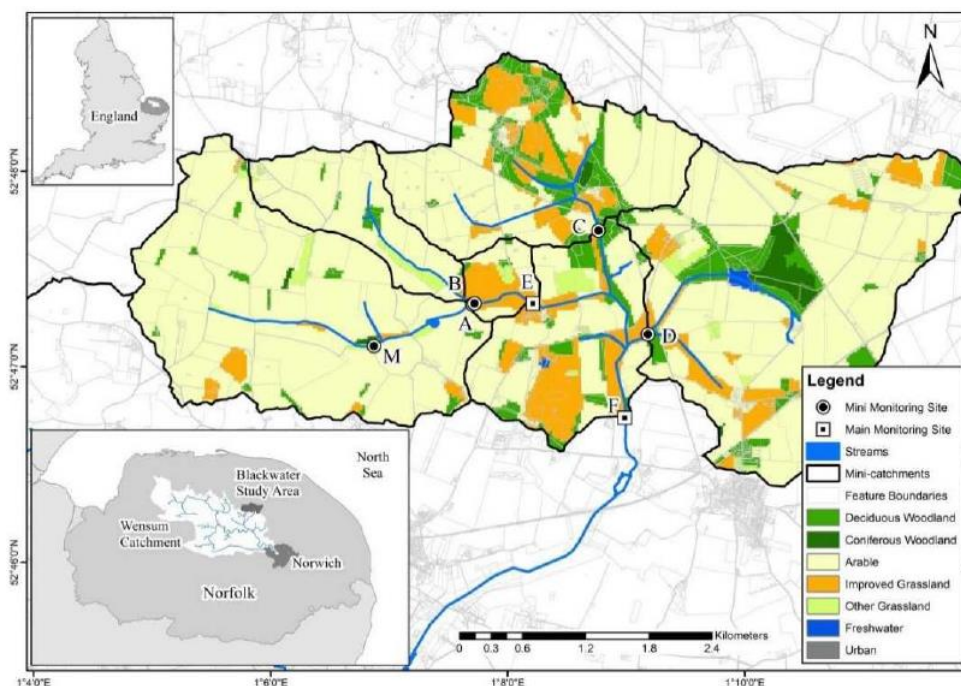


Figure 2.4 Map of the Wensum catchment and within it, the Blackwater sub-catchment. ‘A’, ‘B’, ‘C’, ‘D’ and ‘E’ are the mini-catchments within the Blackwater. This thesis mainly focuses on minicatchment ‘A’ (Chapters 4 and 5). In Chapter 6, mini-catchments ‘A’, ‘B’, and ‘E’ are discussed. From Hama-Aziz (2016).

For the data generated in this study to be placed into context, it is necessary to present the catchment characteristics and physical conditions through which nitrogen must pass. An important transport pathway nitrogen takes as it is transferred from land to aquatic systems is infiltration of rainfall to the soil and subsequent drainage via field drains into ditches and then on to rivers. Additionally, flowpaths through the phreatic and vadose zones represent important pathways. As well as transferring nitrogen from terrestrial to aquatic systems, infiltration also recharges groundwater, which in turn maintains baseflow conditions in rivers and is hence another transport pathway. Fundamental influences on these processes include the hydrology, geology and hydrochemistry of the catchment, as well as the vegetation, soil type and climate, all of which are influenced by physical factors such as geology, topography and geomorphology.

The catchment has a very low relief with the elevation of the river bed declining roughly 60 m over a 73 km drainage path. The Wensum's principal tributaries include the River Tat, Langor Drain, Guist Drain, Wendling Beck, Penny Spot Beck, Blackwater, Swannington Beck and the River Tud. There are also a number of hydraulic controls affecting the Wensum consisting of 14 mill structures and three long-term gauge stations (Sear *et al.*, 2006).

Flow in the Wensum is derived from a number of sources, primarily groundwater baseflow, surface run-off, and direct recharge to the river and drain network. The hydrological profile is typical of a groundwater-fed system with a base flow contribution ranging from 0.85 in the upper reaches to 0.70 at the catchment outlet. Water levels and flows in the surrounding floodplain are significantly influenced by water level management in the Wensum and its drain networks (Sear *et al.*, 2006).

As previously discussed, the intensification of arable agriculture has led to a significant increase in nitrate contamination and a rise in fertiliser use over the past fifty years. East Anglia has been particularly impacted by this due to its relatively (to the rest of the UK) flat terrain and lowland drainage, which are ideal for the use of intensive agricultural practices (Wexler, 2010). In 1993, The Wensum was designated whole-river SSSI status as an exemplar of naturally-enriched calcareous lowland river. Further European protection status was given to the Wensum in 2001 as a Special Area of Conservation (SAC) as recognition of its biodiversity of flora and invertebrate species, which are recognised as internationally important. Under the conservation efforts associated with

this SAC, habitat quality in and around the Wensum must be maintained in order to conserve populations of the protected Bullhead (*Cottus gobio*), Brook Lamprey (*Lampetra planeri*), white-clawed crayfish (*Austropotamobius pallipes*) and Desmoulin's whorl snail (*Vertigo moulinsiana*) as well as for water crowfoot (*Ranunculus fluitans*) and water starwort (*Callitriche palustris*) (Cooper, 2015).

The Blackwater subcatchment is characterised by low elevation, highly variable soil type and minimal riparian zones along the stream network and high Base Flow Index (BFI). Furthermore, its highly variable soil type and range of tillage and cover cropping regimes add to what is an atypical catchment in relation to other systems throughout the UK. As demonstrated in Table 2.4, the soil type within a field can vary from high sand content to high clay content across 0-90cm. Discussed further in Chapter 4, this contributes to a wide range of soil conditions within and between fields in the catchment in terms of soil moisture content and hence oxygen availability, regarded as the main influence on soil denitrification (Groffman *et al.*, 2003). Combined with differing tillage regimes this can alter the nitrification and denitrification potential of a single field dramatically when examined alongside other fields within the catchment. In low permeability, poorly draining peaty catchments such as those in the south west of the UK, the conditions for denitrification would be expected to be limited only by the supply of nitrate, as stocks of organic carbon and anoxic conditions are maintained to a high degree. Therefore, in comparison to the blackwater subcatchment, where nitrogen inputs are high but anoxic conditions and sources of carbon are relatively lower, such peaty catchments might be considered to have a higher denitrification potential. By contrast, freely draining sandy catchments such as those in the south east are expected to be sub-optimal in terms of denitrification, as pH is often low in these soil types and the nature of the soil physical properties is such that anoxic sites are not maintained within the soil profile.

Relating to soil type, but from a land management perspective, the drainage regime in a catchment can have a major role in soil zone nitrogen cycling. The Blackwater subcatchment is a tile-drained system, where soil water is actively removed from the system to enable the land to be cultivated. Catchment scale denitrification rates are typically highest in undrained systems, such as rice paddies in China. Xing *et al* (2002) observed elevated N₂O emissions and enriched $\delta^{15}\text{N}_{\text{NO}_3}$ values in saturated soils in a rice paddy region in China during the rice and wheat growing season, citing a priming effect where nitrogen inputs are higher during these seasons, initiating high rates of

denitrification due to the anoxic and high organic carbon baseline conditions. Such a priming effect is unlikely in the Blackwater subcatchment as the drainage system maintains relatively stable conditions year-round, where water, and with it, dissolved nitrogen species and carbon are removed from the soil zone and conditions are not as anoxic as those in the rice paddy regions throughout the world.

The Blackwater subcatchment is characterised as having a minimal riparian zone in comparison to other systems. This is due to the small stream network and intensively managed nature of the arable land use. Hill (1996) compiled a review considering the role of stream riparian zones in nitrogen export to groundwater from uplands to streams. Hill (1996) suggests that riparian zones have little effect on the export of nitrogen out of a system where the groundwater has limited contact with vegetation and sediments because flow occurs mainly across the surface in these systems. Though the BFI in the Blackwater subcatchment is high, the explanation presented in Hill (1996) is relevant as it highlights one region where denitrification potential is limited in comparison to a system where the riparian zone is more extensive. This introduces an interesting debate over land use policy, where in catchments where riparian zones are maintained, denitrification may be higher than systems where more of the land use is orientated towards intensive agriculture.

Tillage regime is a crucial factor in influencing catchment scale denitrification in the soil zone. Discussed in detail in Chapter 4, different types of tillage regime can alter the soil physical characteristics dramatically, and hence influence soil denitrification. Direct drilling for example minimises soil disturbance and maintains soil temperature, but leaves crop residues in-situ, creating void spaces and increasing infiltration rates (Morris, 2009). The Blackwater subcatchment is under a range of tillage regimes, including conventional, reduced- and direct-drill regimes, and is therefore subject to a highly variable soil zone denitrification potential at the catchment scale in comparison to other systems where a single tillage approach is employed.

BFI has a significant impact on hyporheic zone and in-stream denitrification through its capacity to deliver nitrate to surface water through the groundwater – surface water interface. In Chapter 5, it is shown that groundwater in the Blackwater is nitrate-depleted in the hyporheic zone with no associated evidence for denitrification. In other catchments where BFI is considered to be high, its influence on denitrification is governed by

groundwater nitrate concentrations among other physicochemical characteristics such as dissolved oxygen and carbon availability. In systems where base flow is low in comparison to surface flow, but groundwater nitrate concentrations are elevated, denitrification is restricted to groundwater and hyporheic zone conditions have little influence on the potential for nitrogen removal.

Alongside the ecological impacts associated with elevated nitrate, the overall long-term quality of recharging groundwater (and hence future surface water quality) is compromised by such contamination. The EU Drinking Water Directive (98/83/EC: Council of European Communities, 1998) exists to ensure that water for public supply (primarily sourced from groundwater) remains safe. This legislation places a permissible limit of $50 \text{ mg NO}_3^- \text{ L}^{-1}$ on drinking water and provides the impetus to carry out often costly treatment efforts if this limit is exceeded.

There is an ongoing debate over the potential for high concentrations of nitrate in drinking water to cause adverse health effects such as methaemoglobinemia in infants, implications for fertility, and intestinal cancer (Ward *et al.*, 2005). Therefore, the permissible limit of $50 \text{ mg NO}_3^- \text{ L}^{-1}$ in potable water supplies across the EU is set using the precautionary principle. Given that the Wensum supplies water for the city of Norwich, with a population of ~132,000, and that within the study catchment there are major public supply boreholes, the work presented in this thesis is of wider interest to those working in local public health.

Owing to its significant importance both environmentally and to human health, nitrate is amongst the few contaminants to have been singled out by the EU in the EC Nitrates Directive (91/676/EEC: Council of European Communities, 1991). As such nitrate pollution is now at the heart of the European Water Framework Directive (2000/60/EC: Council of European Communities, 2000), a strict legislation requiring 'good ecological and chemical status' for all surface waters and groundwaters by 2015, which has unfortunately not been achieved. To aid in the protection of potable groundwater supplies, Nitrate Vulnerable Zones (NVZs) were implemented. The introduction of NVZs in England puts in place rules associated with nitrate usage in agriculture to reduce nitrate loss to water bodies in accordance with the Nitrates Directive. The first NVZs were put into place in 1996 with additional areas identified in 2002 and 2008 (DEFRA: Water Quality Division, 2008). As of 2010, ~70% of land in England is identified as a

NVZ. In 2008, the Environment Agency carried out modelling efforts to examine the catchment-wide nitrogen loading from agricultural activities in England and Wales, expressed as confidence in modelled water quality with a 'failure' threshold of 50 mg NO₃⁻ L⁻¹. The outputs from this modelling exercise were then used to revise the way in which NVZs were designated. This evaluation indicates that water quality is predicted to exceed the failure threshold throughout the present study area.

2.4.1 Geology of the Blackwater sub-catchment

A recent report following borehole drilling at the study site carried out by the British Geological Survey (BGS) describes the local geology of the Blackwater sub catchment. The superficial geology, to include the study site consists of a substantial sequence of Quaternary sediments deposited by the interaction between two ice sheets. In the Blackwater sub-catchment within the Wensum, these sediments are made up of tills of different compositions and properties interbedded with glaciofluvial and glaciolacustrine sands and gravels (Table 2.2 and Figure 2.5) (Lewis, 2014).

Table 2.2 Stratigraphic sequence of the Aylsham district. From Lewis (2014)

Aylsham 147		
South West, West and Central part of sheet		East of sheet
Head/Alluvium/River terrace	Head/Alluvium/River terrace	Head/Alluvium
Glaciofluvial sand and gravel, undifferentiated	Glaciofluvial sand and gravel, undifferentiated	Briton's Lane Formation sand and gravel Member (BRLSG)
Briton's Lane Formation (Undifferentiated)	Briton's Lane Formation sand and gravel Member (BRLSG)	
Sherringham Cliffs Formation (SMCL) (undifferentiated)	<p>Locally a chaotic arrangement (especially in the central part) comprising:</p> <ul style="list-style-type: none"> • Chalk-rich till (Weybourne Town Till-WITTI) • Sand rich till (Bacton Green Till – BGTI) <p>Glaciolacustrine sand and clay, glaciofluvial sand and gravel</p>	<p>Glaciofluvial sand and gravel tills:</p> <ul style="list-style-type: none"> • WITTI, BGTI • Glaciofluvial sand and gravel
Lowestoft Formation (LOFT) (undifferentiated)	<ul style="list-style-type: none"> • Walcott Till Member (silt-rich matrix with chalk clasts-WATI) • Glaciolacustrine and/or Glaciofluvial sand and gravel • Lowestoft Till member (clay-rich matrix with chalk clasts) 	<ul style="list-style-type: none"> • WATI • Glaciolacustrine and/or glaciofluvial sand and gravel • Lowestoft Till Member (clay-rich matrix with chalk clasts)
Happisburgh Formation (HPGL) (undifferentiated)	Happisburgh Formation (undifferentiated)	<ul style="list-style-type: none"> • 'Corton Sands' • Happisburgh Till Member (sandy matrix with flint and chalk clasts)
Chalk Formation	Wroxham Crag Formation	Wroxham Crag Formation
	Chalk Formation	Chalk Formation

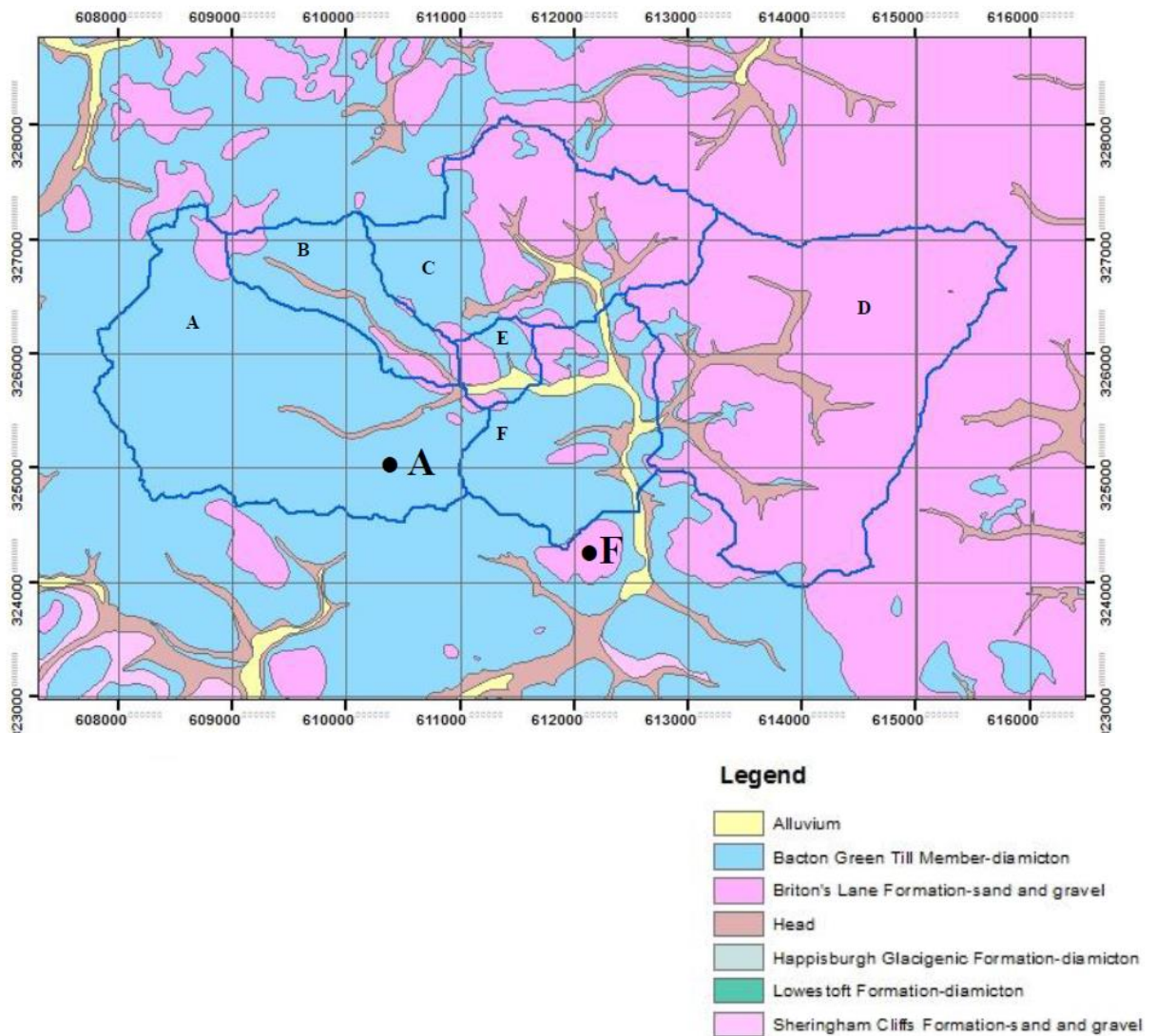


Figure 2.5 Location of the boreholes described in Section 3.2.5 shown in position ‘A’, while position ‘F’ is the location of a set of boreholes near the catchment outlet, not samples in this study from Lewis (2014).

There are three superficial deposits that lie immediately over the chalk bedrock in the west of the Aylsham district. In the East however, the Wroxham Crag intersects these deposits (Figure 2.6). The presence of glacial buried channels complicates the bedrock surface. One of these channels running NNW - SSE bisects mini catchments A and B (Figure 2.4), where a deep borehole to 68.3m depth at Wood Dalling (TG 0883 2699) terminated in superficial deposits at an elevation of 9 m below OD with the lowest 28.8 m identified as chalky till (Lewis, 2014). The boreholes sampled in this project are installed into a complex glacial till sequence, described in Table 2.3. This heterogeneity

overlying the chalk is a key feature in determining nitrogen cycling within the sub surface at the study site, which is discussed in Chapter 5.

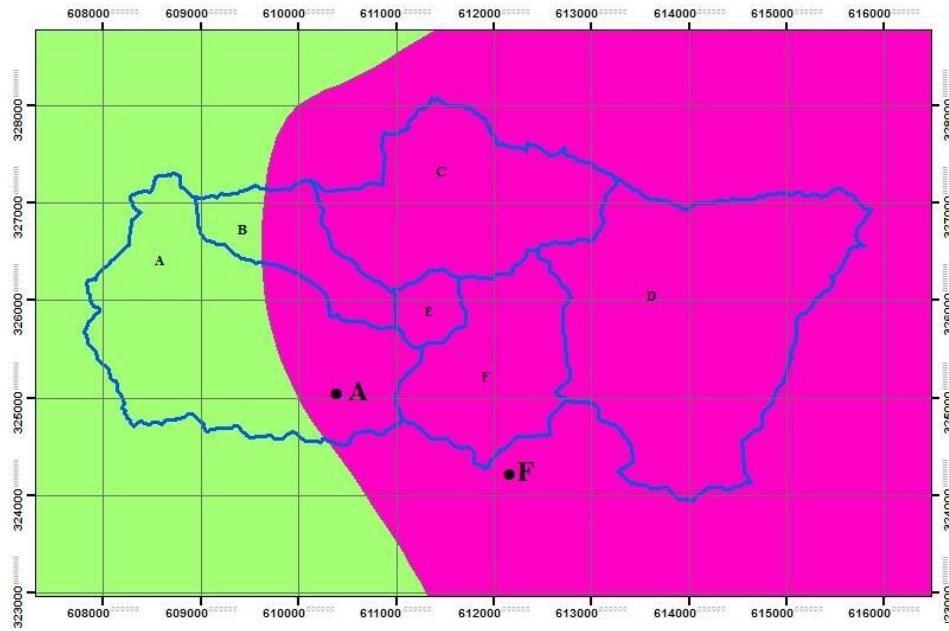


Figure 2.6 Geological map of the study site showing bedrock formation From Lewis (2014). The green section represents the chalk bedrock while the pink section shows the Wroxham crag formation (see Table 2.3)

Table 2.3 Stratigraphy of the 0-50 m geological profile at location 'A' in Figure 2.6 within the Blackwater sub-catchment (Lewis, 2014)

Formation	Description	Depth (m)
Soil		
Sheringham Cliffs Formation – Bacton Green till member	Till, both clasts and matrix chalk-rich. Red chalk clasts may be present	0.0 – 0.2
Sheringham Cliffs Formation – Bacton Green till member	Chalk clasts in an olive grey silty matrix	0.2 – 0.5
Sheringham Cliffs Formation – glaciofluvial and/or glaciolacustrine sands	Sand and gravel	0.5 – 8.2
Lowestoft Formation – Lowestoft till member	Common chalk clasts in a dark grey clay/silt matrix	8.2 – 16.3
Wroxham Crag formation	Sand and gravel, notably quartzite rich	16.3 – 21.5
Chalk		21.5 – 50.0+

2.4.2 Soil physicochemical characteristics of the Blackwater sub-catchment

Figure 2.7 shows the integrated distribution of soil types in the fields surrounding the study reach (highlighted) across the study catchment from 0-30 cm depth while Table 2.4 shows the range of soil chemical characteristics. In Chapter 4, the Dunkirk, Swanhills and Gatehouse fields shown in Figure 2.7 are discussed in detail. Figure 2.8 shows the locations for each sample referenced in Table 2.4. Soil sampling locations were selected as to cover the range of soil types within each field.

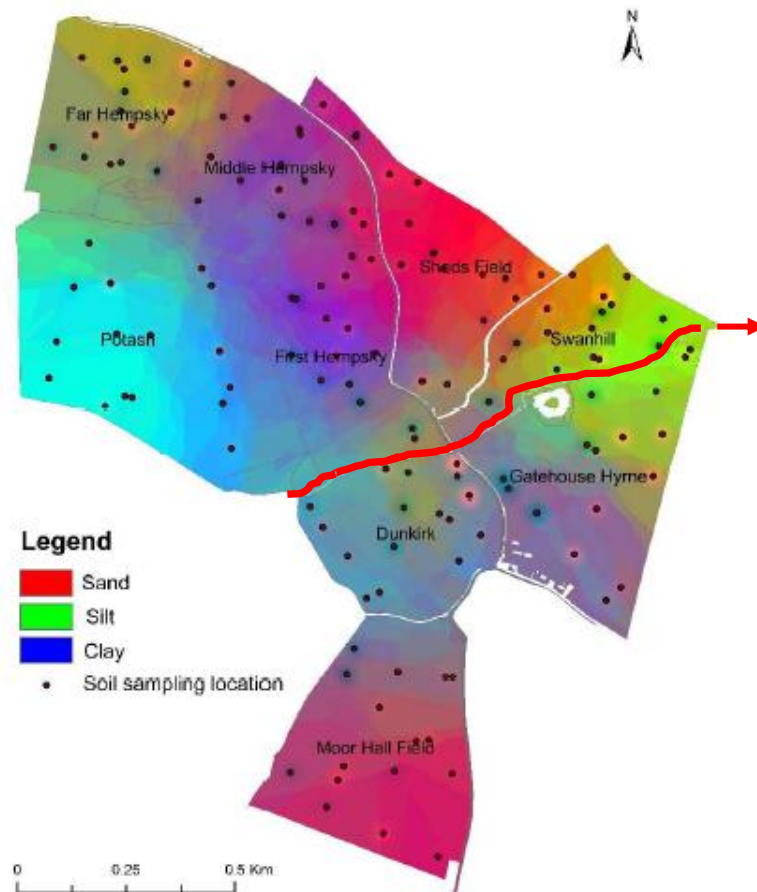


Figure 2.7 Soil fraction distribution throughout the fields surrounding the study reach. Adapted from Hama-Aziz (2016)

Table 2.4 Soil chemical characteristics at 0-30, and particle size distribution at 0-30, 0-60 and 0-90 cm depth for fields associated with sampled field drains (see Chapter 3). Soil major ion concentrations in mg kg⁻¹, sand, silt and clay fractions as percentages.

Field	Sample	0-30cm					30-60cm			60-90cm					
		P	K ⁺	Mg ²⁺	NO ₃	NH ₄ ⁺	Sand	Silt	Clay	Sand	Silt	Clay			
Dunkirk	D1	12.0	73.8	57.4	47.73	0.80	61	22	17	46	31	23	53	20	27
	D2	12.0	72.8	48.2	24.00	1.51	59	24	17	47	36	17	35	23	42
	D3	32.6	173.0	76.4	70.28	0.94	62	22	16	43	25	32	35	23	42
	D4	25.6	57.1	42.8	38.14	0.95	63	21	16	55	30	15	24	27	20
Gatehouse	GH1	51.4	105.0	50.1	17.92	0.90	63	22	15	53	30	17	42	31	27
	GH2	27.0	86.9	58.1	108.29	1.61	61	23	16	43	33	24	38	25	37
	GH3	40.0	148.0	51.1	123.76	1.26	55	23	22	41	24	35	31	24	45
	GH4	20.80	129.0	44.4	160.88	3.67	65	23	12	66	25	9	75	17	8
Swanhills	SW1	30.80	109.0	37.7	156.91	12.80	67	20	13	75	14	7	92	4	4
	SW2	21.20	92.3	55.5	171.50	11.80	66	20	14	55	29	16	45	33	22
	SW3	21.40	108.0	55.0	97.24	0.73	59	24	17	45	34	21	34	29	37
	SW4	12.40	94.0	58.0	127.30	1.17	70	20	10	54	32	14	72	16	12

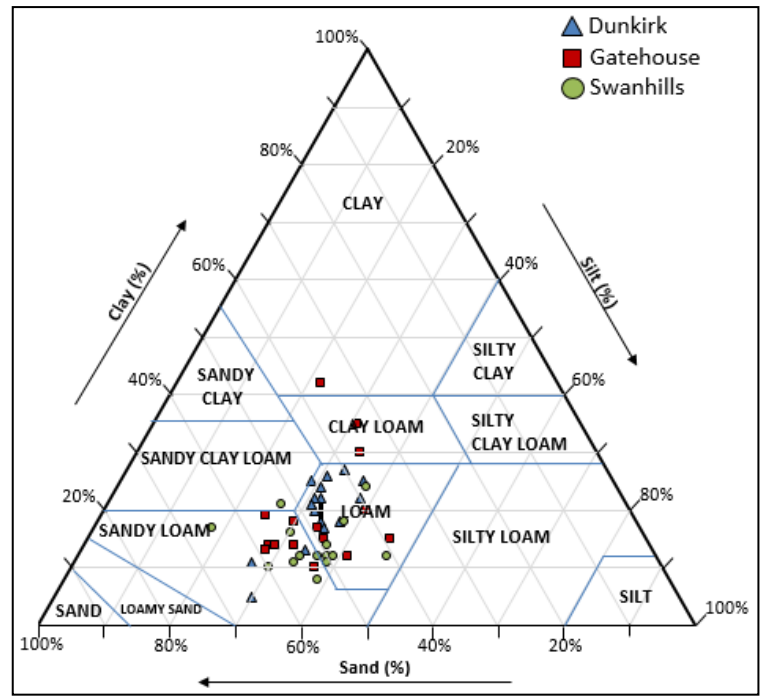


Figure 2.9 Particle size distributions from soil samples taken at the 0-30cm horizon in Dunkirk, Swanhills and Gatehouse. Adapted from Hama-Aziz (2016)

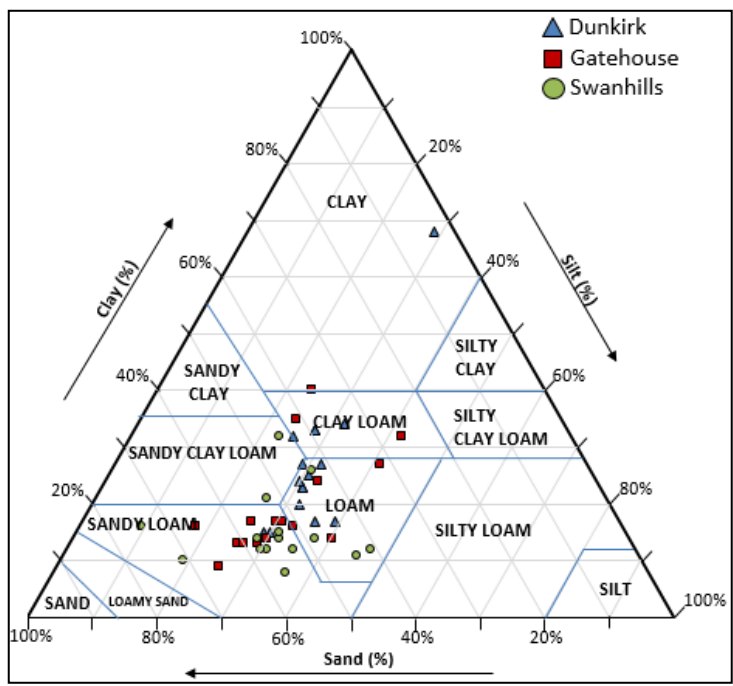


Figure 2.10 Particle size distributions from soil samples taken at the 30-60cm horizon in Dunkirk, Swanhills and Gatehouse. Adapted from Hama-Aziz (2016)

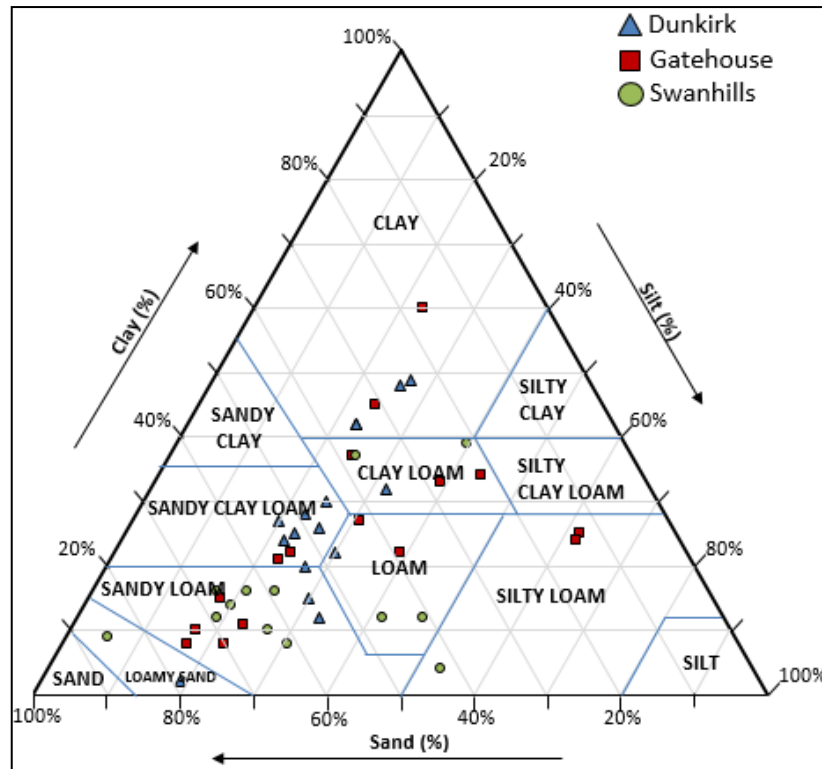


Figure 2.11 Particle size distributions from soil samples taken at the 60-90cm horizon in Dunkirk, Swanhills and Gatehouse. Adapted from Hama-Aziz (2016)

Soil nitrate is highly variable between and within the study fields, though Swanhills contains the most consistent soil nitrate concentration between sampling locations (Table 2.4). Moreover, soil ammonium is higher in Swanhills in comparison to Gatehouse and Dunkirk, suggesting that soil nitrification rates could be elevated in Swanhills with respect to Dunkirk and Gatehouse owing to the larger pool of ammonium available for oxidation, which is consistent with higher soil nitrate concentrations. The distribution of other major soil chemical constituents (P, K⁺, Na⁺, Mg²⁺) is relatively even (to that of nitrate and ammonium). Soil organic carbon within the study catchment was measured by Hama-Aziz (2016), who reported a range of 1.06 – 2.25% in the 0-30 cm profile. This is similar to the 2% threshold associated with a healthy soil as suggested by Loveland and Webb (2003), though some samples were half of this.

2.4.3 Hyporheic zone sediments and piezometer infiltration rates

Sediment coring into the stream bed was undertaken at all piezometer sampling sites.

Unfortunately, it was not possible to collect samples at 1.5 m (see Figures 3.1 and 3.2 for locations), however data regarding particle size distribution are available for the 0.5 and 1.0m depth horizons. Figure 2.12 shows the sediment type at 0.5 m and 1.0 m depth below the stream bed at each site, and Table 2.5 shows the particle size distributions. The majority of sites at 0.5 m and 1.0 m depth are comprised of sandy clay loam or clay sediments, with the 0.5 m depth horizon at Site 2 being loamy sand. Figure 2.13 shows piezometer infiltration rates for a number of sampling occasions at Sites 1 - 4. Because the piezometers at Site 5 would recharge almost immediately it was difficult to record accurate recharge rates, and when the rates were recorded, they were naturally far higher than at Sites 1-4. It is for these reasons Site 5 has been shown separately in Figure 2.14. At Sites 1 and 3, the recharge rate remained relatively similar between depth horizons, while at Sites 2 and 4 there was faster infiltration in one or two piezometers. This could be due to differences in groundwater flow paths, or it is possible that smearing of sediment during installation has impeded the ingress of water into the piezometers in some cases. Figure 2.14 shows highly variable recharge at Site 5, demonstrating the difficulty in taking accurate measurements. Again, this could be an artefact of relatively higher rates of groundwater movement at this site, or the filter membrane may have been damaged during installation, allowing water to flow more easily into the piezometer.

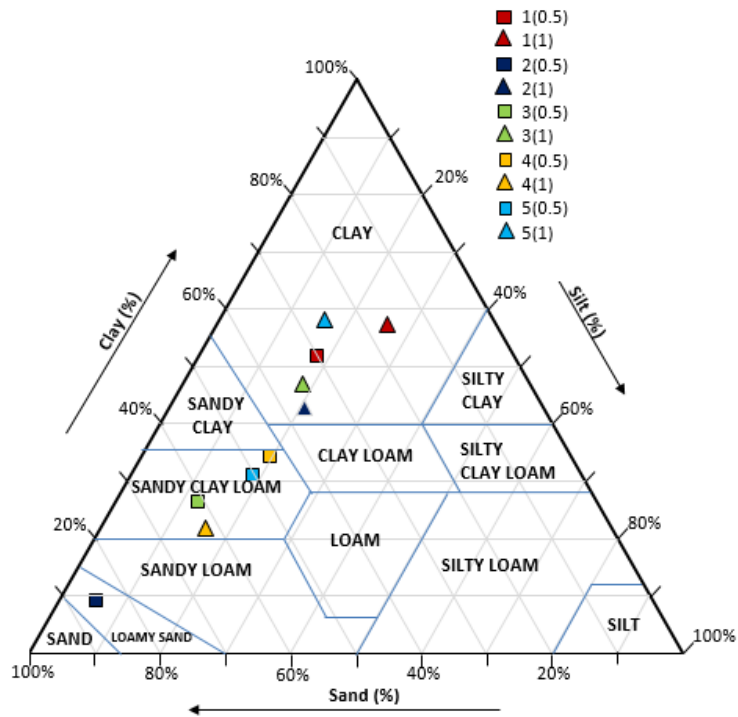


Figure 2.12 Ternary plot showing particle size distributions of subsurface sediments at 0.5 and 1.0m depth across all sampling sites

Table 2.5 Particle size distribution for sediments collected at 0.5 and 1.0 m beneath the stream bed at each sampling site

Sample	Sand (%)	Silt (%)	Clay (%)
1(0.5)	30	19	51
1(1)	17	26	57
2(0.5)	85	6	9
2(1)	36	21	43
3(0.5)	61	13	26
3(1)	35	18	47
4(0.5)	46	20	34
4(1)	62	16	22
(0.5)	50	19	31
5(1)	26	16	58

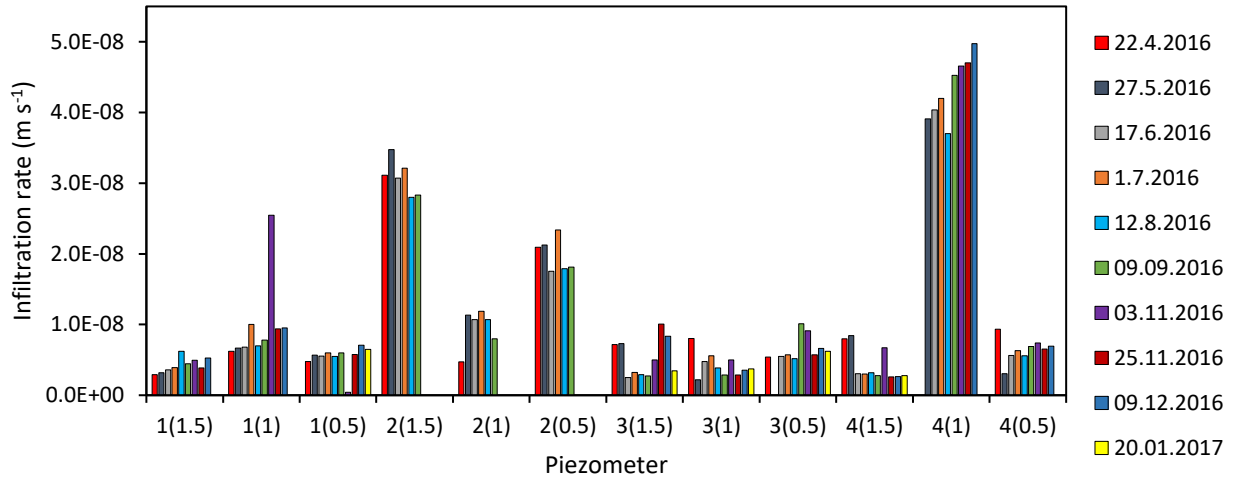


Figure 2.13 . Sites 1-4 piezometer recharge rates between April 2016 and January 2017

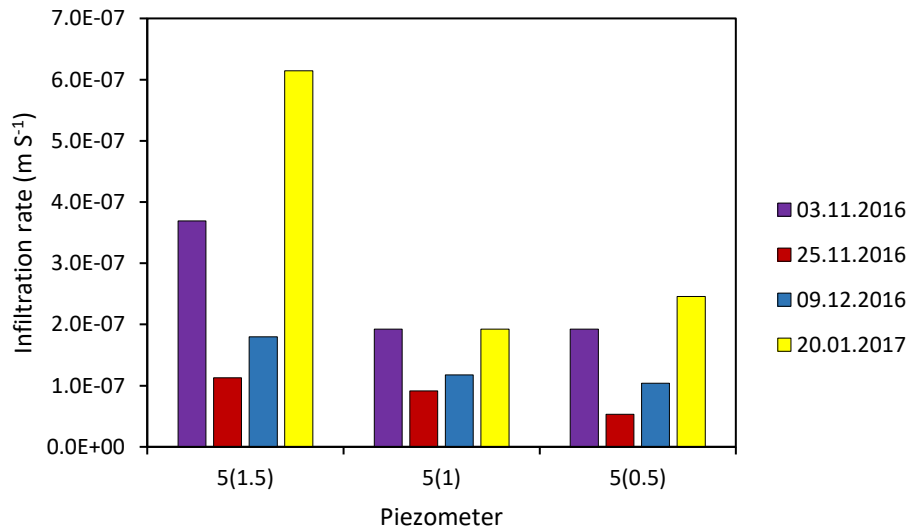


Figure 2.14 Recharge rates for piezometers at Site 5 between November 2016 and January 2017.

Porosity, bulk density and hydraulic conductivity measurements are shown in Table 2.6. Briefly, these measurements were obtained by the following methodologies: Bulk density was calculated by displacement, where a dried sample was sealed in a bag and submerged in a large beaker of water and the amount of water displaced represented the volume of sediment. Bulk density (g cm^{-3}) was then calculated as dry weight of sediment (g) / volume (cm^3). Sediment porosity (%) was calculated as $((\text{wet weight (g)} - \text{dry weight (g)}) / \text{wet weight (g)}) * 100$

Sediment hydraulic conductivity was calculated as $K = Q(-A_i)$ where Q is the rate of infiltration into the piezometer ($\text{m}^3 \text{s}^{-1}$), A is the cross-sectional area of the screened

section on the piezometer (m^2) and i is the hydraulic gradient between adjacent piezometers.

Because individual recharge rate measurements were made on several occasions, and hydraulic conductivity is calculated based on these measurements, the mean of the sediment hydraulic conductivity has been presented. As mentioned, the infiltration rate of the piezometers may have been affected by either smearing of the filter membrane, thus slowing the ingress of water, or damaging the filter membrane which would result in a much faster recharge rate.

Therefore, while every effort has been made to calculate hydraulic conductivity as accurately as possible, these may have been affected by the piezometers themselves. The sediments range between 22% and 58% clay content, with one sample containing 9% clay. Hydraulic conductivities for these sediments are in the $10^{-4} - 10^{-5} m s^{-1}$ range, mostly in agreement with values shown in Hiscock and Bense (2014). This supports the possibility for smearing of the piezometer tip, or in the case of Site 5 where hydraulic conductivities are seemingly considerably higher than expected, damage to the piezometer tip filter membrane.

Table 2.6 Porosity, bulk density (BD) and hydraulic conductivity of sediments at each of the piezometer locations.

Site (depth)	Porosity (%)	BD (g cm ⁻³)	Hydraulic conductivity (m s ⁻¹)	
			mean	range
1(0.5)	2.63	2.36	1.1×10 ⁻⁴	8.6×10 ⁻⁶ – 4.2×10 ⁻⁴
1(1)	22.4	1.0	2.2×10 ⁻⁴	8.1×10 ⁻⁵ – 6.9×10 ⁻⁴
1(1.5)	-	-	3.6×10 ⁻⁴	2.0×10 ⁻⁵ – 9.5×10 ⁻⁵
2(0.5)	12.6	0.19	2.0×10 ⁻⁴	6.1×10 ⁻⁵ – 9.5×10 ⁻⁵
2(1)	17.5	1.20	8.7×10 ⁻⁵	1.8×10 ⁻⁵ – 2.5×10 ⁻⁴
2(1.5)	-	-	7.3×10 ⁻⁴	2.0×10 ⁻⁴ – 2.3×10 ⁻³
3(0.5)	17.8	1.10	5.5×10 ⁻⁵	3.0×10 ⁻⁵ – 8.0×10 ⁻⁵
3(1)	16.7	1.44	6.5×10 ⁻⁵	1.9×10 ⁻⁵ – 2.4×10 ⁻⁴
3(1.5)	-	-	7.4×10 ⁻⁵	2.4×10 ⁻⁵ – 1.9×10 ⁻⁴
4(0.5)	22.3	1.15	3.9×10 ⁻⁵	1.3×10 ⁻⁵ – 1.2×10 ⁻⁴
4(1)	19.9	0.94	2.8×10 ⁻⁴	2.0×10 ⁻⁵ – 9.5×10 ⁻⁵
4(1.5)	-	-	1.4×10 ⁻⁵	5.2×10 ⁻⁶ – 2.7×10 ⁻⁵
5(0.5)	34.8	0.86	1.7×10 ⁻⁵	6.7×10 ⁻⁴ – 2.1×10 ⁻³
5(1)	24.6	1.19	1.7×10 ⁻⁵	1.2×10 ⁻³ – 2.2×10 ⁻³
5(1.5)	-	-	4.0×10 ⁻³	3.2×10 ⁻³ – 6.2×10 ⁻³

The sites chosen for installation of piezometer nests were selected on the basis of their streambed geomorphology. Table 2.7 details such observations made prior to piezometer installation and explanations of predicted direction of water transfer between the stream and hyporheic zone. The goal of selecting piezometer nest sites was to represent a mixture of upwelling and downwelling zones along the study reach. Table 2.7 shows that Sites 1 and 2 were predicted to be overall upwelling zones, whilst Sites 3-5 were predicted to be overall downwelling zones.

Observations during sampling occasions confirm the presence of artesian characteristics in piezometers installed at Sites 1, 3 and 5. From sampling throughout all seasons, it is confirmed that the study reach never runs dry, and so is considered a gaining stream. The observations explained in Table 2.7 may be overruled by measurements of hydraulic head, discussed in Chapter 5.

Table 2.7 Observations made at each of the sites selected for piezometer installation and predictions for groundwater-surface water exchange direction explained.

Site	Stream bed and channel geomorphological observations	Predicted direction of surface water – groundwater exchange
1	Coarse sandy gravel, straight channel, thin sediment layer, numerous riffle sequences, little pooling.	Overall Upwelling zone
2	Majority sand, straight channel, thicker sediment layer than at Site 1, some riffle-pool sequences	Overall Upwelling zone
3	Thick silty sand layer, site is located on a meander with low flow. Evidence of bank collapse increasing bed sediment thickness and causing obstruction in stream.	Overall Downwelling zone
4	Thick silty sand sediment layer, straight channel with low flow, few riffle-pool sequences.	Overall downwelling zone
5	Very thick silty sand bed sediment layer, no riffle features, dense vegetation in spring/summer impedes flow.	Overall Downwelling zone

2.4.4 Hydrology of the Blackwater sub-catchment

The Wensum is described as a meandering lowland river sustained by a high baseflow index (BFI). BFI is useful in describing a river's characteristics as it quantifies the proportion of a river's flow that is sustained from groundwater rather than runoff. A wide range of activities including calibration of hydrological and climate models, studies of basin hydrology and water resource management rely on accurate estimates of base flow (Wexler, 2010). The two flow components of a stream (base flow and runoff) are separated using a stream hydrograph and mathematical functions or software packages are then used to calculate base flow-based discharge data. This is the most widely used approach and is often undertaken without calibration to basin-specific parameters aside from basin area (Lott and Stewart, 2016).

High BFI, along with sustained river flow during particularly dry periods is suggestive of a system with low flashiness (a narrow range of flow conditions). Moreover, a high BFI is an indication that groundwater hydrochemistry will have a significant impact on stream chemistry. The Wensum is monitored by gauging stations operated by the Environment Agency. These gauging stations are located at Fakenham, Swanton Morley and Costessey Mill, flow data are shown in Table 2.7. The BFI shows a slight decrease from the upper catchment to the outlet, demonstrating an increasing fraction of surface accretion. Within the Wensum catchment, there are 10 wastewater treatment facilities with two major sources of effluent discharge located on the upper river at Fakenham and in the southern catchment at East Dereham from the Wending Beck tributary which meets the Wensum upstream of Swanton Morley. The remaining eight wastewater sources comprise minor sewage works servicing the smaller towns and villages within the catchment and release treated effluent into the river system. In the more rural parts of the catchment, septic tanks are often installed at residential dwellings which may leak and thus contribute to the effluent discharge into the river network.

Table 2.8 Hydrological and abstraction data for the Wensum catchment at Environment Agency gauging stations (Entec, 2007; Marsh and Hannaford, 2008; Centre for Ecology and Hydrology, 2009, Environment Agency, 2009a; Environment Agency, 2009b). Data originally tabulated in Wexler (2010).

Gauging station	Fakenham	Swanton Morley	Costessey Mill
	34011 (TG 919294)	34014 (TG 020184)	34004 (TG 177128)
Catchment area (km ²)	162	398	571
Mean flow (m ³ s ⁻¹)	0.87	2.64	4.04
Base Flow Index (BFI)	0.83	0.75	0.74
Effluent volume ^a (m ³ s ⁻¹)	0.028	0.036	-
Groundwater abstractions (MI/d)		33.0 ^b	
Surface water abstractions (MI/d)		46.4 ^b	

^aEffluent volumes calculated based on population served by the wastewater works at 180 litres per person per day

^bAbstractions from the Wensum catchment estimated from long-term averages (1970-2003)

2.4.5 Hydrogeology of the Wensum Catchment

The hydrogeology of the Wensum catchment is mostly dominated by the Chalk aquifer. The majority of the Chalk in the Wensum catchment is confined by the Lowestoft Till in the interfluves. There are outcrops located in the west of the catchment and erosion has exposed areas of the Chalk in the river valley. Given the low permeability of the Lowestoft Till, recharge to the Chalk is restricted, however recharge through the till may occur through preferential flow paths as a result of its highly spatially varied thickness and incorporation of sand lenses (Toynton, 1979). Furthermore, the Wensum catchment is characterised by large areas of sands and gravels in hydraulic continuity with the Chalk surrounding the river channel in the Wensum Valley (Moseley *et al.*, 1976).

Hiscock *et al.* (1996) described Norfolk's Chalk bedrock geology, reporting high spatial variation in transmissivity and storativity as a result of the distribution of overlying Pleistocene deposits. Fissuring is poorly developed in the confined areas of the Chalk beneath the till, with transmissivities of < 100 m²/day. In the valleys and areas of outcropping, fissuring is more widespread, resulting in transmissivities of up to 2000

m²/day. The mean storativity and transmissivity of the Wensum catchment Chalk is estimated as 0.064 ± 0.029 and 685 ± 260 m²/day, respectively (Toynton, 1979).

Nitrate in groundwater in the Wensum is typically slow to transfer through the catchment, with groundwater flow mainly restricted to fissuring within the Chalk. The undifferentiated till above the Chalk therefore represents a far more efficient pathway for the delivery of nitrate and is discussed further in Chapter 5.

2.4.6 Hydrochemistry of the Blackwater sub-catchment

The Chalk groundwater of the Wensum catchment is key in governing its hydrochemistry, producing Ca-HCO₃⁻ dominated waters of circum-neutral pH. Work by Edwards (1973) on major ion concentrations at the Wensum catchment outlet showed a wide range in nitrate concentrations (12 – 62 mg NO₃⁻ L⁻¹), which revealed a positive correlation with flow. Furthermore, Hiscock (1993) observed high spatial variability in Chalk groundwater nitrate concentrations, ranging from undetectable to 62 mg/L.

The high degree of spatial variability seen in riverine major ion concentrations (NO₃⁻, HCO₃⁻, Cl⁻, SO₄²⁻, Na⁺, K⁺, and Ca⁺) is representative of the wider ranges found in Norfolk's groundwater whereas values for riverine magnesium and silica can be below the lower limit of the range typically shown for chalk groundwater (Wexler, 2010). There are a number of influences identified which contribute to the high spatial variability in concentrations of the above ions found in the chalk groundwater, including the hydrologic characteristics of the overlying deposits and hydrogeological conditions (Hiscock, 1993). In terms of nitrate, river valley chalk groundwater has been shown to be high in nitrate as it is generally either exposed or is overlain by only a thin layer of permeable material, whereas in the interfluves (regions between valleys), the Chalk aquifer shows nitrate at levels below the limit of detection (Hiscock, 1993).

2.4.7 Topography and land use in the Blackwater sub-catchment

Situated at 30 – 50 m above sea level, the Blackwater sub-catchment is ideal for arable farming in terms of its topography as it slopes gently (typically not exceeding 0.5°). As a result, the majority of the land use in this area is intensive arable farming, ranging from 60% in the sandy loam soils in mini-catchment C, to 92% in mini-catchment A, where

the soil type is clay loam (see Figure 2.4). A seven-year crop rotation consisting of winter wheat, winter and spring barley, sugar beet, oilseed rape and spring beans is established within the western half of the Blackwater sub-catchment. The non-arable land use is comprised of improved grassland (12%), rough grassland (2%), mixed woodland (11%), freshwater (<1%) and rural settlements (1%).

2.4.8 Climate in East Anglia and the Wensum

The Blackwater sub-catchment is situated in East Anglia, one of the driest counties in the UK. An average of 601 mm rainfall per year fell between 1961 and 1990 with only 114 days per year during this period exceeding 1 mm (Met Office, 2009). October – December is the wettest period, though the summer months are typically associated with high rainfall. The Wensum catchment (1961 – 1990) show a 30-year average precipitation of 672 mm (Centre for Ecology and Hydrology, 2009), slightly higher than the mean for East Anglia. Yusoff *et al.* (2002) reported an average rate of groundwater recharge for East Anglia (as effective precipitation) of 140 mm per annum. The mean monthly temperatures in East Anglia range from a minimum of 0.6°C in January and February to a maximum of 21°C in July and August (Met office, 2009).

2.4.9 Selection of study fields

The selection criteria for the Dunkirk, Gatehouse and Swanhills fields within minicatchment A of the Blackwater subcatchment (Figure 2.8) was based on consideration of differences in soil type, tillage regime and fertiliser application history. Table 2.4 shows the soil particle size distribution in these fields from ground level to 90cm depth. Further discussed in Chapter 4, the overall soil clay content of the study fields increased from Dunkirk > Swanhills > Gatehouse, providing the opportunity to examine denitrification in soils where the clay content evolves along a gradient.

Tillage regime also varied between the study fields, again discussed in further detail in Chapter 4. The Dunkirk and Gatehouse fields were under a reduced tillage regime, whilst the Swanhills field was managed by the direct drill method. The influence of tillage regime is briefly introduced in Section 2.4.s and discussed in detail in Chapter 4. Selecting fields under different tillage regimes allowed for the comparison of the influence of management approach on soil denitrification.

The fertiliser application history and crop type grown in each of the three fields studied is discussed in Chapter 6. Overall, each field received a comparable amount of nitrogen fertiliser in the years preceding and during the study period. Therefore, given the differences in soil type and tillage regime, nitrogen fertiliser applications are not considered to be a variable when comparing the Dunkirk, Swanhills and Gatehouse fields in terms of soil denitrification rates. As such, these fields were selected as it also allowed for discussion of the influence of tillage regime on soil denitrification as demonstrated by soil leachate nitrate isotope values.

2.5 Summary

The aim of this chapter was to provide the necessary context for the data presented in Chapters 4, 5 and 6. Nitrate within the surface water – groundwater continuum originates in a range of sources, undergoes numerous transformations and is often mixed with a wide variety of other water sources. Combined, these processes act to influence the concentration and isotopic composition of the remaining nitrate. One important location within any catchment is the hyporheic zone (HZ), representing the surface water – groundwater interface. Within the HZ, conditions for denitrification are environmentally ideal, with abundant sources of nitrate, organic material and anoxic microsites. However, these conditions are heavily reliant on the hydrological connectivity of the surface water and groundwater within a given system.

The fundamentals of stable isotope theory were discussed, and the influence of different aspects of the nitrogen cycle on nitrate isotopic composition was discussed.

Denitrification enriches both the nitrogen and oxygen isotopes of nitrate whilst nitrification often results in a depletion of $^{15}\text{NNO}_3$. The merits of a dual isotope approach include the ability to separate sources of, or processes affecting nitrate, which have overlapping ^{15}N ranges.

Finally, a description of the study site was provided, discussing the socioeconomic and ecological significance of the Wensum catchment. The study site is underlain by a bedrock geology of Chalk and Wroxham Crag through which the groundwater supporting the majority of the hydrological regime. Given the geological setting, the local hydrology is dominated by Ca-HCO_3^- type water, with solute concentrations occupying a wide range, as governed by flow through the catchment. Land use in the Black water sub-catchment is dominated by intense arable farming, where a seven year crop rotation is

carried out within the Western half. The topography allows for such intense agriculture to be maintained, owing to its low elevation and flat relief. The soil type within the Blackwater ranges from sandy loam to clay loam, though there is high variation in soil physical characteristics, even within fields. Climate in the Blackwater is dry relative to much of the UK.

Chapter 3 Research methods

3.1 Experimental design

The study site is shown in Figure 3.1. There were five sampling sites located along a 1.6 km stream reach (between Site 1 and Site 5). At each sampling site, samples from a field drain, the stream and three piezometers, installed to 0.5, 1.0, and 1.5 m beneath the stream bed were collected. Site 5 shows six piezometers, though only three were sampled, the other three were from a previous project, not installed to the correct depths. The GPS coordinates and elevation for each of the 15 piezometers is shown in Table 3.1.

The field drains sampled at Sites 1 and 2 drain the ‘Dunkirk’ field, at Site 3 the ‘Swanhills’ field drain was sampled and at Site 4 the ‘Gatehouse Hyrne’, referred to herein as ‘Gatehouse’ field drain was sampled. At Site 5, a field drain connected to an adjacent unused field was sampled. In the following, the sites mentioned refer to those shown in Figure 3.1.

The aim of this study was to investigate denitrification in different locations within an agriculturally impacted catchment. To this end, sampling took place in two main areas: (1) field drains, representing the soil zone, discussed in Chapter 4, and (2) along the surface water – subsurface continuum, where stream water, benthic sediment pore water and shallow groundwater from the piezometers, representing the hyporheic zone, were sampled (Chapter 5). Samples were collected between 19/11/2015 and 20/01/2017, covering two winters.

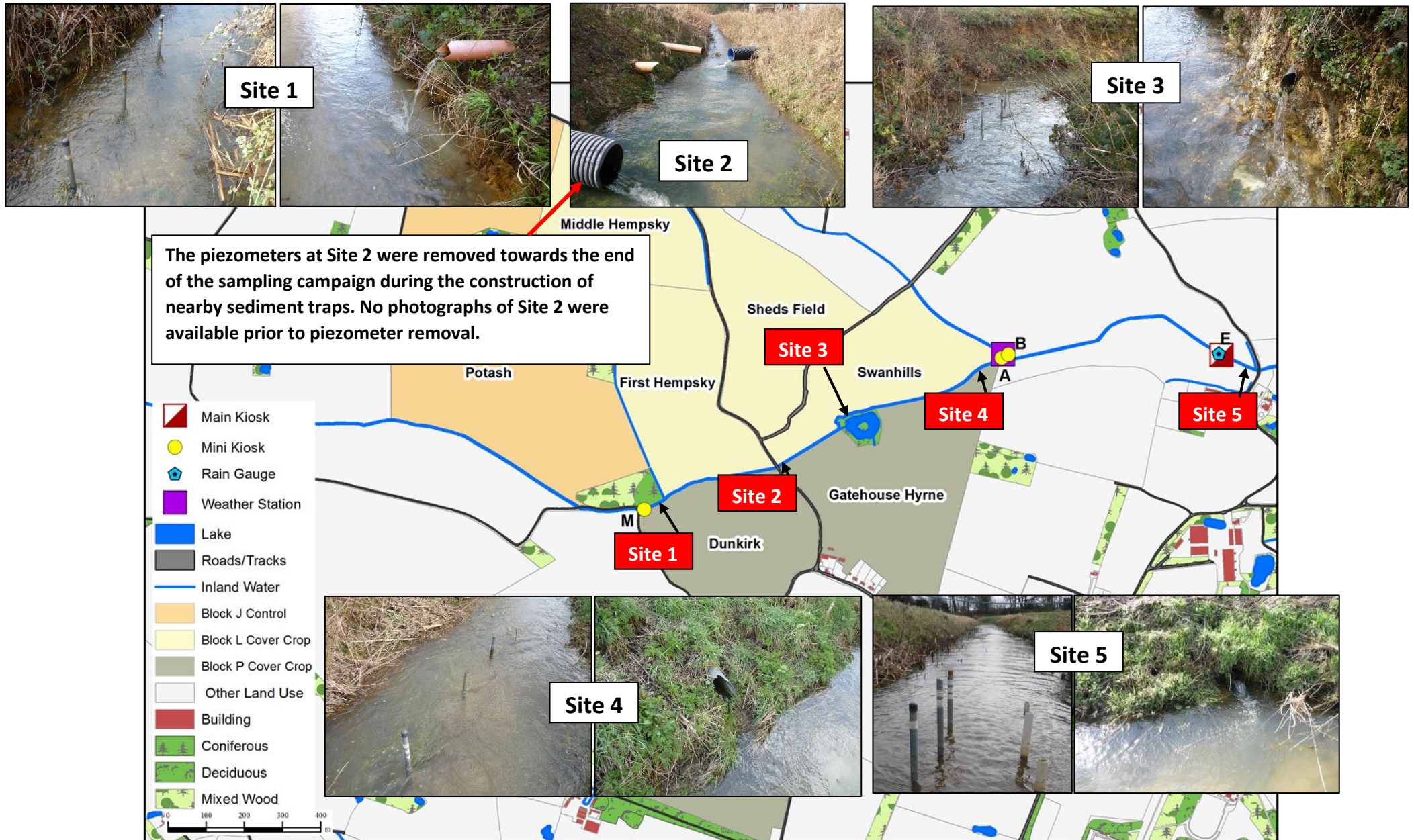


Figure 3.1 Images and locations of the five sites at which the piezometers were installed and sampled. Field drain and stream samples were also collected at each of the sampling sites

Table 3.1 GPS coordinates and elevation of the top of each piezometer above Ordinance Datum for each of the 15 piezometers installed and sampled during the project. There is ~1.6 km between the piezometers at Site 1 and at Site 5.

Piezometer	Easting	Northing	Elevation (m)
1(0.5)	610133.703	325287.915	38.67
1(1.0)	610134.396	325288.024	38.67
1(1.5)	610134.964	325288.092	38.72
2(0.5)	610473.261	325392.23	37.57
2(1.0)	610473.949	325392.421	37.58
2(1.5)	610474.387	325392.536	37.58
3(0.5)	610641.409	325527.267	36.78
3(1.0)	610641.884	325527.551	36.62
3(1.5)	610642.349	325528.117	36.56
4(0.5)	611090.236	325676.496	34.20
4(1.0)	611090.919	325676.628	34.09
4(1.5)	611091.601	325676.791	34.09
5(0.5)	611663.534	325684.25	32.66
5(1.0)	611663.265	325684.382	32.67
5(1.5)	611663.096	325684.541	32.61

3.2 Field sampling

3.2.1 Piezometer installation and sampling

Three drive-tip piezometers were installed in the stream bed at each of the five locations along the study reach, totalling 15 piezometers. Piezometers were constructed of galvanised steel, with a screened tip section containing a filter membrane (Marton Geotechnical Services LTD). At the sampling locations, piezometers were driven into the stream bed using a fence post driver so that the centre of the screened tip section reached 0.5, 1.0 or 1.5 m below the stream bed.

Before sampling, piezometer water column height was recorded using a well dipper. During sampling, the piezometers were first emptied using a hand siphon pump before being allowed to re-fill over a period of ~3 hours. Following recharge, piezometer water column heights were once again measured, and the data were used to calculate infiltration rates and estimate the hydraulic conductivity (described in Chapter 2) of the subsurface sediments at 0.5, 1.0 and 1.5 m below the stream bed. Water samples were collected using a bespoke bailer system, developed for the project. Figure 3.2 shows the process by which the bailer collected a sample from the piezometers, while Figure 3.3 shows a photograph of the bailer and tubing, tubing is 2 m in length. After a sample was withdrawn from the piezometer, it was transferred to a plastic syringe with one way stop cock valve at the open end. Transferring piezometer samples to syringes allowed for excess air to be pushed out of the syringe to minimise contact with the atmosphere.

Syringes were prepared by first being left in a Decon 90 bath overnight before rinsing 10 times with MilliQ water. They were then left overnight in a 10% HCl acid bath and rinsed again with MilliQ water. Finally, the syringes were oven dried for 24h at 60°C and stored in clean plastic bags until use. Syringes containing samples were stored in a cool bag containing ice packs until the end of the sampling run where field measurements were taken, and frozen until analysis.

Following the collection of all water samples, measurements of temperature, dissolved oxygen, pH and electrical conductivity were taken using a Hanna HI9025 pH meter, Hanna HI9146 dissolved oxygen meter and a Fisher Scientific Accumet AP75 electrical conductivity meter. An air thermometer was used to take temperature readings of the water samples.

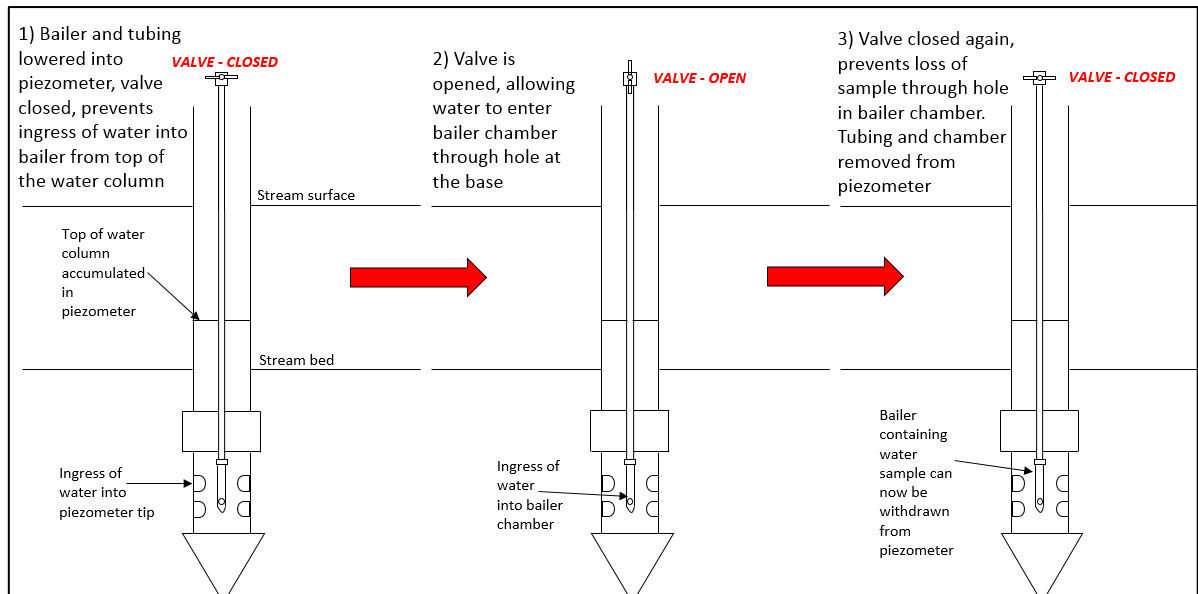


Figure 3.2 Schematic showing the process by which the bailer is used to collect a sample from a piezometer following purging and refilling of the piezometer



Figure 3.3 Bailer and tubing used to collect piezometer samples

3.2.3 Subsurface sediment sampling

Sediment samples were collected from 0.5 and 1.0 m beneath the stream bed, collection of sediment from 1.5 m below the stream bed was not possible within the limitations of the equipment. To collect a sediment sample from below the stream bed, a coffer dam constructed of a plastic ring was pushed into the stream sediment. The dam was then bailed out using plastic buckets until empty. When the sediment was exposed with minimal water inside the dam, an auger was used to core into the hyporheic zone sediments, markers at 0.5 and 1.0 m along the auger handle were used to allow for accurate depth of coring. Where the water was too deep for the coffer dam, two dams were stacked, attached by a ring of parafilm to ensure no water entered the dam through the join. Samples were stored in plastic bags with as much air removed as possible until physical measurements were carried out in the lab. Figures 3.4a-c show photographs of the sediment coring process.



Figure 3.4 Cofferdam installed next to piezometers prior to bailing



Figure 3.5 Cofferd dam empty following bailing, ready for augering



Figure 3.6 Dual height cover dam for use in deeper water

3.2.4 Stream and field drain sampling

In the field, 50ml centrifuge tubes were first flushed with sample (either field drain or stream) before being completely filled with water. Samples were stored in a cool bag containing ice packs until the end of the sampling run when field measurements were taken (Section 3.2.1). Following the field measurements, the samples were filtered using 0.2 μm syringe filters into clean centrifuge tubes and frozen until analysis. Centrifuge tubes were prepared in the same way as the syringes used for piezometer samples, described in Section 3.2.1.

3.2.5 Borehole sampling

Four boreholes were sampled a number of times during the sampling campaign, located at position 'A' in Figure 2.5. The boreholes were installed by the British Geological Survey to depths of 3.6, 12, 15.3 and 50 m, prior to the beginning of this project. The 50 m borehole was drilled into the Chalk, whilst the three shallower boreholes were drilled in order to monitor the overlying Quaternary deposits. Before sampling, three times the volume of the screened section of each borehole was pumped out. Table 3.2 shows the volume of water removed before sampling. Following purging, a bucket was flushed with sample before being filled and field measurements were taken (described in Section 3.2.1) before being filtered using 0.2 µm syringe filters into 50 ml centrifuge tubes, prepared as described in Section 3.2.4. Samples were frozen until analysis. The pump used for the borehole sampling was a Monsoon DTW 120ft submersible pump powered by a Low Flow Power Booster 3 controller from RS Hydro attached to two 12v batteries from Multicell Ltd. To measure pH, dissolved oxygen and electrical conductivity, probes were inserted into a bucket of water collected using the borehole pump, and gently moved around in the water until a stable reading could be taken. For all other samples, the probes were inserted directly into the syringe or centrifuge tube (depending on sample type) and a reading was taken once the probe had reached a stable value. After the field measurements were taken, the samples were filtered through 0.2µm syringe filters into clean syringes and frozen until analysis.

Table 3.2 Borehole diameter, length of screened section and volume of water removed prior to sampling calculated as $3(\pi \times r^2 \times h)$

Borehole	Diameter of screened section (m)	Length of screened section (m)	Volume of water removed (L)
1 (50 m)	0.074	25.0	323.0
2 (15.3 m)	0.05	3.0	18.0
3 (12 m)	0.05	7.0	41.0
4 (3.6 m)	0.05	2.6	15.0

3.2.6 Diffuse Equilibrium in Thin Films probe deployment and sample processing

Shallow sediment pore water profiles of nitrate, nitrite, chloride and sulphate were generated through the use of Diffuse Equilibrium in Thin Films (DET) probes. DET probes are constructed of a plastic frame housing a 1.2 mm layer of polyacrylamide gel. DET probe housings were marked at 2.5 cm intervals along the gel strip and inserted into the stream sediment. In total, five probes were installed at the most downstream sampling site along the study reach (Site 5). Probes were deployed on 17/02/2017 and retrieved on 20/02/2017. Upon retrieval of the probes, the gel strips were sliced with a clean plastic blade at the 2.5cm intervals marked on the probe housing. The gel slices were then transferred to pre-weighed 15 ml centrifuge tubes, prepared as described in Section 3.2.1, and stored on ice until returning to the lab. Once in the lab, the centrifuge tubes containing the gel slices were weighed, and 5 ml MilliQ water was added to each sample. The samples were then placed on ice on a shaker table for 24 h before removing the gel slices from the centrifuge tubes and filtering the eluent through a 0.2 μm syringe filter into clean centrifuge tubes. Samples were then frozen until analysis for anions and nitrate stable isotopic composition, described in Section 3.3.

Following eluent anion concentration (comprising nitrate, nitrite, chloride and sulphate) analysis using liquid chromatography, sediment pore water concentrations were calculated as follows:

1) Mass of solute in eluent (mg) = eluent concentration (mg L^{-1}) \times (volume of gel (L) + volume of eluent (L))

2) Concentration of solute in gel slice (mg L^{-1}) = Mass of solute in eluent (mg) / volume of gel slice (L)

3.2.7 Sediment particle size distribution

Sediment core particle size distribution was measured on a Malvern 2000 particle size analyser. 10 g of dried sample was placed in a Malvern 2000G sample bath and agitated for two minutes per sample. Samples were run in triplicate or until there was reasonable agreement between replicates.

3.3 Laboratory techniques

3.3.1 Major ions and dissolved organic carbon

Concentrations of nitrate, nitrite, chloride and sulphate in all samples were measured by liquid chromatography using a Dionex ICS 2000. Mixed standards were prepared, and contained $\text{K}_2\text{SO}_4^{2-}$, NaNO_2 , NaCl and NH_4Cl . Standards ranged from 0.5 – 7.5 mg L^{-1} . Each sample was diluted by a factor of 50 due to high Cl^- concentrations. Samples were run alongside blanks of deionised water (typically 8 – 10 in each run) and limits of detection were calculated as three times the standard deviation of solutes in the blanks. A single run of 20 blanks was also carried out in order to calculate limits of detection. A certified reference multi element anion standard (Sigma-Aldrich) was used to ensure accuracy of measurements.

Ammonium concentrations were measured in a number of samples by liquid chromatography using a Dionex ICS 5000. Calibration standards were produced containing NH_4Cl covering a range of 0.5 – 7.5 mg L^{-1} . Samples were diluted two times prior to analysis. Cations (Ca^{2+} , Mg^{2+} , Na^+ , K^+) were measured by Inductively Coupled Plasma Optical Emission Spectroscopy (ICP-OES) using a Varian Vista Pro axial ICP-OES. 900 μL of sample were acidified with 100 μL conc. HNO_3 prior to analysis. Standards of the measured cations were all created by dilution of single element stock (1000 mg kg^{-1}). Standard ranges were different for all cations, all starting at 0.5 mg L^{-1} with the highest concentration standards for calcium, potassium, magnesium and sodium of 20, 5, 5 and 15 mg L^{-1} , respectively Table 3.3 shows the limit of detection and precision of the Varian Vista Pro axial ICP-OES and Dionex ICS 2000 for each of the analytes measured.

Dissolved organic carbon (DOC) concentrations were measured by high temperature combustion using a Skalar FormacsHT TOC/TN analyser equipped with a LAS-160 sampler and nondispersive infrared (NDIR) detector. The method had been created to convert all organic carbon in a sample to CO_2 by addition of 3M HCl . Samples were then stirred and sparged to remove the CO_2 . The remaining organic carbon was then oxidised

at 850°C to CO₂ and measured by the NDIR detector. Calibration standards consisting of potassium hydrogen phalate (C₈H₅KO₄) were used encompassing the predicted range of DOC in the samples, and the concentrations were certified using NWCANBERRY-0 lake water certified reference material (CRM). Blanks consisting of ultrapure MilliQ water were run at the beginning and end of each analysis. Table 3.3 shows the precision and limit of detection for the Skalar FormacsHT TOC/TN.

Table 3.3 Precision and limit of detection (LOD) for each of the analytes measured in stream, field drain, piezometer and borehole samples.

Analyte	Precision	LOD (mg L ⁻¹)	Instrument
NO ₃ ⁻	+/- 0.12%	0.03	Dionex ICS 2000
NO ₂ ⁻	+/- 0.10%	0.001	Dionex ICS 2000
SO ₄ ²⁻	+/- 0.30%	0.6	Dionex ICS 2000
Cl ⁻	+/- 0.39%	0.3	Dionex ICS 2000
Ca ²⁺	+/- 0.5 mg L ⁻¹	0.36	Varian Vista Pro axial ICP - OES
K ⁺	+/- 0.08 mg L ⁻¹	0.06	Varian Vista Pro axial ICP - OES
Mg ²⁺	+/- 0.3 mg l ⁻¹	0.02	Varian Vista Pro axial ICP - OES
Na ⁺	+/- 1.53 mg L ⁻¹	0.07	Varian Vista Pro axial ICP - OES
NH ₄ ⁺	+/- 2.25%	0.16	Dionex ICS 5000
DOC	+/- 12%	1	Skalar FormacsHT TOC/TN analyser

Prior to particle size distribution, the sediment bulk density and porosity were calculated (described in Chapter 2).

Sediment core particle size distribution was measured on a Malvern 2000 particle size analyser. 10g of dried sample was placed in a Malvern 2000G sample bath and agitated for two minutes per sample. The particle size distribution was measured using Malvern

software. Samples were run in triplicate or until there was reasonable agreement between replicates.

3.3.4 Nitrate stable isotopes

3.3.4.1 Production of media and agar plates

The measurement of $\delta^{15}\text{N}_{\text{NO}_3^-}$ and $\delta^{18}\text{O}_{\text{NO}_3^-}$ values followed the well-established denitrifier method (Sigman *et al.*, 2001, Casciotti *et al.*, 2002). A brief summary of the methodology is presented in the following sections.

The media for growing bacteria cultures was produced using the following recipe to make 4 bottles (445 ml each):

- 1.8g KNO_3 , 0.45g $(\text{NH}_4)_2\text{SO}_4$, 11.7g K_2HPO_4 , 54g Tryptic Soy Broth added to 1800ml ring main water.
- Stir with magnetic stirrer for ~15 minutes.
- Transfer to 4 500ml media bottles (445 ml each).
- Autoclave bottles (50 min), leave to cool overnight.
- Crimp seal using autoclaved butyl septa and store in the dark.

Nitrate free media (NFM) was produced as follows:

- 0.5g $(\text{NH}_4)_2\text{SO}_4$, 13g K_2HPO_4 , 60g Tryptic Soy Broth added to 2000ml ring main water.
- Stir with magnetic stirrer for ~15 minutes.
- Pour into small bottles (80 ml each).
- Autoclave bottles and caps for 30 min, then replace caps.
- Store in a dark place.

Agar plates for growing bacterial cultures were produced as follows:

- 0.5g KNO_3 , 0.125g $(\text{NH}_4)_2\text{SO}_4$, 3.25g K_2HPO_4 , 15g Tryptic Soy Broth, 25g Tryptic Soy Agar added to 500ml ring main water.
- Stir with heated magnetic stirrer for ~15 minutes.
- Pour into bottles and autoclave for 30 minutes.

- Remove from autoclave when cooled to 54°C and replace lid.
- In a microbiology safety cabinet, pour agar into plates.
- Leave plates to dry over night with the lids on, once dry seal with parafilm.

3.3.4.2 Preparation of bacteria cultures

The bacterial species used for this study was *Pseudomonas chlororaphis* subsp. *Aureofaciens* (ATCC # 13985). This species is a facultative anaerobe which uses nitrate and nitrite as electron acceptors during anaerobic respiration under low oxygen conditions. This particular strain of bacteria lacks the nitrous oxide reductase activity. As a result, the typical denitrification sequence, terminating at the production of N₂ gas, is limited to the production of N₂O as shown in Equation 3.1



Initially, a small amount of freeze dried bacteria stock (ATCC# 13985) was suspended in a 15 ml centrifuge tube containing ~10ml of media (described in Section 3.3.4.1). The centrifuge tube was left on a shaker table inside an incubator set to 20°C overnight. The following morning, ~2ml of the contents of the centrifuge tube was injected through the septa of the media bottles described in Section 3.3.4.1. On a typical week, two media bottles would be inoculated. The inoculated media bottles were then returned to the shaker table inside the incubator for six to ten days. Following the incubation period, the bacteria were concentrated by centrifuging the incubated media and discarding the supernatant. The colonies were then transferred to bottles containing 80ml of nitrate free media (NFM) (described in Section 3.3.4.1) and resuspended. Antifoam was also added to the NFM to avoid excess bubbling when purging.

3.3.4.3 Preparation of sample vials

1 ml of the concentrated bacteria suspended in NFM was added to autoclaved, 20 ml glass vials. 5 ml of MilliQ water was also added and the vials were crimp sealed with autoclaved rubber stoppers. On a typical run, four blanks were included, one of which was comprised of 1 ml of bacterial culture and no MilliQ water. Venting needles were then pushed through the septa and the vials were inverted and placed on to needles set in a manifold connected to a helium canister. Vials were purged for 45 minutes to create anoxic conditions. Following purging, the vials were placed on a shaker table within an

incubator set to 20°C and left overnight. The vials were then purged again for 45 minutes to remove any residual oxygen before being injected with the samples. The volume of sample injected into the vials was calculated based on the concentration of nitrate measured using liquid chromatography. The volume of sample injected needed to contain 20 nM of nitrate. The majority of samples required injection volumes ranging between ~150 µL for stream and field drain samples, containing high concentrations of nitrate, to ~8 mL, for low nitrate piezometer samples. For all injections over 1 mL, a venting needle was used to avoid overpressuring the vials. If more than 10 ml of sample was required, it could not be analysed as the volume of the vial was too small. Once injected with sample, the vials were inverted and left overnight to allow for the conversion of nitrate to nitrous oxide. Samples were then lysed using 0.2 mL of 6 M hydrogen peroxide. Alongside the samples, standards were prepared using 50 uL of 400 µM NO₃⁻ concentration. Bacterial blanks were also prepared, where no nitrate was added.

The standards were international nitrate isotope calibration standards, containing accepted isotopic compositions within a range expected of the samples. Three international reference standards were used, with isotopic compositions reported in Bohlke *et al.* (2003), shown in Table 3.4. The nitrogen isotopic composition is reported in reference to air, whilst the oxygen isotopic composition is in reference to Vienna Standard Mean Ocean Water (V-SMOW). In addition to international standards, an in-house reference from UEA broad was used, with a known beam area, as well as 20 ppm N₂O reference gas.

Table 3.4 Isotopic composition of international nitrate standards, values reported in Bohlke et al (2003)

Isotopic composition of international nitrate standards	δ¹⁵N_{NO3} (‰)	δ¹⁸O_{NO3} (‰)
USGS 34 KNO ₃	-1.8	-27.9
USGS 35 NaNO ₃	2.7	57.5
IAEA N3 KNO ₃	4.7	25.6

3.3.4.4 Running samples on the GEO 2020 isotope ratio mass spectrometer

As discussed, the dissolved nitrate in the samples was converted to N₂O by the denitrifier method (Sigman *et al.*, 2001; Casciotti *et al.*, 2002). The isotopic signature of the produced N₂O was measured in relation to a laboratory cylinder N₂O reference gas, using a Europe Geo 20:20 continuous flow gas chromatograph isotope ratio mass spectrometer (GCIRMS). Prior to isotopic analysis, N₂O was extracted from sample vials and purified by purge and trap. This process is dependent on the different boiling and freezing points of N₂O, N₂, He, H₂O and CO₂. N₂O from each sample was purged for 500 seconds from the vial headspace using helium before being passed through a steel loop immersed in liquid nitrogen, then cryo-focussed in a second liquid nitrogen-immersed steel loop. The mixture of helium carrier gas and vial headspace was purified by first passing through a Nafion drier reverse-flow and magnesium perchlorate trap to remove any water. CO₂ was removed by a Carbosorb trap, and volatile organic compounds were removed using a Supelco F trap (Kaiser *et al.*, 2007). Following cryo-focussing, the N₂O was passed through a Varian Poraplot/Q pre-column in order to separate any remaining compounds present that could interfere with the signal. A short delay between CO₂ and N₂O peaks in the GC was achieved by passing the N₂O through an HP-PLOT/Q GC column, maintained at 30°C. A schematic for the path of N₂O through the system is shown in Figure 3.5. A typical run consisted of four bacterial blanks (three containing 1ml of culture and 5 ml of deionised water and one without deionised water), five sets of standards, each in double (i.e. an entire run would contain 10 each of USGS34, USGS35 and IAEA N3), one in house reference from UEA broad and 44 samples. At least four reference gas vials containing 20 ppm N₂O were also included in every run. The constraints of the Calisto software meant that a reference gas pulse as the reference for each sample was not possible. To circumvent this issue, sample vials purged with 20ppm N₂O (at a rate of 30 ml/min for 15 minutes) were used. As such, measured isotope ratios from the samples were converted to δ values, described in Chapter 2 where R_{standard} was the isotope ratio from the 20 ppm N₂O vial in the first position of every run. As a failsafe, every run began with four 20 ppm N₂O vials, where if the first 20 ppm N₂O vial measurement was anomalous, the next vial was used as a reference, and so on. Run times were around 14 – 17 hours, to ensure that the liquid nitrogen used in the trapping of sample N₂O did not run out overnight, a timed liquid nitrogen pump would fill the dewar at regular intervals.

N₂O with masses of 44, 45 and 46 were measured in the Geo 20:20. A heated filament within the mass spectrometer source produces electrons that bombard the N₂O molecules released from the sample, ionising the N₂O, forming N₂O⁺. The N₂O⁺ molecules are then accelerated along a flight tube passing through a magnetic section, where the enriched ions (i.e. those of the heaviest mass, containing ¹⁵N and ¹⁸O) move along a wider trajectory than those of a lighter mass. After separation, ions with different masses are collected in separate Faraday cups where their signal is amplified, and the ⁴⁵N₂O:⁴⁴N₂O and ⁴⁶N₂O:⁴⁴N₂O ratios are calculated within the Sercon Callisto software.

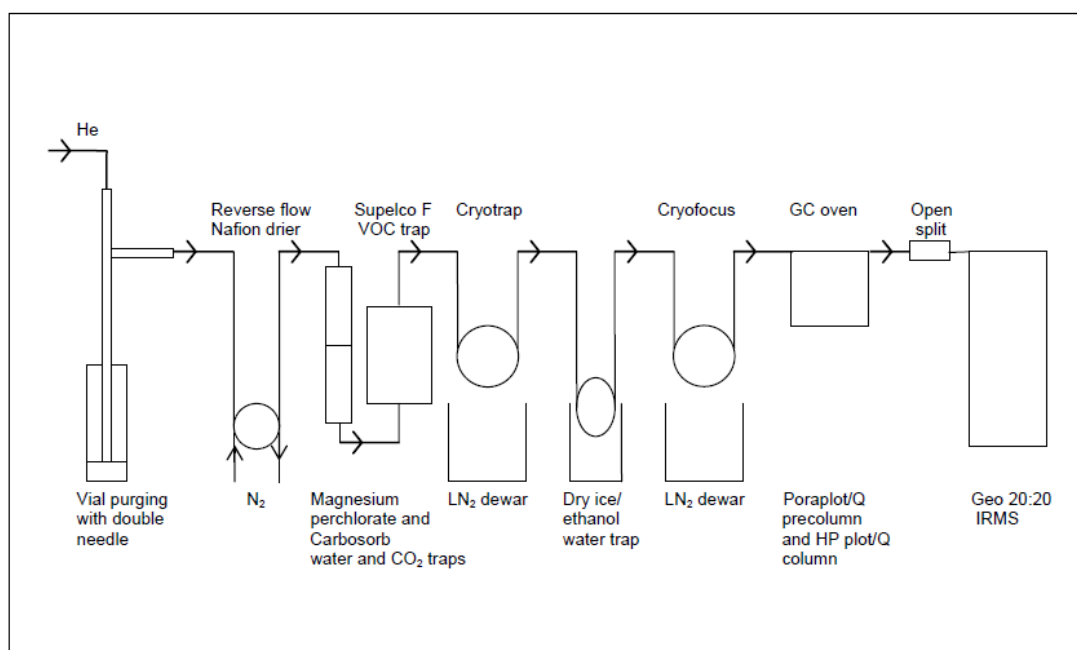


Figure 3.7 Schematic showing N₂O extraction and purification using the Geo 20:20. From Wexler (2010)

3.3.4.5 Data reduction

The data reduction procedure undertaken achieved a number of tasks: correction for introduction of nitrate from blanks, drift correction, ¹⁷O anomaly correction associated with the use of USGS 35, quantification of the amount of oxygen retained and the relative size of the bacterial blank and generation of calibration curves.

The first phase of the data reduction was to correct for any nitrate contribution from the blanks. This was achieved by subtracting the average $\delta^{15}\text{N}$ and $\delta^{18}\text{O}$ values measured in the first three blanks (containing 1 ml bacterial culture and 5 ml MQ water) from each of the samples and standards subsequently analysed.

Before each sample, a pulse of N₂O reference gas was injected into the Geo 20:20, comprised of 99.999% volume N₂O purity grade 5. This reference gas was used to correct measurements made of the N₂O from the samples for drift within the mass spectrometer. Isotope ratios of the reference gas and sample N₂O were converted to δ values, where $R_{standard}$ was the first N₂O reference gas pulse in the run (set to 0.0‰) and $R_{standard}$ was the subsequent reference gas pulses, allowing for δ values of the reference gas to be generated. Assuming that the sample vials were affected by the same drift as the reference gas, δ values associated with drift within the instrument were subtracted from the sample δ values, completing the first phase of data reduction. It should be noted that using the N₂O reference gas drift to determine the drift in the instrument throughout an analysis run assumes that there is no drift associated with the entire prep line (Figure 3.5). This is because the N₂O reference gas pulses were injected directly into the mass spectrometer to assess drift within the instrument. Therefore interferences throughout the prep line were not accounted for in the drift assessment. An improvement in this method would be to measure the drift in the standards that were analysed throughout each run as these were subject to the entire prep line. The existing data reduction method was set up to use the N₂O reference gas instead prior to the start of this research.

Following drift correction, the next stage of the data reduction was to correct for the ¹⁷O contribution to N₂O to account for the ¹⁷O contribution to standard USGS35. ¹⁴N¹⁴N¹⁷O has a mass of 45, and can hence introduce bias towards ¹⁵N, where an N₂O molecule can also be comprised of ¹⁵N¹⁴N¹⁶O. This was achieved using Equation 3.2 from McIlvin and Altabet (2005):

$$\delta^{15}\text{N}_{\text{N}_2\text{O}_{\text{sample}}} = \delta^{45}\text{N}_{\text{N}_2\text{O}_{\text{sample}}} [1 + {}^{17}\text{R}_{\text{std}}/(2^{15}\text{R}_{\text{std}})] - \delta^{17}\text{O}_{\text{NO}_3} [{}^{17}\text{R}_{\text{std}}/(2^{15}\text{R}_{\text{std}})]$$

Eq. 3.2

¹⁷R_{std} and ¹⁵R_{std} are the ¹⁷O:¹⁶O and ¹⁵N:¹⁴N ratios of the N₂O reference gas. $\delta^{17}\text{O}_{\text{NO}_3}$ is the ¹⁷O content of the sample or standard, including the contribution of ¹⁷O as an anomaly (referred to as $\Delta^{17}\text{O}$). Kaiser *et al.* (2007) measured the ¹⁷O anomaly of the USGS 35 international standard as $\Delta^{17}\text{O}$ 20.87 ‰. As such, the correction for the ¹⁷O anomaly of the USGS 35 international standard was achieved by Equation 3.3, completing the second phase of the data reduction:

$$(\delta^{18}\text{O}_{\text{N}_2\text{O}} \times 0.528) + 20.87 \quad \text{Equation. 3.3}$$

The third phase of the data reduction process was to examine amount of oxygen exchange between the water in which the bacteria were suspended, and the nitrate in the sample. Across 13 runs, the mean oxygen exchange calculated was $3.03 \pm 1.2\%$. The mean beam area of the blank was $0.81 \pm 0.35\%$ of that of the standards, below the accepted 5% reported by Sigman *et al.* (2001) and Casciotti *et al.* (2002).

Calibration curves were then generated from cross plots of mean corrected $\delta^{15}\text{N}$ and $\delta^{18}\text{O}$ values from N_2O produced by denitrification of the international standards relative to their accepted δ_{NO_3} values. The best fit equations from these plots were used to create the calibration curves against which the $\delta^{15}\text{O}_{\text{NO}_3}$ and $\delta^{18}\text{O}_{\text{NO}_3}$ values for the samples were calibrated, using Excel. The range of $\delta^{15}\text{N}_{\text{NO}_3}$ values covered by the international standards is narrow and did not cover entire isotopic range of nitrogen associated with agricultural sources (discussed in Chapter 2). Wexler (2010) carried out similar research using the same instrument (GEO 20:20) and international standards. To overcome this narrow range of $\delta^{15}\text{N}_{\text{NO}_3}$ values, Wexler (2010) also included a KNO_3 laboratory standard (SIL-TF), which had $\delta^{15}\text{N}$ and $\delta^{18}\text{O}$ values of $+13.3 \pm 0.1 \text{ ‰}$ and $+29.2 \pm 0.1 \text{ ‰}$, respectively. Wexler (2010) commented that because the $\delta^{15}\text{N}$ and $\delta^{18}\text{O}$ values of SIL-TF had not been verified independently, they could not be used with the same confidence as the international standards (USGS 34, USGS 35 and IAEA N3). After the analysis was completed, Wexler (2010) calculated a second set of calibration curves including SIL-TF in order to validate the use of the international standards for use in measurement of samples with an extended range of $\delta^{15}\text{N}_{\text{NO}_3}$. Since the use of the international standards had previously been verified by Wexler (2010), this was not repeated in the presented research. Figures 3.6 and 3.7 show a typical calibration curve and associated equation used in each run.

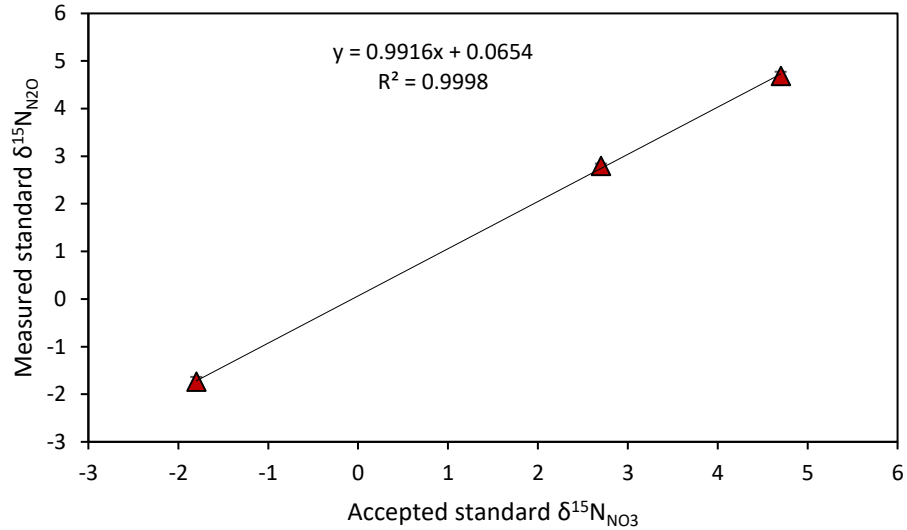


Figure 3.8 Example of calibration curve for $\delta^{18}\text{O}_{\text{N}_2\text{O}}$ (relative to reference gas) against the accepted $\delta^{18}\text{O}_{\text{NO}_3}$ values of the international standards (USGS 34, USGS 35 and IAIA – N3) from one analysis run, where 10 of each standard was analysed. Error bars show \pm standard deviation around the mean

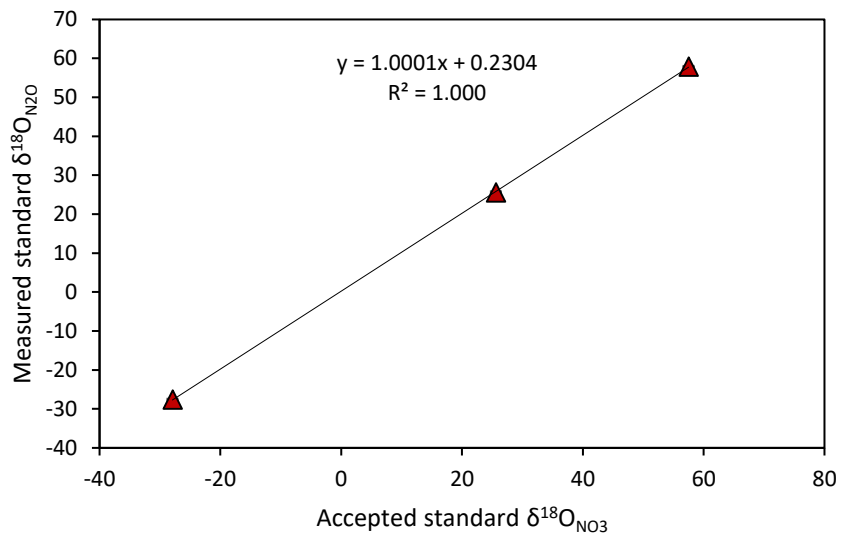


Figure 3.9 Example of calibration curve for $\delta^{15}\text{N}_{\text{N}_2\text{O}}$ (relative to reference gas) against the accepted $\delta^{15}\text{N}_{\text{NO}_3}$ values of the international standards (USGS 34, USGS 35 and IAIA – N3) from one analysis run, where 10 of each standard was analysed. Error bars show \pm standard deviation around the mean

As a quality control check, an in-house reference (IHR) sample collected from the River Yare at UEA campus was also included in each run. The reference was unverified, however had previously been analysed using the Geo 20:20 several hundred times. Therefore if the measured $\delta^{15}\text{N}$ and $\delta^{18}\text{O}$ values of the IHR fell within the range (mean \pm 1 standard deviation), it was deemed that the instrument was working correctly and that there was no interference aside from the factors mentioned in the above paragraphs.

3.3.4.6 Precision

The overall uncertainty in the $\delta^{15}\text{N}_{\text{NO}_3}$ and $\delta^{18}\text{O}_{\text{NO}_3}$ values for the samples collected was calculated as 1 standard deviation around the mean of the standards. The average within-run standard deviation was ± 0.13 and ± 0.27 ‰ for $\delta^{15}\text{N}_{\text{NO}_3}$ and $\delta^{18}\text{O}_{\text{NO}_3}$, respectively. This within-run standard deviation represents the uncertainty for all $\delta^{15}\text{N}_{\text{NO}_3}$ and $\delta^{18}\text{O}_{\text{NO}_3}$ values reported throughout this thesis.

3.3.5 Water isotope analysis

The water isotopic composition ($\delta^{18}\text{O}_{\text{H}_2\text{O}}$ and $\delta^2\text{H}_{\text{H}_2\text{O}}$ values) was measured for the majority of the samples collected. Sub-samples were transferred to 1ml vials that had been rinsed thoroughly and oven dried at 60°C overnight or until completely dry. Batches of samples were run in rotation using a Picarro V1102 – *i* liquid water isotope analyser. Samples were analysed six times, with the final three replicates used to calculate the average $\delta^{18}\text{O}_{\text{H}_2\text{O}}$ and $\delta^2\text{H}_{\text{H}_2\text{O}}$ values. This was to overcome memory effects within the instrument (where water remaining in the instrument from the previous sample could affect the measurement of the next sample). The amount of sample injected with each replicate was 2.6 μL . International standards were used to calibrate the sample δ values, consisting of USGS 64444 ($\delta^{18}\text{O}$ -51.14 ‰, $\delta^2\text{H}$ -399.1 ‰) and USGS 67400 ($\delta^{18}\text{O}$ -1.97 ‰, $\delta^2\text{H}$ +1.2 ‰). The international standards used were secondary standards, relative to V-SMOW for USGS 67400 and Standard Light Antarctic Precipitation (SLAP) for USGS 64444. In addition to the international standards, Norwich tap water was also analysed ($\delta^{18}\text{O}$ -7.2 ‰, $\delta^2\text{H}$ -47.0 ‰) in order to validate the calibration. Standards were analysed ten times each to overcome the memory effects associated with the instrument. Because the range in δ values for the standards was large, the standards were run more times than the samples. The precision of the water isotope analysis was for ± 0.25 ‰

$\delta^{18}\text{O}_{\text{H}_2\text{O}}$ and $\pm 2\text{‰}$ for $\delta^2\text{H}_{\text{H}_2\text{O}}$ values, all plots showing water isotope data are subject to this level of uncertainty.

3.4 Statistical analysis

Statistical analysis was carried out using the statistical package SPSS (v. 20, IBM). The way in which the data presented in Chapters 4 and 5 are separated (i.e. by spring/summer and autumn/winter, or by sampling site) meant that low population groups of data were often compared. The majority of statistical comparisons were between median values, given the often large range in the data (Chapters 4 and 5). As such, Mann-Witney U tests were used to determine significance between two sets of data (defined as $P < 0.05$).

Where mean values were compared, Independent samples t-tests were used. Because the populations of data sets were often low, comparing means using t-tests became difficult when data sets were not normally distributed (given the low number of data points), which was common even when converting to \log_{10} values. Normality was assessed using a Shapiro-Wilks test where $P > 0.05$ indicated a normally distributed data population and $P < 0.05$ was not normally distributed. Additionally, kurtosis and skewedness z scores were calculated by dividing the kurtosis and skewedness values by the standard deviation of each dataset. Those datasets that had kurtosis and skewedness z scores outside of the range of -1.96 to +1.96, and also had P values for the Shapiro-Wilk's test of < 0.05 were deemed non-normally distributed. Where data were not normally distributed, the values were first converted to \log_{10} values, if this did not change the distribution, Mann-Witney U tests were used.

Chapter 4 Soil zone denitrification: evidence from field drain hydrochemical and isotope data

4.1 Introduction

In this chapter, evidence for microbially-mediated denitrification is presented through nitrate stable isotope data from field drain samples. Supporting data, covering major ion concentrations and soil physical characteristics are also presented in order to place these stable isotope data in the wider context of field-scale nitrogen cycling. The field drains here are treated as an analogue for soil processes in terms of transformations and attenuation of nitrogen in the soil profile.

Denitrification in agricultural soils is a key consideration in crop production. As nitrogen is a major component in crop production, denitrification represents an important loss process from many agricultural systems (Tiedje, 1988). Furthermore, applications of ammonium nitrate fertilisers have been shown to increase production of nitrous oxide in the soil zone (N_2O , is a bi-product of denitrification and a well-documented potent greenhouse gas) (Clayton *et al.*, 1997).

Owing to its highly reactive nature, nitrogen cycling in soils is a profoundly complex process with many contributing factors, both direct and indirect in nature. Nitrate in agricultural soils is elevated through applications of ammonium nitrate fertilisers. Rates of soil nitrate production (and as a result, N_2 , N_2O and NO through subsequent denitrification) from fertiliser-derived ammonium and subsequent removal of nitrate by denitrification are influenced by the availability of an electron donor and acceptor (carbon and nitrate respectively), because denitrification is an anaerobic process, oxygen availability is the most important component (Hofstra and Bouwman, 2005). These factors are intrinsically linked to climate and management practices which in turn govern soil conditions (Tiedje, 1988).

Soil pH has been shown to affect rates of denitrification, with more acidic conditions typically inhibiting denitrification, while as with many biological processes, an optimum temperature range also exists (Simek *et al.*, 2000). For denitrification to progress, nitrate must first be present, either through production by nitrification or applied as ammonium

nitrate fertiliser (which is nitrified in the soil), manure or atmospheric deposition. Rates of nitrification are linked to the availability of ammonium, which is itself affected by the cation exchange capacity of soils, hence soil type is also an important factor in regulating rates of denitrification (Hofstra and Bouwman, 2005).

Due to the influencing factors discussed above, rates of denitrification can be highly variable and are often dynamic in time and space. This gives rise to the presence of 'hot spots' and 'hot moments', where spatial heterogeneity of soil physico-chemical characteristics and seasonal variations in climate and agricultural management (e.g. fertiliser application rate, method and timing, and applications of animal manure) drive denitrification in dynamic and discreet ways (McCclain *et al.*, 2003).

Additionally, crop types can affect denitrification in that different species take up nitrogen from the soil in different amounts with different timings, and the amount of nitrogen input from crop residues is variable with crop type (Hofstra and Bouwman, 2005). Certain crops such as legumes and clover are also capable of fixing nitrogen in the soil, increasing the pool of reactive nitrogen for cycling.

Baggs *et al.* (2008) gave an overview of the use of stable isotopes in N₂O source partitioning in soils, highlighting the key roles isotope measurements play in elucidating the processes through which N₂O is produced. While this thesis mainly addresses the process of denitrification based on a discrepancy in the nitrogen budget at the study site, Baggs *et al.* (2008) explain that to gain a full understanding the N₂O budget of a system and hence develop appropriate management strategies, all components of the nitrogen cycle must be examined and that stable isotopes are a valuable resource to achieve this. In this study, the dual stable isotopes of nitrate (¹⁵N and ¹⁸O), as measured from water samples through the denitrifier method (Sigman *et al.*, 2001; Casciotti *et al.*, 2002). These data collected from field drain water are used to identify the occurrence of microbially-mediated denitrification in the soil zone.

Snider *et al.* (2017) used $\delta^{15}\text{N}_{\text{NO}_3}$ measurements of nitrous oxide from soil cores to determine the processes driving rapid transformations of nitrogen immediately following liquid manure applications. The results showed high rates of coupled nitrification-denitrification (that is, denitrification of nitrate produced through nitrification) based on N₂O emissions and isotopic analyses. Previous incubation experiments carried out on the same soils (Snider *et al.*, 2015) showed flux-weighted $\delta^{18}\text{O}_{\text{N}_2\text{O}}$ values to be lower than

expected as a result of denitrification, such that they overlapped with the range typically associated with nitrification. Snider *et al.* (2015) attributed this to oxygen exchange with the soil water during the process of denitrification (where an oxygen atom from a water molecule is exchanged for one derived from air, thus altering the isotopic composition of the N₂O produced from denitrification), and warn that ¹⁸O must be treated with caution when identifying nitrogen transformation processes. One of the strongest features of adopting a dual stable isotope approach is that this potential uncertainty associated with δ¹⁸O_{NO₃} values can be overcome by combining these data with δ¹⁵N_{NO₃} data (and nitrate concentration measurements). The results of such an approach are presented and discussed in the following sections.

4.2 Results

A map of the sampling sites within the study catchment was shown in Chapter 3.

Throughout this chapter there are numerous references to the individual sampling sites, therefore for convenience they are repeated again in Figure 4.1.



Figure 4.1 Locations of the sampling sites at which piezometer, stream and field drain water samples were collected. At each site, three piezometers were installed in the stream bed with the screened section at 0.5m, 1.0, and 1.5m beneath the stream bed. Sites 1 and 2 are the ‘Dunkirk’ field drains, Site 3 is the ‘Swanhills’ field drain and Site 4 is the ‘Gatehouse Hyrne’ field drain. Site 5 is a field drain from an unused field where data on previous cropping were not available.

4.2.1 Results of field measurements and overview of hydrochemical data

Temperature, dissolved oxygen (DO), pH and electrical conductivity (EC) measurements are presented in Tables 4.1 and 4.2. Spring/summer and autumn/winter samples have been combined as individual seasons contain too few samples for statistical analysis but some preservation of temporal variation is necessary for the consideration of seasonal cycles. Drain DO concentrations were similar to those measured in the stream samples (presented in Chapter 5) and so can be considered saturated in terms of DO.

Hydrochemical data comprising major ions were collected for each sample. Unfortunately, sample volumes and resources prevented direct measurement of bicarbonate and so concentrations have been calculated through ion balance using the hydrochemical modelling software PHREEQC (ver. 2.0). Hydrochemical data are presented in Tables 4.3 and 4.4 showing spring/summer and autumn/winter measurements, respectively. Atmospheric deposition of major ions for which data were available are presented in Table 4.5.

At all sites in both the spring/summer and autumn/winter samples, DO far exceeded that considered to be the threshold for the onset of anaerobic denitrification (0.5 mg L^{-1} , Zumft, 1997). Averages of 5.65 and 6.02 mg L^{-1} were measured across all sites in the spring/summer and autumn/winter samples respectively, suggesting the presence of discrete anoxic microsites within the soil zone. All samples were circum-neutral in terms of pH, with the exception of Site 4 in the autumn/winter samples which were more acidic than the other sites with an average pH of 6.66.

Table 4.1 . Field measurements of field drain samples collected between March-August 2016

Temperature (°C)				Dissolved oxygen (mg L ⁻¹)			pH			Electrical conductivity (µS cm ⁻¹)		
Site	Range	Mean	<i>n</i>	Range	Mean	<i>n</i>	Range	Mean	<i>n</i>	Range	Mean	<i>n</i>
1	6.0-15.0	11.7	3	6.16-6.27	6.12	2	7.43-7.57	7.52	3	494-775	682	4
2	6.5-16.0	12.5	5	5.38-5.46	5.41	3	7.00-7.81	7.39	4	564-807	723	6
3	7.0-16.0	12.3	5	5.20-7.56	6.35	3	6.75-7.53	7.18	4	557-922	816	5
4	6.5-16.0	12.9	5	4.09-4.97	4.41	3	6.83-7.66	7.21	4	550-764	668	6
5	6.4-16.0	11.6	5	5.34-6.47	5.97	3	7.34-8.03	7.77	4	382-770	646	5

Table 4.2 Field measurements of field drain samples collected between September-February 2016/17

Temperature (°C)				Dissolved oxygen (mg L ⁻¹)			pH			Electrical conductivity (µS cm ⁻¹)		
Site	Range	Mean	<i>n</i>	Range	Mean	<i>n</i>	Range	Mean	<i>n</i>	Range	Mean	<i>n</i>
1	5.0-10.0	7.7	6	5.45-7.95	6.17	6	6.86-8.40	7.47	7	438-667	519	9
2	5.0-16.0	8.9	6	5.32-6.73	5.82	7	7.11-7.70	7.41	7	458-772	568	9
3	6.0-10.5	8.1	7	5.18-7.77	6.32	8	6.51-8.05	7.27	9	416-800	569	11
4	6.0-15.5	10.1	4	5.00-5.56	5.35	4	6.39-6.94	6.66	4	423-716	532	7

Table 4.3 Major ion concentrations (mg L-1) in field drain samples collected between March-August 2016

Site	NO ₃ ⁻		Cl ⁻		SO ₄ ²⁻		HCO ₃ ⁻		Ca ²⁺		Mg ²⁺		K ⁺		Na ⁺	
	Range	Median	Range	Median	Range	median	Range	Median	Range	Median	Range	Median	Range	Median	Range	Median
1	7.79- 22.67	16.86 <i>n</i> = 4	29.66- 42.21	39.27 <i>n</i> = 4	29.43- 57.06	41.68 <i>n</i> = 4	191.67- 342.48	325.5 <i>n</i> = 4	75.80- 155.11	136.08 <i>n</i> = 4	3.06- 4.49	3.78 <i>n</i> = 4	0.62- 5.86	1.41 <i>n</i> = 4	12.15- 15.51	14.65 <i>n</i> = 4
2	4.00- 25.64	13.74 <i>n</i> = 6	32.06- 45.46	38.56 <i>n</i> = 6	9.26- 34.63	29.99 <i>n</i> = 6	214.17- 417.95	384.7 <i>n</i> = 6	40.88- 153.87	135.09 <i>n</i> = 6	3.16- 4.86	3.72 <i>n</i> = 6	0.54- 45.75	0.66 <i>n</i> = 6	16.18- 43.22	16.45 <i>n</i> = 6
3	36.25- 44.29	41.29 <i>n</i> = 6	51.28- 72.93	65.06 <i>n</i> = 6	46.17- 60.05	52.55 <i>n</i> = 6	125.71- 518.34	345.8 <i>n</i> = 6	77.43- 162.40	158.47 <i>n</i> = 6	4.19- 4.48	4.35 <i>n</i> = 6	1.34- 9.31	4.60 <i>n</i> = 6	18.09- 23.56	18.60 <i>n</i> = 6
4	27.86- 66.53	51.67 <i>n</i> = 6	40.38- 72.62	49.71 <i>n</i> = 6	26.34- 30.45	27.96 <i>n</i> = 6	143.66- 300.41	293.9 <i>n</i> = 6	78.28- 133.40	116.76 <i>n</i> = 6	3.12- 5.21	4.11 <i>n</i> = 6	0.88- 11.78	3.82 <i>n</i> = 6	11.63- 18.87	16.68 <i>n</i> = 6
5	15.50- 31.84	23.32 <i>n</i> = 4	28.54- 34.14	36.73 <i>n</i> = 6	22.64- 31.45	27.48 <i>n</i> = 6	117.43- 395.80	350.7 <i>n</i> = 6	50.53- 141.42	127.69 <i>n</i> = 6	3.85- 5.12	4.59 <i>n</i> = 6	5.27- 9.39	6.75 <i>n</i> = 6	12.87- 15.01	14.77 <i>n</i> = 6

Table 4.4 Major ion concentrations (mg L⁻¹) in field drain samples collected between November 2015 – February 2016 / September 2016 – January 2017

	NO₃⁻		Cl⁻		SO₄²⁻		HCO₃⁻		Ca²⁺		Mg²⁺		K⁺		Na⁺	
Site	Range	Median	Range	Median	Range	Median	Range	Median	Range	Median	Range	Median	Range	Median	Range	Median
1	3.93- 39.32	14.07 <i>n</i> = 10	26.94- 69.05	43.16 <i>n</i> = 10	5.61- 43.10	30.58 <i>n</i> = 10	111.65- 233.03	159.7 <i>n</i> = 10	65.01- 135.46	78.44 <i>n</i> = 10	1.09- 6.25	3.64 <i>n</i> = 10	0.39- 13.51	5.09 <i>n</i> = 10	8.79- 17.15	15.56 <i>n</i> = 10
2	8.91- 34.12	25.64 <i>n</i> = 9	29.19- 80.61	45.36 <i>n</i> = 9	21.15- 33.70	27.48 <i>n</i> = 9	107.31- 413.44	191.1 <i>n</i> = 9	66.92- 148.56	85.83 <i>n</i> = 9	0.97- 4.66	3.19 <i>n</i> = 9	0.30- 30.19	9.78 <i>n</i> = 9	7.36- 24.39	14.80 <i>n</i> = 9
3	0.73- 44.29	34.92 <i>n</i> = 11	1.12- 89.21	48.58 <i>n</i> = 11	0.96- 57.59	40.88 <i>n</i> = 11	97.63- 555.49	144.6 <i>n</i> = 11	64.76- 159.63	77.90 <i>n</i> = 11	2.22- 4.89	4.07 <i>n</i> = 11	0.65- 56.30	3.28 <i>n</i> = 11	9.88- 20.36	17.40 <i>n</i> = 11
4	30.21- 69.05	60.86 <i>n</i> = 6	31.79- 89.21	34.99 <i>n</i> = 6	20.16- 26.70	23.56 <i>n</i> = 6	105.23- 298.30	118.1 <i>n</i> = 6	62.80- 123.46	82.42 <i>n</i> = 6	1.22- 12.21	3.15 <i>n</i> = 6	0.18- 7.78	3.91 <i>n</i> = 6	7.17- 37.19	11.18 <i>n</i> = 6
5	2.81- 39.34	22.80 <i>n</i> = 6	28.42- 53.97	39.74 <i>n</i> = 6	15.97- 33.15	29.70 <i>n</i> = 6	109.06- 367.84	187.9 <i>n</i> = 6	58.13- 134.26	69.77 <i>n</i> = 6	1.27- 5.09	3.26 <i>n</i> = 6	0.52- 16.92	10.60 <i>n</i> = 6	5.44- 16.74	12.34 <i>n</i> = 6

Table 4.5 Atmospheric deposition of major ion molecules (kg) across the three study fields Dunkirk, Swanhills and Gatehouse calculated based on data sourced from CEH (2008) between 19/11/2015 and 20/01/2017. Mass of solutes is calculated from annual precipitation-weighted concentrations between 1986 and 2007.

Field	NO ₃ ⁻	NH ₄ ⁺	Cl ⁻	SO ₄ ²⁻	Ca ²⁺	Mg ²⁺	Na ⁺
Dunkirk	269 ± 38	135 ± 28	252 ± 54	306 ± 96	58 ± 16	20 ± 5	140 ± 28
Swanhills	231 ± 32	116 ± 24	216 ± 47	262 ± 82	49 ± 14	17 ± 4	120 ± 24
Gatehouse	391 ± 55	196 ± 41	366 ± 79	445 ± 140	84 ± 23	29 ± 7	204 ± 41

4.2.2 Nitrate

Nitrate concentrations varied across all sites (Figure 4.2). Across all sites the mean range of concentrations was large in the spring/summer samples (21.59 mg L⁻¹) with the largest range observed at Site 4 (38.67 mg L⁻¹). During the autumn/winter period, the range was larger still across all sites (mean 35.91 mg L⁻¹) with the largest range observed at Site 3. The wide range of nitrate concentrations reflects the high mobility of nitrate within a system, and the variable conditions throughout the sampling period. Comparisons of temporal variation within sites (for example, mean nitrate concentration during the spring/summer period versus that in the autumn/winter at Site 1) are also shown in Figure 4.3. There was no significant difference between the mean spring/summer and autumn/winter nitrate concentrations at any site ($P > 0.05$).

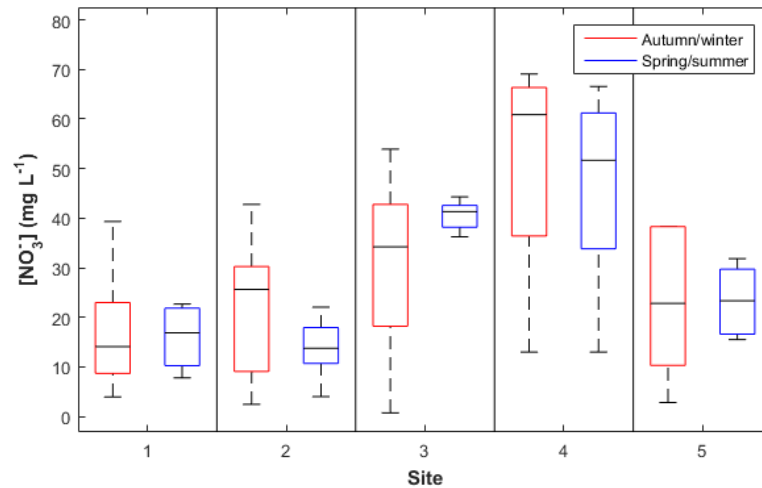


Figure 4.2 Box and whisker diagram showing intra-site comparison of median nitrate concentrations between spring/summer and autumn/winter. The range of concentrations is shown by the whiskers and the boxes illustrate the interquartile range of nitrate concentrations.

Despite being combined, the spring/summer and autumn/winter sample sets still comprised relatively few samples, though enough to carry out simple statistical analyses. Given the low number of samples however, a single sample can generate proportionally high variation within the dataset, for example at Site 5 in the autumn/winter samples collected on 26/11/2015, where the lowest nitrate concentration measured was 2.81 mg L⁻¹ while the median average was 22.80 mg L⁻¹ in a dataset of just 4 samples. The same applies to many of the other major ions measured and where appropriate, individual samples will be discussed.

4.2.3 Chloride

The spatial distribution of chloride in the spring/summer and autumn/winter samples is shown in Figure 4.3. The variance between sites during the autumn/winter sampling period was lower than that during the spring/summer. There was no significant difference between any sites during the autumn/winter period ($P > 0.05$ in all cases). Despite very similar median chloride concentrations across sites ($39.97 - 48.31 \text{ mg L}^{-1}$), the autumn/winter samples had much higher variability within sites with a mean average range of 52.92 mg L^{-1} as opposed to 17.62 mg L^{-1} in the spring/summer samples.

This is due to consistently higher maximum values and in part down to one very low value measured at Site 3, collected on 03/11/2016 (1.12 mg L^{-1}). Although the variability was relatively much higher in the autumn/winter samples with respect to the spring/summer samples, chloride concentrations showed no statistically significant difference between seasons at any site ($P > 0.05$) between seasons.

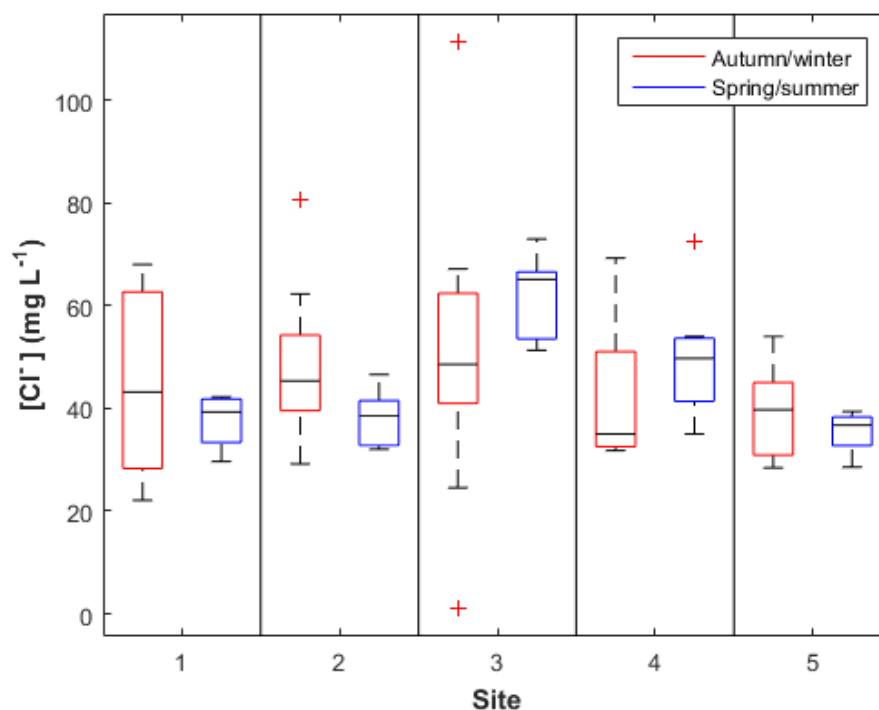


Figure 4.3 Box and whisker diagram showing intra-site comparison of median chloride concentrations between spring/summer and autumn/winter. The range of concentrations is shown by the whiskers and the boxes illustrate the interquartile range of chloride concentrations. Red crosses represent outliers in the data set.

4.2.4 Sulphate

Median field drain sulphate concentrations in the spring/summer and autumn/winter samples are shown in Figure 4.4. The mean range between sites was higher in the autumn/winter samples than in the spring/summer samples (26.41 and 15.49 mg L⁻¹ respectively). One sample collected on 03/11/2016 at Site 3 in the autumn/winter samples contributes significantly to this variation (0.96 mg L⁻¹). Another relatively (to the majority of the samples) low concentration (9.92 mg L⁻¹) sample was collected at the same site on 19/11/2015. There were statistically significant seasonal differences in sulphate concentrations observed at Sites 1, 3 and 4.

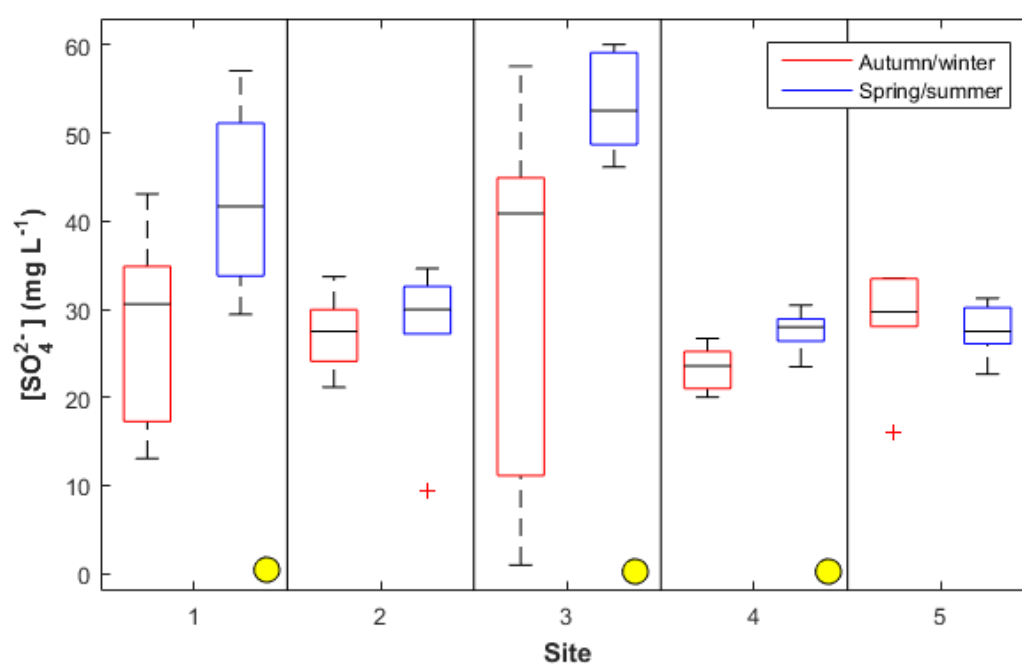


Figure 4.4 Box and whisker diagram showing intra-site comparison of median sulphate concentrations between spring/summer and autumn/winter. The range of concentrations is shown by the whiskers and the boxes illustrate the interquartile range of sulphate concentrations. Red crosses represent outliers in the data set. Yellow circles show significantly different median concentrations following a Mann-Whitney U test ($P < 0.05$)

4.2.5 Bicarbonate

Median spring/summer and autumn/winter bicarbonate concentrations at all sites are shown in Figure 4.5. The spring/summer samples contained consistently less bicarbonate than the autumn/winter samples, though this difference was only significant at Sites 1 and 2 ($P < 0.05$). Within-site variation was higher in the spring/summer than in the autumn/winter samples, with mean ranges across all sites of 300 and 229 mg L^{-1} , respectively. As mentioned previously, bicarbonate concentrations have been calculated based on ionic charge balance due to lack of sample volume for direct measurement. As such, the variations in bicarbonate concentration for each sample are intrinsically linked to variations in concentrations of all other major ions. Whilst care was taken to process and analyse samples to the highest possible standard, interpretations of bicarbonate data should take this into account.

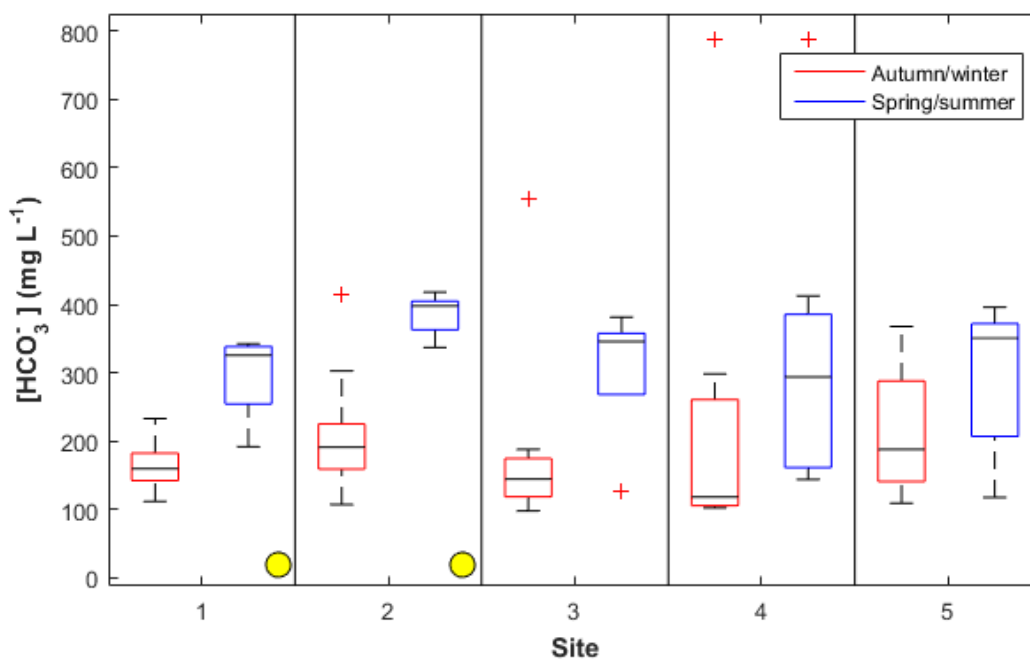


Figure 4.5 Box and whisker diagram showing intra-site comparison of median bicarbonate concentrations between spring/summer and autumn/winter. The range of concentrations is shown by the whiskers and the boxes illustrate the interquartile range of bicarbonate concentrations. Red crosses represent outliers in the data set. Yellow circles show significantly different median concentrations following a Mann-Whitney U test ($P < 0.05$)

4.2.6 Calcium

Median spring/summer and autumn/winter field drain calcium concentrations across all sites are shown in Figure 4.6. The mean range in calcium concentrations across all sites was similar in the spring/summer and autumn/winter samples (105.24 and 102.93 mg Ca²⁺ L⁻¹ respectively). Moreover, spring/summer calcium concentrations were consistently higher than in samples collected in the autumn/winter period across all sites, though this was not statistically significant at any site (P>0.05)

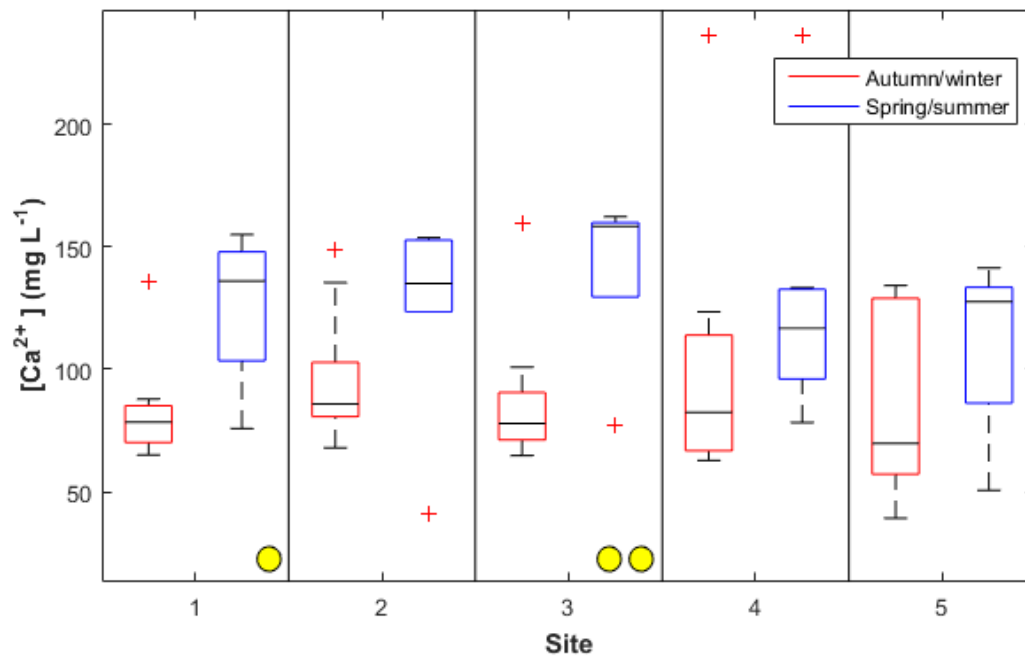


Figure 4.6 . Box and whisker diagram showing intra-site comparison of median calcium concentrations between spring/summer and autumn/winter. The range of concentrations is shown by the whiskers and the boxes illustrate the interquartile range of calcium concentrations. Red crosses represent outliers in the data set. Yellow circles show significantly different median concentrations following a Mann-Whitney U test (P < 0.05), double yellow circles show significance at P < 0.01.

4.2.7 Magnesium

Median spring/summer and autumn/winter field drain magnesium concentrations across all sites is shown in Figure 4.7. Magnesium concentration variation was similar between spring/summer and autumn/winter samples, with all sites within 0.92 mg L^{-1} , though mean within site variations were larger (averaging 5.23 mg L^{-1}). This is due to the consistently lower minimum values and a single sample measured on 09/09/2016 at Site 4. Temporal variations showed no significant difference between autumn/winter and spring/summer samples at any site ($P > 0.05$).

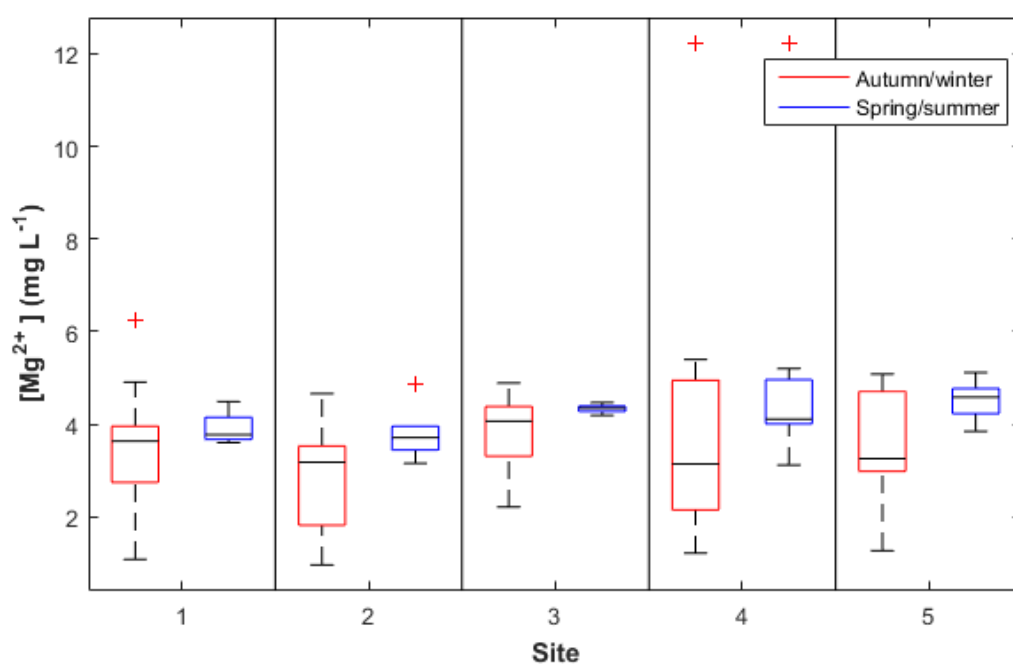


Figure 4.7 Box and whisker diagram showing intra-site comparison of median magnesium concentrations between spring/summer and autumn/winter. The range of concentrations is shown by the whiskers and the boxes illustrate the interquartile range of magnesium concentrations. Red crosses represent outliers in the data set.

4.2.8 Potassium

Median site spring/summer and autumn/winter potassium concentrations are shown in Figure 4.8. The lowest concentration measured in the autumn/winter samples was similar to that of the spring/summer samples (0.18 and 0.54 mg L^{-1} respectively). The variations in potassium concentrations was large, for example at Site 2 in the spring/summer samples, the range in concentrations was $0.54 - 47.75$ mg L^{-1} . The mean range across all sites in the spring/summer and autumn/winter samples is 14.69 and 23.58 mg L^{-1} , respectively, despite this range being far higher than many of the measured concentrations. This is due to a number of very high (in comparison to the majority of the samples) concentrations. Figure 4.9 also shows the median concentrations of the spring/summer and autumn/winter samples at all sites. Despite the high variability, no statistically significant temporal differences were observed ($P > 0.05$).

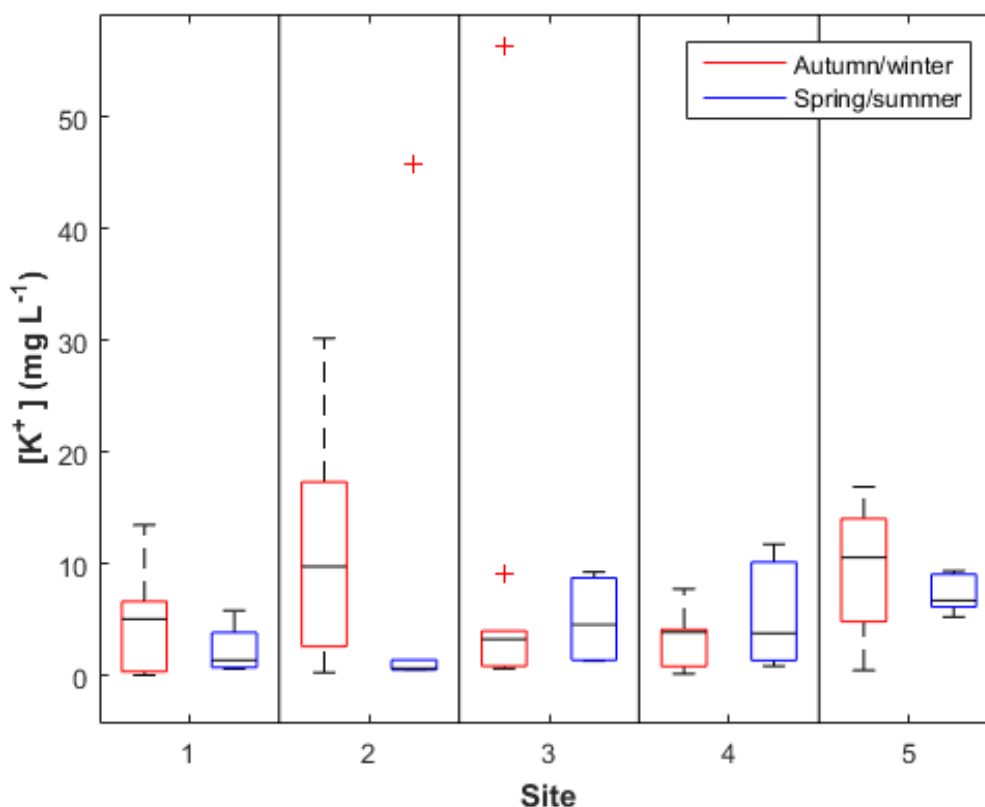


Figure 4.8 Box and whisker diagram showing intra-site comparison of median potassium concentrations between spring/summer and autumn/winter. The range of concentrations is shown by the whiskers and the boxes illustrate the interquartile range of potassium concentrations. Red crosses represent outliers in the data set.

4.2.9 Sodium

The median spring/summer and autumn/winter sodium concentrations are shown in Figure 4.9. Mean variation across all sites in the spring/summer and autumn/winter samples was similar (12.08 and 15.60 mg L⁻¹). Much of this variation is due to a few high concentration samples, for example at Site 2 in the spring/summer samples where a single sample collected on 7/3/2016 had a concentration of 43.22 mg L⁻¹ (with the average of the other samples collected from this site at 16.42 mg L⁻¹). There were a small number of other samples with similarly high concentrations. Concentration ranges are shown in Table 4.3. Figure 4.10 shows the temporal variations in sodium concentrations, illustrating no significant difference between spring/summer and autumn/winter samples at any site ($P > 0.05$).

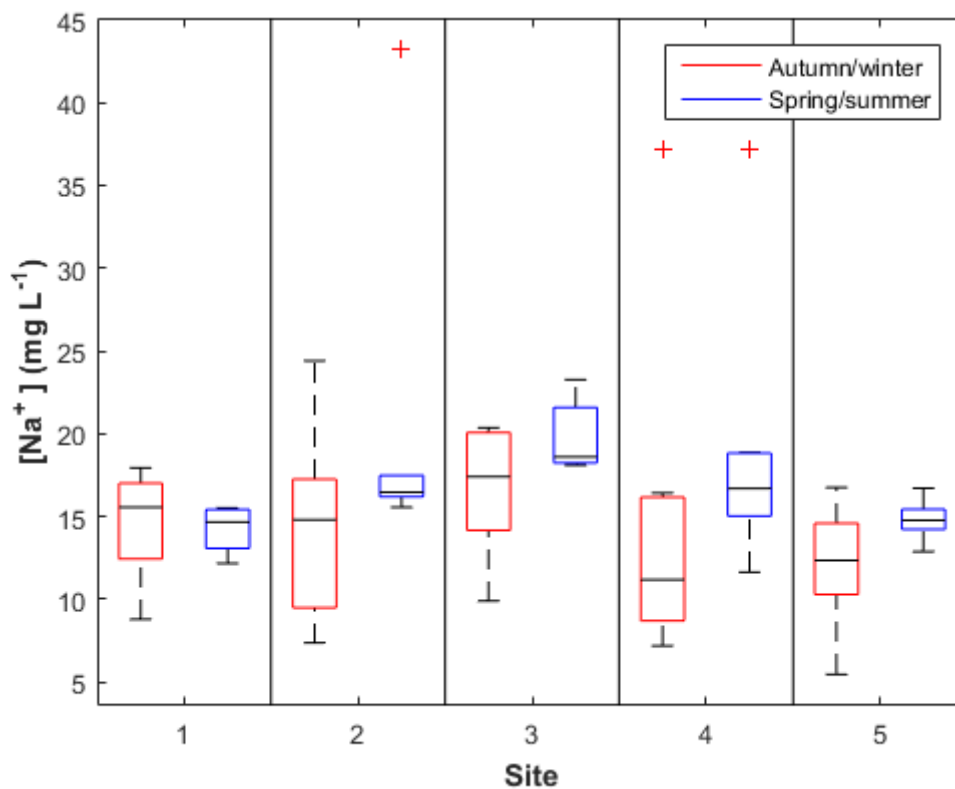


Figure 4.9 Box and whisker diagram showing intra-site comparison of median sodium concentrations between spring/summer and autumn/winter. The range of concentrations is shown by the whiskers and the boxes illustrate the interquartile range of sodium concentrations. Red crosses represent outliers in the data set.

4.2.10 Dissolved organic carbon

Dissolved organic carbon (DOC) was analysed in a number of field drain, piezometer and borehole samples. Unfortunately, sample volume constraints restricted extensive measurements. Nevertheless, the field drain DOC concentrations are presented in Table 4.6. There was high variability in the DOC concentrations between and within sites, for example at Site 3 where spring/summer DOC concentrations are between 1.4 - 39.1 mg L⁻¹ and autumn/winter samples fall between 1.3 and 4.7 mg L⁻¹, and at Site 1 the median autumn/winter DOC concentration is 3.2 mg L⁻¹ while Site 4 sees autumn/winter median concentrations of 30.6 mg L⁻¹, albeit from fewer measurements.

Table 4.6 Field drain DOC concentrations (mg L⁻¹) across all sites during spring/summer (SS) and autumn/winter (AW) sampling periods covering March – August and September-February respectively. Median concentrations presented at the bottom of each column in bold.

Site 1		Site 2		Site 3		Site 4		Site 5	
SS	AW	SS	AW	SS	AW	SS	AW	SS	AW
21.8	1.6	2.8	20.7	1.4	3.2	57.1	27.9	3.9	5.3
3.9	0.9	58.4	9.7	2.4	3.6	4.0	4.9	11.8	-
-	3.2	12.0	19.9	2.1	2.8	3.9	33.4	54.1	-
-	3.5	9.7	17.5	47.9	3.2	10.8	40.5	4.7	-
-	1.6	-	5.0	2.5	1.3	-	-	-	-
-	3.5	-	4.9	39.1	4.7	-	-	-	-
-	3.4	-	4.5	-	-	-	-	-	-
-	-	-	4.0	-	-	-	-	-	-
12.9	3.2	10.9	7.4	2.4	3.2	7.4	30.6	8.2	-

4.2.11 Nitrite and ammonium

Concentrations of nitrite and ammonium are shown in Table 4.7. Nitrite was negligible in all samples with no significant variation between sites ($P > 0.05$). Ammonium concentrations occupied a wide range, however there were no significant differences between sites ($P > 0.05$). Given that nitrite and ammonium concentrations were extremely low in comparison to nitrate, nitrate is the dominant species in the nitrogen chemistry of the study system and suggests that oxidising conditions are prevalent, though zones where reducing conditions prevail are present, as discussed in later sections of this chapter. Site 4 was not included in statistical analyses because there were only two data points available which were too few for any comparisons with other sites. Because the concentrations of these two analytes were low, nitrite and ammonium were not included in the ion balance where bicarbonate concentrations were calculated.

Table 4.7 Nitrite and ammonium concentrations in field drain samples collected from all sites

Site	Nitrite (mg L^{-1})		Ammonium (mg L^{-1})	
	Range	Mean	Range	Mean
1	0.002 – 0.057	0.026 $n = 14$	0.01 – 2.39	0.90 $n = 8$
2	0.009 – 0.060	0.032 $n = 15$	0.01 – 8.88	1.90 $n = 6$
3	0.002 – 0.061	0.028 $n = 17$	0.02 – 2.49	1.18 $n = 7$
4	0.004 – 0.057	0.030 $n = 13$	0.04 – 1.69	0.86 $n = 2$
5	0.006 – 0.067	0.032 $n = 11$	0.86 – 2.34	1.66 $n = 4$

4.2.12 Stable isotopic composition of nitrate

The $\delta^{15}\text{N}_{\text{NO}_3}$ and $\delta^{18}\text{O}_{\text{NO}_3}$ values for all field drain samples are presented in Figures 4.10 and 4.11, respectively. The $\delta^{15}\text{N}_{\text{NO}_3}$ and $\delta^{18}\text{O}_{\text{NO}_3}$ values were progressively significantly lower from Sites 1 – 4 in that the $\delta^{15}\text{N}_{\text{NO}_3}$ and $\delta^{18}\text{O}_{\text{NO}_3}$ values measured at Site 1 were significantly higher than Site 2 which were significantly higher than at Site 3 and so on ($P < 0.01$ in all cases). The $\delta^{15}\text{N}_{\text{NO}_3}$ and $\delta^{18}\text{O}_{\text{NO}_3}$ values measured at Site 5 were significantly higher than those at Sites 3 and 4 ($P < 0.01$). The highest variation in spring/summer $\delta^{15}\text{N}_{\text{NO}_3}$ values was measured at Site 2 whilst Site 4 was least variable. $\delta^{18}\text{O}$ values were most variable at Site 5 and least variable at Site 1. Median $\delta^{15}\text{N}_{\text{NO}_3}$ and $\delta^{18}\text{O}_{\text{NO}_3}$ values were lowest at Site 4 and highest at Site 1.

As with the spring/summer samples, the highest mean $\delta^{15}\text{N}_{\text{NO}_3}$ and $\delta^{18}\text{O}_{\text{NO}_3}$ values for the autumn/winter samples were measured in samples from Site 1, while the lowest were from Site 4. The most variation was seen in samples from Site 1, while Site 5 was the most consistent between sampling occasions. The autumn/winter samples follow the same pattern in terms of $\delta^{15}\text{N}_{\text{NO}_3}$ values as the spring/summer samples, while the $\delta^{18}\text{O}_{\text{NO}_3}$ values were significantly higher than the spring/summer samples at Sites 1 and 2 ($P < 0.05$).

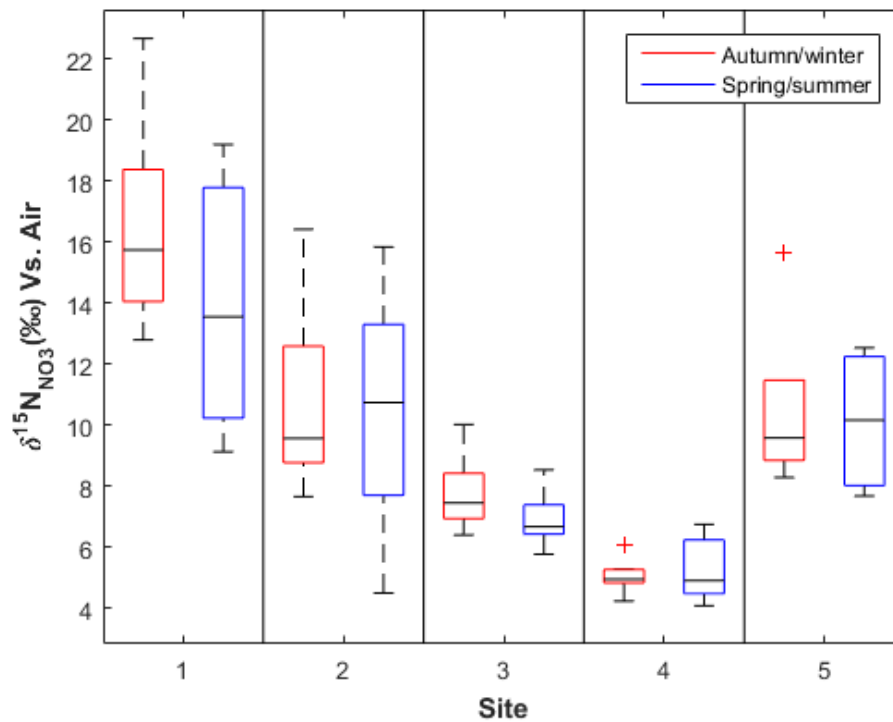


Figure 4.10 Box and whisker diagram comparing autumn/winter and spring/summer $\delta^{15}\text{N}_{\text{NO}_3}$ values at each site. The whiskers show the range across the entire data set and the boxes show the interquartile range of $\delta^{15}\text{N}_{\text{NO}_3}$ values. Red crosses show outliers in the data set.

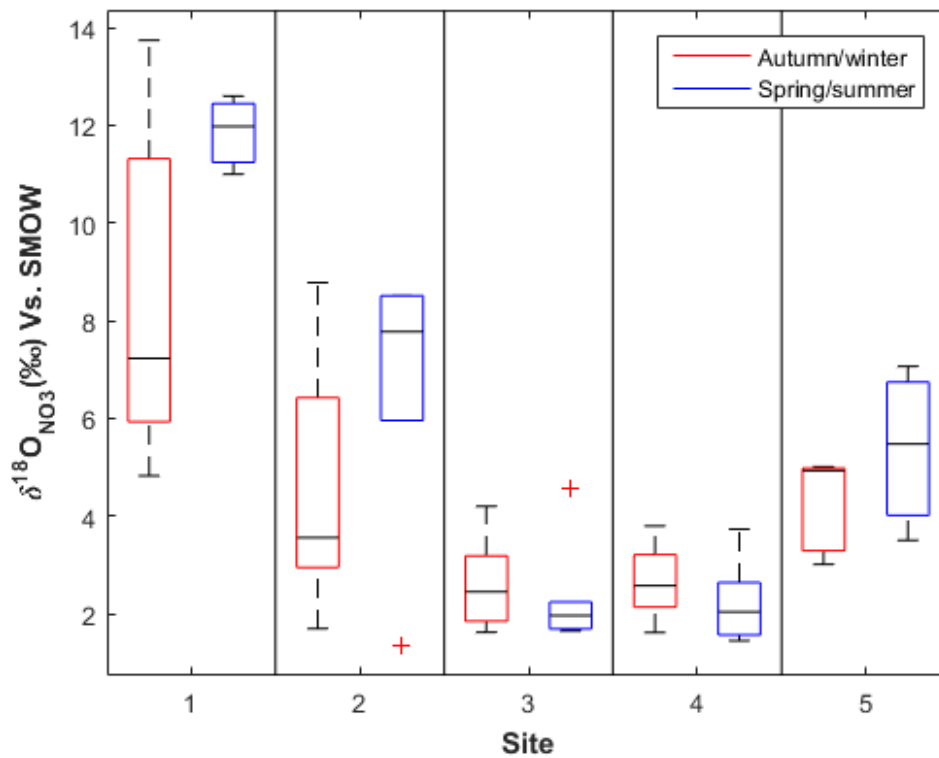


Figure 4.11 Box and whisker diagram comparing autumn/winter and spring/summer $\delta^{18}\text{O}_{\text{NO}_3}$ values at each site. The whiskers show the range across the entire data set and the boxes show the interquartile range of $\delta^{18}\text{O}_{\text{NO}_3}$ values. Red crosses show outliers in the data set.

4.3 Discussion of denitrification in the soil zone

Figures 4.10 and 4.11 show a clear distinction between sampling sites in terms of $\delta^{15}\text{N}_{\text{NO}_3}$ and $\delta^{18}\text{O}_{\text{NO}_3}$ values. When examined as a cross-plot (Figure 4.12), the nitrate isotope data show a trend that is indicative of denitrification, as discussed in Chapter 2. Figure 4.12 shows enrichment of both ^{15}N and ^{18}O (measured with respect to the international standards AIR and V-SMOW - Vienna Standard Mean Ocean Water respectively) in the residual nitrate. The slope of the best fit line on Figure 4.12 is 0.62. This is within the range reported in the literature associated with denitrification (0.35 – 0.76, Bottcher *et al.*, 1999; Aravena and Robertson, 1998; Mengis *et al.*, 1999; Cey *et al.*, 1999; Panno *et al.*, 2006; Wexler *et al.*, 2014; Fukada *et al.*, 2003) suggesting microbially-mediated denitrification was occurring within the soil zone. $\delta^{15}\text{N}_{\text{NO}_3}$ and $\delta^{18}\text{O}_{\text{NO}_3}$ from the field drain samples in a range of +4.5 to +22.7 for $\delta^{15}\text{N}_{\text{NO}_3}$ and +1.4 to +13.7 for $\delta^{18}\text{O}_{\text{NO}_3}$. This indicates that the source of nitrate is a combination of nitrified soil ammonium, and manure and septic waste (Chapter 2, Kendall *et al.*, (2007)). Since the study site is an arable system, hence no manure or septic waste is present, those samples with $\delta^{15}\text{N}_{\text{NO}_3}$ and $\delta^{18}\text{O}_{\text{NO}_3}$ values that fall within the range associated with manure and septic waste are likely demonstrating enrichment of both N and O isotopic species of nitrified and subsequently denitrified soil ammonium.

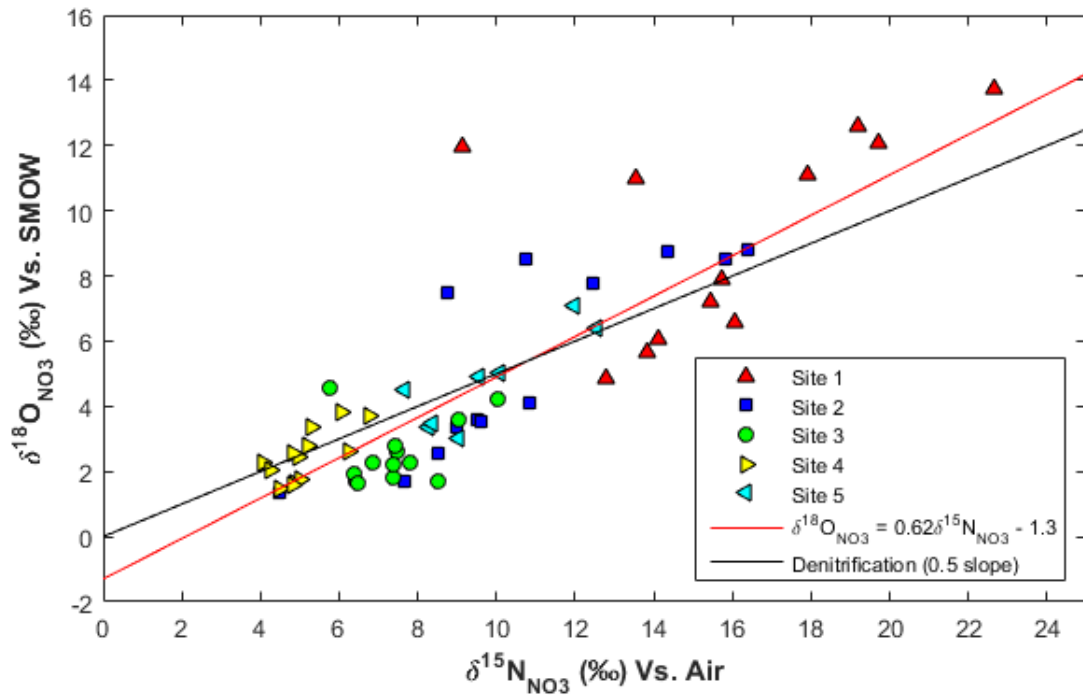


Figure 4.12 Cross-plot of $\delta^{15}\text{N}_{\text{NO}_3}$ and $\delta^{18}\text{O}_{\text{NO}_3}$ values of samples from all sites collected between November 2015 and January 2017. The red line represents the best fit line for the data with a slope of 0.62, while the black line shows the theoretical slope of 0.5 associated with dual fractionation of $^{15}\text{N}_{\text{NO}_3}$ and $^{18}\text{O}_{\text{NO}_3}$ as a result of microbially-mediated denitrification.

Another indicator of denitrification is decreasing nitrate concentration with increasing $\delta^{15}\text{N}_{\text{NO}_3}$ and $\delta^{18}\text{O}_{\text{NO}_3}$ values as shown in Figures 4.13 and 4.14, respectively. Figures 4.13 and 4.14 clearly show that the samples with the highest nitrate concentration are associated with the lowest level of fractionation (i.e. lowest $\delta^{15}\text{N}_{\text{NO}_3}$ and $\delta^{18}\text{O}_{\text{NO}_3}$ values) and vice versa, where Site 4 represents the former and Site 1, the latter. An inverse relationship between nitrate concentration and $\delta^{15}\text{N}_{\text{NO}_3}$ and $\delta^{18}\text{O}_{\text{NO}_3}$ values is indicative of denitrification as nitrate is consumed during denitrification, which in turn enriches the remaining pool of nitrate in ^{15}N and ^{18}O .

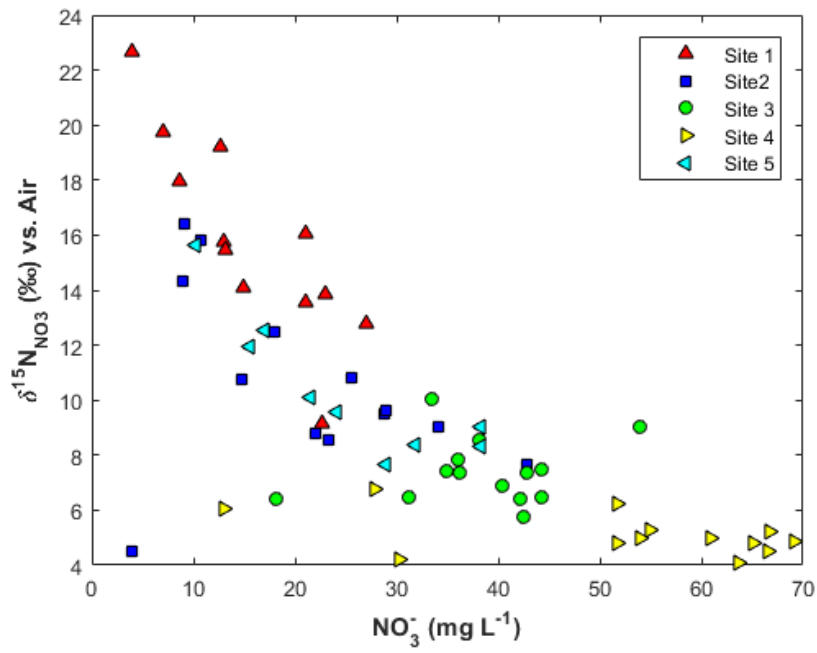


Figure 4.13 Nitrate concentration plotted with $\delta^{15}\text{N}_{\text{NO}_3}$ values of samples collected between November 2015 and January 2017.

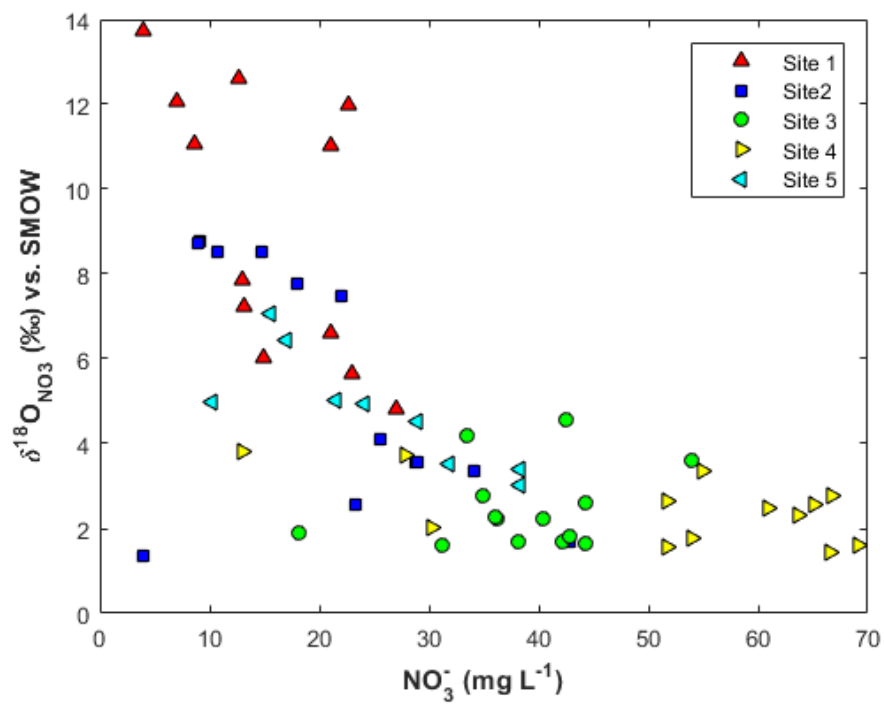


Figure 4.14 Nitrate concentration plotted with $\delta^{18}\text{O}_{\text{NO}_3}$ values of samples collected between November 2015 and January 2017

4.3.1 The influence of soil physical characteristics on denitrification

The distinction between sampling sites is likely the result of difference in the soil conditions at each sampling site, primarily soil type and how this interacts with oxygen availability. In Chapter 2, it is shown that the soil type varies across the study catchment, and that the three fields covered by Sites 1 – 4 (Dunkirk, Sites 1 and 2, Swanhills, Site 3 and Gatehouse, Site 4) contain a range of soil clay content. Site 5 drains a field not used for arable crops during the time frame of this study. As a result, no soil sampling was undertaken, and no nitrogen inputs were recorded for this field. Consequently, though the data from the field drain sampling at Site 5 have been collected and presented but fall within the middle of the range of $\delta^{15}\text{N}_{\text{NO}_3}$ and $\delta^{18}\text{O}_{\text{NO}_3}$ values, Site 5 is omitted from the discussions presented in the following sections.

Figures 4.12 – 4.14 provide strong evidence for microbial denitrification within the soil zone, based on the nitrate stable isotope and concentration data. The majority of studies regarding denitrification within the soil zone involve identifying denitrification by measuring soil N_2O emissions due to its significance in climate change (e.g. Kool *et al.*, 2011; Lewicka-Szczebak *et al.*, 2015; Zhang *et al.*, 2015). In this study, soil field drain data are used to describe processes in the soil zone. It is the soil leachate that provides information regarding the labile chemical species, and combined with soil texture data, will provide the context within which the measured field drain $\delta^{15}\text{N}_{\text{NO}_3}$ and $\delta^{18}\text{O}_{\text{NO}_3}$ values are discussed.

The aim of this study was not to assess soil processes and the soil environment in particular, rather the potential for denitrification in the various environments within the study catchment. As such, exhaustive soil analysis has not been carried out and so the field drain samples are presented as a proxy for soil processes.

The data presented in this chapter show that the nitrate in samples collected from Sites 1 and 2 is the most isotopically enriched, while Sites 3 and 4 are the least fractionated, suggesting that Sites 1 and 2 contain more favourable conditions for denitrification than Sites 3 and 4, namely zones of anoxia within the soil. It is well established that soil texture is a significant contributor to microbial nitrogen cycling owing to its influence on oxygen availability as a result of water retention, with nitrification commonly associated with moderate to dry conditions, and denitrification favoured by waterlogged soil, low oxygen conditions (De Klein and Van Logtestijn, 1994; Menyailo and Hungate, 2006).

The pore connectivity and water filled pore space of a soil matrix are determined by its texture and structure, this in turn has a significant impact on the cycling of nutrients within and between microsites (Castellano *et al.*, 2013). For example, Palta *et al.* (2014) explained that coupled nitrification-denitrification is inhibited in compacted soils characterised by high clay content and low porosity because the exchange of substrates between aerobic and sub-oxic pores is suppressed, while nitrate production and removal within soils is supported where there is high porosity and water flow paths are relatively short, typically within coarser grained soils. It follows then that for soil denitrification to occur, the soil texture must be within a narrow window of intergranular structure, where the pore connectivity is such that diffusion of substrates between oxic and sub-oxic zones can occur, but still maintain anaerobic conditions. The nitrate concentration and stable isotope data suggest that the soil at Sites 1 and 2 lies within this narrow range of conditions, whilst soil conditions at Sites 3 and 4 may be more variable.

The most enriched (i.e. highest $\delta^{15}\text{N}_{\text{NO}_3}$ and $\delta^{18}\text{O}_{\text{NO}_3}$ values) samples were collected from the drains in the most clay-rich fields, supporting the importance of soil texture in soil denitrification. An extensive search of the literature indicates that studies relating soil leachate nitrate isotopic composition to texture are non-existent. Figure 4.15 shows the soil clay and moisture content alongside field drain $\delta^{15}\text{N}_{\text{NO}_3}$ and $\delta^{18}\text{O}_{\text{NO}_3}$ values. Figure 4.15 indicates that the soil texture is contributing significantly to conditions favourable to denitrification through its influence on soil moisture and hence oxygen availability. However, Site 4 contained a significantly ($P < 0.05$) higher fraction of clay than Site 3, despite the drain samples collected there being significantly ($P < 0.05$) less enriched in ^{15}N and ^{18}O , demonstrating that soil texture alone is not responsible for the onset of denitrification.

Examining the nitrate isotope data in field drain samples collected from Sites 3 and 4 alongside soil moisture (unfortunately, soil moisture data were not available for Sites 1 and 2) allows for some further interpretation into the soil oxygen availability that might have been present at these sites during the sampling campaign, above that of inferring from clay content. Site 4, the Gatehouse field had a cover crop established and was under reduced tillage cultivation during the sampling campaign. This might be key in explaining that whilst the clay content and average soil moisture over 0-90cm was higher, the enrichment of nitrogen isotopes was lower in relation to Site 3, the Swanhills field which also had a cover crop cultivated but was under direct-drill regime. Morris

(2009) explained that in reduced tillage regimes, such as in the Gatehouse field (Site 4), a stale seed bed is cultivated, and weeds are sprayed with herbicides. Under a direct-drill cultivation regime, as is carried out on Swanhills (Site 3), stubble from the previous crop is left in the soil and weeds are sprayed off and new seeds are drilled directly into the undisturbed surface. Because at Site 4 (the Gatehouse field, reduced tillage) crop residues are incorporated into the soil following harvest, void spaces generated through root growth are maintained, increasing hydrological connectivity. It follows that due to the differences in cultivation regime between Swanhills (Sites 3, cover crop, direct-drill) and Gatehouse (Site 4, cover crop, reduced tillage), infiltration rates are likely higher at Site 4, despite the higher soil moisture content. Higher infiltration rates at Site 4 both increase the oxygen availability within the soil profile, and the flow of water through it, hence providing fewer regions of saturation in the subsurface, i.e. even though the average soil moisture content in the Gatehouse field over 0-90cm was higher, throughput of soil water could have been faster, resulting in greater fluctuations in saturated conditions. These conditions are sub-optimal for denitrification because water residence time is low, and the requisite anoxic conditions/microsites are reduced. This demonstrates that while soil texture is contributing to the level of fractionation of the nitrate in the leachate, it may only do so up to a certain threshold, beyond which, agricultural management regimes may begin to dominate. Sites 1 and 2 were two field drains measured from the same field, the Dunkirk field, hence the clay content is reported as the same. The differences in nitrate isotope values yet identical clay content likely lies in the variation in clay content across the field. Soil particle size distribution was measured in a soil samples collected from a number of locations within each field, as reported in Hama-Aziz (2016). Since the two drains are located at either end of the Dunkirk field, it is probable that the most clay rich soil can be found at the end of the field which is drained at Site 1. The error bars in Figure 4.15 indicate that clay content does vary significantly throughout each field.

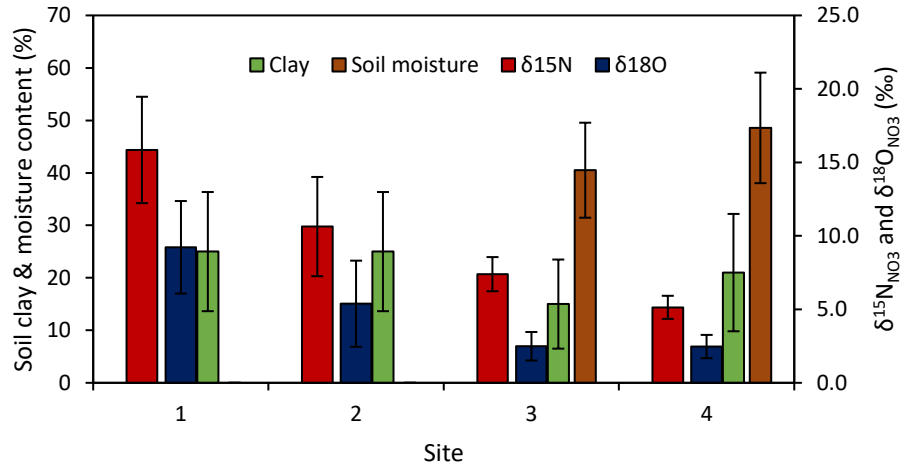


Figure 4.15 $\delta^{15}\text{N}_{\text{NO}_3}$ and $\delta^{18}\text{O}_{\text{NO}_3}$ values for sites 1-4 plotted with average clay content and soil moisture content (%) across 0-90 cm depth for corresponding fields. Field Sites 1 and 2 drain Dunkirk, Site 3 drains Swanhills and Site 4 drains Gatehouse.

Wier *et al.* (1992) used the acetylene inhibition method to measure the effect of water-filled pore space, soil nitrate and available carbon on total denitrification ($\text{N}_2\text{O} + \text{N}_2$ production) in packed soil cores which were brought to 60, 75 and 90% water-filled pore space. The results showed that the loss of nitrogen from the cores by denitrification typically increased as soil texture became finer and more saturated with water.

Wiodarczyk *et al.* (2005) examined the influence of redox conditions on N_2O production and consumption in soils of varying textures. Soil samples reflecting a range of sand, silt and clay configurations were collected and incubated under anaerobic conditions for 35 days and N_2O emissions were measured daily. The results showed that the range of amount of N_2O released from the soils derived from soil nitrate was 13-44% of the initial nitrate content, with average daily N_2O production positively correlated with the soils containing increasing 0.05 – 0.002 and < 0.002 mm grain size fractions, whilst N_2O production was negatively correlated with the > 0.05 mm fraction. Wiodarczyk *et al.* (2005) attributed these results to increased capacity of the finer soil textures to sustain reducing conditions favourable for denitrification in relation to soils with coarser textures.

Sites 3 and 4 (Swanhills and Gatehouse fields, respectively) were associated with the highest nitrate concentrations in the field drains. Given that nitrogen fertiliser

applications (as ammonium nitrate) were similar in all fields (as will be discussed in chapter 6), it is possible that at these sites, generation of nitrate through nitrification of the applied ammonium is the same (or higher) than at Sites 1 and 2 (the Dunkirk field) (where the concentrations of nitrate are lowest), potentially due to the lower clay content and therefore more aerobic conditions. The result of this would be, at Sites 3 and 4, a combination of increased nitrate production due to the relatively (to Sites 1 and 2) aerobic nature of the soil coupled with nitrification-denitrification inhibited because the soil is not anoxic enough to bring about the onset of denitrification. What is most likely is that the Dunkirk (Sites 1 and 2) field soil contains more anaerobic microsites owing to its higher clay content and therefore more ‘hot spots’ of denitrification are present in this field compared to Swanhills (Site 3) and Gatehouse (Site 4).

Biogeochemical ‘hot spots’ are defined by McClain *et al.* (2003) as areas associated with “disproportionately higher reaction rates” in relation to the immediately adjacent matrix. Palta *et al.* (2014) defined ‘hot spots’ as sampling points that show rates of denitrification higher than the 3rd quartile value of the overall dataset. In this study, quantification of denitrification ‘hot spots’ was not attempted and so the suggestion that one field might contain more ‘hot spots’ than another is based on speculation relating to data on soil texture.

The interpretation of biogeochemical activity at any scale larger than ‘micro’ usually relies on identifying or predicting ‘hot spots’ and/or ‘hot moments’ (Palta *et al.*, 2016; McClain, *et al.*, 2003). This is because rates of denitrification are governed by soil biogeochemical conditions which evolve over time and between sites (Palta *et al.*, 2016). This variation is difficult to predict particularly where soil conditions are managed by human input, for example in an agricultural setting such as in the study site examined in this thesis.

Hofstra and Bouwman (2005) synthesised data collected from 336 studies of denitrification in agricultural soils relating to a number of factors, one of which was soil type. A model was constructed to calculate global rates of denitrification. Results from this study revealed that rates were highest in agricultural settings with high nitrogen applications and poorly drained soils. As discussed in the previous sections of this chapter, this is due to the influence of soil texture on oxygen availability.

Palta *et al.* (2016) investigated the factors controlling denitrification rates in an urban wetland system in New Jersey, USA with highly heterogeneous soils. Soil cores comprised of a wide range of textures were used to examine the interaction between denitrification rates, denitrification enzyme activity, available inorganic carbon and soil water retention. Contrary to the notion that denitrification rates are highest in low grain size, poorly draining soils (Hofstra and Bouwmann, 2005), Palta *et al.* (2016) reported the highest rates of denitrification in cores collected from the lowest elevation that were characterised by high macroporosity and low variation in pore space. This open intergranular structure allows for the accumulation of microbial biomass within the soil pore space, hence these soils facilitate the development of robust microbial communities. Palta *et al.* (2016) also explained that denitrification is often coupled with nitrification in soils, where nitrate accumulates in aerated pores (through nitrification), and then diffuses into anaerobic pores where it is denitrified. Rates of this diffusion and presence/absence of anoxic pore spaces relies heavily on the soil texture. Tillage regime can also have a significant influence on nitrification-denitrification regimes in the soil as different tillage approaches result in drastically different aeration of the soil. Denitrification rates are therefore closely linked to these rates of nitrate diffusion and presence of anoxic pore spaces. Based on comments by Palta *et al.* (2016), it is likely that soil texture must occupy a narrow range in structural characteristics where pore spaces are large enough for microbial communities to accumulate, but not so large that anoxic conditions cannot develop. Therefore, on a continuum from Site 1 to 4, it is suggested that soil pore size, nitrate diffusion rates (between pore spaces) decrease, therefore reducing the denitrification potential from Sites 1 – 4.

Whilst the influence of soil texture on $\delta^{15}\text{N}_{\text{NO}_3}$ values have been discussed, it is important to acknowledge the possibility of differences in source $\delta^{15}\text{N}$ from soil organic matter (SOM) between the study fields. The $\delta^{15}\text{N}_{\text{NO}_3}$ values measured in field drain discharge may have differed between fields where e.g. the SOM in the Dunkirk field may have been more enriched with respect to that in the Swanhills field, generating the more isotopically enriched $\delta^{15}\text{N}_{\text{NO}_3}$ values measured in field drain in Dunkirk relative to Swanhills. The $\delta^{15}\text{N}$ value of SOM in soils is influenced by the rate and extent of organic matter decomposition and source material, where SOM resulting from plant litter decomposition by soil microbes is isotopically lighter than the source plant litter (Kendall *et al.*, 2007). Soil conditions and amount of organic matter incorporated into soils in

agricultural settings are strongly affected by tillage regime. As discussed above, the Dunkirk, Swanhills and Gatehouse fields were under different tillage regimes and are characterised by different soil clay content, but all underwent cover cropping. It follows that differences in soil physical conditions (i.e. temperature and moisture) and the degree to which plant material is incorporated into soils could have a strong influence on the $\delta^{15}\text{N}_{\text{NO}_3}$ values measured in the field drains at each of the study fields. An improvement in this study would have been to collect $\delta^{15}\text{N}$ data from SOM samples across the three study fields. This would have allowed for confirmation that the interpretation of the nitrate stable isotope data collected from the field drains was indeed due to differences in soil denitrification rate between the fields.

In Chapter 6 it is discussed that throughout the wider Blackwater Subcatchment, different crops were grown in different fields during the time period covered by this study. However, it is shown in Chapter 6 that the Dunkirk, Swanhills and Gatehouse fields were all used to grow the same type of crop, winter barley during the study period. Furthermore, all three fields were subject to the same fertiliser type applications. Therefore, if there were appreciable differences in the nitrogen isotope values in SOM between the fields, these must have been governed by soil physical conditions and tillage regime. Again, were SOM nitrogen isotope data collected within the presented study, this hypothesis could have been tested fully.

The $\delta^{18}\text{O}_{\text{NO}_3}$ data shown in Figure 4.11 show that the dissolved nitrate in the field drain samples has $\delta^{18}\text{O}_{\text{NO}_3}$ values across all fields of +1.4 to +13.7‰, indicative of soil N, with a range of -5 to +15‰ reported in Kendall *et al.* (1998) and below the range occupied by nitrate fertiliser (+15 to +25‰) (Kendall *et al.*, 1998). Therefore, there is little evidence of direct export of nitrate derived fertiliser from the fields. Sebilo *et al.* (2013) showed that labelled ^{15}N incorporated into agricultural soils can persist as soil organic matter for up to 30 years post application as soil organic matter so it is likely that the dissolved nitrate measured in the field drain samples is derived from mineralisation of soil organic matter, suggesting that of the fertiliser derived nitrate applied to the fields, a portion is immobilised in soil organic matter and later mineralised and lost as subsurface through-flow.

4.3.2 Soil water hydrochemistry and stoichiometry

Aside from nitrogen fertiliser (Nuram35+S which contains 35% nitrogen and 7% SO_3), there were no additions of fertilisers or liming agents to the three fields for which the field drain data were obtained. Furthermore, atmospheric deposition of NO_3^- , NH_4^+ , Cl^- , SO_4^{2-} , Ca^{2+} , Mg^{2+} and Na^+ was negligible in comparison to the major ions supplied from fertiliser applications and soil weathering (Table 4.5). As such, sources of major ions in the soil must originate in soil organic matter (SOM) and weathering of soil minerals. In the case of chloride, since atmospheric depositions were shown to be low (Table 4.5), Sylvanite applications, which contain chloride, to nearby sugar beet fields may have contributed to soil chloride through dust deposition. The atmospheric deposition data are derived from a UK-wide dataset published by the Centre for Ecology and Hydrology (2008) and so it is likely that this local source is not represented. Moreover, soil organic matter has been shown to contain chloride in amounts roughly equivalent to that of phosphorus (Oberg, 1998).

Dissolution of soil minerals is facilitated by the interaction between carbonic acid and soluble organic compounds. Primary mineral weathering results in the generation of weathering reaction products (HCO_3^- and CO_3^{2-}), base cations, and Cl^- and SO_4^{2-} (found in many minerals and soil organic matter) which typically remain in solution (Essington, 2004).

Since hydrolysis of soil minerals occurs at higher rates when there are more available H^+ ions (i.e. lower pH) (Huang, 2004), higher solute concentrations should be associated with lower pH. This is not the case however, as there is very little correlation between major ions and pH, though the range presented in this study is narrow (Figure 4.16), indicating that pH alone is not a major factor in the weathering of soil minerals in this system. This stands to reason as pH values in all samples are circum-neutral (6.39-8.03). What the field drain pH can indicate however, is the extent of chemical weathering the soil has undergone. Chadwick and Chorover (2001) explained that as acid is produced within a soil (through biogenic processes) or deposited from the atmosphere. Ca, Mg and Na carbonates neutralise this acidity. Once the carbonates are fully depleted, a rapid decline in pH occurs as the buffering capacity of the soils is removed but the weathering of primary minerals continues. H^+ and Al^{3+} ions replace the base cations (Ca^{2+} , Mg^{2+} , K^+ and Na^+) on the exchange complex of the minerals. The result of this process is that

cations and anions are leached from the soil profile which lowers the pH from circum-neutral to around 5.5.

If this were the case and no other factors were involved, then it would be expected that the lower pH field rain samples contain higher concentrations of major ions. However newly mobilised mineral components are taken up by the crops growing in the fields and are assimilated by soil microbiota and so it is possible that the lower pH samples are indeed collected from relatively more weathered soils (compared to other soils in the catchment) but the concentrations of secondary minerals in the leachate do not reflect this as they are utilised before being leached from the soil profile. Since very few samples had a pH of < 6 , the soils through which the drain water passes cannot be considered ‘extensively’ weathered (i.e. the soils in Dunkirk, Swanhills and Gatehouse). This system is characterised by chalky boulder clay and is hence dominated by calcium and bicarbonate ions however, and it is likely that the pH is being maintained in the range of 6-8 by carbonate buffering.

Dissolved carbon dioxide, bicarbonate, carbonate, calcium and magnesium species react to maintain the pH through their production and consumption of H^+ ions. It is for this reason that pH-major ion relationships in systems containing high concentrations of bicarbonate are limited in their use.

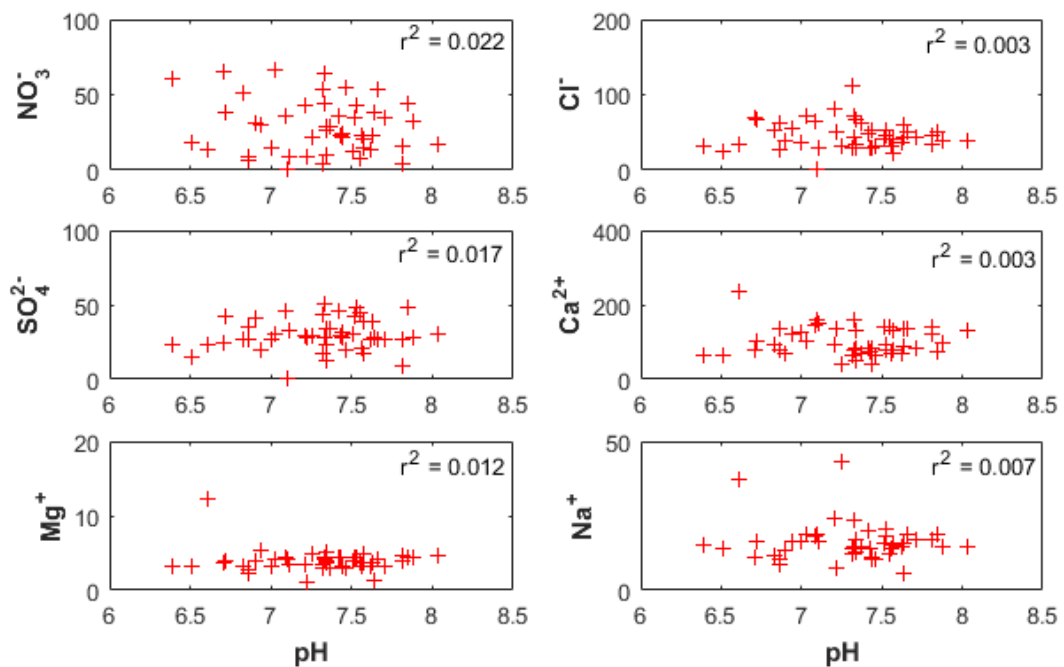


Figure 4.16 Relationship between pH and major ions in field drain samples

With respect to the discussion of the hydrochemical characteristics of the field drain samples presented above, the amount of nitrogen removed from the soil zone via denitrification is estimated below, using the difference between the mass of nitrogen applied to the study fields (Dunkirk, Swanhills and Gatehouse) and the mass of dissolved nitrogen exported to the adjacent stream in soil leachate.

The amount of nitrogen leached from Dunkirk, Swanhills and Gatehouse was calculated using farm nitrogen fertiliser application data obtained from the Salle Farms Co. Gatekeeper record, supplied by Lister Noble. A detailed explanation of how this was calculated is available in Chapter 6. In brief, nitrogen inputs are calculated as:

Amount of fertiliser applied to field (kg) × nitrogen fraction of the fertiliser × (1-crop export coefficient) = amount of fertiliser-derived nitrogen available for leaching from field (kg)

The mass of nitrogen leached from each field, based on the above equation is presented in Box 4.1

Box 4.1. Mass of nitrogen outputs from each study field in soil leachate

The predicted soil leachate concentration for each of the three study fields is shown below, calculated as:

(Mass of nitrogen leached (mg) / Volume of water in field drain (L)) * 4.42.

The volume of water leaving the fields through the drainage network is calculated at Field area (m²) × Average annual effective precipitation (m a⁻¹)

The volume of water in each field drain is based on an average UK annual effective precipitation rate of 140mm a⁻¹ as reported in (Yusoff *et al.*, 2002). An average soil leachate concentration of 111 mg NO₃⁻ L⁻¹ across all three study fields has been used in the following calculations.

Field (site)	Field area (m ²)	Nitrogen leached (kg)	Drain volume (L)	Soil leachate concentration (mg NO ₃ ⁻ L ⁻¹)
Dunkirk (1 & 2)	129100	528	19365000	120
Swanhills (3)	110800	396	16620000	105
Gatehouse (4)	187800	682	28170000	107

The average dissolved soil leachate nitrate concentration across the three study fields (i.e. Sites 1 – 4) was $29.21 \pm 18.94 \text{ mg L}^{-1}$. Assuming a pre-denitrification leachate concentration volume of $111 \text{ mg NO}_3^- \text{ L}^{-1}$, there is a discrepancy of $62.93 - 100.73 \text{ mg NO}_3^- \text{ L}^{-1}$ unaccounted for in the soil leachate entering the stream.

The amount of fertiliser-derived nitrogen incorporated into the soil organic matter pool in this scenario is yet to be accounted for however. Sebilo *et al.* (2013) used ^{15}N -labelled fertiliser-derived nitrate to identify the long-term fate of nitrogen applied to agricultural soils in fertiliser over 30 years. Sebilo *et al.* (2013) showed that 61-65% of applied fertiliser nitrogen was taken up by plants during this period, and of the nitrogen that was not taken up by plants, 32-37% was incorporated into the soil organic matter pool, representing approximately 11 – 14% of total applied fertiliser-derived nitrogen. Based on this rate of incorporation of fertiliser-derived nitrogen into soil organic matter presented in Sebilo *et al.* (2013), it can be estimated that of the discrepancy of $62.93 - 100.73 \text{ mg NO}_3^- \text{ L}^{-1}$ in soil leachate nitrate concentration discussed above, 11 – 14% is accounted for as incorporation of nitrogen into the soil organic matter pool, not denitrification. Therefore after taking into account the incorporation of nitrogen into soil organic matter, the discrepancy between assumed pre-denitrification soil leachate nitrate concentration and actual measured soil leachate concentration was estimated to be $54.12 - 89.65 \text{ mg L}^{-1}$.

A stoichiometric approach has been taken to identify the present electron donors involved in the assumed soil zone denitrification as demonstrated by nitrate isotope data obtained from field drain sampling over a 12-month period. Where carbon is an electron donor, as is the case in the majority of soil zone denitrification scenarios, the reaction is as follows:



This produces a stoichiometric ratio of C:NO₃⁻ of 1.25:1.

In cases where FeS₂ is the electron donor, typically where *Thiobascillus denitrificans* is the dominant denitrifier species, the reaction is:



This produces a stoichiometric ratio of $\text{FeS}_2:\text{NO}_3^-$ of 0.35:1.

Given the range of discrepancies in field drain dissolved nitrate concentration, for carbon to be the primary electron donor supplying energy for the removal of 54.12 – 89.65 mg L^{-1} of nitrate, this equates to a minimum Dissolved Organic Carbon (DOC) concentration required in the soil water of 67.65 – 112.06 mg L^{-1} . In the case of FeS_2 being the primary electron donor, dissolved field drain FeS_2 was not measured, however SO_4^{2-} was. In this instance, based on the above equation, for every mole of NO_3^- denitrified, 1.4 moles of SO_4^{2-} would need to be produced if FeS_2 is the primary electron donor during denitrification. Therefore, for FeS_2 to be the primary electron donor in denitrification, a minimum SO_4^{2-} concentration in the soil water of 75.77 – 125.51 mg L^{-1} would be required.

Field drain DOC concentrations were lower than the required amount to reduce the discrepancy between the soil leachate nitrate concentration and that measured in the field drain samples (0.9 – 49.9 mg L^{-1} , Table 4.6). The field drain SO_4^{2-} concentrations were also too low if oxidation of Fe_2S were responsible for denitrification within the soil zone. Tables 4.3 and 4.4 show median field drain sulphate concentrations ranging between ~20 - 50 mg L^{-1} , with high variation between individual samples. Neither DOC nor sulphate can explain the loss of nitrate in terms of their roles as potential electron donors involved in denitrification. Furthermore, there is no apparent correlation between DOC and nitrate concentrations as shown in Figure 4.17 ($r^2 = 0.043$).

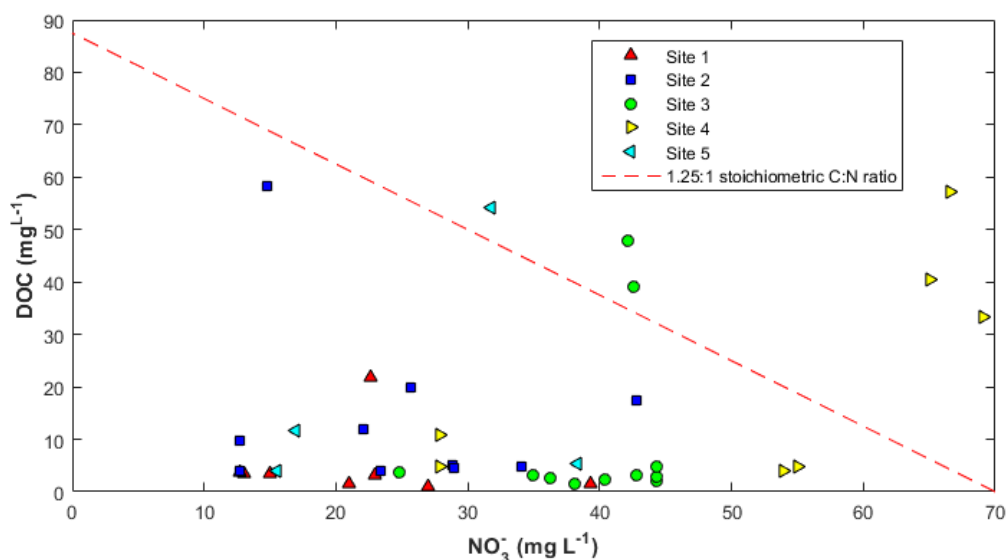


Figure 4.17 Relationship between DOC and NO_3^- concentrations in all field drain samples. The dashed line represents modelled successive removal of nitrate following equation 4.4, illustrating that not enough DOC is present in the majority of the samples for it to be the primary electron donor for denitrification in the soil zone.

Since there is a known 1.25:1 C:N stoichiometric ratio associated with denitrification with carbon as an electron donor (Equation 4.2), the absence of a correlation between nitrate and DOC shown in Figure 4.17 ($r^2 = 0.043$) suggests that DOC may not be the primary electron donor driving denitrification. Given that DOC only represents the soluble form of carbon, it is possible that other forms of carbon are influencing rates of denitrification. It is likely that solid phase soil organic carbon (SOC) is driving denitrification, demonstrating that DOC data should be treated with caution in this context. Figure 4.18 shows the correlation between nitrate and sulphate, where for every mole of nitrate reduced by denitrification, 1.4 moles of sulphate should be produced if Fe_2S is the electron donor. Figure 4.18 shows that while there are a number of samples where the sulphate concentration is high enough based on this 1.4:1 $\text{NO}_3^-:\text{SO}_4^{2-}$ stoichiometric ratio, the correlation is poor ($r^2 = 0.0219$), indicating that Fe_2S within the soil is not the primary electron donor for denitrification, with other sources of sulphate contributing to the higher concentrations. Figure 4.18 does show that samples from Sites 3 and 4 contain higher concentrations of sulphate than Sites 1 and 2, however the isotopic evidence shows that Sites 1 and 2 are associated with more denitrification than Sites 3 and 4. If oxidation of Fe_2S where sulphur is the electron donor for denitrification were

responsible for the production of the high sulphate concentration at Sites 3 and 4, then these same samples would contain low concentrations of nitrate which is not the case.

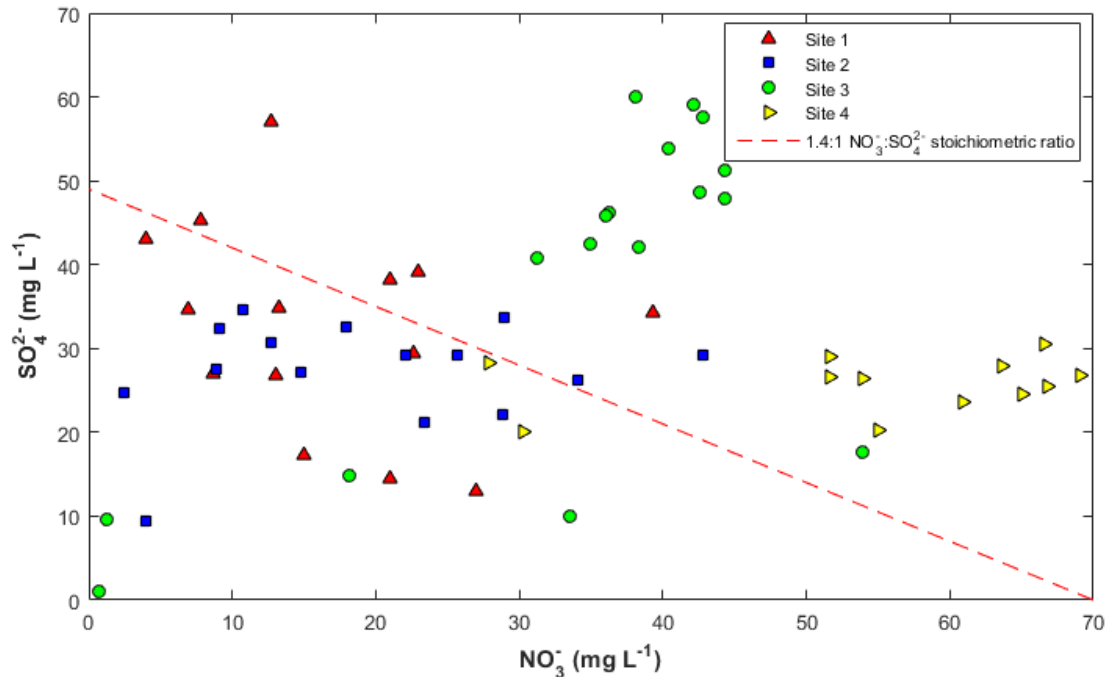


Figure 4.18. Relationship between SO_4^{2-} and NO_3^- concentrations in all field drain samples. The dashed line represents modelled successive removal of nitrate following equation 4.3, illustrating a weak relationship between SO_4^{2-} and NO_3^- , r^2 0.022.

The relationship between nitrate and bicarbonate is another indicator of denitrification. Figure 4.19 shows the relationship between bicarbonate and nitrate (spring/summer and autumn/winter combined) demonstrating a general decrease in bicarbonate with increasing nitrate, or in other words, the samples with the highest nitrate are typically associated with the lowest bicarbonate. The trend is weak though (r^2 0.184). Nevertheless Figure 4.19 shows the expected relationship between nitrate and bicarbonate in a system where denitrification is present, in that bicarbonate is produced due to the production of CO_2 and hydroxide (OH^-) which may react to form bicarbonate (Drill *et al.*, 1995).

Figure 4.19 also shows a stoichiometric ratio for $\text{NO}_3^-:\text{HCO}_3^-$ as 1:1 based on Equation 4.2. Equation 4.2 was used as it provides the maximum bicarbonate yield for the reaction. Figure 4.19 shows that far more bicarbonate is present in the samples than would be provided if denitrification were the sole source. The oxidation of organic matter and/or

reaction of carbonate with CO₂ within the soil zone therefore accounts for the majority of bicarbonate in the samples.

Trudell *et al.* (1986) presented equation 4.5, that accounts for elevated bicarbonate due to pH buffering, which yields a nitrate:bicarbonate stoichiometric ratio of 2.5:



Following pH buffering in the soil, the bicarbonate concentration calculated for the field drain samples are still higher than predicted from equation 4.5, as mentioned oxidation of soil organic matter is the likely source of the excess bicarbonate in the field drain samples.

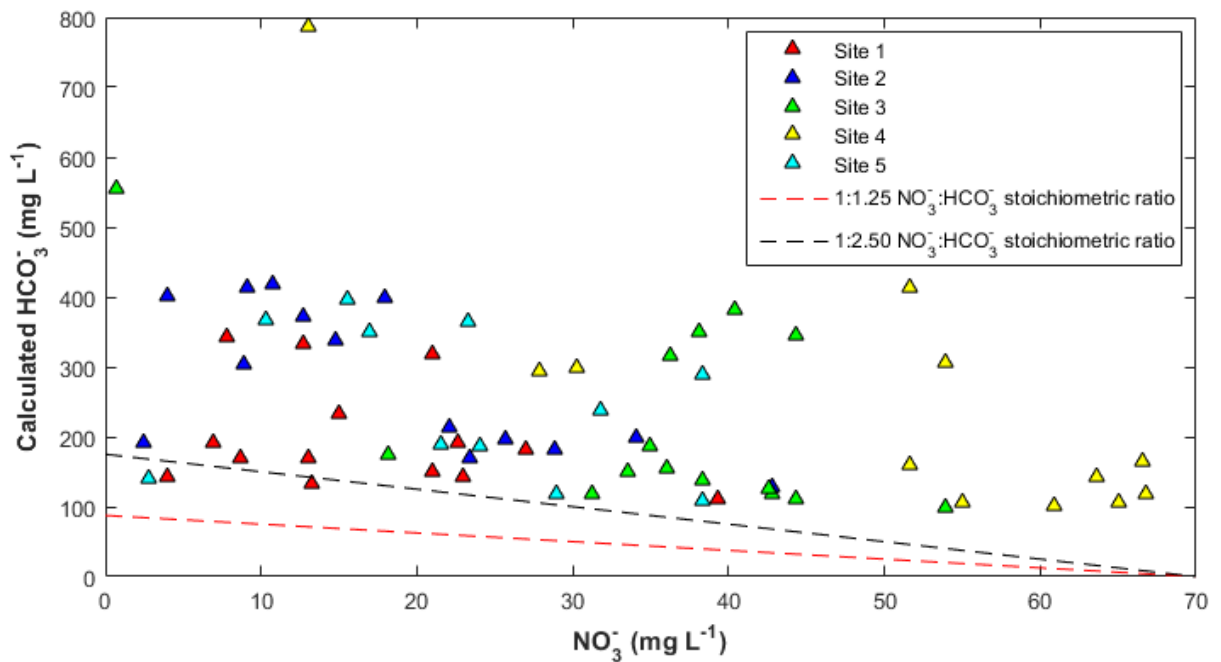


Figure 4.19 Relationship between measured NO₃⁻ and calculated HCO₃⁻ concentrations in all field drain samples collected between November 2015 and January 2017. - - - illustrates the production of 1.25 moles of bicarbonate for every 1 mole of nitrate denitrified following equation 4.2. - - - shows buffering of the pH in the soil due to the reaction of H⁺ from carbonic acid with calcite in the soil described in Equation 4.6, resulting in a 1:2.5 nitrate:bicarbonate ratio.

Previous studies have related rates of denitrification to DOC, such as Hill *et al.* (2000). Hill *et al.* (2000) examined denitrification rates in a forest riparian zone along the Boyne River, Ontario, USA. Two hypotheses were tested: that denitrification in the subsurface is restricted to localised zones, and that denitrification is stimulated where subsurface

flow paths deliver nitrate to supplies of available organic carbon. Using the acetylene block technique, Hill *et al.* (2000) observed a strong inverse relationship between nitrate and N₂O concentration and DOC, suggesting that oxidised forms of nitrogen are consumed under reducing, high DOC conditions.

Stow *et al.* (2005) measured N₂O emissions from the Neuse River watershed in North Carolina, USA. Measurements of dissolved oxygen, nitrate, total nitrogen, ammonium and DOC were also carried out. Standard linear models and classification and regression trees (CART) showed a positive relationship between N₂O emissions and DOC concentrations. Stow *et al.* (2005) explained that the significance of DOC in the water is closely linked to the sediments, in that sediments with high organic content will be less dependent on the water itself as a source of carbon. Furthermore, analyses from this study show high rates of N₂O emissions at low DOC concentrations where nitrate concentrations are high, suggesting that when nitrate concentrations are high, the system is 'primed' for denitrification (i.e. that any incorporation of carbon will immediately initiate denitrification), further reinforcing the significance of carbon limitation. The data presented in this chapter are different to that of Stow *et al.* (2005) in that Stow *et al.* (2005) examined riverine denitrification whereas here, soil processes are being discussed. However comments made by Stow *et al.* (2005) regarding the presence of DOC in the water and sediment pore water can be applied to soil processes. If sediments with high organic content are less reliant on water as a source of carbon, as suggested by Stow *et al.* (2005), then it follows that soil containing high soil organic carbon (SOC) are less affected by the DOC within percolating surface water.

Contrary to Hill *et al.* (2000) and Stow *et al.* (2005), other studies have found no relationship between DOC and denitrification rates. Davidsson and Stahl (2000) examined the importance of SOC in conjunction with the influence of additional DOC on nitrogen transformations in wetlands. Davidsson and Stahl (2000) used ¹⁵N labelled nitrate to examine the nitrogen transformations in soil cores comprised of forest peaty soil, field peaty soil, silt loam, loam and sandy loam. Nitrogen removal was considerable in all five cores, with the highest rates measured in the peaty soil (73% removal) and the lowest rates in the sandy loam (11%). The addition of DOC (in the form of glucose) did not have any impact on soil nitrogen transformations, suggesting that where carbon is not limiting, the dissolved fraction is not the primary source utilised in microbial respiration. Furthermore, the soils used in Davidsson and Stahl (2000) represent a wide range in

organic matter content and even in the least organic matter rich soil (sandy loam), DOC was not found to influence rates of nitrogen removal, indicating that the threshold for DOC utilisation in terms of overall carbon availability is high.

Bernhardt and Likens (2002) studied the interdependence of carbon and nitrogen cycling in forested streams by continuously adding DOC as potassium acetate to a stream in the Hubbard Brook Experimental Forest, New Hampshire, USA. Nitrate and ammonium concentrations were monitored for two months prior to six weeks of DOC additions. Nitrate uptake rates and lengths were also estimated through short term ammonium enrichments in the study and control streams. The change in nitrate and ammonium concentrations was used as an indication of whole-stream nitrification. Results showed that the addition of DOC immediately stimulated bacterial growth and activity, characterised by rapid removal of DOC from the water column and a reduction in nitrate concentration consistent with shortened nitrate uptake lengths.

Bernhardt and Likens (2002) commented that the bacterial growth was so rapid following the additions that it was visible to the naked eye, indicating a strongly carbon limited system prior to the DOC additions. Denitrification was not affected by the addition of DOC, instead the study system was nitrogen limited and it was suggested that any potential advantage gained by denitrifiers through the addition of DOC was probably offset by the reduction in nitrate availability through nitrification (the cause of the decline in nitrate concentration during the DOC enrichment) following the sudden trigger in bacterial growth.

Therefore, the addition of DOC increased competition (for ammonium) between nitrifiers and other heterotrophs rather than stimulating denitrification, where Bernhardt and Likens (2002) explained that nitrifiers are poor competitors. This study highlights the subtle nuances in the coupled carbon and nitrogen cycles and illustrates the significance of limitation of one or the other compound in terms of the impact of any additions on nitrogen cycling. The results from the aforementioned studies all indicate that the solubility of the carbon may not be what governs its availability and quality, suggesting that it is the chemical structure (i.e. bioavailability) that influences its efficacy as an electron donor for denitrification.

The soil zone presented in this study is not nitrogen limited, and carbon stocks were similar to those associated with the 2% threshold for a healthy soil (1.06 – 2.25%,

Chapter 2). From previous studies, it is apparent that DOC is not a reliable measure of carbon availability in terms of its influence on nitrogen transformations, and its true impact is dependent on C or N limitation. Figure 4.19 clearly shows no correlation between DOC and nitrate in the field rain samples and is consistent with Davidsson and Stahl (2000) and Bernhardt and Likens (2002). This infers that DOC is only an important source of carbon under certain circumstances, i.e. where C or N is strongly limiting. SOC is probably more important as an electron donor for denitrification. DOC only represents the dissolved fraction of carbon within a system, where percolating water containing nitrate probably utilises the carbon that is adsorbed to the soil particle surface, explaining why clay content and soil water residence time is so important in facilitating denitrification.

In Chapter 2, the soil physicochemical characteristics were presented and a map of SOC across the study site is shown, from Hama-Aziz (2016). Hama-Aziz (2016) commented that soils with higher clay content are typically associated with higher SOC in relation to sandy soils. The reasons for this are two-fold, firstly, because decomposition rates are lower in soils with high clay content due to the bonds between the clay surface particles and the organic matter. Secondly, high clay content increases the potential for aggregation within the matrix, resulting in organic matter molecules being physically protected from mineralisation (Bot and Benites, 2005).

Given the SOC content of the soil at the study site, it would be reasonable to suggest that SOC is not a limiting factor contributing to the higher nitrate and lower $\delta^{15}\text{N}_{\text{NO}_3}$ and $\delta^{18}\text{O}_{\text{NO}_3}$ values measured at Sites 3 and 4 relative to Sites 1 and 2. Rather, the cultivation practice (in the case of Swanhills, Site 3), clay content and soil water residence time are key determining factors.

4.5 Summary

In this chapter, hydrochemical and nitrate isotopic field drain data have been presented alongside soil physical characteristics. The field drains in this context represent major soil zone processes, namely denitrification and the data were used in combination to elucidate the fate of nitrogen connected to the oxidation of carbon and sulphur as electron donors. Through nitrate isotopic analysis it was demonstrated that denitrification is present within the soil zone, with more fractionation of $^{15}\text{N}_{\text{NO}_3}$ and $^{18}\text{O}_{\text{NO}_3}$ isotopes occurring where the soil texture was more clay rich. At Site 3, the clay content is lower than at Site 4 but the isotopic enrichment of nitrate was lower. Site 3 was under a different cultivation regime than Sites 1, 2 and 4 in that it is managed using reduced tillage. It was suggested that in this case, the presence of crop residues in the subsurface resulted probably in higher infiltration rates and more oxygenated soil conditions where shorter water residence times and the absence of anoxic sites restricted the isotopic enrichment of the soil water nitrate through denitrification.

The pool of available carbon is a key component of soil nitrogen transformations. There was no correlation between soil water DOC and nitrate concentrations. The reliability of DOC data as a representative of soil available carbon was scrutinised, and the evidence for this from the literature is mixed. If percolating water containing nitrate passes through soil with SOC adsorbed to its particle surfaces, then this provides an electron donor for microbial denitrification. Clay rich soils tend to contain more SOC owing to the charge on the particle surfaces. Furthermore, clay rich soil is more water retentive and hence will foster longer water residence times (hence more opportunity for denitrification). Given the similar nitrogen applications across all three fields encompassing Sites 1 – 4 and the identical climate experienced, the isotopic evidence for denitrification and its spatial distribution across the study site can be explained by the differences in soil texture.

Chapter 5 Evidence for denitrification in the stream – hyporheic zone continuum

5.1 Introduction

In this chapter, the stream and piezometer field measurement, hydrochemical and isotopic data are presented, representing a continuum from the surface water to the hyporheic zone (up to 1.5 m below the stream bed). Nitrogen cycling is discussed along this continuum facilitated by nitrate isotopic data and discussed within the context of both hydrochemical and water isotope data, and the local hydrogeological regime. As explained in Chapter 2, the hyporheic zone in this study is recognised as 15 cm – 1.5 m below the stream bed, with the benthic zone classified as 2.5 – 15 cm beneath the stream bed. The piezometers installed to 0.5, 1.0 and 1.5 m then represent three separate strata within the hyporheic zone.

The hyporheic zone describes the area directly beneath, and to the sides of a stream bed, a detailed discussion of the hyporheic zone was presented in Chapter 2. Hyporheic zone denitrification is primarily driven by the delivery of nutrients and carbon from downwelling surface water. A parcel of water travelling downstream will inevitably meet an obstruction such as a gravel bar. While most of the water will circumvent this obstacle, some will be forced downwards into the hyporheic zone where its velocity will be slowed significantly. Within the hyporheic zone, the water (containing dissolved nutrients and carbon) will come into contact with biofilms (comprised of bacteria) that cover the sediment particles. These microbial communities then utilise the carbon dissolved in the newly incorporated water as a source of energy to carry out biochemical reactions (including the oxidation of ammonia and nitrite in nitrification and reduction of nitrate in denitrification) that govern downstream water quality (Zarnetske 2014).

Such exchanges of water, nutrients and organic matter are driven by changes in streambed topography, porosity and discharge. Where water is upwelling through the hyporheic zone, the overlying stream receives nutrients from the groundwater, and in downwelling zones, dissolved oxygen and organic matter are delivered to the hyporheic zone. Redox potential (Eh) is a key driver of biochemical (microbially mediated)

reactions within the hyporheic zone (i.e. nitrification and denitrification) (Boulton *et al.*, 1998) as gradients in Eh determine where oxidation (e.g. of nitrite to nitrate during nitrification) or reduction (e.g. of nitrate to N₂O and N₂ during denitrification) occur.

Liu *et al.* (2017) recently investigated hyporheic zone nitrogen transformations using sediment packed-columns. The focus of this work was to examine how changes in the mixing of surface water and groundwater influence the transformation of nitrogen in the hyporheic zone in relation to microbial community function. Results from Liu *et al.* (2017) showed that rates of denitrification, nitrification and dissimilatory nitrate reduction to ammonium (DNRA) were highly responsive to changes in sediment and water chemistry, water residence time and exchange of ground- and surface water. Such changes in physicochemical conditions were associated with the distribution of denitrification functional genes along a flow path following elution of the columns with 'synthetic' groundwater (comprising 0.46 mM NO₃⁻ and no O₂). The step change in microbial functional potential towards denitrification coincided with accelerated reduction of nitrate and was unaffected by short-term exchange of groundwater and surface water, indicating that prolonged or heavy periods of precipitation can have an effect on the capacity of the hyporheic zone to cycle nitrogen but that shorter or less intense rainfall events do not have the same influence.

Briody *et al.* (2016) studied the impact of a small flooding event under low-flow conditions on biogeochemical processes and surface water-groundwater mixing through sampling of well transects located perpendicular to the Lower Colorado River, USA. Analysis of samples included concentrations of major ions, nutrients, carbon and water isotopes ($\delta^2\text{H}_{\text{H}_2\text{O}}$ and $\delta^{18}\text{O}_{\text{H}_2\text{O}}$ values), alongside well water levels. Sampling was carried out every 2h over a 24h period covering a short flooding event. Results showed that the small flood pulse did not have any profound impact on mixing of surface water and groundwater as ascertained from water isotope analysis. Furthermore, there was no apparent denitrification in response to this flooding event. Briody *et al.* (2016) commented that a large flooding event may be required to bring about any substantial mixing of surface water and groundwater within the hyporheic zone. These findings are consistent with those of Liu *et al.* (2017) who explained that rapid changes in microbial community activity in terms of rates of denitrification do occur within the hyporheic zone, but only where sufficient and prolonged mixing is achieved. Therefore, the hyporheic zone can be thought of as an important zone of nitrogen cycling, but only

where sufficient perturbation occurs, resulting in sustained delivery of surface water (and hence carbon) to the hyporheic zone; and it is the rate of denitrification at baseline conditions that is responsible for the removal of nitrate on a diurnal basis. Such elevated exchange of surface water and groundwater through the hyporheic zone can be considered ‘hot moments’ in terms of denitrification. Briggs *et al.* (2014) described ‘hot moments’ as periods of time during which rates of denitrification are disproportionately higher than at baseline conditions.

Nitrogen in streams and rivers is cycled in close connection to carbon, with potentially significant amounts of nitrogen being removed by denitrification between the catchment and the ocean. There is currently a lack of understanding regarding the significance of exchange surface water and the catchment within which it is located. In particular, the mediation of processes and reactions performed by hyporheic sediments as water is exchanged through this boundary in either direction (Trimmer *et al.*, 2012).

In terms of regulation of denitrification within streams and hyporheic sediments, there is considerable evidence to suggest that denitrification rates are determined either by the availability of organic electron donors and/or electron acceptors (in the form of nitrite and nitrate) at the fine, intergranular scale (e.g. Mulholland *et al.*, 2008). Meanwhile at the reach scale, the scale at which the discussions in this chapter are based, the proportion of nitrogen removed by denitrification is considered to be determined by river discharge and total nitrate flux, where high river discharge and nitrate flux is associated with low water residence time and contact time with sediments (Seitzinger *et al.*, 2006). Despite the understanding of stream and hyporheic zone denitrification generated through recent research, there still exist gaps in our knowledge related to the magnitude of denitrification in hyporheic zone sediments (Trimmer *et al.*, 2012).

Heppell *et al.* (2014) demonstrated that patterns in porewater chemistry reflect spatial variability in sources of water, where oxic conditions were associated with discharge of groundwater and reducing conditions were considered reflective of lateral fluxes of water through riparian zones and/or hyporheic zones. In Heppell *et al.* (2014) it was demonstrated that under baseflow conditions, a zone of preferential discharge (of groundwater into the stream) represented 4-9% of nitrate being transported through the reach in surface water. Given the potential significance of such preferential discharge

zones, Heppell *et al.* (2014) explained that there is a need to improve our understanding of the spatial distribution of preferential discharge zones at the reach scale.

Much of the existing work on hyporheic zone denitrification has focussed on the upper few centimetres and therefore largely ignores the role of groundwater flow paths which may influence the chemical activity of this zone. This focus is partially justified as microbial activity has been shown to be limited by the availability of organic carbon at depth, however the delivery of organic carbon to shallow sediments in systems where groundwater flow paths are complex can be potentially significant (Wondzell, 2006). Krause *et al.* (2009) examined the spatial and temporal distribution of nitrate along a groundwater-surface water continuum in an upwelling flow path under baseflow in the River Leith, UK over a two-year period. Krause *et al.* (2009) commented that the magnitude of variation in nitrate concentration along the upwelling flow path was mainly influenced by sediment structure and physical characteristics along the study reach. The results presented in Krause *et al.* (2009) indicate that variations in redox conditions and resultant pore water nitrate concentrations in the hyporheic zone could arise in depths greater than the top few centimetres. Despite these findings, Krause *et al.* (2009) commented that the fate of nitrogen along an upwelling flow path from groundwater to surface water is still poorly understood and that further work is necessary to expand the conceptual model of hyporheic sediment nutrient cycling beyond the immediate groundwater-surface water interface.

Currently, differing mechanisms of nitrate removal in terms of denitrification and dissimilatory nitrate reduction to ammonium (DNRA) in surface water and benthic sediments is underrepresented in the literature. Lansdown *et al.* (2012) quantified potential pathways of DNRA and denitrification in the hyporheic zone using ¹⁵N labelled nitrogen-bearing substrates. Lansdown *et al.* (2012) explained that denitrification was dominant, though DNRA was also found to be active. Potential rates of denitrification were highest in shallow sediments, and clear differences in sediments from riffle and pool sequences were emerged. Though Lansdown *et al.* (2012) presented compelling evidence for the distribution between anaerobic denitrification and DNRA in hyporheic zone sediments based on stream bed geomorphology, there is a paucity of such studies in the wider literature. As such, another key knowledge gap emerges in terms of the influences of physicochemical characteristics of sediments and their influence on nitrogen removal pathways.

Byrne *et al.* (2014) explained that climate change models predict an intensification in storm activity during summer periods that could result in an increase in the frequency and magnitude of high flow conditions in many catchments across the globe. The classical view of the hyporheic zone is that it is dynamic, with its boundaries considered to expand and withdraw under high and low flow scenarios, respectively. Westhoff *et al.* (2011) observed the expansion of the hyporheic zone during periods of high river stage as a result of increased downwelling of surface water into the subsurface. Byrne *et al.* (2014) suggested that this downwelling results in longer water residence time in the hyporheic zone and could potentially enhance nutrient cycling by speeding up reaction rates. However, Byrne *et al.* (2014) commented that the influence of river stage variability on hyporheic zone biological activity remains relatively unknown and is considered to be another knowledge gap in terms of the role of the hyporheic zone in nutrient cycling.

This chapter aims to contribute to the resolution of these gaps in our knowledge by presenting nitrate isotope and concentration data from deeper (in relation to the majority of studies) within the hyporheic zone, along a stream reach characterised by a range of geomorphologic features. Discussion of these findings is placed in the context of nitrogen removal pathways.

5.2 Results

The major ion chemistry from all stream and piezometer samples is presented in the following sections. Since the stream reach sampled was short (1.6 km) in relation to the length of the network within the catchment, seasonal differences in hydrological connectivity between the surface and subsurface are of interest. The five sampling sites have therefore been combined and separated into spring/summer and autumn/winter categories. In this instance, each individual site represents a repeat within the sampling campaign, where for example the 0.5m piezometer was sampled at Sites 1-5, these represent five repeat samples from the same reach.

A map of the sampling sites within the study catchment was shown in Chapter 3. Throughout this chapter there are numerous references to the individual sampling sites, therefore for convenience they are repeated again in Figure 5.1.



Figure 5.1 Locations of the sampling sites at which piezometer samples were collected. At each site, three piezometers were installed in the stream bed with the screened section at 0.5m, 1.0, and 1.5m beneath the stream bed.

5.2.1 Overview of field measurement and major ion data

Spring/summer and autumn/winter field measurements are shown in Table 5.1 and Spring/summer and autumn/winter hydrochemical data are presented in Tables 5.2 and 5.3 respectively. As with the field drain data (Chapter 4), bicarbonate concentrations in the stream and piezometer samples have been calculated using the geochemical modelling software PHREEQC (v.2) though ion balance. As such, the bicarbonate concentrations reported in Section 5.2.6 were subject to variations in concentrations of all other major ions measured. While every effort was made to ensure the highest analytical accuracy (Chapter 3), this should be taken into consideration when examining the bicarbonate concentrations reported in this chapter.

Table 5.1 Field measurements of samples collected from stream, 0.5m, 1.0m and 1.5m piezometers along a 1.6 km study reach between November 2015 and January 2017.

Autumn/winter – November 2015 – February 2016 / September 2016 – January 2017												
	pH			Dissolved oxygen (mg L ⁻¹)			Temperature (°C)			Electrical conductivity (µS)		
	Range	Mean	<i>n</i>	Range	Mean	<i>n</i>	Range	Mean	<i>n</i>	Range	Mean	<i>n</i>
Stream	6.79 – 8.17	7.53	47	4.28 – 9.30	6.70	42	3.0 – 15.5	8.5	38	329 - 1305	678	49
0.5m	6.49 – 8.12	7.27	30	3.07 – 7.78	5.45	28	6.0 – 19.0	10.5	28	298 - 1438	564	40
1.0m	6.22 – 8.05	7.16	28	1.49 – 8.44	5.16	26	6.0 – 18.0	10.6	29	338 - 1314	607	37
1.5m	6.42 – 8.12	7.37	29	2.25 – 7.39	5.27	13	5.5 – 17.5	10.8	30	308 - 1882	639	36
Spring/summer – March 2016 – August 2016												
	Range	Mean	<i>n</i>	Range	Mean	<i>n</i>	Range	Mean	<i>n</i>	Range	Mean	<i>n</i>
Stream	7.13 – 8.16	7.68	20	4.95 – 8.26	6.13	15	5.5 – 19.0	12.9	25	524 - 1183	798	20
0.5m	6.25 – 7.96	7.10	13	3.00 – 4.65	3.68	6	6.0 – 22.0	13.6	20	323 - 1665	619	25
1.0m	6.43 – 7.61	7.15	12	2.50 – 5.81	4.09	8	6.5 – 19.0	14.3	21	425 - 1333	645	23
1.5m	6.6 – 7.74	7.43	13	3.15 – 5.63	4.15	9	7.5 – 19.0	15.2	20	421 - 1245	622	27

Table 5.2 Major ion concentrations (mg L⁻¹) in stream, 0.5m, 1.0m and 1.5m piezometer samples collected from five sites along the 1.6 km study reach between spring and summer 2016.

		NO ₃ ⁻			Cl ⁻			SO ₄ ²⁻			HCO ₃ ⁻		
Depth	range	median	<i>n</i>	range	median	<i>n</i>	range	median	<i>n</i>	range	Median	<i>n</i>	
Stream	0.69-38.33	25.89	28	11.83-148.83	48.61	29	6.46-45.28	28.44	29	107-511	286	28	
0.5m	0.31-9.82	2.02	24	23.5-120.3	40.2	25	3.77-38.4	17.92	25	125-509	266	24	
1.0m	0.15-16.66	1.93	24	22.52-239.39	38.86	25	12.38-129.11	22.51	25	146-409	244	23	
1.5m	0.27-5.21	1.74	27	22.87-242.31	39.83	28	5.08-242.31	25.17	29	125-344	262	26	
		Ca ²⁺			K ⁺			Mg ²⁺			Na ⁺		
Depth	range	median	<i>n</i>	range	median	<i>n</i>	range	median	<i>n</i>	range	median	<i>n</i>	
Stream	60.16-174.24	129.26	29	0.32-11.29	1.25	25	2.22-5.07	3.89	29	9.95-23.62	17.24	29	
0.5m	43.69-139.72	91.39	24	0.88-281.8	3.04	24	1.83-5.19	3.82	24	7.29-26.12	16.46	23	
1.0m	61.36-145.59	93.49	24	1.27-124.62	2.32	24	1.88-8.94	3.07	24	9.93-22.82	14.68	24	
1.5m	61.84-128.51	96.1	26	1.15-186.41	3.38	26	2.75-7.12	4.05	26	10.81-22.55	16.35	26	

Table 5.3 Major ion concentrations (mg L⁻¹) in stream, 0.5m, 1.0m and 1.5m piezometer samples collected from five sites along the 1.6 km study reach between November 2015 – February 2016 and September 2016 and January 2017.

		NO ₃ ⁻			Cl ⁻			SO ₄ ²⁻			HCO ₃ ⁻		
Depth	Range	Median	<i>n</i>	Range	Median	<i>n</i>	Range	Median	<i>n</i>	Range	Median	<i>n</i>	
Stream	1.61-38.75	27.24	56	22.81-181.91	46.14	56	10.78-56.93	25.70	56	51-410	144	55	
0.5m	0.11-33.20	1.07	45	18.86-312.58	41.16	43	6.65-52.79	20.69	43	104-388	193	37	
1.0m	0.17-46.27	1.50	39	18.98-320.78	41.54	40	10.18-151.81	28.50	40	44-431	162	37	
1.5m	0.16-17.07	0.92	40	18.58-412.97	45.58	40	5.08-119.28	30.41	44	54-361	176	35	
		Ca ²⁺			K ⁺			Mg ²⁺			Na ⁺		
Depth	Range	Median	<i>n</i>	Range	Median	<i>n</i>	Range	Median	<i>n</i>	Range	Median	<i>n</i>	
Stream	46.40-139.04	67.10	55	0.16-134.87	3.98	55	0.61-8.11	3.44	55	3.48-24.39	13.43	55	
0.5m	47.53-124.22	70.57	37	0.47-230.23	5.85	37	0.79-9.58	3.69	37	3.64-26.73	14.25	37	
1.0m	30.15-152.82	65.97	37	0.49-156.05	5.97	37	0.43-9.98	3.04	37	1.75-22.82	13.55	37	
1.5m	30.87-127.90	69.70	35	0.58-392.19	14.93	35	0.83-7.01	3.22	35	4.74-26.28	16.34	35	

5.2.2 Field measurements

The temperature measurements reflect seasonality in the piezometers at all three depths (0.5m 1.0m and 1.5m below the stream bed) (Table 5.3). Overall, the piezometer sample temperatures ranged from 5.5°C during the autumn/winter in the 1.5m piezometer and 22.0°C during the spring/summer in the 0.5 m piezometer, close to the range reported by Farr *et al.* (2017) in an urban setting (9.1 – 16.1°C), and in a rural agricultural setting reported by Kellner and Hubbart (2015) (7.5 – 16.8°C). The values reported here include an appreciably lower minimum value than those of the ranges found in the literature, although the majority of the temperature measurements fall within this range.

Because of the long recharge time of the piezometers (2-3h, necessary for the accumulation of enough sample volume for the analyses), dissolved oxygen (DO) measurements must be treated tentatively, as this recharge period would allow for some oxygen from the overlying atmosphere to be dissolved into the water before being sampled. It is also for this reason that measurements of redox potential were not attempted for these samples. Nevertheless, DO measurements from all sites and piezometer depths are all above the upper threshold beyond which the environment is considered too well oxygenated for the onset of anaerobic denitrification (0.5 mg L⁻¹, Hübner, 1986). The spring/summer mean DO range across all piezometer depths was 3.86 – 4.15 mg L⁻¹, lower than observed in the stream (4.95 – 8.26). During the autumn/winter, the piezometer DO range was 5.15 – 5.45 mg L⁻¹ and the stream DO range was 4.28 – 9.30 mg L⁻¹. This was higher than during the summer, likely as a result of the lower water temperature and hence increased oxygen solubility. In both cases (spring/summer and autumn/winter), the stream DO concentrations measured were higher than in the piezometer samples, demonstrating a less oxic environment in the subsurface relative to the stream, however as explained above exposure to the atmosphere during recharge of the piezometers will have incorporated some oxygen into the hyporheic zone samples from the air column in the piezometer tube.

All pH values measured were circum-neutral, with little difference between surface (stream) and subsurface (piezometer) samples, or between spring/summer and autumn/winter samples. The range in mean spring/summer piezometer pH values across the three depths was 7.10 – 7.68 whilst the mean stream pH was 7.68. During the autumn/winter sampling period, the range in mean piezometer pH values was 7.16 – 7.37 across all depths and the stream mean pH was 7.53. Ideally, denitrification occurs within

a pH range of 7-8 (Feast *et al.*, 1998). The data presented here show that pH was not a limiting factor in denitrification within the subsurface of the study catchment. Table 5.3 shows that there were some samples collected in the stream and all piezometer depths where the pH was below 7, though these were few in number.

Mean spring/summer stream electrical conductivity (EC) was $798 \mu\text{S cm}^{-1}$ where the mean EC across the piezometer depths showed little variation, ranging between $616 - 645 \mu\text{S cm}^{-1}$. The autumn/winter samples were consistently lower than the spring/summer samples in EC, where the mean stream EC was $678 \mu\text{S}$ and the mean piezometer EC ranged between $564 - 639 \mu\text{S}$. Only in the stream samples was this difference between mean autumn/winter and spring/summer samples statistically significant ($P < 0.05$). At no depth (0.5m, 1.0m or 1.5m) were the autumn/winter piezometer samples significantly lower than the spring/summer samples ($P > 0.05$). Table 5.2 shows high variation in EC within the stream and piezometer samples, with higher minimum values during the spring/summer. This high variation in EC reflects the large range of major ion concentrations measured in all samples (Table 5.3) due to dilution by rain water and road salt runoff.

5.2.3 Nitrate

Figure 5.2 shows the nitrate concentration profile from the stream to 1.5m depth below the stream surface at all sites. Median stream nitrate concentrations were significantly higher ($P < 0.01$) than in the piezometers (0.5, 1.0 and 1.5m depth below the stream bed). Median nitrate concentrations remained similar with depth ($P > 0.05$), with the spring/summer samples consistently slightly higher than the autumn/winter samples, though not significantly so ($P > 0.05$). A small number of high nitrate concentrations were observed, within the considerable range measured in the chalk groundwater in Norfolk ($< 0.1 - 104.8 \text{ mg L}^{-1}$; Feast *et al.*, 1998), though the nitrate concentration in the chalk groundwater measured at Salle (the same study site as presented in this thesis) by Feast *et al.* (1998) was 14.8 mg L^{-1} , lower than the highest concentrations shown in Figure 5.2. Figure 5.2 illustrates that these high (in relation to the majority of samples) nitrate concentrations were virtually always measured in the samples collected during the autumn/winter period. Important to discussions in Section 5.3.4, the nitrate concentration in the 12 m borehole located close to Site 1 (Figure 5.1) was $3.75 \pm 0.32 \text{ mg L}^{-1}$. The location of the borehole is shown in Figure 2.5.

Diffuse Equilibrium in Thin films (DET) probes were installed at Site 5 in order to gain a higher (2.5cm) resolution, shallow sediment depth profile of nitrate (and sulphate, chloride and nitrite) covering 2.5 – 15.0 cm into the benthic sediments. Figure 5.3 shows that median nitrate concentrations decline with depth until 10 cm, beyond which the concentration remains similar. Variation was high in the upper 10 cm of benthic sediment and the only statistically significant differences were between the 5.0cm and 12.5, and 12.5 and 15.0 cm depth horizons ($P < 0.05$). Figure also 5.3 shows that variability in nitrate concentrations decreased with depth in the shallow sediment profiles.

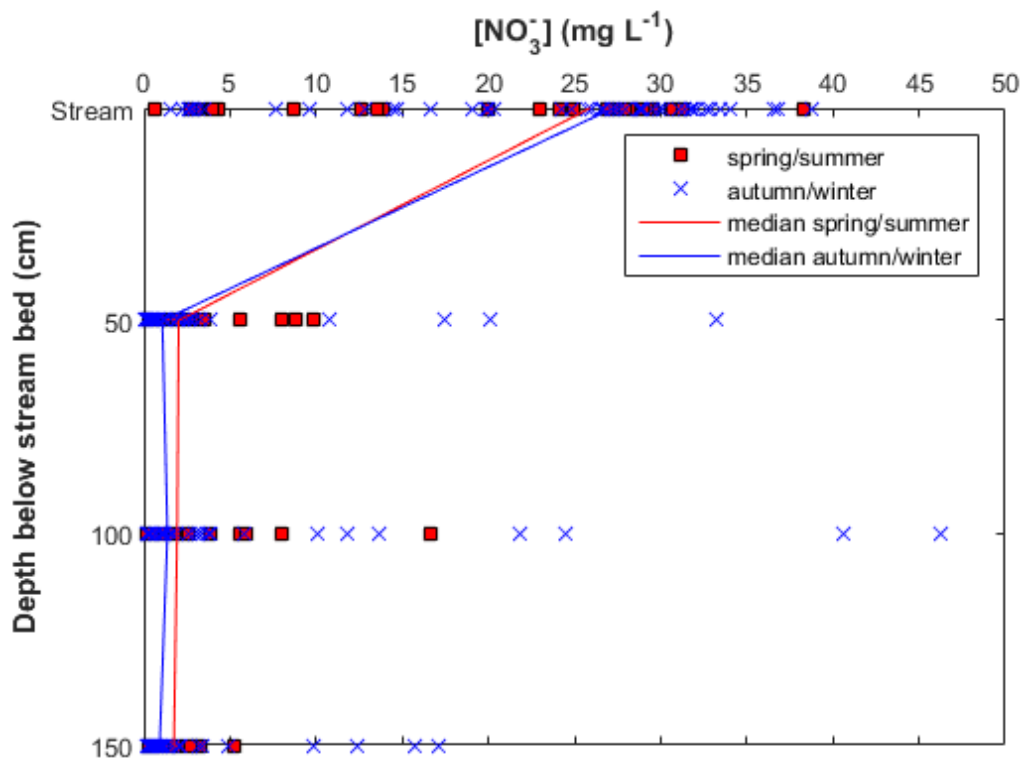


Figure 5.2 Depth profile of nitrate concentrations from the stream to 1.5m below the streambed from spring/summer, collected between 7/3/2016 – 12/8/2016 (red) and autumn/winter (blue) samples collected between 19/11/2015 – 5/2/2016 and 9/9/2016 – 20/1/2017. The red and blue lines show the median values for spring/summer and autumn/winter samples respectively.

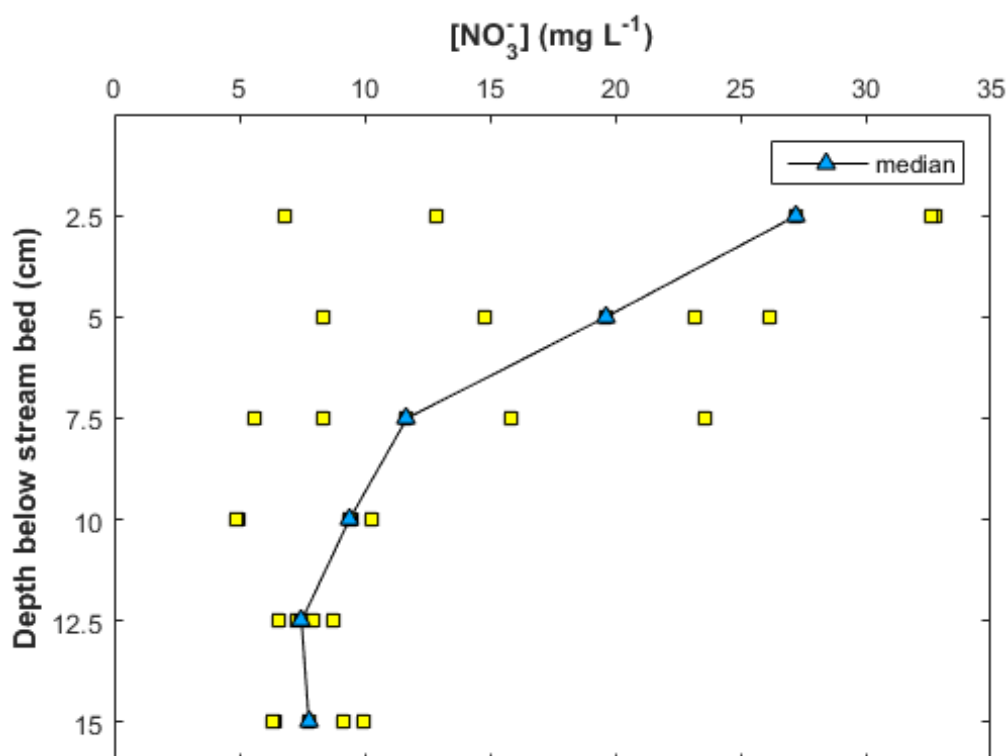


Figure 5.3 Stream sediment pore water nitrate concentration depth profile from 2.5cm to 15.0cm beneath the stream bed from DET probe deployments. DET probes were deployed at a Site 5 along the study reach on 17/2/2017 and retrieved on 20/2/17.

5.2.4 Nitrite and ammonium

Nitrite concentrations were negligible in comparison to nitrate in all samples with no statistically significant variation between spring/summer and autumn/winter at any depth horizon ($P > 0.05$). Despite being low, the majority of samples contained measurable amounts of nitrite all within a narrow range of $\sim 0.01 - 1.00 \text{ mg L}^{-1}$. Ammonium concentrations were higher than nitrite ranging from $0.02 - 2.15 \text{ mg L}^{-1}$ (Table 5.4). Due to sample volume and analytical restraints, fewer samples were analysed for ammonium and unfortunately the spring/summer samples were significantly underrepresented. Whilst it appears that minimum ammonium concentrations in the few spring/summer samples were higher than the lowest autumn/winter samples, the paucity of spring/summer samples makes any seasonal comparisons impossible. Based on the autumn/winter samples, the ammonium concentrations in the stream samples were significantly lower than those at all piezometer depths ($P < 0.05$). Due to the low concentrations, these two ions have not been included in the ion balance used to calculate bicarbonate concentrations (Section 5.2.7).

Table 5.4 Nitrite and ammonium concentrations for all stream and piezometer samples

	NO_2^- (mg L ⁻¹)				NH_4^+ (mg L ⁻¹)			
	spring/summer		autumn/winter		spring/summer		autumn/winter	
	range	mean	range	mean	range	mean	range	mean
Stream	0.01 – 0.06	0.04 <i>n</i> = 29	0.01 – 0.06	0.02 <i>n</i> = 56	-	-	0.02 – 2.79	0.08 <i>n</i> = 30
0.5m	0.01 – 1.108	0.03 <i>n</i> = 25	0.01 – 0.06	0.02 <i>n</i> = 45	1.02 – 1.59	1.31 <i>n</i> = 2	0.01 – 2.37	1.33 <i>n</i> = 27
1.0m	0.01 – 0.06	0.03 <i>n</i> = 24	0.01 – 0.06	0.04 <i>n</i> = 40	1.23 – 1.51	1.37 <i>n</i> = 2	0.01 – 6.16	1.20 <i>n</i> = 24
1.5m	0.001 – 0.998	0.03 <i>n</i> = 28	0.01 – 0.07	0.03 <i>n</i> = 37	1.33 – 1.47	1.36 <i>n</i> = 3	0.01 – 2.15	1.24 <i>n</i> = 25

5.2.5 Chloride

Figure 5.4 shows the stream – 1.5m depth profile of measured chloride concentrations during the spring/summer and autumn/winter sampling periods. Unlike nitrate, the stream chloride concentrations were similar to those measured in the piezometers and maintained a relatively stable concentration throughout the profile. There were no significant differences in the median concentrations observed between depth horizons ($P > 0.05$) and no statistically significant difference between spring/summer and autumn/winter chloride concentrations at any depth horizon ($P > 0.05$). There were a small number of samples that contained higher (than the bulk of the samples) concentrations creating a large range of chloride concentrations (18.6 – 414.0 mg L⁻¹), though 84% of the data were within the 18.6 – 96.0 mg L⁻¹ range. Hence, the highest values only comprise a small fraction of the whole dataset. This range was similar to the range measured by Feast *et al.* (1998) in a chalk aquifer in Norfolk, who reported a range of 21.4 - 174.8 mg L⁻¹. Similar to nitrate, the highest chloride concentrations were measured in the samples collected during the autumn/winter.

A shallow (2.5 – 15.0cm) sediment chloride concentration profile was generated at Site 5 through installation of DET probes. Figure 5.5 shows an increasing concentration with depth, though the variation was high and there was no statistical significance between depth horizons ($P > 0.05$).

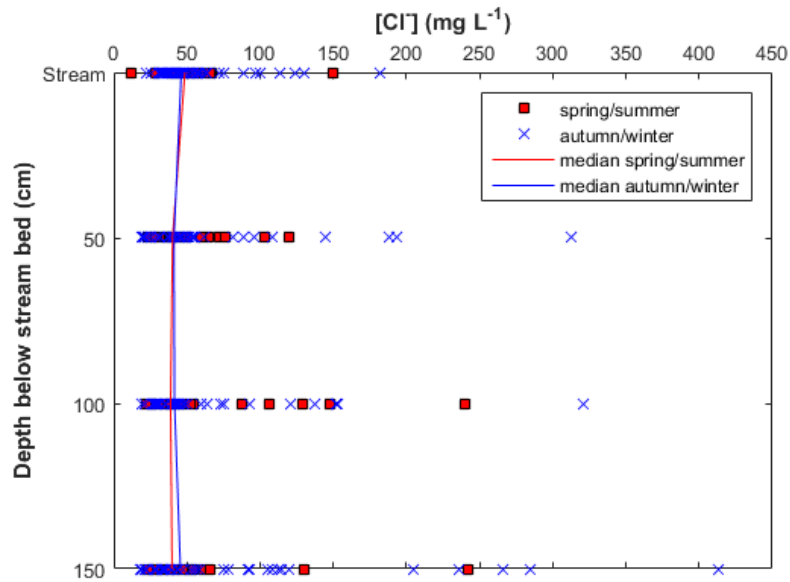


Figure 5.4 Depth profile of chloride concentrations from the stream to 1.5m below the streambed from spring/summer, collected between 7/3/2016 – 12/8/2016 (red) and autumn/winter (blue) samples collected between 19/11/2015 – 5/2/2016 and 9/9/2016 – 20/1/2017. The red and blue lines show the median values for spring/summer and autumn/winter samples respectively.

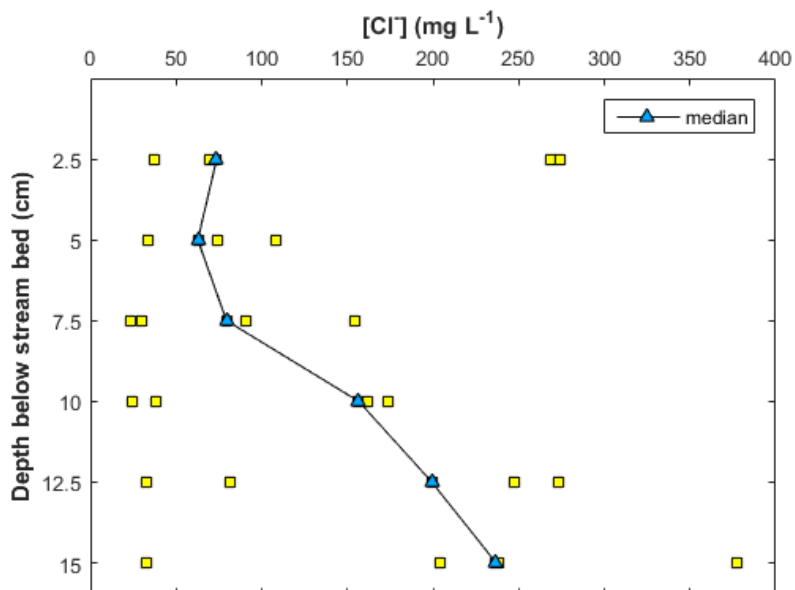


Figure 5.5 Stream sediment pore water chloride concentration depth profile from 2.5cm to 15.0cm beneath the stream bed from DET probe deployments. DET probes were deployed at a single site along the study reach on 17/2/2017 and retrieved on 20/2/17.

5.2.6 Sulphate

The stream – 1.5m depth profile of sulphate concentrations is shown in Figure 5.6. Stream and subsurface sulphate concentrations were similar, though there was considerable variation at all horizons within the profile including a number of markedly higher (than the majority of the samples) concentrations. These high concentration samples were collected during the autumn/winter sampling campaign, though the highest concentration was measured in a spring/summer sample. There were no statistically significant differences between the spring/summer and autumn/winter sulphate concentrations at any depth horizon including the stream. Between depths in the spring/summer samples, the median stream concentration was significantly higher than the 0.5m piezometer ($P < 0.01$); and the 0.5m piezometer was significantly lower than the 1.5m piezometer in both seasonal datasets ($P < 0.05$). There were no other significant differences between depth horizons. In the autumn/winter samples, more variability between depths was observed, with median stream samples significantly lower in sulphate than the 1.0 and 1.5m piezometers ($P < 0.05$). Furthermore, despite being similar, concentrations significantly increased with depth ($P < 0.05$). In the shallow depth profile, generated by the DET probes, sulphate concentrations remained roughly constant (Figure 5.7), with no statistically significant differences observed with depth. Relative to the deeper (piezometer) horizons however, sulphate concentrations in the 2.5-15.0cm profile were considerably higher.

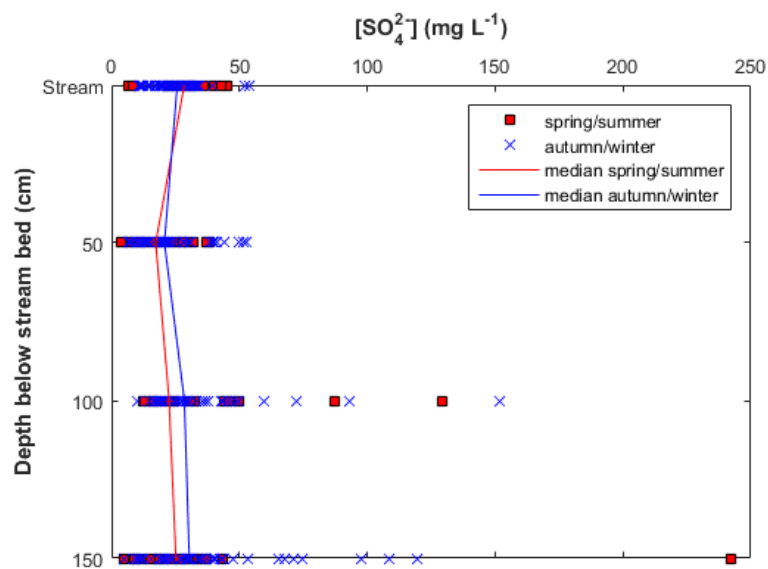


Figure 5.6 Depth profile of sulphate concentrations from the stream to 1.5m below the streambed from spring/summer, collected between 7/3/2016 – 12/8/2016 (red) and autumn/winter (blue) samples collected between 19/11/2015 – 5/2/2016 and 9/9/2016 – 20/1/2017. The red and blue lines show the median values for spring/summer and autumn/winter samples respectively.

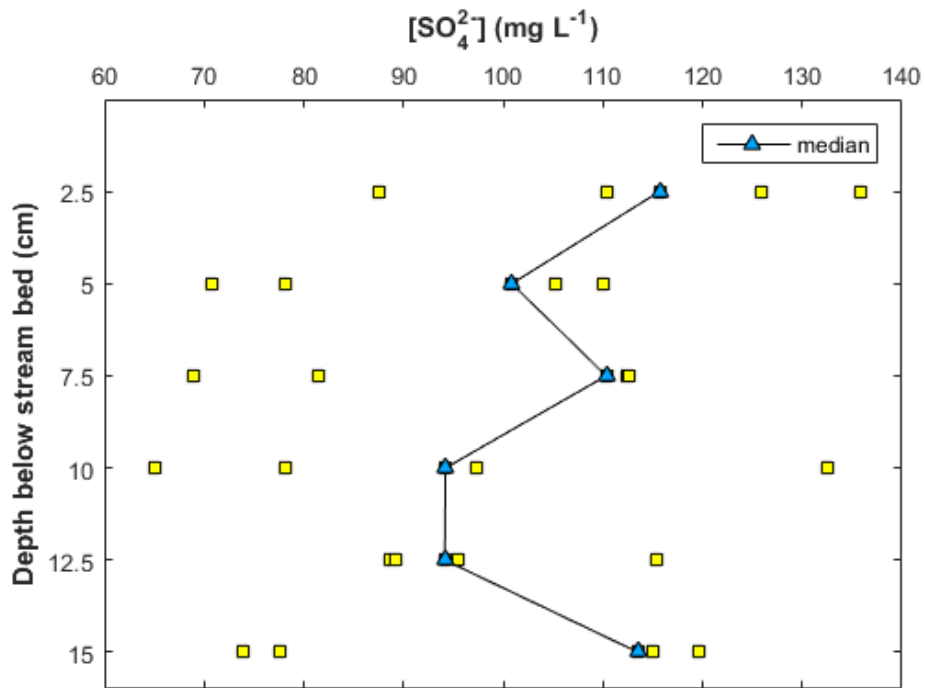


Figure 5.7 Stream sediment pore water sulphate concentration depth profile from 2.5cm to 15.0cm beneath the stream bed from DET probe deployments. DET probes were deployed at a single site along the study reach on 17/2/2017 and retrieved on 20/2/17.

5.2.7 Bicarbonate

Figure 5.8 shows the spring/summer and autumn/winter bicarbonate concentration profiles. Stream and subsurface bicarbonate concentrations were similar, with little variation in median concentration with depth. Concentrations were consistently higher in the samples collected during the spring/summer period, and significantly so ($P < 0.01$) at all depth horizons other than the stream, despite the spring/summer samples being demonstrably higher in the stream as well as at 0.5, 1.0 and 1.5m below the stream bed. As previously mentioned, concentrations of bicarbonate were not directly measured, instead calculated from ion balance. As such, though every effort was made to ensure accurate measurement, the bicarbonate concentrations reported in this chapter are subject to variations in all other major ions measured, especially the calcium concentrations.

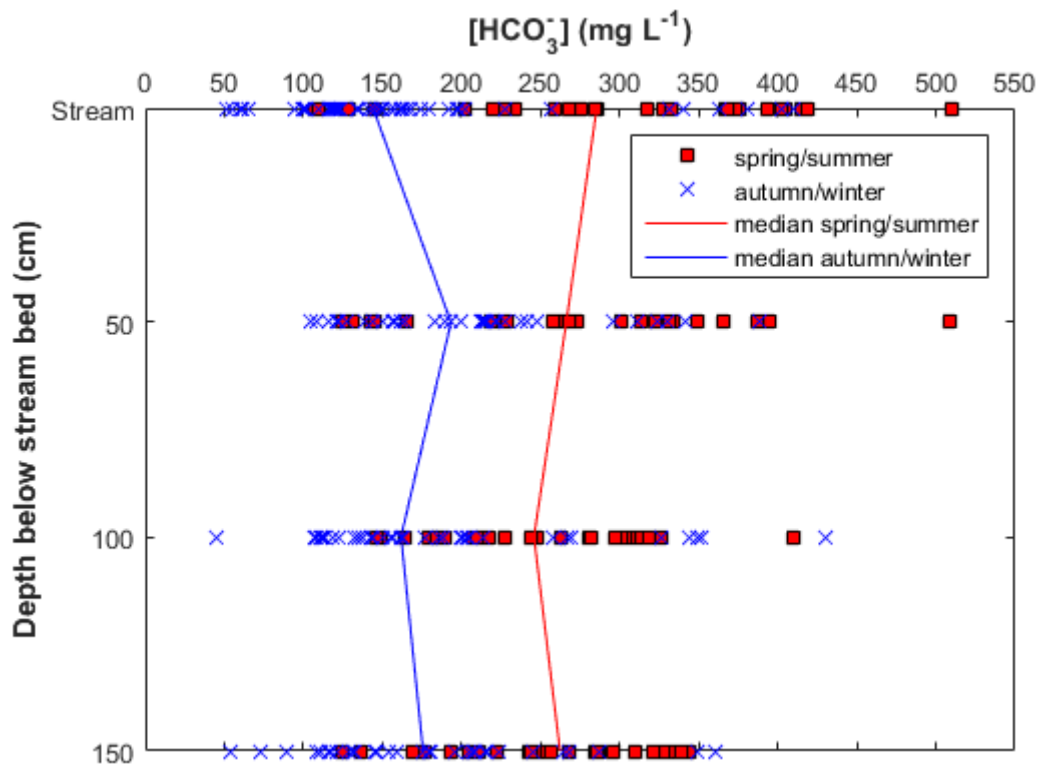


Figure 5.8 Depth profile of bicarbonate concentrations calculated from ion balance from the stream to 1.5m below the streambed from spring/summer, collected between 7/3/2016 – 12/8/2016 (red) and autumn/winter (blue) samples collected between 19/11/2015 – 5/2/2016 and 9/9/2016 – 20/1/2017. The red and blue lines show the median values for spring/summer and autumn/winter samples respectively.

5.2.8 Calcium

Spring/summer and autumn/winter calcium concentration profiles are shown in Figure 5.9. Similar to the bicarbonate concentrations (which are closely coupled to calcium), the spring/summer calcium concentrations were consistently significantly higher than in the autumn/winter samples at all depth horizons including the stream ($P < 0.01$). Variations in the calcium concentrations and the observed higher spring/summer concentrations would have impacted bicarbonate calculations and explain the observed seasonal differences. Of all the major ions, calcium had the biggest influence on the calculate bicarbonate concentrations given the local geology, discussed in Chapter 2. Calcium concentrations remained similar with increasing depth, though the stream spring/summer samples contained significantly higher concentrations than those from the subsurface ($P < 0.01$). The highest concentrations measured may be the result of dissolution of minerals contained in the sediment.

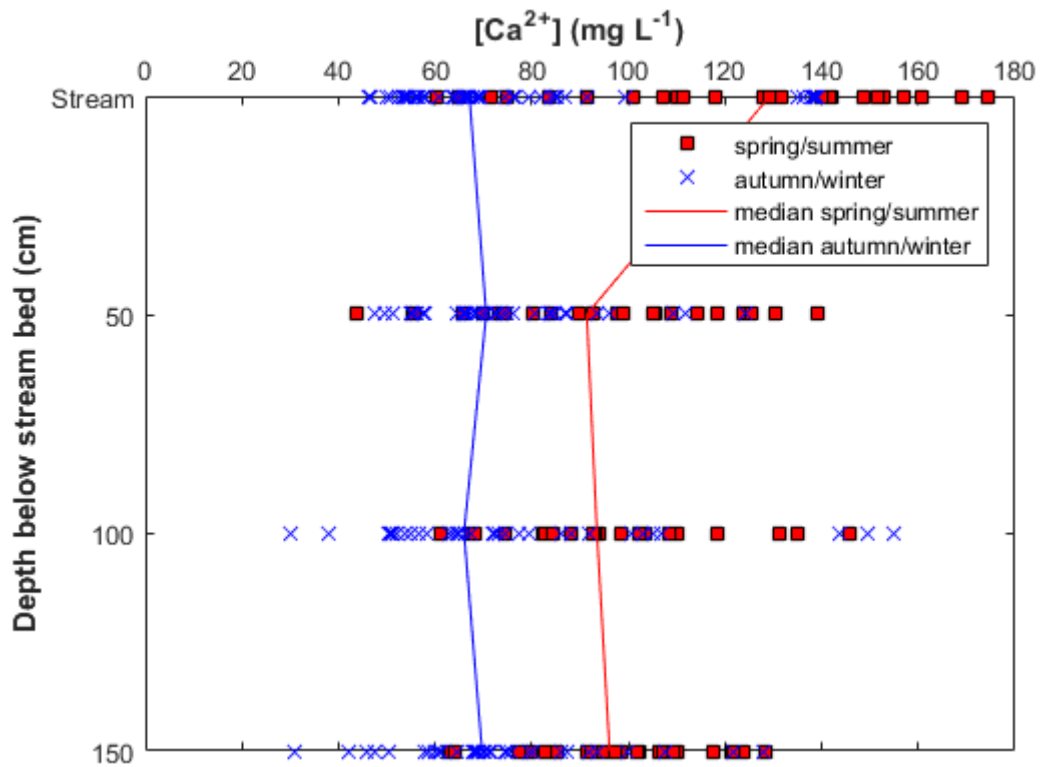


Figure 5.9 Depth profile of calcium concentrations from the stream to 1.5m below the streambed from spring/summer, collected between 7/3/2016 – 12/8/2016 (red) and autumn/winter (blue) samples collected between 19/11/2015 – 5/2/2016 and 9/9/2016 – 20/1/2017. The red and blue lines show the median values for spring/summer and autumn/winter samples respectively.

5.2.9 Potassium

Spring/summer and autumn/winter depth profiles of potassium concentrations are shown in Figure 5.10. Median stream and subsurface concentrations were similar at all depth horizons, changing very little from the stream to 1.5m below the stream bed. There are a number of high concentration samples which are in stark contrast to the majority of the data. The greatest range was measured in the 1.5m piezometer (1.66 – 392.19 mg L⁻¹). Feast *et al.* (1998) measured potassium concentrations in chalk groundwater in Norfolk, reporting a range of 0.60 - 34.4 mg L⁻¹. The total range of subsurface potassium concentrations presented in this chapter is 0.47 – 392.19 mg L⁻¹, with 20% of the dataset exceeding the maximum value reported in Feast *et al.* (1998). One explanation for these high concentration samples is that the filter membrane for some piezometers may have been damaged during installation, allowing for ingress of sediment into the screened section. Samples were filtered upon collection, however as with calcium, dissolution of minerals contained within the sediment may have provided an additional source of potassium in some samples.

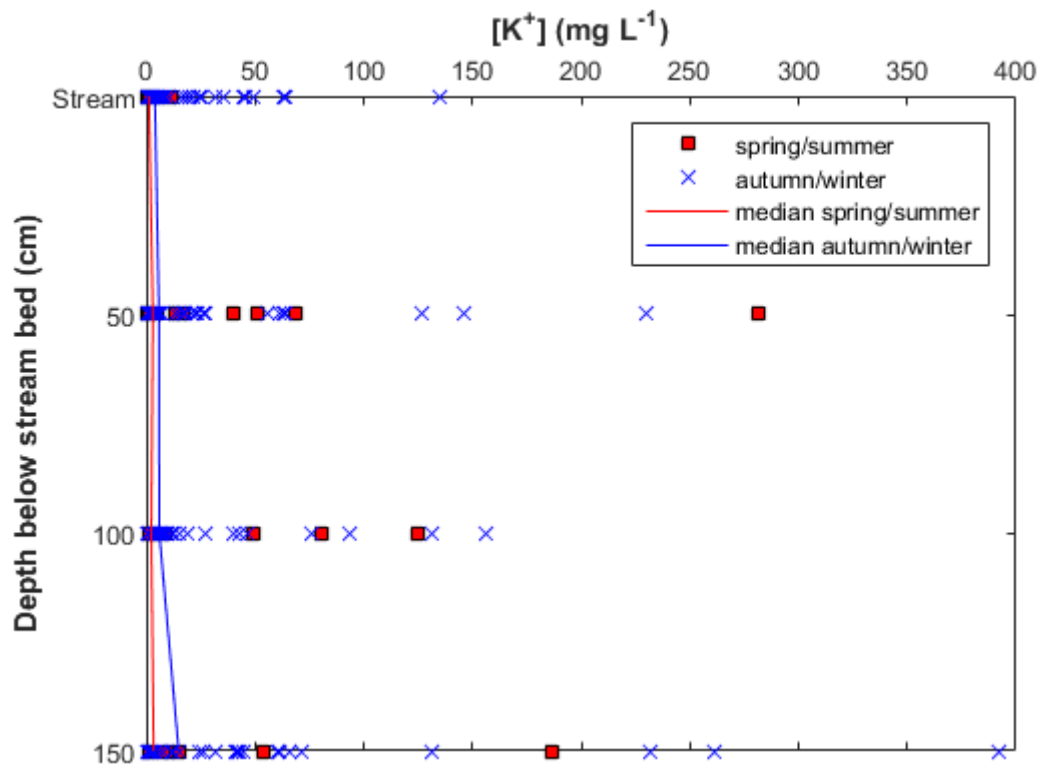


Figure 5.10 Depth profile of potassium concentrations from the stream to 1.5m below the streambed from spring/summer, collected between 7/3/2016 – 12/8/2016 (red) and autumn/winter (blue) samples collected between 19/11/2015 – 5/2/2016 and 9/9/2016 – 20/1/2017. The red and blue lines show the median values for spring/summer and autumn/winter samples respectively.

5.2.10 Magnesium

Depth profiles of spring/summer and autumn/winter magnesium concentrations are shown in Figure 5.11. As with the majority of the other major ions, stream magnesium concentrations were similar to those in the subsurface. There was a high degree of variability in the sample concentrations, especially at 1.0m below the stream surface. Seasonal variations were significant in the stream and 1.5m piezometer samples ($P < 0.05$ and $P < 0.01$, respectively) where the spring/summer samples contained higher magnesium concentrations. Median values were similar across the whole stream – 1.5m depth continuum and variability within depth horizons was roughly equivalent between both seasonal datasets (Tables 5.1 and 5.2).

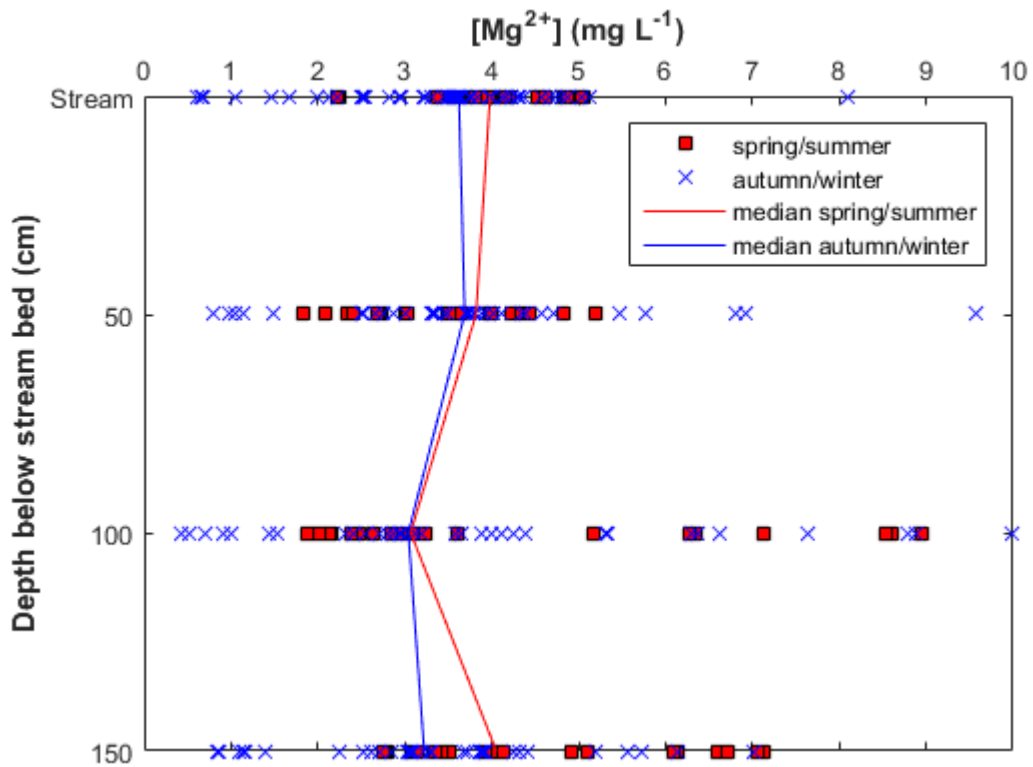


Figure 5.11 Depth profile of potassium concentrations from the stream to 1.5m below the streambed from spring/summer, collected between 7/3/2016 – 12/8/2016 (red) and autumn/winter (blue) samples collected between 19/11/2015 – 5/2/2016 and 9/9/2016 – 20/1/2017. The red and blue lines show the median values for spring/summer and autumn/winter samples respectively.

5.2.11 Sodium

Sodium concentration profiles are shown in Figure 5.12. Median concentrations remained similar throughout the depth profile. The only significant difference between the spring/summer and autumn samples was in the stream samples, where the spring/summer samples had a significantly higher median sodium concentration ($P < 0.01$). There was a high degree of variability at all depth horizons, mainly due to a number of low concentration autumn/winter samples.

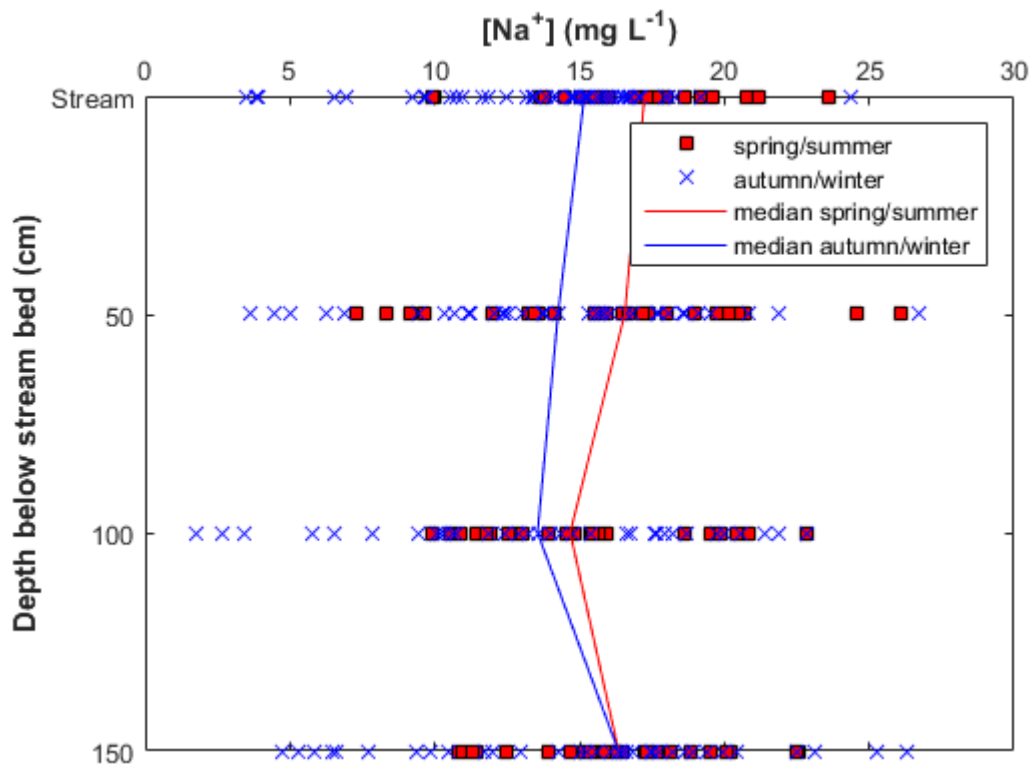


Figure 5.12 Depth profile of sodium concentrations from the stream to 1.5m below the streambed from spring/summer, collected between 7/3/2016 – 12/8/2016 (red) and autumn/winter (blue) samples collected between 19/11/2015 – 5/2/2016 and 9/9/2016 – 20/1/2017. The red and blue lines show the median values for spring/summer and autumn/winter samples respectively.

5.2.12 Dissolved organic carbon

Due to sample volume restrictions, not all samples were analysed for DOC concentration. As a result, DOC concentrations from only two spring/summer samples from each piezometer, and four from the stream were available, rendering a seasonal comparison impossible. Nevertheless, enough data were available to compare DOC concentrations from the stream to 1.5m depth, as shown in Figure 5.13. The range in the stream samples was narrower than in the piezometers and the median DOC concentration was significantly lower than the 0.5 and 1.0m piezometers ($P < 0.05$). There was no statistically significant difference in median DOC concentration between the 0.5, 1.0 and 1.5m piezometers.

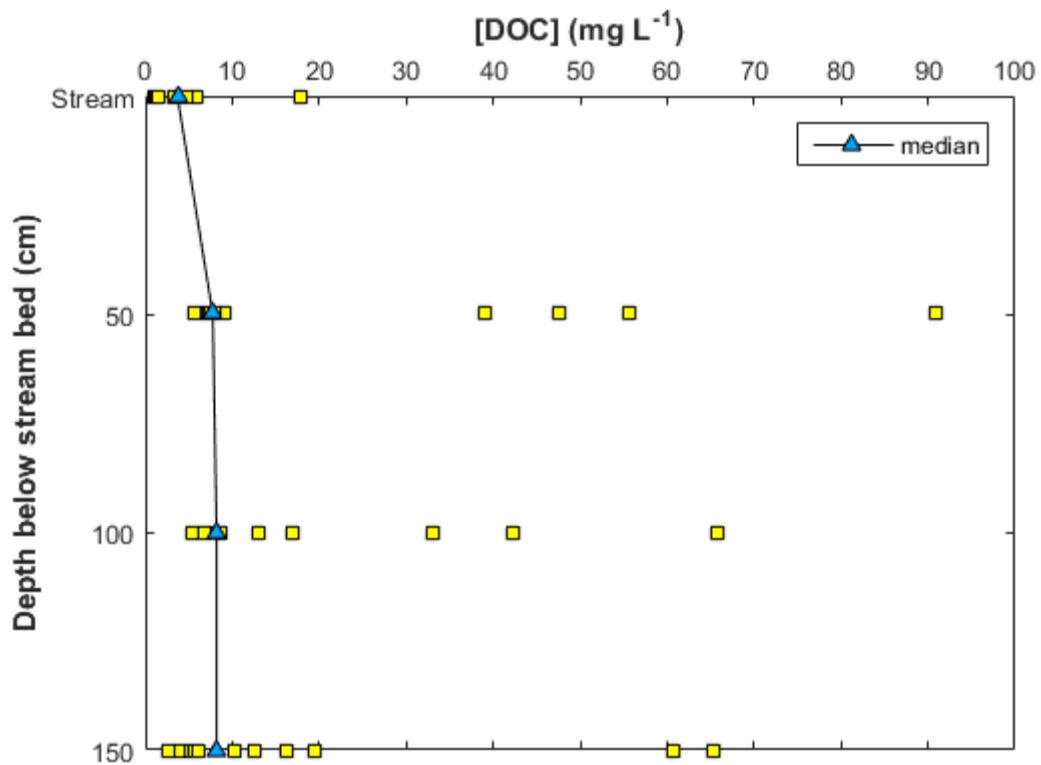


Figure 5.13 Depth profile of DOC concentrations from the stream to 1.5m below the streambed collected along a 1.6 km study reach. Samples were collected during the period of 19/11/2015 – 20/01/2017

5.2.13 Piezometer hydraulic head measurements and hydraulic gradients

Throughout the sampling campaign, groundwater head within the piezometers was measured to allow for calculation of the vertical direction of flow and hence to ascertain whether the sites at which the piezometer nests were installed (i.e. Sites 1-5) were zones of upwelling or downwelling. This empirical approach builds upon the visual interpretation of sediment loading and streambed geomorphology at each site described in Chapter 2. Table 5.5 shows the mean averaged head measurements above Ordinance Datum (aOD) in each of the piezometers between 22/04/2018 and 20/01/2017. Table 5.5 shows that Sites 2 and 5 were zones of groundwater discharge into the stream and that Sites 1, 3 and 4 were zones of surface water incorporation into the hyporheic zone, demonstrating that the piezometer nest sites covered both downwelling and upwelling zones during the sampling campaign. Vertical hydraulic gradients were calculated as $\frac{dh}{dz}$ where dh is the difference in hydraulic head between the 1.5m and 0.5m piezometers at a given site and dz is the difference in elevation at the centre of the screened section of the 1.5m and 0.5m piezometers, set to 1m.

Table 5.5. Piezometer nest mean vertical hydraulic gradient at Sites 1-5 covering a period between 22/04/2018 – 20/01/2017. Head measurements were collected with reference to ordnance datum and are expressed as metres above ordnance datum (aOD).

Piezometer	Head (m aOD)	Vertical hydraulic gradient at site	Overall direction of groundwater flow
1(0.5)	38.46	-0.34	Downwelling
1(1)	38.61		
1(1.5)	38.12		
2(0.5)	37.13	0.27	Upwelling
2(1)	37.33		
2(1.5)	37.39		
3(0.5)	36.24	-0.61	Downwelling
3(1)	36.00		
3(1.5)	35.63		
4(0.5)	33.80	-0.56	Downwelling
4(1)	33.84		
4(1.5)	33.24		
5(0.5)	32.41	0.01	Upwelling
5(1)	32.39		
5(1.5)	32.42		

5.2.14 Stable isotopes of nitrate along the stream - hyporheic zone continuum

Figure 5.14 shows the $\delta^{15}\text{N}_{\text{NO}_3}$ and $\delta^{18}\text{O}_{\text{NO}_3}$ values in the shallow sediment pore water profile (2.5 – 15cm) collected from the DET probes. The $\delta^{15}\text{N}_{\text{NO}_3}$ values show high variability along the 2.5 – 15cm sediment depth profile, though no statistically significant difference between depths was found ($P > 0.05$). The $\delta^{18}\text{O}_{\text{NO}_3}$ values show increasing levels of enrichment in $^{18}\text{O}_{\text{NO}_3}$ with depth up to 10cm, beyond which median values stabilise. Though such a trend was observed, the differences in $\delta^{18}\text{O}_{\text{NO}_3}$ values between depths were not significant ($P > 0.05$).

Stream and piezometer $\delta^{15}\text{N}_{\text{NO}_3}$ and $\delta^{18}\text{O}_{\text{NO}_3}$ values are shown in Figure 5.15. The $\delta^{15}\text{N}_{\text{NO}_3}$ values occupy a much narrower range than the $\delta^{18}\text{O}_{\text{NO}_3}$ values, with a small number of spring/summer samples in the 0.5m piezometer containing more enriched $^{15}\text{N}_{\text{NO}_3}$ than the bulk of the data. With the exception of the stream samples, autumn/winter $\delta^{15}\text{N}_{\text{NO}_3}$ values were slightly higher at all piezometer depths, though this difference was not statistically significant ($P > 0.05$). There were no significant differences in $\delta^{15}\text{N}_{\text{NO}_3}$ values between the stream and piezometers, or between piezometer depths ($P > 0.05$).

The $\delta^{18}\text{O}_{\text{NO}_3}$ values measured in stream and piezometer samples were highly variable, with the stream samples showing a much narrower range than the piezometers. The

stream sample $\delta^{18}\text{O}_{\text{NO}_3}$ values were significantly different in relation to all three piezometer depths ($P < 0.01$). In the 1.0m piezometer, the spring/summer samples were significantly more enriched in $^{18}\text{O}_{\text{NO}_3}$ than the autumn/winter samples ($P < 0.05$).

The $\delta^{15}\text{N}_{\text{NO}_3}$ and $\delta^{18}\text{O}_{\text{NO}_3}$ values in the stream samples fall within the range of nitrified soil ammonium and manure (Chapter 2) for the autumn/winter and spring/summer samples. In the piezometers, the $\delta^{15}\text{N}_{\text{NO}_3}$ and $\delta^{18}\text{O}_{\text{NO}_3}$ values were also within the range of nitrified soil ammonium and manure, though the $\delta^{18}\text{O}_{\text{NO}_3}$ values in some samples indicate the incorporation of some precipitation-derived nitrate.

For discussions in Section 5.3.4 it is important to show the $\delta^{15}\text{N}_{\text{NO}_3}$ and $\delta^{18}\text{O}_{\text{NO}_3}$ values measured in the 12 m borehole mentioned in Section 5.2.3. The $\delta^{15}\text{N}_{\text{NO}_3}$ and $\delta^{18}\text{O}_{\text{NO}_3}$ values measured in samples collected from this borehole were $+20.9 \pm 0.6 \text{ ‰}$ and $+17.8 \pm 0.6 \text{ ‰}$, respectively ($n = 5$).

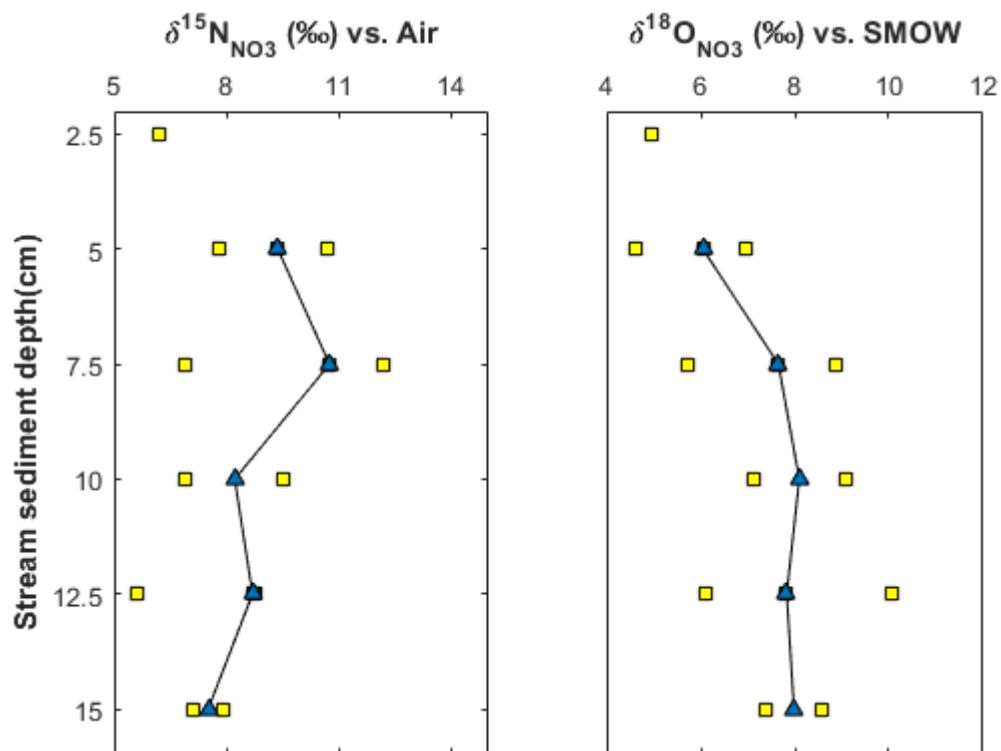


Figure 5.14 Shallow sediment pore water $\delta^{15}\text{N}_{\text{NO}_3}$ and $\delta^{18}\text{O}_{\text{NO}_3}$ values along a 2.5 – 15.0 cm profile from DET probes deployed at sampling Site 5 on 17/02/2017. Probes were retrieved on 20/02/20.

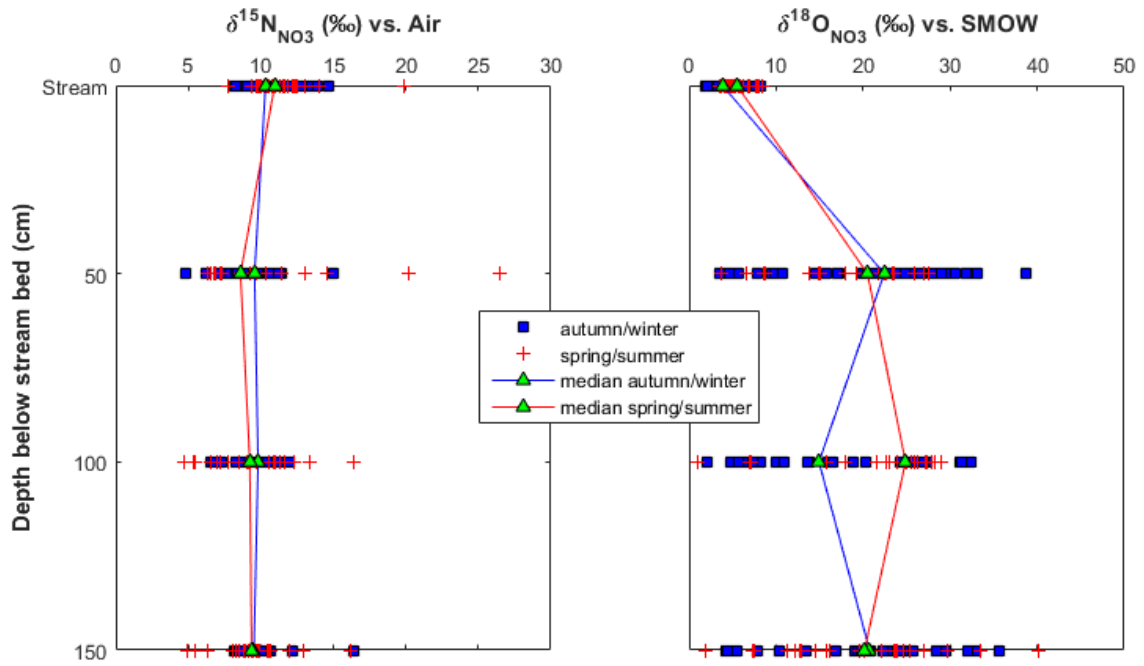


Figure 5.15 Stream, 0.5m, 1.0m and 1.5m piezometer $\delta^{15}\text{N}_{\text{NO}_3}$ and $\delta^{18}\text{O}_{\text{NO}_3}$ values in samples collected from five locations along the study reach. Samples collected between 19/11/2015 – 05/02/2016 and 09/09/2016 – 20/01/2017 represent the autumn/winter period, and samples collected between 07/03/2016 and 12/08/2016 represent the spring/summer period. Median values for both data sets are shown by the green triangles and corresponding coloured lines.

5.2.15 $\delta^{18}\text{O}_{\text{H}_2\text{O}}$ and $\delta^2\text{H}_{\text{H}_2\text{O}}$ values of stream and piezometer samples

Seasonal variations within precipitation $\delta^{18}\text{O}_{\text{H}_2\text{O}}$ and $\delta^2\text{H}_{\text{H}_2\text{O}}$ values exist as a result of fractionation processes relating to temperature and rainfall amount, as demonstrated in George (1998) for rainfall collected within the same study catchment, where the warmer, drier months are associated with isotopically heavier precipitation than the cooler, wetter months. Figure 5.16 compares the $\delta^{18}\text{O}_{\text{H}_2\text{O}}$ values in the stream and piezometer samples between seasons. Contrary to George (1998), there were no statistically significant differences between $\delta^{18}\text{O}_{\text{H}_2\text{O}}$ values when spring, summer, autumn and winter samples were compared for the stream and piezometer samples ($P > 0.05$). There was only one exception to this, in the 1.0m piezometer samples, where autumn $\delta^{18}\text{O}_{\text{H}_2\text{O}}$ was significantly more enriched than in the winter and spring samples ($P < 0.001$). In Figure 5.17, seasonal $\delta^{18}\text{O}_{\text{H}_2\text{O}}$ values are compared between depth horizons from the stream to 1.5m depth below the stream bed. In all seasons, the stream $\delta^{18}\text{O}_{\text{H}_2\text{O}}$ values were significantly higher than the piezometer samples ($P < 0.01$). During the winter, the 0.5m piezometer samples were significantly isotopically more enriched in ^{18}O than at 1.0m depth ($P < 0.05$). In the spring samples the 0.5m and 1.5m samples were significantly

more enriched than at 1.0m depth ($P < 0.05$). The summer samples showed significantly higher $\delta^{18}\text{O}_{\text{H}_2\text{O}}$ values in the 0.5m piezometer than at 1.0m depth ($P < 0.05$). The autumn samples showed no significant differences between the piezometer samples.

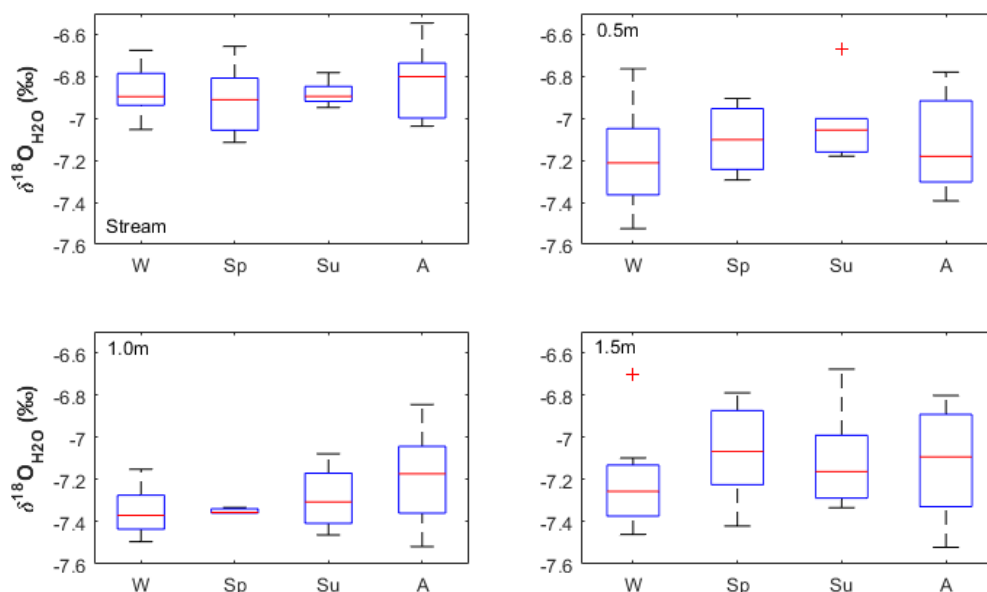


Figure 5.16 Boxplots comparing $\delta^{18}\text{O}_{\text{H}_2\text{O}}$ values along the stream - 1.5m depth profile by season in samples collected between November 2015 and January 2017. W = winter, Sp = spring, Su = summer, A = autumn. The range of concentrations is shown by the whiskers and the boxes illustrate the interquartile range of nitrate concentrations. The red crosses represent outliers. Horizontal lines represent the median $\delta^{18}\text{O}_{\text{H}_2\text{O}}$.

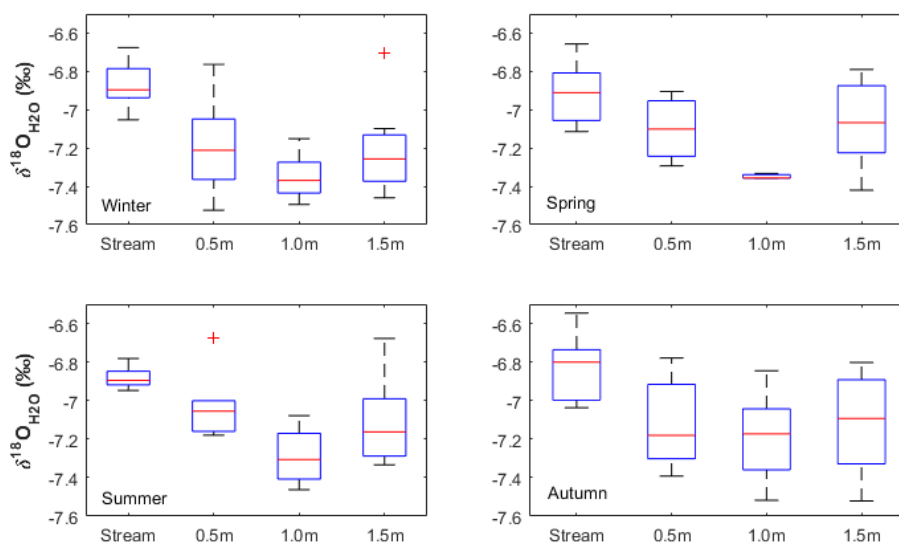


Figure 5.17 Boxplots comparing seasonal $\delta^{18}\text{O}_{\text{H}_2\text{O}}$ values by depth along the stream - 1.5m continuum in samples collected between November 2015 and January 2017. W = winter, Sp = spring, Su = summer, A = autumn. The range of concentrations is shown by the whiskers and the boxes illustrate the interquartile range of nitrate concentrations. The red crosses represent outliers. Horizontal lines represent the median $\delta^{18}\text{O}_{\text{H}_2\text{O}}$.

The stream $\delta^2\text{H}_{\text{H}_2\text{O}}$ values presented as a cross-plot in Figure 5.18 cover a wide range with little partitioning between seasons, while the $\delta^{18}\text{O}_{\text{H}_2\text{O}}$ values are within one per mille. The exception is during the summer. Summer $\delta^{18}\text{O}_{\text{H}_2\text{O}}$ and $\delta^2\text{H}_{\text{H}_2\text{O}}$ values were more discretely clustered than the spring, autumn and winter seasons. The stream samples were all more enriched in $\delta^{18}\text{O}_{\text{H}_2\text{O}}$ and $\delta^2\text{H}_{\text{H}_2\text{O}}$ than the volume weighted average precipitation value from George (1998) and also the chalk groundwater. There was no preservation in the seasonal signal in the 0.5m piezometer samples (Figure 5.19). In the 1.0 and 1.5 m piezometer samples, the seasonal signal of $\delta^{18}\text{O}_{\text{H}_2\text{O}}$ and $\delta^2\text{H}_{\text{H}_2\text{O}}$ values was preserved to some extent (Figures 5.20 and 5.21). The winter values consistently occupied the lower end of the range, though some autumn, summer and spring values were also similar to the winter values. Furthermore, at 1.0 m depth it is autumn values, not the spring or summer values that showed the heaviest isotopic signature.

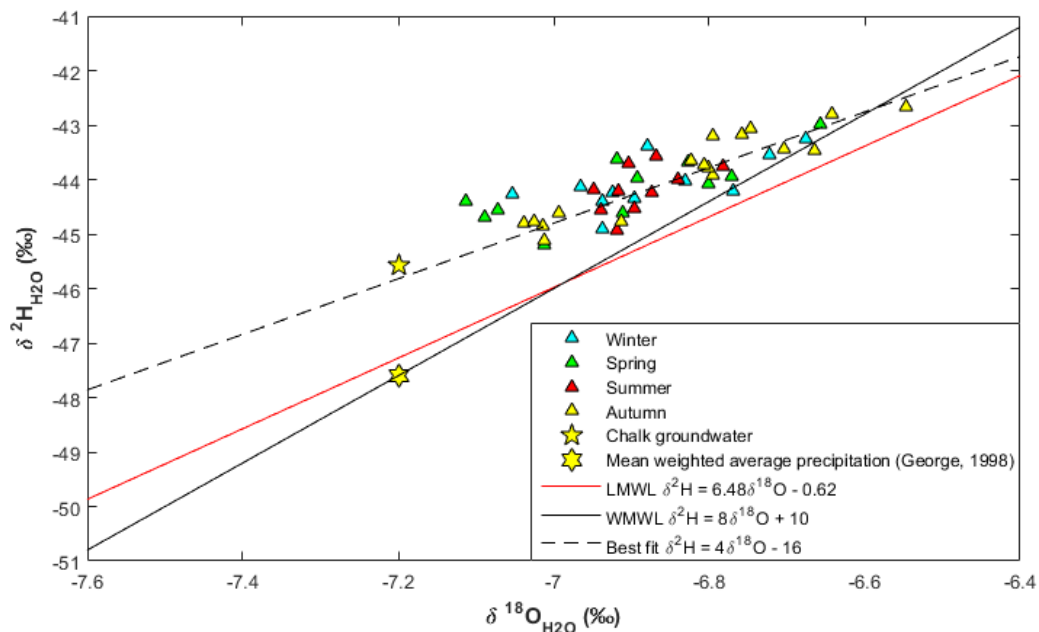


Figure 5.18 $\delta^{18}\text{O}_{\text{H}_2\text{O}}$ and $\delta^2\text{H}_{\text{H}_2\text{O}}$ values for stream samples. The black line represents the world meteoric water line and the red line shows the local meteoric water line, the black dashed line is the best fit line for the data. Chalk groundwater from 50m below the ground surface and the volume weighted average precipitation and local meteoric water line (LMWL) from George (1998) are also shown. The world meteoric water line (WMWL) is from Craig (1961).

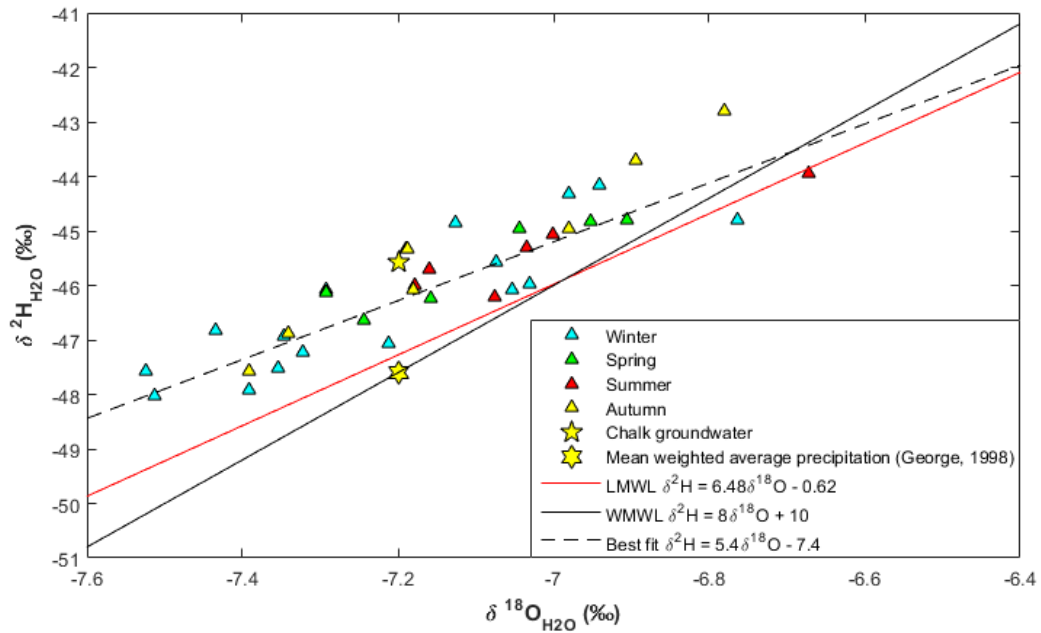


Figure 5.19 $\delta^{18}\text{O}_{\text{H}_2\text{O}}$ and $\delta^2\text{H}_{\text{H}_2\text{O}}$ values for 0.5 m piezometer samples. The black line represents the world meteoric water line and the red line shows the local meteoric water line, the black dashed line is the best fit line for the data. Chalk groundwater from 50m below the ground surface and the volume weighted average precipitation and local meteoric water line (LMWL) from George (1998) are also shown. The world meteoric water line (WMWL) is from Craig (1961).

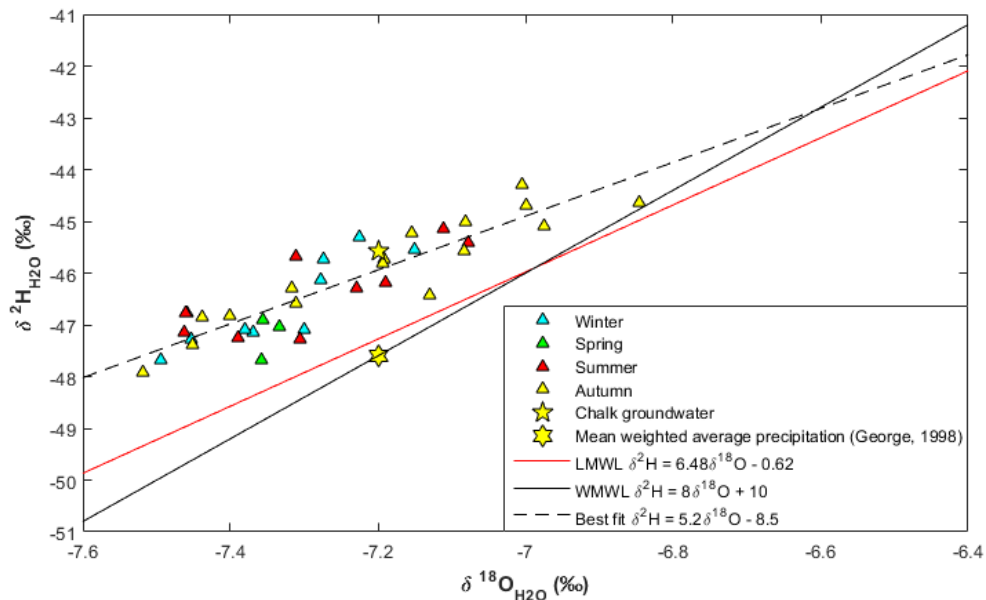


Figure 5.20 $\delta^{18}\text{O}_{\text{H}_2\text{O}}$ and $\delta^2\text{H}_{\text{H}_2\text{O}}$ values for 1.0 m piezometer samples. The black line represents the world meteoric water line and the red line shows the local meteoric water line, the black dashed line is the best fit line for the data. Chalk groundwater from 50m below the ground surface and the volume weighted average precipitation and local meteoric water line (LMWL) from George (1998) are also shown. The world meteoric water line (WMWL) is from Craig (1961).

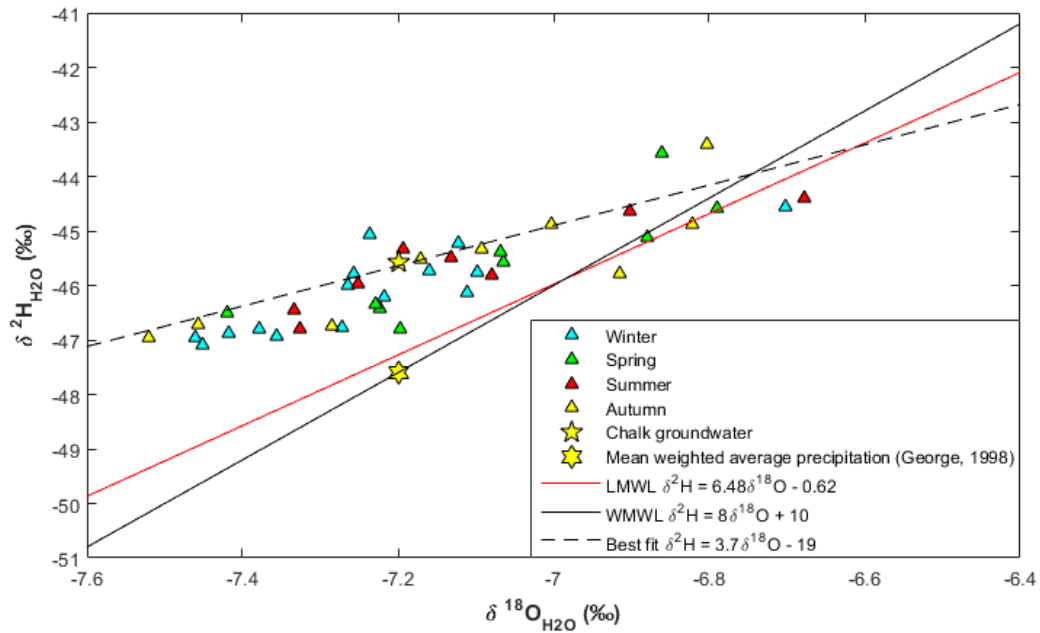


Figure 5.21 $\delta^{18}\text{O}_{\text{H}_2\text{O}}$ and $\delta^2\text{H}_{\text{H}_2\text{O}}$ values for 1.5 m piezometer samples. The black line represents the world meteoric water line and the red line shows the local meteoric water line, the black dashed line is the best fit line for the data. Chalk groundwater from 50m below the ground surface and the volume weighted average precipitation and local meteoric water line (LMWL) from George (1998) are also shown. The world meteoric water line (WMWL) is from Craig (1961).

The distribution of the complete data set of $\delta^{18}\text{O}_{\text{H}_2\text{O}}$ and $\delta^2\text{H}_{\text{H}_2\text{O}}$ values between the stream and piezometer samples is shown in Figure 5.22. In Figure 5.22 the data have not been separated temporally, rather by depth horizon along the vertical profile (stream, 0.5, 1.0 and 1.5 m beneath the stream bed). As discussed, the stream samples were isotopically most enriched while the piezometer samples occupy a wider range, with little distinction between depth horizons. The majority of the 1.0m piezometer samples were at the lighter end of the range, whilst the 1.5m piezometer samples forming two distinct groups, with the lighter group comprised of the majority of the winter samples at this depth.

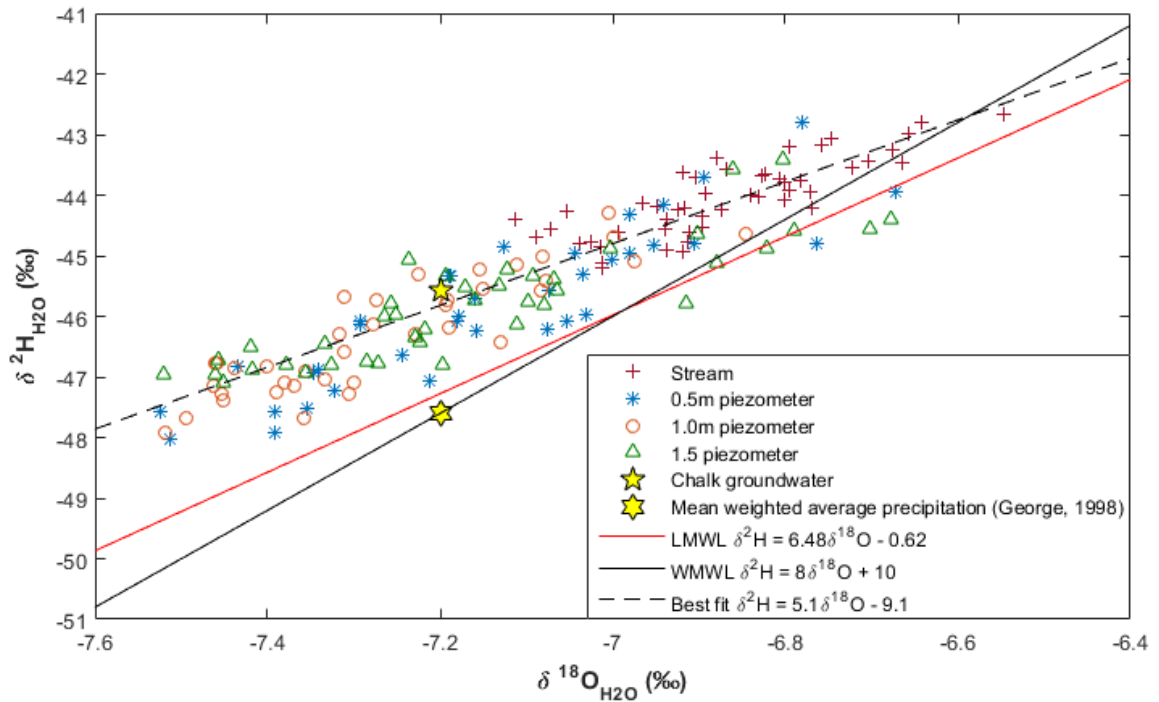


Figure 5.22 $\delta^{18}\text{O}_{\text{H}_2\text{O}}$ and $\delta^2\text{H}_{\text{H}_2\text{O}}$ values for all stream and piezometer samples. The black line represents the world meteoric water line and the red line shows the local meteoric water line. Chalk groundwater from 50m below the ground surface and the volume weighted average precipitation and local meteoric water line (LMWL) from George (1998) are also shown. The world meteoric water line (WMWL) is from Craig (1961).

5.3 Discussion

5.3.1 Isotopic evidence for denitrification in the stream, benthic sediment and hyporheic zone

The stream $\delta^{15}\text{N}_{\text{NO}_3}$ and $\delta^{18}\text{O}_{\text{NO}_3}$ values are shown as a cross-plot in Figure 5.23. Stream samples show dual fractionation of ^{15}N and ^{18}O , a relationship associated with denitrification, discussed in Chapter 2. The gradient of the best fit line was 0.88 however, above the range reported in the literature associated with microbially-mediated denitrification where the fractionation of nitrogen to oxygen atoms occurs in a roughly 2:1 ratio (resulting in a slope of 0.5 when $\delta^{15}\text{N}_{\text{NO}_3}$ and $\delta^{18}\text{O}_{\text{NO}_3}$ values are plotted together) (0.35 – 0.76, Bottcher *et al.*, 1999; Aravena and Robertson, 1998; Mengis *et al.*, 1999; Cey *et al.*, 1999; Panno *et al.*, 2006; Wexler *et al.*, 2014; Fukada *et al.*, 2003). There was a reasonable correlation between $\delta^{15}\text{N}_{\text{NO}_3}$ and $\delta^{18}\text{O}_{\text{NO}_3}$ values ($r^2 = 0.61$). The $\delta^{15}\text{N}_{\text{NO}_3}$ and $\delta^{18}\text{O}_{\text{NO}_3}$ values measured in the stream samples fell within the range of manure and septic waste, as demonstrated in Chapter 2. The study site was within an arable system, hence there was no livestock contributing manure to the pool of reactive nitrogen. Therefore, it is possible that the isotopic composition of the nitrate measured in the stream water was the result of progressive denitrification of nitrified and subsequently denitrified soil ammonium. There were some turkey manure additions made to fields elsewhere in the study catchment, however these were applied August/September 2015 and so the later samples would not have incorporated this.

Examining $\delta^{15}\text{N}_{\text{NO}_3}$ and $\delta^{18}\text{O}_{\text{NO}_3}$ values in relation to nitrate concentration can introduce an extra layer of detail when attempting to identify the cause of isotopic fractionation such as that shown in Figure 5.23. Figures 5.24 and 5.25 show stream $\delta^{15}\text{N}_{\text{NO}_3}$ and $\delta^{18}\text{O}_{\text{NO}_3}$ values plotted against nitrate concentrations. If denitrification were responsible for the trend in the $\delta^{15}\text{N}_{\text{NO}_3}$ and $\delta^{18}\text{O}_{\text{NO}_3}$ values shown in Figure 5.23, then it would be expected that nitrate ^{15}N and ^{18}O composition to increase as the nitrate concentration decreased, as is demonstrated in the field drain samples presented in Chapter 4. This relationship is not shown in the stream samples, indicating that either denitrification was not the cause of the dual isotopic fractionation, or that some process is acting to maintain stream nitrate concentrations. Since the stream is well mixed, with sources from groundwater, surface runoff, soil leachate and precipitation, the expected relationship between nitrate concentration and $\delta^{15}\text{N}_{\text{NO}_3}$ and $\delta^{18}\text{O}_{\text{NO}_3}$ values was probably masked.

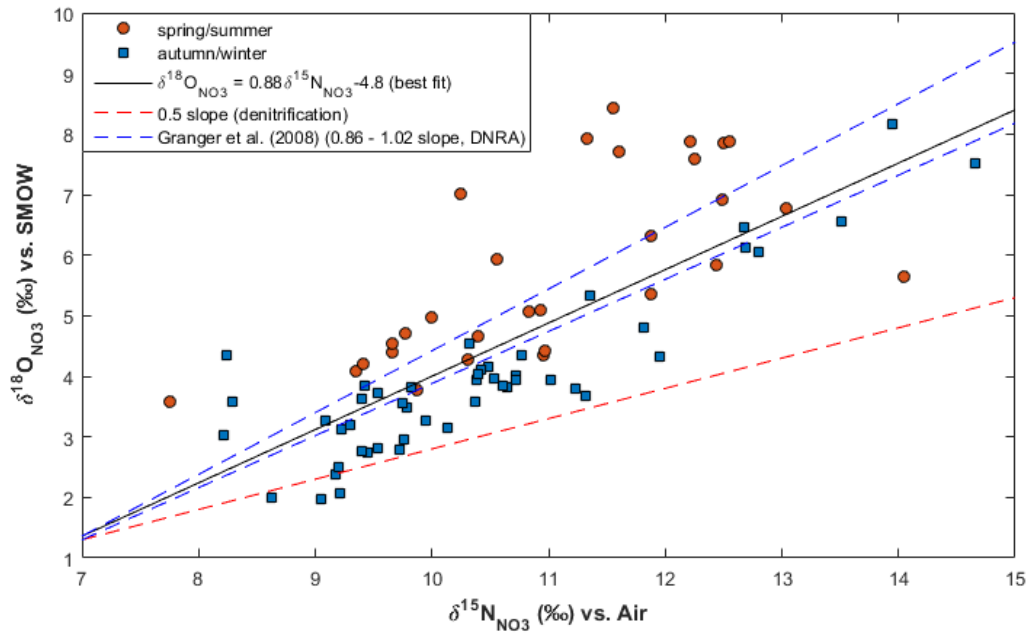


Figure 5.23 Crossplot of $\delta^{18}\text{O}_{\text{NO}_3}$ vs $\delta^{15}\text{N}_{\text{NO}_3}$ values measured in stream samples separated into spring/summer samples, collected between 7/3/2016 – 12/8/2016 (red) and autumn/winter (blue) samples collected between 19/11/2015 – 5/2/2016 and 9/9/2016 – 20/1/2017. Samples were collected from five locations along the 1.6 km study reach. The solid black line represents the best fit line for the data, the dashed red line represents a theoretical 0.5 slope resulting from the ideal 2:1 nitrogen:oxygen isotope fractionation associated with denitrification. The dashed blue lines show the range of slopes presented in Granger et al. (2008) associated with dissimilatory reduction of nitrate to

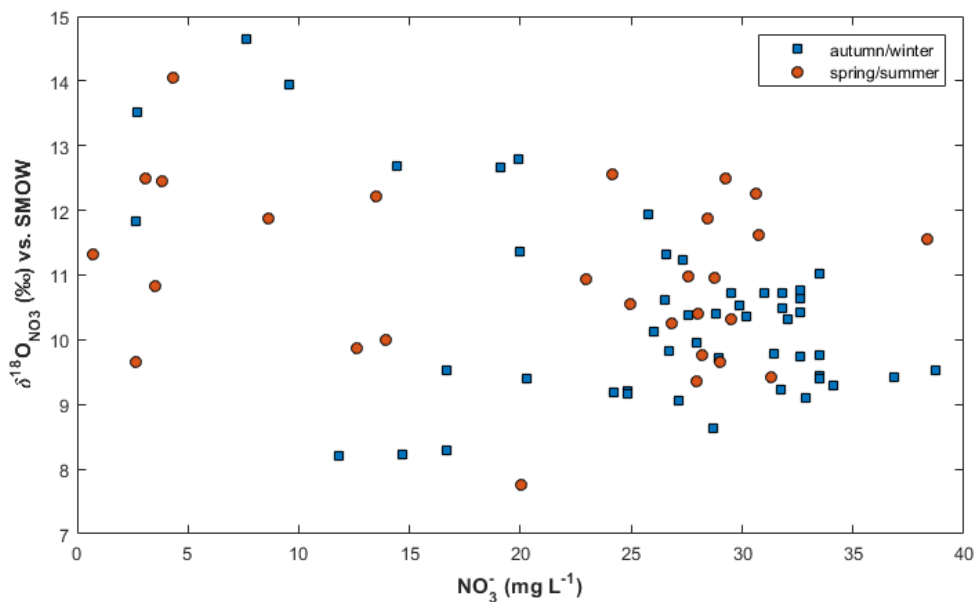


Figure 5.24 Relationship between $\delta^{15}\text{N}_{\text{NO}_3}$ values and stream nitrate concentrations. Samples separated into spring/summer samples, collected between 7/3/2016 – 12/8/2016 (red) and autumn/winter (blue) samples collected between 19/11/2015 – 5/2/2016 and 9/9/2016 – 20/1/2017. Samples were collected from five locations along the 1.6 km study reach.

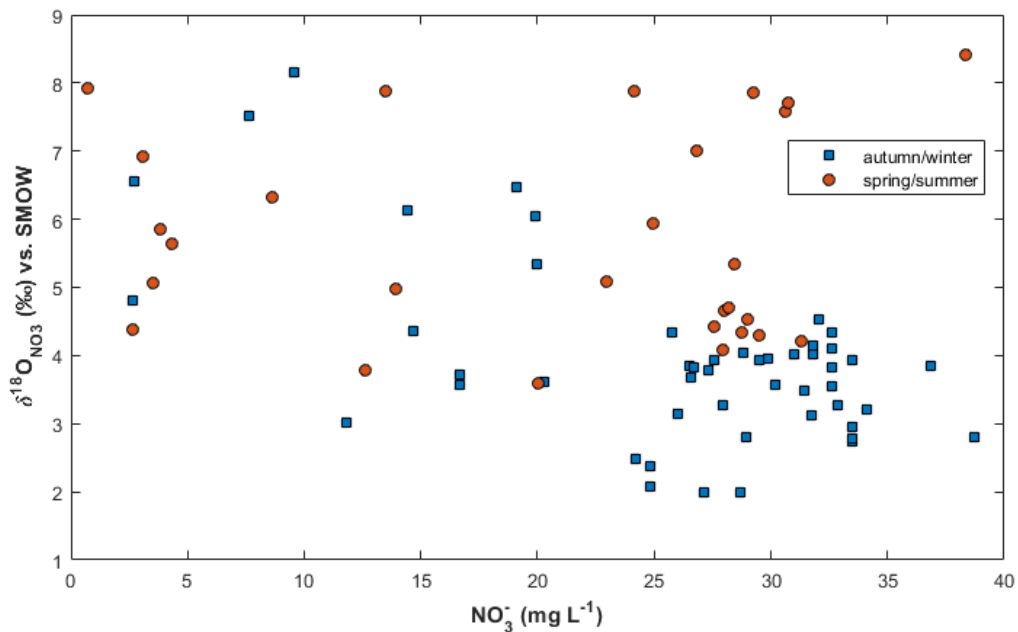


Figure 5.25 Relationship between $\delta^{18}\text{O}_{\text{NO}_3}$ values and stream nitrate concentrations. Samples separated into spring/summer samples, collected between 7/3/2016 – 12/8/2016 (red) and autumn/winter (blue) samples collected between 19/11/2015 – 5/2/2016 and 9/9/2016 – 20/1/2017. Samples were collected from five locations along the 1.6 km study reach.

Unfortunately, not all of the DET samples were suitable for nitrate isotope analysis, consequently $\delta^{15}\text{N}_{\text{NO}_3}$ and $\delta^{18}\text{O}_{\text{NO}_3}$ values for the shallow stream benthic sediment depth profile (2.5 – 15.0cm) are sparse. Figure 5.26 shows potential dual fractionation of $\delta^{15}\text{N}_{\text{NO}_3}$ and $\delta^{18}\text{O}_{\text{NO}_3}$ values within the stream sediment, however because the data are few in number the trend is weak (r^2 0.14), therefore this is only suggested tentatively. Benthic sediments do typically contain conditions that are favourable for microbially-mediated denitrification (Rahimi *et al.*, 2015), discussed in section 5.3.2. The source signal of the nitrate isotopes in the benthic sediment was similar to that of the stream, suggesting that soil ammonium acts as the pool of reactive nitrogen. There was no distinction between depth horizons within the sediment in terms of $\delta^{15}\text{N}_{\text{NO}_3}$ and $\delta^{18}\text{O}_{\text{NO}_3}$ values, though the data were too few in number to perform statistical analyses in order to ascertain whether or not the depth horizons were truly significantly different from one another.

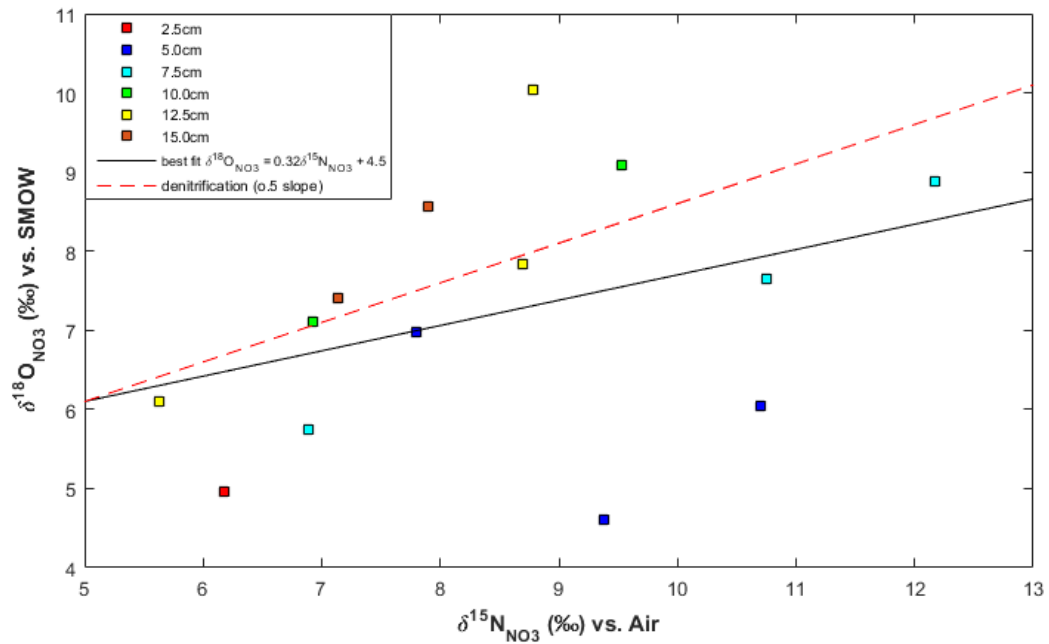


Figure 5.26 Shallow sediment profile (2.5 – 15.0cm below the stream bed) of $\delta^{15}\text{N}_{\text{NO}_3}$ and $\delta^{18}\text{O}_{\text{NO}_3}$ values. The black line represents the best fit line for the data with a slope of 0.32. The red dashed line represents a theoretical 0.5 slope associated with microbially-mediated denitrification.

There was no indication of hyporheic zone denitrification based on the $\delta^{15}\text{N}_{\text{NO}_3}$ and $\delta^{18}\text{O}_{\text{NO}_3}$ values from samples collected from the piezometers (Figure 5.27 – 5.29). A small subset of samples from the 0.5 m piezometers did appear to show a linear correlation between the $^{15}\text{N}_{\text{NO}_3}$ and $^{18}\text{O}_{\text{NO}_3}$ isotopic composition. But the vast majority of this sample subset was collected between March 2016 and July 2016 and so were subject to different climatic and hydrological conditions, hence there was no correlation between the data points and no suggestion that this apparent trend should be due to denitrification. In all piezometer depths, the data occupied a narrow $\delta^{15}\text{N}_{\text{NO}_3}$, and wide $\delta^{18}\text{O}_{\text{NO}_3}$ range. The piezometer samples showed markedly different ranges of $\delta^{15}\text{N}_{\text{NO}_3}$ and $\delta^{18}\text{O}_{\text{NO}_3}$ values with respect to the stream and DET samples. In the piezometers, the source of nitrate appears to be a combination of nitrified soil ammonium, nitrate fertiliser and a small number of samples contain nitrate originating from atmospheric deposition.

The classical understanding of exchange of water across the groundwater-surface water interface is that where downwelling occurs, dissolved oxygen and carbon is transferred to the groundwater, and in zones of upwelling, nitrate rich, low oxygen water is delivered to the surface. Table 5.5 shows that Sites 2 and 5 were zones of groundwater discharge into

the stream and that Sites 1, 3 and 4 were zones of surface water incorporation into the hyporheic zone, demonstrating that the piezometer nest sites covered both downwelling and upwelling zones during the sampling campaign. Table 5.1 shows the dissolved oxygen concentrations measured in all piezometer samples across the sampling sites. When examined individually, there is no statistically significant difference in the mean dissolved oxygen or nitrate concentration measured in the piezometer samples at each site and any depth (1.5, 1.0 or 0.5m). Furthermore, Figure 5.13 shows the DOC concentration measured in each piezometer. Again, when examined individually, there is no significant difference between sites in terms of DOC concentration between sampling sites. The same lack of isotopic evidence exists at each sampling site. Therefore, it is suggested that the direction of flow of water across the groundwater-surface water boundary was not a determining factor in hyporheic denitrification in this instance, possibly due to the relatively oxic conditions measured in all piezometer samples. The dissolved oxygen concentration measured in the piezometer samples ranged from 1.49-9.30mg L⁻¹, indicating oxic conditions within the hyporheic zone and hence indicates a lack of anoxic conditions necessary for the onset of denitrification at 0.5-1.5m below the stream bed along the study reach. This helps to explain the lack of isotopic evidence for denitrification at depth beneath the stream bed.

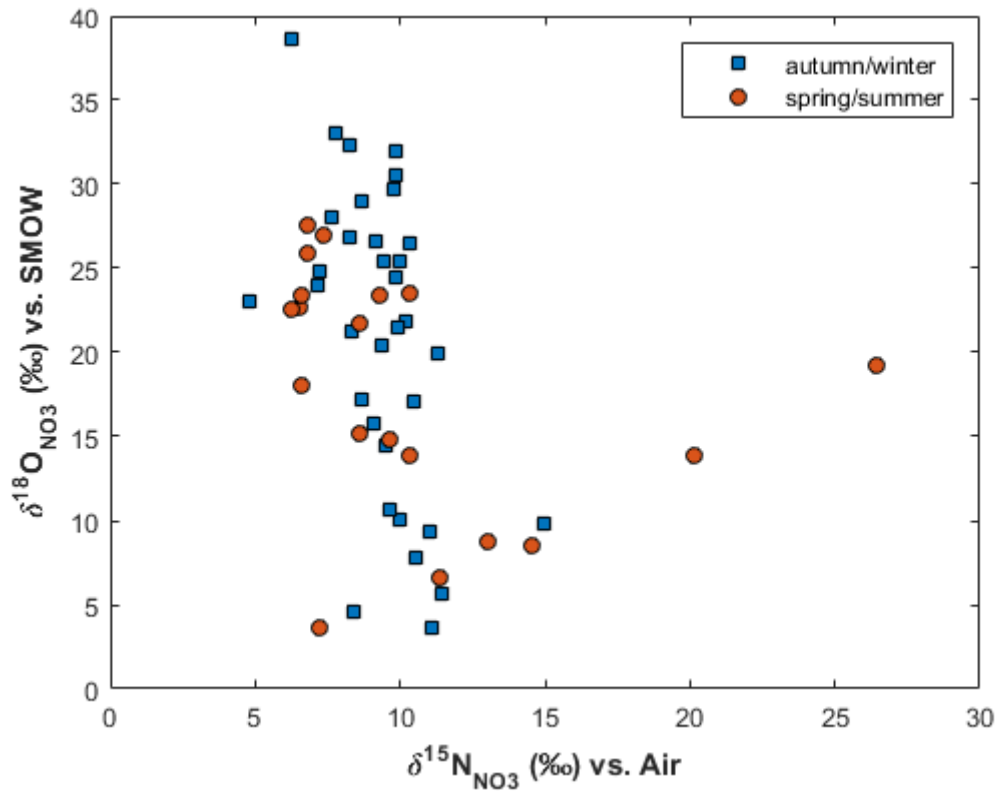


Figure 5.27 Cross-plot of $\delta^{15}\text{N}_{\text{NO}_3}$ and $\delta^{18}\text{O}_{\text{NO}_3}$ values measured in 0.5 m piezometer samples separated into spring/summer samples, collected between 7/3/2016 – 12/8/2016 (red) and autumn/winter (blue) samples collected between 19/11/2015 – 5/2/2016 and 9/9/2016 – 20/1/2017. Samples were collected from five locations along the 1.6 km study reach.

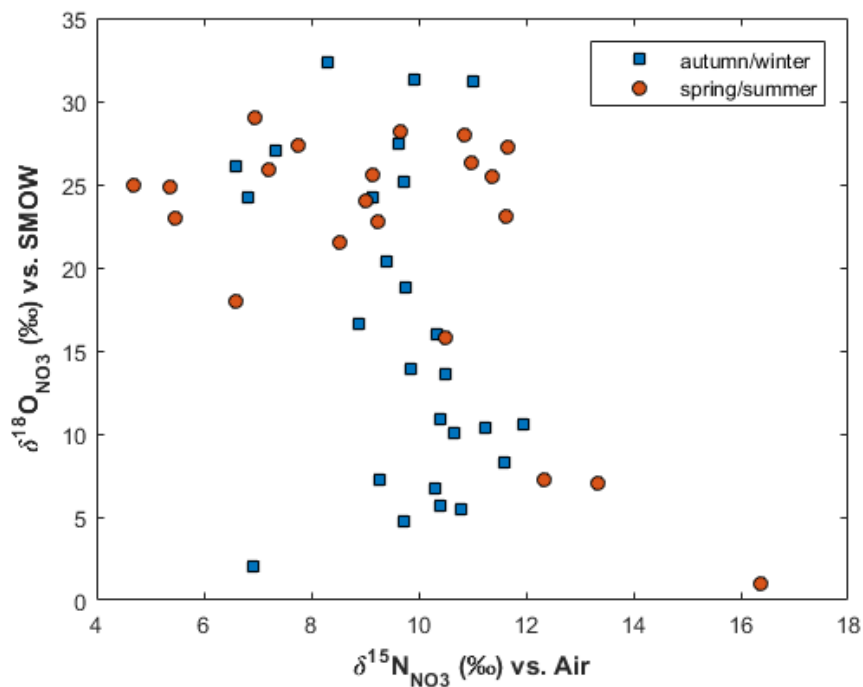


Figure 5.28 Cross-plot of $\delta^{15}\text{N}_{\text{NO}_3}$ and $\delta^{18}\text{O}_{\text{NO}_3}$ values measured in 1.0 m piezometer samples separated into spring/summer samples, collected between 7/3/2016 – 12/8/2016 (red) and autumn/winter (blue) samples collected between 19/11/2015 – 5/2/2016 and 9/9/2016 – 20/1/2017. Samples were collected from five locations along the 1.6 km study reach.

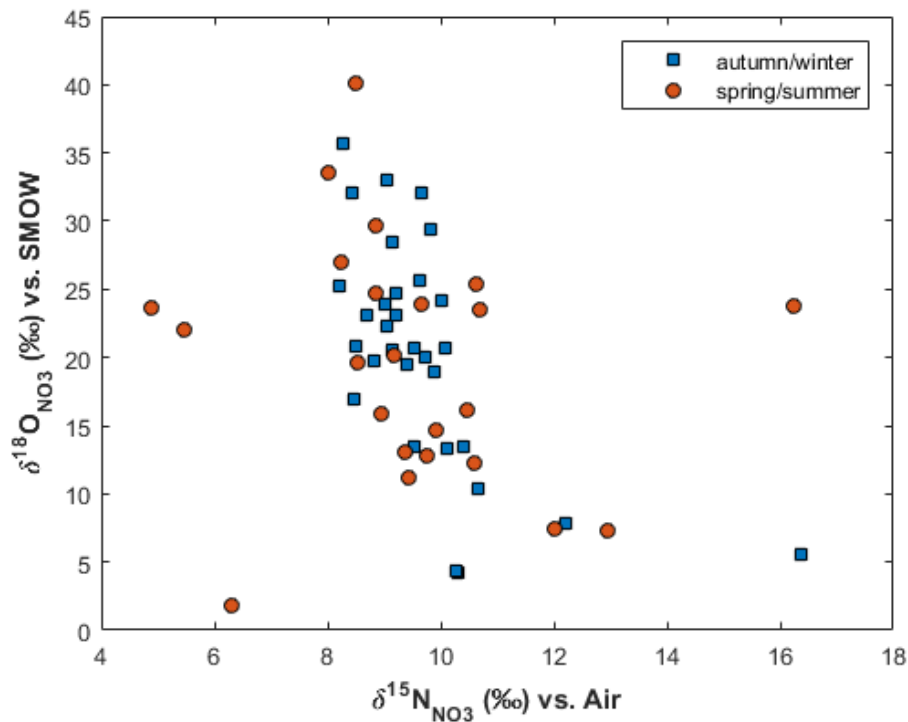


Figure 5.29 Cross-plot of $\delta^{15}\text{N}_{\text{NO}_3}$ and $\delta^{18}\text{O}_{\text{NO}_3}$ values measured in 1.5 m piezometer samples separated into spring/summer samples, collected between 7/3/2016 – 12/8/2016 (red) and autumn/winter (blue) samples collected between 19/11/2015 – 5/2/2016 and 9/9/2016 – 20/1/2017. Samples were collected from five locations along the 1.6 km study reach.

5.3.2 Transfer of water across the groundwater - surface water interface

As discussed in Chapter 2, the hydrological regime in the study site is characterised by a high baseflow index, hence stream flow is dominated by groundwater inputs. This is reflected in the summer stream $\delta^{18}\text{O}_{\text{H}_2\text{O}}$ and $\delta^2\text{H}_{\text{H}_2\text{O}}$ values, where the data are discretely clustered in relation to data from the other seasons, indicating little variation in precipitation and runoff, while the other seasons, which relative to the summer receive more variable precipitation events. The higher range in the $\delta^{18}\text{O}_{\text{H}_2\text{O}}$ and $\delta^2\text{H}_{\text{H}_2\text{O}}$ values for the spring, autumn and winter reflects the antecedent conditions within the study area (Figure 5.18). Ali and Roy (2010) explained that when the antecedent conditions are wet, the spatial connectivity of a catchment is increased and that runoff responses are likely heavily influenced by pre-event water. In other words, if a catchment is wet prior to a storm event, it is this existing water that dominates the flux of water and nutrients, rather than the event water because the system is considered primed, so any additional water from a precipitation event will quickly increase the hydrological connectivity. If the connectivity of the catchment was increased under wet antecedent conditions, then two scenarios might arise: (1) as the stream gauge rises due to precipitation, more stream

water is pushed into the subsurface as a result of the increasing pressure. (2) As the water table rises due to wetter conditions throughout the catchment, more groundwater is discharged into the stream. This additional groundwater influence would be masked as a result of the coinciding additional runoff. Therefore, only under baseflow conditions is the groundwater contribution to the stream detectable as a discrete component.

Where stream water is pushed into the subsurface due to increasing stream gauge under high precipitation conditions, it is likely that this would only be detectable in the 0.5 m piezometer, if at all. Figure 5.19 shows the seasonal $\delta^{18}\text{O}_{\text{H}_2\text{O}}$ and $\delta^2\text{H}_{\text{H}_2\text{O}}$ values from samples collected from the 0.5 m piezometers. Since the stream water isotopic signature was heavier than the majority of the 0.5 m piezometer samples (Figure 5.22), the autumn and winter samples should be isotopically heavier at this depth than during the drier months if a higher (than during the spring/summer) proportion of stream water was incorporated into the subsurface. Instead, the range in the $\delta^{18}\text{O}_{\text{H}_2\text{O}}$ and $\delta^2\text{H}_{\text{H}_2\text{O}}$ values for the 0.5 m piezometers reflects the seasonal precipitation trend, where isotopically lighter water infiltrates into the hyporheic zone during the wetter months due to rain out effects and reduced evaporation relative to the warmer months (George, 1998).

There were winter samples at the more enriched end of the range of $\delta^2\text{H}_{\text{H}_2\text{O}}$ values however, potentially suggesting that stream water can be transported to 50 cm below the stream bed, but it is likely that this can only happen during prolonged or heavy rainfall events (Briody *et al.*, 2016; Liu *et al.*, 2017), and that the typical precipitation regime does not cause incorporation of stream water to this depth horizon. Figure 5.30 shows the 0.5 m piezometer $\delta^{18}\text{O}_{\text{H}_2\text{O}}$ values against precipitation. Figure 5.30 shows that while there were some more enriched (than the mean) $\delta^{18}\text{O}_{\text{H}_2\text{O}}$ values measured in samples following heavy rainfall events (e.g. samples collected on 7/3/16), isotopically depleted values were also recorded following such events (e.g. 8/1/16) and vice versa, where isotopically enriched samples were collected on sampling days where there was no preceding heavy rainfall (e.g. 12/8/16). The averaged $\delta^{18}\text{O}_{\text{H}_2\text{O}}$ values are obtained from samples collected on the same day but at different points along the study reach (e.g. the average $\delta^{18}\text{O}_{\text{H}_2\text{O}}$ values for 7/12/15 are comprised of samples from Sites 1-5). Given the high variability as illustrated by the large error bars shown in Figure 5.30, it is possible that there was variation in the connectivity between the stream and subsurface along the study reach, suggesting the possibility of preferential flow paths where at one sampling site along the

study reach, stream water enters the 0.5 m piezometer more readily than at another site. If there was variation in the exchange of surface water and groundwater along the stream, then the exchange of nutrients and organic material would also vary downstream, hence potentially generating discrete zones where denitrification potential is higher, or ‘hot spots’. In this case, the intensity of rainfall events might not be as important as the presence or absence of preferential flow paths. It is possible that at shallower (than 0.5 m) depths the introduction of stream water into the subsurface following rainfall events is more pronounced, however water isotope data for the 0-0.5 m depth profile were not available. Given the lack of isotopic evidence for denitrification in any piezometers (Figures 5.27 – 5.29) however, and the evidence for denitrification in the shallow depth profile (0-15 cm below the stream bed) (Figure 5.26), it is likely that the benthic sediment contains conditions better suited for denitrification than at the depths to which the piezometers were installed. DET probes were only installed at Site 5 and so comparison of the variation in nitrate isotopic signature in the benthic sediments between sites was not possible.

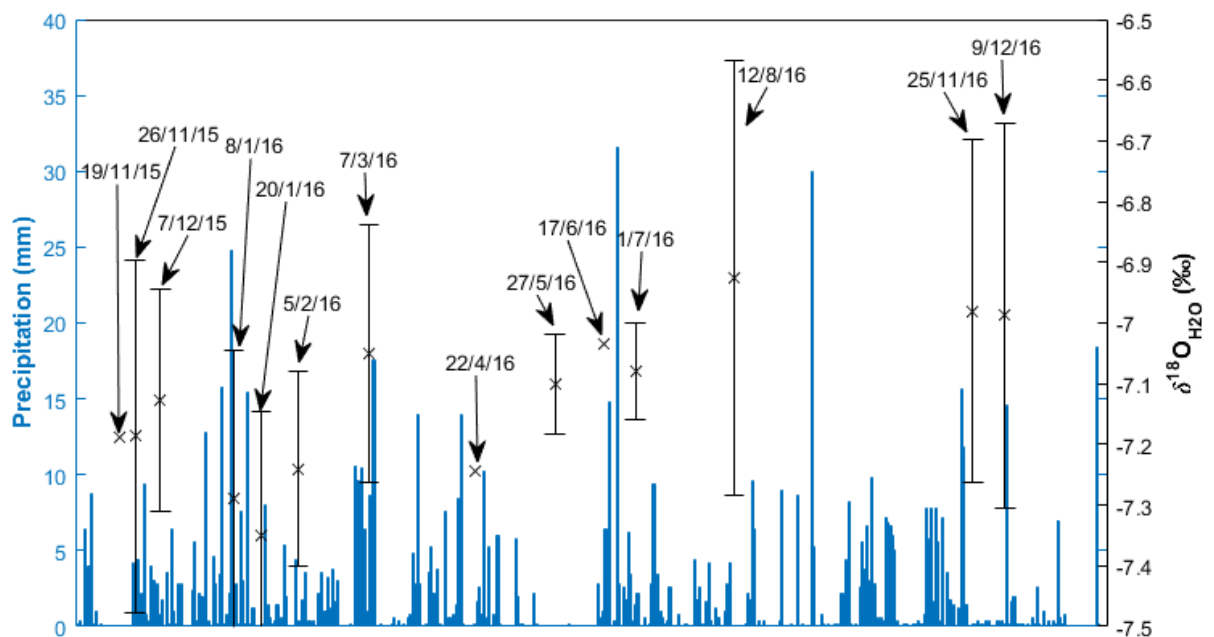


Figure 5.30 Mean $\delta^{18}\text{O}_{\text{H}_2\text{O}}$ values from 0.5m piezometer samples collected between 19/11/15 and 9/12/16 plotted with daily precipitation. Samples were collected from up to five locations along a 1.6km reach.

5.3.3 Nitrogen cycling in the stream

The fractionation of both $^{15}\text{N}_{\text{NO}_3}$ and $^{18}\text{O}_{\text{NO}_3}$ in the stream samples suggests the presence of denitrification within the stream itself. However, when examined alongside the nitrate concentration data this does not appear to be the case, as the most fractionated (i.e. isotopically heaviest) samples do not correspond to the lowest nitrate concentrations (Figures 5.24 and 5.25). The stream represents the result of mixing of surface runoff, soil leachate, precipitation and groundwater and so the inputs of many different sources of water with a large variation in sources (and hence isotopic compositions). There are two possible explanations for the observed dual fractionation of nitrate isotopes in stream water but lack of corresponding reduction in nitrate concentration. These are presented in Sections 5.3.2.1 and 5.3.2.2.

5.3.3.1 Denitrification in the stream sediment coupled with nitrification

Kellman and Hillarie-Marcel (1998) used $\delta^{15}\text{N}_{\text{NO}_3}$ isotopic signatures of stream water draining a heavily fertilised agricultural catchment to identify in-stream denitrification. The results from this study demonstrated the significant potential for in-stream denitrification over a short 600 m distance, where up to 50% removal of downstream nitrogen was observed corresponding to an enrichment of $\delta^{15}\text{N}_{\text{NO}_3}$ values of up to +10‰. Kellman and Hillarie-Marcel (1998) commented that while stream waters typically contain denitrifying bacteria, they are also associated with high dissolved oxygen concentrations which inhibit the onset of anaerobic denitrification. Instead, the majority of in-stream denitrification occurs in benthic sediments as a result of diffusion of nitrate into the stream bed from the water column above.

Table 5.3 shows that dissolved oxygen concentrations in the stream samples were higher than the 0.5 mg L^{-1} threshold below which denitrification begins to take place (Hubner, 1986). Therefore, water column nitrate isotope fractionation should be limited since denitrification may only be occurring in the benthic sediments. This supports the limited data from the DET probes presented in this study, where dual fractionation of stream sediment pore water $^{15}\text{N}_{\text{NO}_3}$ and $^{18}\text{O}_{\text{NO}_3}$ was tentatively identified and suggests that more data might show a stronger relationship.

Kellman and Hillarie-Marcel (1998) also presented evidence for the presence of denitrification by comparing $\delta^{15}\text{N}_{\text{NO}_3}$ values to the natural logarithm of nitrate concentrations, explaining that a linear, inverse relationship signifies denitrification.

Kendall *et al.* (2007) explained that if the nitrate in a body of water is present as the result of mixing of other sources of water with distinct $\delta^{15}\text{N}_{\text{NO}_3}$ values, then the relative contributions of the two different sources can be calculated, providing no subsequent fractionation takes place following mixing. If the dissolved nitrate contained in a body of water truly does derive from a mixture of two different sources, then the concentration in the mixed water body (in this study, the stream samples) must plot along a mixing line between the end members. Kendall *et al.* (2007) went on to explain that these mixing lines are only straight lines when the concentrations of the two end members is the same, if they are not, the mixing line becomes hyperbolic. To this end, a useful test to examine whether $\delta^{15}\text{N}_{\text{NO}_3}$ and $\delta^{18}\text{O}_{\text{NO}_3}$ values are the result of mixing of water sources is to plot the isotope values against $\ln[\text{NO}_3^-]$, where a mixing line becomes curved if the end member nitrate concentrations are different. Denitrification is represented by a straight line. This is demonstrated in Figure 5.31 from Kendall *et al.* (2007), where fractionation of the nitrogen isotope due to denitrification is shown as a straight line.

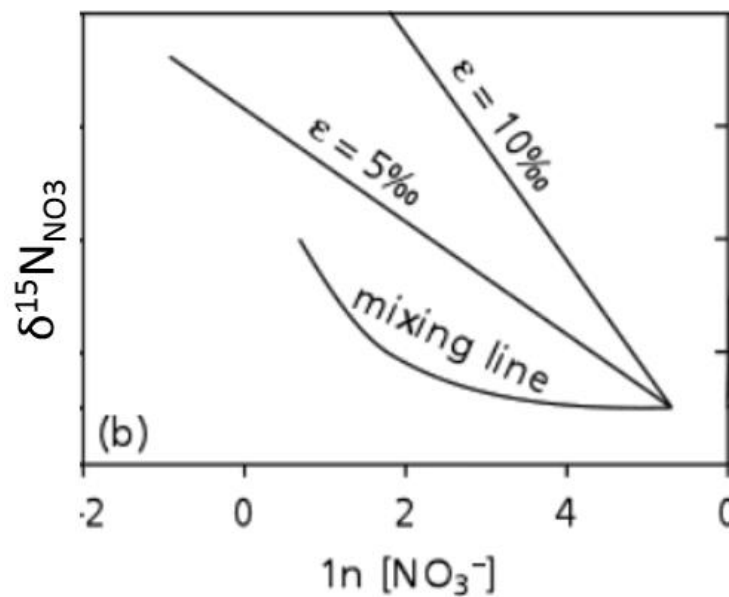


Figure 5.31 Deriving the process responsible for fractionation of $^{15}\text{N}_{\text{NO}_3}$ by plotting $\ln[\text{NO}_3^-]$ vs $\delta^{15}\text{N}_{\text{NO}_3}$. A straight line indicates denitrification whereas a curve suggests mixing as the cause of the $\delta^{15}\text{N}_{\text{NO}_3}$ value (y axis). Adapted from Kendall et al (2007).

Applying the same analysis to the data presented in this study yields Figure 5.32. When plotted against $\ln[\text{NO}_3^-]$, neither $\delta^{15}\text{N}_{\text{NO}_3}$ nor $\delta^{18}\text{O}_{\text{NO}_3}$ exhibit the trend associated with denitrification or mixing of two end members. Figure 5.30 shows that a slope of -5 or -10 is indicative of denitrification, while Figure 5.32 shows slopes of -0.5 and -1.7 for $^{15}\text{N}_{\text{NO}_3}$

and $^{18}\text{O}_{\text{NO}_3}$, respectively. One explanation for this is that the stream samples represent mixing of more than two sources. The addition of additional sources of water may then complicate the mixing regime, thus affecting the relationship observed in Figure 5.32. Since there is strong evidence for the presence of denitrification in the soil zone (as discussed in Chapter 4), any further denitrification in the stream would result in a lower stream nitrate concentration than measured in the field drains. The average field drain nitrate concentration (across all sites) was $29.85 \pm 18.61 \text{ mg L}^{-1}$ whilst the average stream concentration was $24.28 \pm 18.66 \text{ mg L}^{-1}$, slightly lower but not significantly so ($P > 0.05$). Since the stream receives low nitrate concentration groundwater, this lower (than the field drains) concentration is probably the result of the baseflow component and not due to in-stream denitrification.

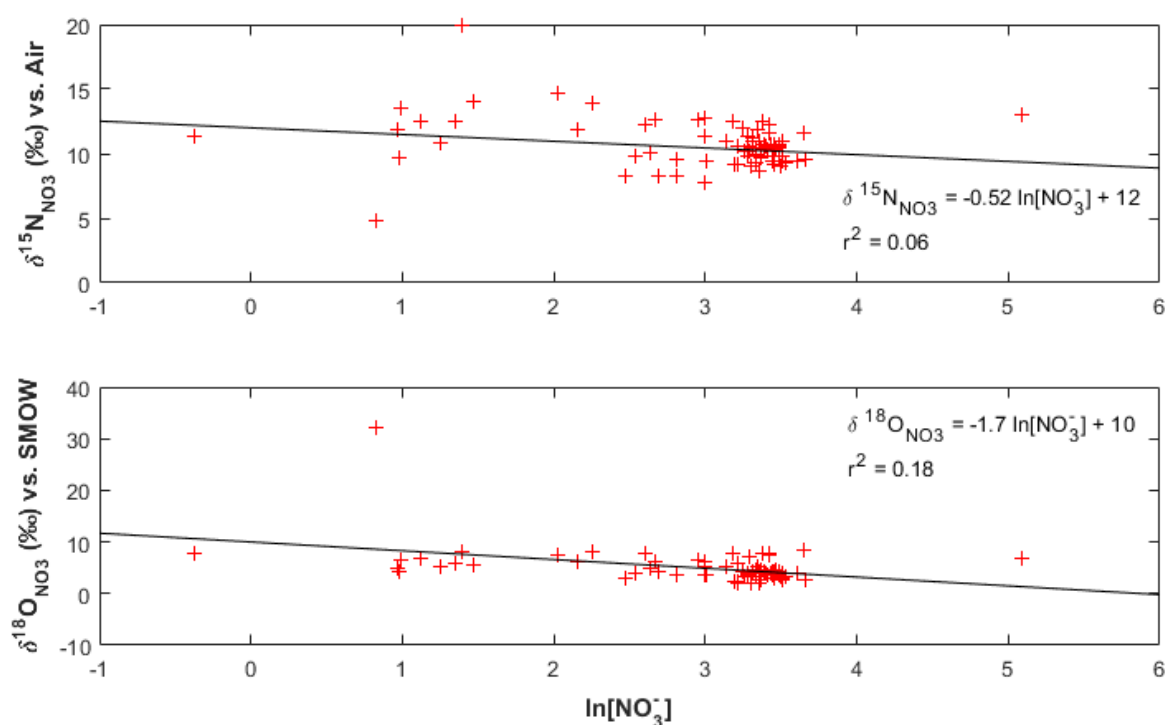


Figure 5.32 Correlation between $\delta^{15}\text{N}_{\text{NO}_3}$ and $\delta^{18}\text{O}_{\text{NO}_3}$, and the natural log of the nitrate concentrations measured in stream samples collected from five locations along a 1.6 km study reach between November 2015 and January 2017. The black line represents the best fit line for the data.

Since both the correlation of $\ln[\text{NO}_3^-]$ and nitrate isotopic composition, and nitrate concentration versus $\delta^{15}\text{N}_{\text{NO}_3}$ and $\delta^{18}\text{O}_{\text{NO}_3}$ values rely on nitrate concentration data, then it is possible that in stream coupled nitrification-denitrification could interfere with the expected trends. This is because, whilst fractionation of $^{15}\text{N}_{\text{NO}_3}$ and $^{18}\text{O}_{\text{NO}_3}$ in nitrate

resulting from denitrification was shown in the stream nitrate isotope data, nitrification may simultaneously maintain the nitrate concentration, thus negating the expected decrease in concentration with increases in $\delta^{15}\text{N}_{\text{NO}_3}$ and $\delta^{18}\text{O}_{\text{NO}_3}$ values. Given the low concentrations of nitrite and ammonium in the stream samples (0.031 and 0.608 mg L⁻¹ respectively), it is possible that nitrification is taking place within the stream with its rate being limited by the supply of ammonium. Mineralisation of organic material within the benthic sediments could supply the ammonium necessary for nitrification.

As discussed in Chapter 2, it is well established that denitrification causes the $\delta^{15}\text{N}_{\text{NO}_3}$ and $\delta^{18}\text{O}_{\text{NO}_3}$ values of the residual nitrate pool to increase in an approximate 2:1 ratio. Therefore, if denitrification is responsible for the dual fractionation of $\delta^{15}\text{N}_{\text{NO}_3}$ and $\delta^{18}\text{O}_{\text{NO}_3}$ values, the slope of a best fit line should be close to 0.5. However, a number of studies have shown $\delta^{15}\text{N}_{\text{NO}_3}$ and $\delta^{18}\text{O}_{\text{NO}_3}$ values that when plotted against one another show best fit lines with slopes of 0.35 – 0.76 (Bottcher *et al.*, 1999; Aravena and Robertson, 1998; Mengis *et al.*, 1999; Cey *et al.*, 1999; Panno *et al.*, 2006; Wexler *et al.*, 2014; Fukada *et al.*, 2003), with the upper end closer to that reported in this study (0.89) regarding the stream samples, though still lower. Furthermore, Wunderlich *et al.* (2012) reported slopes of 0.91 – 0.97 in a study examining the different carbon substrates on nitrate isotope fraction during denitrification, though it is important to note that the slopes reported in Wunderlich *et al.* (2012) were from batch laboratory experiments under ideal anaerobic conditions where the sources of nitrate were controlled, and not from field data. Since atmospheric nitrate is typically associated with heavily enriched $\delta^{18}\text{O}_{\text{NO}_3}$ values (+63 ‰ to +94‰, Elliot *et al.*, 2006), it is possible that contributions of atmospheric nitrate to the stream samples was responsible for the steep slope of the best fit line for the stream nitrate isotope data, and that without the introduction of atmospheric nitrate, the slope of this best fit line would fall within the range reported in the literature. Given the proportionally (to agricultural and soil-borne sources of nitrate) high $\delta^{18}\text{O}_{\text{NO}_3}$ values associated with precipitation, even if precipitation were a small contributor to the nitrate in the stream, this may be enough to skew the stream $\delta^{18}\text{O}_{\text{NO}_3}$ values, incorporating more enriched $\delta^{18}\text{O}_{\text{NO}_3}$ values.

In this instance, nitrate concentrations may be maintained through nitrification within the stream, which is subsequently denitrified in the benthic sediments, facilitating the dual fractionation of $^{15}\text{N}_{\text{NO}_3}$ and $^{18}\text{O}_{\text{NO}_3}$ shown in Figure 5.23, but not showing any negative correlation between nitrate concentration and $\delta^{15}\text{N}_{\text{NO}_3}$ and $\delta^{18}\text{O}_{\text{NO}_3}$ values as

demonstrated in Figures 5.24 and 5.25. In combination with atmospheric inputs, the slope of the line suggests that denitrification is occurring, likely in the benthic sediments because the water column contains too much dissolved oxygen to bring about the onset of anaerobic respiration but is steeper than the range cited in the literature. As Kellman and Hillarie-Marcel (1998) discussed, benthic denitrification results in minimal isotopic fractionation. Since dual nitrate isotope fractionation in the stream samples was observed, on first inspection this suggests that denitrification in the stream was not diffusion limited and therefore may not be occurring in the benthic sediments. However, it is discussed in Section 5.3.2 that there may have been certain locations along the study reach where the exchange of stream and groundwater was high relative to other locations. In this instance, rates of diffusion of nitrate into the stream sediments from the overlying water column may not inhibit isotopic fractionation as much, resulting in the detectable nitrate isotope fractionation in the stream samples.

The effects of DNRA and nitrification on nitrate isotopes act in opposite directions, where DNRA enriches the residual pool of nitrate in ^{15}N and ^{18}O , and nitrification produces nitrate that is isotopically depleted in ^{15}N and ^{18}O . The $\delta^{15}\text{N}_{\text{NO}_3}$ and $\delta^{18}\text{O}_{\text{NO}_3}$ values for the stream samples were +7.8 to +19.9‰ and +2.0 to +8.9‰, respectively, within the ranges typically associated with nitrification of ammonium fertiliser and soil organic matter (~-4 to +7.5 ‰ for $\delta^{15}\text{N}_{\text{NO}_3}$ and ~-5 to +15‰ for $\delta^{18}\text{O}_{\text{NO}_3}$, Kendall *et al.*, 1998). If DNRA were the only mechanism influencing the isotopic signature of the stream water nitrate, then it could be expected that both $\delta^{15}\text{N}_{\text{NO}_3}$ and $\delta^{18}\text{O}_{\text{NO}_3}$ values measured in these samples would be greater than the observed values. Since Figure 5.23 indicates a denitrification pattern similar to the typical dual enrichment of both nitrogen and oxygen in nitrate, but no associated decrease in nitrate concentration, then the suggestion that in-stream nitrification was maintaining nitrate concentrations is supported by the measured $\delta^{15}\text{N}_{\text{NO}_3}$ and $\delta^{18}\text{O}_{\text{NO}_3}$ values that fall within the range associated with nitrification of fertiliser ammonium and soil organic matter. In this case, the pool of reactive nitrogen available for denitrification or DNRA in the stream water was probably comprised of nitrified soil organic nitrogen and fertiliser-derived ammonium, which acted to ‘temper’ the enrichment of nitrate isotopes resulting from DNRA.

5.3.3.2 Dissimilatory reduction of nitrate to ammonium in the stream sediments coupled with nitrification

The second explanation for stream water nitrate isotopic composition showing dual fractionation of $^{15}\text{N}_{\text{NO}_3}$ and $^{18}\text{O}_{\text{NO}_3}$ but no corresponding reduction in nitrate concentration is the dominance of dissimilatory reduction of nitrate to ammonium (DNRA). As discussed in Chapter 2, DNRA is a nitrogen cycling pathway where microbially-mediated dissimilatory conversion of nitrate to ammonium (i.e. where the nitrogen is not incorporated into bacterial cells) is carried out (Burgin and Hamilton, 2007). Fermentative DNRA receives electrons from organic matter in the following reaction, after Robertson *et al.*, 1996:



The conditions necessary for the onset of denitrification and DNRA are similar, in that both processes occur under anoxic conditions and require available electron donors (organic carbon) and acceptors (nitrate). Whether DNRA or denitrification is favoured depends on which substrate (organic carbon or nitrate) is limiting. Rivett *et al.*, (2007) explained that DNRA is typically favoured in nitrate-limiting environments where bioavailable organic carbon is in abundance and denitrification dominates where carbon is limited, and nitrate is in high supply. Tiedje (1988) suggested that this was because environments where labile carbon is abundant favour organisms that utilise electron acceptors most efficiently. Tiedje (1988) went on to explain that for every mole of nitrate reduced by DNRA, eight electrons are transferred, whereas during denitrification, only five are transferred. Therefore, in nitrate limiting, high carbon conditions, microbiota capable of carrying out DNRA can out compete denitrifying organisms.

The ammonium produced through DNRA in the sediments is available for nitrification, which would conserve the nitrate concentration within the stream through further nitrification. Figures 5.24 and 5.25, and Table 5.4 are consistent with a lack of change in downstream nitrate concentrations due to nitrification resulting from DNRA, and subsequent oxidation of ammonium during nitrification. The resultant ammonium could also be taken up via assimilation which would have the same effect on ammonium concentrations but would not maintain nitrate concentrations. For nitrification to maintain high stream water nitrate and low ammonium, the oxidation of ammonium produced from DNRA must be rapid.

Since denitrification in the soil zone was identified through isotopic and nitrate concentration analysis of field drain samples (Chapter 4) which drain into the stream, then further denitrification in the stream would show lower nitrate concentrations than measured in the field drains, a characteristic that was not observed, as explained in Section 5.2.3.1. In this instance, given that nitrate concentrations in the stream and field drains were similar, it is suggested that the fate of ammonium produced by potential DNRA in the benthic sediments is its utilisation in nitrification, rather than its uptake by assimilation.

As discussed in Section 5.3.2.1, the slope of the best fit line for the stream samples was 0.88, above the upper end of the range cited in the literature for denitrification (~0.5). Granger *et al.* (2008) reported the first measurements of nitrogen and oxygen fractionation associated with DNRA from laboratory studies in cultures of denitrifying bacteria. Two seawater strains (*Pseudomonas stutzeri* and *Ochrobactrum* sp.) and three freshwater strains (*Paracoccus denitrificans*, *Pseudomonas chlororaphis*, and *Rhodobacter sphaeroides*) were used in this study. The results showed that when the $\delta^{18}\text{O}_{\text{NO}_3}$ and $\delta^{15}\text{N}_{\text{NO}_3}$ values were plotted together, the slope of the best fit line across all species was 0.86 – 1.02, with the exception of *R.sphaeroides* which plotted a slope of 0.62. The best fit line for the stream nitrate isotope data is within this range, and hence suggests DNRA as a possible cause of dual nitrate isotope fractionation.

As discussed however, DNRA is thought to only dominate over denitrification when nitrate is limited, and organic carbon is in abundance. Figure 5.33 demonstrates that in the stream, the opposite was observed, where DOC was low and nitrate concentrations were high. Since DNRA would likely only occur in the stream sediments due to the relatively anoxic conditions compared to the stream water, the stream samples may not reflect benthic conditions. Sediment pore water nitrate concentrations along a 2.5 – 15.0 cm depth profile, were ~5 to ~33 mg L⁻¹, not indicative of nitrate limitation. DOC concentrations for the 2.5 – 15.0 cm depth profile were not available. Furthermore, Megonigal *et al.* (2004) compiled ranges of nitrogen uptake due to DNRA as a percentage of total nitrogen uptake from a number of ecosystems. In river sediments in Northern Ireland, this range was estimated to be ~5 – 10%, with the balance assumed to be due to denitrification. Therefore, it is unlikely that DNRA is the dominant nitrogen cycling process in the stream water samples presented in this chapter, though there are

existing few studies investigating DNRA in freshwaters and so DNRA cannot be entirely ruled out.

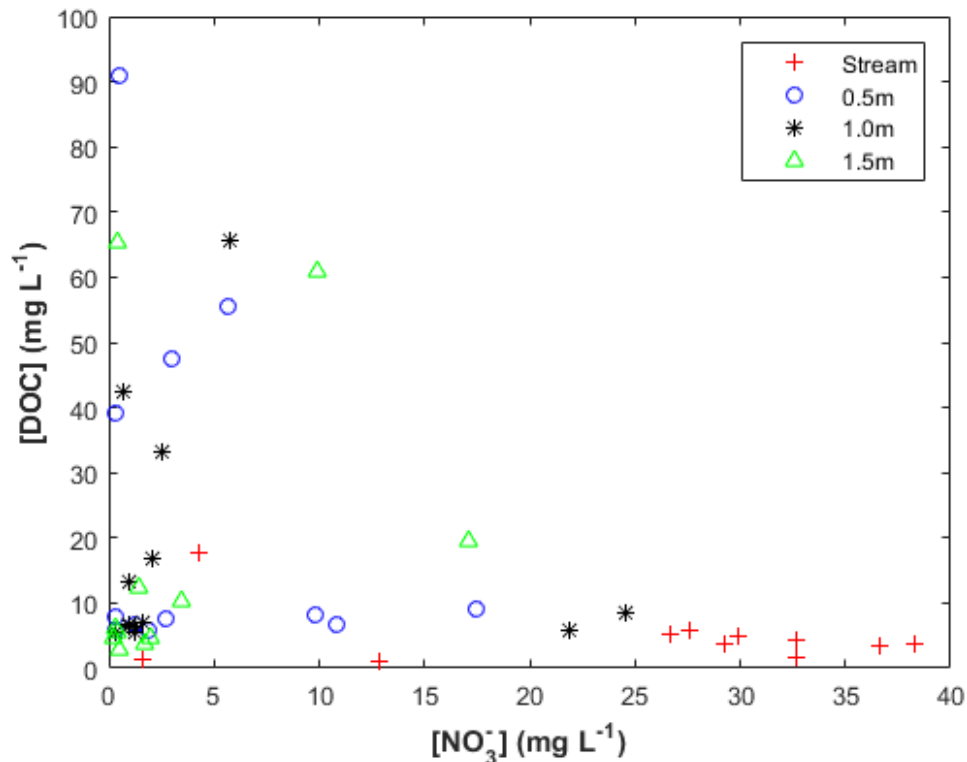


Figure 5.33 Relationship between DOC and nitrate concentration along the stream-1.5m continuum in samples collected at five sets of piezometers along the 1.6 km study reach between November 2015 and January 2017.

Both scenarios, described in the above and in Section 5.3.2.1, provide evidence of isotopic fractionation of stream water nitrate due to DNRA and denitrification, respectively. Neither scenario is without contradictory evidence however and is it likely that a combination of the two is responsible for the dual fractionation of nitrate isotopes but lack of concurrent reduction in nitrate concentrations in the stream. Further mesocosm studies using stream water and benthic sediments collected from the study site would be needed to isolate the nitrogen transformation pathways, as this would eliminate the introduction of highly-enriched atmospheric nitrate, and exchange of surface water and groundwater contributing to the scenario presented in Section 5.3.2.1. Both scenarios share the same coupled nitrification as an explanation for the maintained (from the field drains) nitrate concentrations in the stream water.

5.3.4 Nitrogen cycling in the hyporheic zone

The stratigraphy of the study site is presented in Table 2.2. In Chapter 2 and shows that the majority of the piezometers at 0.5 and 1.0 m depth were installed into sandy clay loam or clay, where microbial growth may not be as inhibited as it would be deeper in the subsurface where chalk is dominant (as the pore space is too small for denitrifying bacteria to enter). Nevertheless, there was no indication of denitrification in the piezometer samples demonstrated by the nitrate isotope data shown in Figures 5.27 – 5.29.

The sediment porosity, bulk density and hydraulic conductivity measurements for the 0.5 and 1.0 m strata shown in Chapter 2 demonstrate the heterogeneity of the sediments at these depths, reflecting a wide spatial range of potential water residence times within the hyporheic zone. If the physical properties of the sediments were solely responsible for rates of denitrification, then it would be expected that the sites where hydraulic conductivity is lowest would be associated with relatively higher (than sites with higher hydraulic conductivity) fractionation of nitrate isotopes, and lower nitrate concentrations (providing isotopic fractionation was not inhibited by slow rates of nitrate diffusion between oxic and anoxic pore spaces). This was not observed however, as all piezometer depths show the same lack of nitrate dual isotopic fractionation and low concentrations.

Given the low nitrate and high DOC concentrations in the piezometer samples, it is possible that denitrification was inhibited in the hyporheic zone because the shallow groundwater was nitrate limited as it was upwelled to the surface (through the hyporheic zone). This would produce the lack of isotopic evidence for denitrification in the hyporheic zone (0.5 1.0 and 1.5 m below the stream bed). Feast *et al.* (1998) inferred denitrification within the heterogeneous glacial till at the same study site as presented in this thesis as elevated dissolved $N_2: Ar$ ratios measured in the deeper chalk groundwater. Briefly, the chalk groundwater contained elevated dissolved $N_2: Ar$ ratios, yet the lowest nitrate concentration samples were not associated with the most enriched $\delta^{15}N_{NO_3}$ values and so it was suggested that denitrification in the upper weathered till during recharge was responsible for the chalk groundwater dissolved $N_2: Ar$ ratios. Therefore, the cause of the low nitrate concentrations in the hyporheic zone samples presented in this thesis could be because the water was denitrified prior to arriving at the hyporheic zone. The isotopic signal for denitrification (dual enrichment of $\delta^{15}N_{NO_3}$ and $\delta^{18}O_{NO_3}$) in the hyporheic zone samples presented in this chapter must then be obscured by mixing of

different sources of groundwater. This is consistent with the borehole isotope data. Though few in number ($n = 5$), the 12 m borehole showed $\delta^{15}\text{N}_{\text{NO}_3}$ and $\delta^{18}\text{O}_{\text{NO}_3}$ values of $+20.9 \pm 0.9 \text{ ‰}$ and $+17.8 \pm 0.6 \text{ ‰}$, respectively. The $^{15}\text{N}_{\text{NO}_3}$ was far more enriched at 12 m than at the shallower 0.5 – 1.5 m depth ($+9.64 \pm 2.62 \text{ ‰}$), though the $^{18}\text{O}_{\text{NO}_3}$ is not ($+19.68 \pm 8.61 \text{ ‰}$ at 0.5 – 1.5 m depth), probably due to the incorporation of precipitation derived nitrate, with high $\delta^{18}\text{O}_{\text{NO}_3}$ in the shallower piezometer samples. The mean concentration of nitrate in the borehole was 3.75 mg L^{-1} , higher than the majority of the piezometer samples. This suggests that the samples collected from the borehole were only partially denitrified, and that further denitrification may occur at a shallower depth between 12 m and 1.5 m (the deepest piezometer depth).

The lack of evidence for denitrification in the hyporheic zone supports the findings reported in Smith *et al.* (2009), who developed a novel classification scheme to assess the pollutant natural attenuation potential at the groundwater-surface water interface across England and Wales. The classification scheme was based on hydrogeological data pertaining to sediment thickness and permeability, reflecting water residence time within the groundwater-surface water interface and baseflow index, and reflecting stream-subsurface connectivity. Geochemical data relating to sediments were also used, including sediment cation exchange capacity and organic, and total inorganic carbon fractions. The geochemical data were used to represent the sediment retardation capacity of anions, organic contaminants and acids. To each of the described parameters, a score was allocated representing high (3), medium (2) or low (1) in relation to its foreseen impact on nutrient attenuation potential. Scores for each parameter were then combined, generating an overall score for each of the 7816 surface water bodies within England and Wales analysed. Results showed that within the Wensum catchment (containing the study site examined in this thesis), a score of ‘low’ was attributed to the nutrient attenuation potential of the groundwater – surface water interface, in agreement with the primary data presented in this chapter.

Though the same parameters were not measured (i.e. those measured in this study and those used to generate the classification system in Smith *et al.*, 2009), the findings of Smith *et al.* (2009) can offer some further discussion surrounding the lack of isotopic evidence for denitrification in the 0.5, 1.0 and 1.5m piezometer samples. Table 5.8, recreated from Smith *et al.* (2009) shows an explanation of the parameters and how their relative scores influence natural attenuation potential. In Smith *et al.* (2009), the

sediments described refer to the fine mobile sediment and so the discussions surrounding data presented in this chapter may pertain to a deeper zone beneath the stream than that described in Smith *et al* (2009). Nevertheless, the isotopic and nitrate concentration data presented in this chapter and the findings of Smith *et al.* (2009) are in agreement, and so some interpretation remains relevant. At all three piezometer depths, the median DOC concentrations were similar (8.1, 7.8 and 8.2 mg L⁻¹ in the 0.5, 1.0 and 1.5 m piezometers, respectively), and would not be considered limiting (Zarnetske *et al.*, 2011a reported hyporheic zone denitrification occurring at DOC concentrations of 0.80 – 1.54 mg L⁻¹) and so in the context of Smith *et al.* (2009) are not considered low. In Chapter 2, it is demonstrated that within the study catchment, the quaternary deposits are heterogeneous, furthermore there was high variation in the particle size distribution of sediment samples collected along the study reach at 0.5 and 1.0 m depth below the stream bed, also shown in Chapter 2. Therefore, the sediment at the depth to which the piezometers were installed may contain areas where permeability is high, resulting in low nitrate residence time, and reducing denitrification potential at these depths. The baseflow index for the study area is high, and so groundwater flux into the overlying stream is also high, however groundwater nitrate concentrations were low, hence delivery of nitrate into the groundwater – surface water interface was low. Overall, observations made from data collected at the study site are in agreement with Smith *et al.* (2009), however there are some differences regarding the hydrological regime.

Table 5.8 Influence of parameters used by Smith et al. (2009) to qualitatively classify the groundwater-surface water interfaces of surface water bodies across England and Wales. Adapted from Smith et al. (2009). Sediment fOC refers to the organic carbon fraction of a sediment.

Natural attenuation potential	Sediment <i>foc</i>	Sediment permeability	Sediment thickness	Baseflow index (BFI)	Predicted impact on river nitrate
High	High <i>foc</i> results in greater pollutant retardation potential and denitrification	Low permeability increases pollutant residence time in sediments	Thick sediments increase pollutant residence time	High BFI increases groundwater flux into surface water	Decreased riverine nitrate
Medium	Moderate <i>foc</i>	Moderate permeability	Moderate thickness	Moderate BFI	Close to mean of all surface water bodies
Low	Low <i>foc</i> results in low pollutant retardation potential and denitrification	High permeability reduces pollutant residence time in sediments	Thin sediments reduce pollutant residence time	Low BFI reduces groundwater flux into surface water	Increased riverine nitrate

5.4 Summary

In this chapter, nitrogen cycling along shallow hyporheic zone - stream continuum was discussed. The continuum covers the stream, through the benthic sediments as a shallow profile from 2.5 – 15 cm below the stream bed at 2.5cm resolution, to 0.5, 1.0 and 1.5 m below the stream bed (representing the hyporheic zone). There was isotopic evidence for denitrification within the stream as demonstrated by dual fractionation of $^{15}\text{N}_{\text{NO}_3}$ and $^{18}\text{O}_{\text{NO}_3}$. This was not concurrent with a reduction in nitrate concentration however, where if denitrification were consuming nitrate, then the samples with the lowest nitrate concentration should also be associated with the highest $^{15}\text{N}_{\text{NO}_3}$ and $^{18}\text{O}_{\text{NO}_3}$ values. This is likely the result of coupled nitrification-denitrification within the stream, where nitrification was maintaining nitrate concentrations, thus confounding an expected inverse relationship between nitrate concentration and $\delta^{15}\text{N}_{\text{NO}_3}$ and $\delta^{18}\text{O}_{\text{NO}_3}$ values. Furthermore, the slope of the best fit line in the nitrate isotope data was 0.88, higher than the range found within the literature (0.35 – 0.76). This could be the result of incorporation of heavily enriched atmospheric $^{18}\text{O}_{\text{NO}_3}$. It was suggested that areas along the study reach that are characterised by preferential exchange of surface and subsurface water (i.e. where there is a preferential flow path) were responsible for overcoming the restricted isotopic fractionation associated with benthic denitrification (where rates of nitrate diffusion into the sediments cause low isotopic fractionation). Alternatively, the steep slope of the best fit line in the stream $\delta^{15}\text{N}_{\text{NO}_3}$ and $\delta^{18}\text{O}_{\text{NO}_3}$ values might be the result of dissimilatory reduction of nitrate to ammonium within the benthic sediments, not denitrification. The same resultant nitrification of the ammonium produced by dissimilatory reduction of nitrate to ammonium (DNRA) would explain the moderate stream water nitrate concentrations, though DNRA requires nitrate limited conditions, something that is not evident in the sediment pore water nitrate concentrations.

In the benthic sediment profile, Diffuse Equilibrium in Thin Films (DET) probes were installed at the downstream sampling site and analysed for major ion concentrations and $\delta^{15}\text{N}_{\text{NO}_3}$ and $\delta^{18}\text{O}_{\text{NO}_3}$ values. The data were limited, however do tentatively suggest that denitrification was occurring within the stream sediments, though more data are necessary to confirm this. The DET data support the discussion of stream isotope data where denitrification is more prevalent in the benthic sediments than in the water column due to sediment pore waters containing less dissolved oxygen than surface water bodies, though a dissolved oxygen profile in the stream sediments was not possible.

Nitrogen cycling deeper within the hyporheic zone at 0.5, 1.0 and 1.5 m below the stream bed was then discussed, using data from samples collected from piezometers. There was no isotopic evidence for denitrification at 0.5, 1.0 or 1.5 m below the stream bed, despite very low nitrate concentrations in the samples. The most likely explanation for the observations in the piezometer nitrate isotope data suggested to be mixing with other sources of low nitrate water. The groundwater borehole (12 m below the surface) showed more enriched $\delta^{15}\text{N}_{\text{NO}_3}$ than the piezometer (hyporheic zone) samples, suggesting that the explanation for the low nitrate concentration measured in the hyporheic zone is because the groundwater is denitrified before it arrives at the hyporheic zone. This is consistent with findings by Feast *et al.* (1998) who inferred denitrification in the groundwater within the same study catchment, based on Chalk groundwater dissolved N_2 : Ar ratios. Further denitrification in the hyporheic zone is then inhibited due to a lack of substrate (nitrate).

Chapter 6 Catchment nitrogen mass balance

6.1 Introduction

In this chapter, a nitrogen mass balance for the study catchment is presented. The purpose of this chapter is to identify the potential proportion of nitrogen inputs to the study site that are removed through denitrification and to draw together the observations made in Chapters 4 and 5 through presentation of a catchment conceptual model. Such information is useful in terms of improving farm scale nutrient management to minimise economic losses and environmental impact.

A mass balance approach to quantifying nitrogen inputs and outputs within a system is rooted in the principle of substance flow analysis (SFA). The objective of SFA is to provide relevant information in order to inform an overall management strategy. In this case, a strategy is required to manage the export of nitrogen from the Blackwater subcatchment. SFA is typically conducted by a three-step process: firstly, the system must be clearly defined in space and time. Second, an overview of stocks and flows of the given substance must be obtained, and these stocks and flows must be quantified. Finally, the results must be interpretable in a meaningful way, depending on the goal of the SFA. All three stages involve a range of choices and specific requirements which are determined by the goal of the SFA. For example, the time frame covered by the analysis might be dictated by that land use.

SFA of nutrients in agricultural scenarios is a powerful tool in informing management practices from an environmental and economic perspective and is easily implemented as explained in further detail below. Briefly, in agricultural settings, crop rotations follow strict temporal cycles and so the time period for which any SFA is carried out in this type of system will likely be governed by such seasonal agricultural cycles. Additionally, the spatial demarcation of an agricultural SFA can be easily understood on a catchment or field scale, as much like the temporal aspect, field and catchment sizes are clearly defined. Quantification of nutrient stocks and flows is also easily achieved as fertiliser application rates and cropping data are well documented, as demonstrated in this chapter.

Given the importance of SFA, nutrient mass balances are often rooted in this principle, though their purpose and consideration of factors (i.e. sources/sinks if a given nutrient) vary from study to study.

Nutrient budgets are produced through inventory of all of the inputs and outputs of a substance (in this case, nitrogen) in a defined system over a given time period. A nutrient budget is rooted in the underlying principle of mass balance, that is, the nutrient inputs minus the nutrient exports from a system represents the change in storage of a given nutrient within the system in question (Meisinger and Randall, 1991). In an agricultural setting, the amount of nutrients incorporated into a system, and the methods through which they are applied vary significantly between farming systems and even between fields. This is the case for the study site presented in this thesis, where different tillage regimes and fertiliser applications are used to maintain separate fields. Nutrient mass balance calculations provide an overall framework within which every agricultural system should be represented (Watson *et al.*, 2002). A basic schematic of nutrient budgeting is illustrated in Figure 6.1.

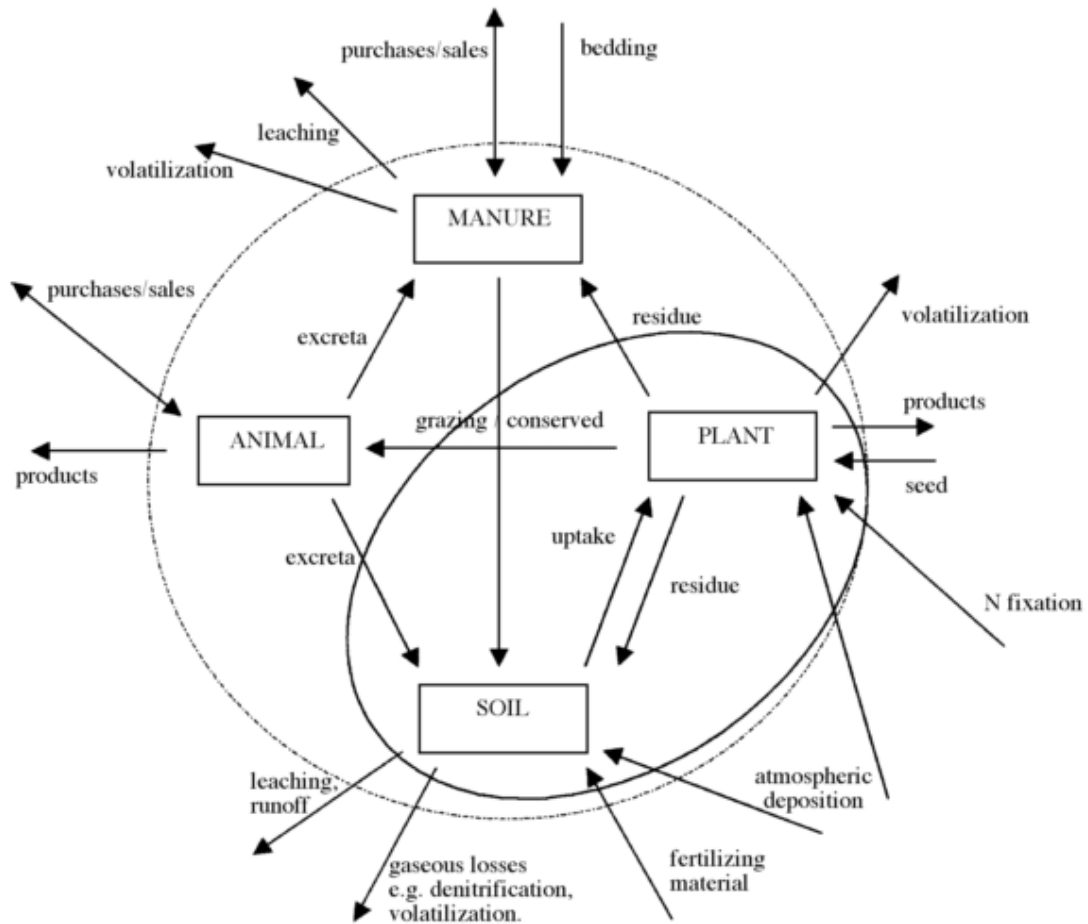


Figure 6.1 Basic diagram of potential nutrient flows within a farm. The dashed line represents the farm boundary including cropped and uncropped land, the unbroken line represents the crop rotation boundary from surface to rooting depth (Watson et al., 2002)

There are a range of types of nutrient budgets, with the distinction between them being where the system boundary is identified, the presence/absence of internal flows and which inputs and outputs are represented (Watson and Atkinson., 1999). Jarvis (1999) described three main types of nutrient budgets

- **Gate budgets:** These budgets are typically only concerned with the flow of controlled nutrient inputs (e.g. nitrate fertilisers). Inputs that are not in the direct control of the farmer or land manager such as biological nitrogen fixation and atmospheric inputs are not incorporated within gate budgets. This method is therefore not suitable for organic systems, though its simplistic and well constrained approach makes it a common tool in policy analysis and development.

- **Surface budgets:** This approach centres on the discrepancy between total inputs of a nutrient and its removal through uptake by crops (or grazing in livestock farming). Surface budgets do account for uncontrolled nutrient inputs but not their fate or origin. Surface budgets are most common in assessments of crop nutrient requirements.
- **System budgets:** System budgets are the most thorough of the three common budget types. They provide information regarding nutrient inputs, exports and internal cycling covering a range of system components (i.e. soil, crops etc). Given their complexity, system budgets require much more data than gate or surface budgets.

Oenema and Heinen (1999) commented that when carrying out a nutrient budget exercise, there is no one correct approach. Instead, the methodology of the exercise should be governed by its purpose. The nitrogen budgeting approach taken in this chapter is primarily based on the gate budget. As will be discussed in Section 6.2.1, atmospheric inputs of nitrogen are minor, and biological nitrogen fixation is not accounted for, leaving only the fertiliser applications as significant inputs of nitrogen. Uptake of nitrogen through crops is accounted for in this budget however, so the methodology is primarily based on the gate budget, but does include some elements of a surface budget. The fate of nitrogen within the system was discussed in Chapters 4 and 5. Briefly, in Chapter 4 nitrate isotope and concentration data strongly indicate the presence of denitrification within the soil zone as demonstrated by field drain water samples. In Chapter 5, no evidence for denitrification in groundwater was found based on nitrate isotope and concentration data, though some evidence for in-stream (likely in the benthic sediments) denitrification was presented.

Because nutrient budgets are used for discrete systems, the definition of the system is crucial. Watson *et al.* (2002) explained that whilst including all of the land within a farm boundary (that is, not just land given over to cultivation) gives a truly holistic representation of the study environment, it is common for only the managed land to be included. This is a source of uncertainty because field margins are then not included in field sizes, and areas of woodland are not included in the budget. Whether or not this uncertainty is significant enough to confound the mass balance calculation, depends on its purpose and the percentage of unmanaged land within the catchment.

Another key consideration is the temporal range of the budget. Again, dictated by its purpose. The temporal range can cover a single growing season, a calendar year, or a hydrological year. In some cases, where nutrients are applied on a less than yearly basis, a single year will not be sufficient. In organic systems, data that cover complete cropping rotations are crucial, in particular where the purpose of the budget is to assess the environmental impact of the nutrients in question. Nitrate losses from the ploughing of grassland have been shown to be high immediately following cultivation, but when averaged over the entire rotation period, losses are typically much lower (Stopes *et al.*, 2002). Long term-records are useful as they allow for comparison between years. This enables the user to assess the impact of agricultural regimes and climate. Examining budgets that span several crop rotations also allows for comparison of management practices (Messinga *et al.*, 2010).

Watson *et al.* (2002) compiled 88 farm scale nutrient budgets for organic farms across nine temperate countries (Austria, Canada, Germany, Netherlands, New Zealand, Norway Sweden and UK). The data showed a nitrogen average surplus (that is, an excess of nitrogen following all uptake and leaching calculated through mass balance) of $83.2\text{kg N ha}^{-1}\text{ yr}^{-1}$, with the highest nitrogen use efficiency associated with arable systems. Of these 88 nutrient budgets, four were from the UK, all either mixed arable and dairy, or dairy only. UK farms averaged a nitrogen surplus of $135.5\text{kg ha}^{-1}\text{ yr}^{-1}$. The range of nitrogen surplus across all 88 budgets was $1.2\text{ kg ha}^{-1}\text{ yr}^{-1}$ in arable systems to $395.6\text{ kg ha}^{-1}\text{ yr}^{-1}$ in horticultural systems. It should be noted that of the 88 systems for which data were presented in Watson *et al.* (2002), only two were arable and the majority (67) were dairy. Nitrogen surplus in arable systems varied widely between these two systems from $1.2\text{ kg ha}^{-1}\text{ yr}^{-1}$ to $50.0\text{ kg ha}^{-1}\text{ yr}^{-1}$. Since these systems were so different in terms of nitrogen mass balance, but were both arable, more nitrogen mass balance calculations (such as the one presented in this chapter) on UK arable farms would improve the understanding of how nitrogen is cycled through these systems and therefore enable more informed and better management strategies. Watson *et al.* (2002) commented that the large range in nitrogen surplus between and within farm types suggests that future research relating to farm-scale nutrient budgets needs to address the scope for increasing nutrient use efficiency, focusing more on management practices.

The study site presented in this thesis is not organic, and is arable only, therefore making the drawing of comparisons with those cases presented in Watson *et al.* (2002) difficult. However, Watson *et al.* (2002) do set out a useful baseline for nitrogen use efficiency across Europe.

Gentry *et al.* (2009) explained that simple nitrogen input/output analyses of agricultural systems are a useful tool in assessing the nutrient management performance of a given scenario. Gentry *et al.* (2009) went on to explain that such analyses typically rely on large scale assumptions, excluding important factors such as soil leaching, denitrification or annual depletion of soil nitrogen. Gentry *et al.* (2009) carried out an extensive nitrogen mass balance for the Big Ditch watershed, Illinois, in which a two-year study of soil nitrogen mineralisation, soybean N₂ fixation, tile drain and river nitrogen loading, and groundwater and in-stream denitrification were measured. Gentry *et al.* (2009) reported that total nitrogen inputs were less than the outputs due to large losses of nitrogen through leaching and assumed soil zone denitrification. Gentry *et al.* (2009) attributed the change in soil nitrogen storage to the balance in this shortfall. Whilst the mass balance in this chapter is not as extensive as that presented in Gentry *et al.* (2009), it does attempt to address one of the major assumptions described: that of assumed denitrification within the Blackwater subcatchment as the balance between known nitrogen inputs and the mass of nitrogen removed via riverine export.

One important consideration in a nitrogen mass balance, especially within an agricultural setting where nitrogen inputs are high, is the storage of fertiliser-derived nitrogen in soil organic matter as demonstrated by Sebilo *et al.* (2013). Puckett *et al.* (1999) conducted a nitrogen mass balance budget in an intensively managed agro-ecosystem in Minnesota, USA to improve understanding of nitrate contamination of groundwater in the region. The mass balance undertaken by Puckett *et al.* (1999) included inputs of nitrogen from fertiliser applications, biological fixation, atmospheric deposition and animal feed whilst outputs were quantified from crop harvests, animal product exports, volatilisation from fertiliser and manure. The balance was assumed to be representative of denitrification. Denitrification was estimated to remove approximately half of the excess nitrate that leached below the rootzone, however storage of nitrogen in soil organic matter was not accounted for, and so the results presented in Puckett *et al.* (1999) may have overestimated the role of denitrification in the study system. The mass balance presented

in this chapter does account for the storage of nitrogen in soil and so aims to address this component of nitrogen mass balance overlooked in Puckett *et al.* (1999).

6.2 Setting up the nitrogen mass balance model

6.2.1 Delineation of nutrient budget boundary

A clear boundary is key for any nutrient budget exercise. Figure 6.2 shows the whole of the Blackwater sub-catchment, with the area for which the nitrogen budget is carried out marked by the thicker red line. The highlighted area, comprised of mini catchments A, B and E and encompassing 714.07 ha, contain the fields discussed in Chapter 4, the whole of the study stream reach (from which the stream samples were collected and where all of the piezometers were installed, discussed in Chapter 5), and also the contributing upstream water sources. The kiosk at the boundary of mini catchment E represents the integration of the three mini catchments and recorded high resolution nitrate concentration and flow data which are used in the mass balance calculations.

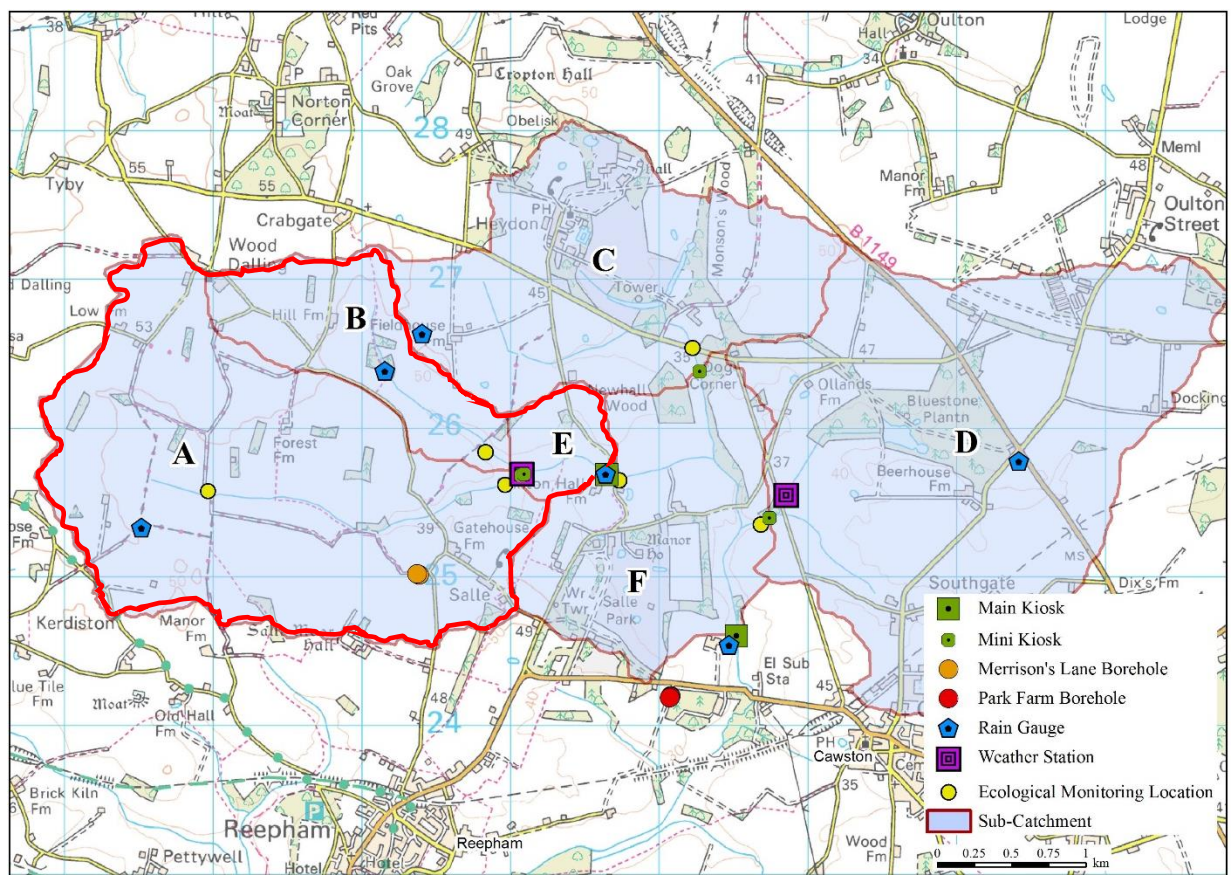


Figure 6.2 Map of the Blackwater sub-catchment with the area encompassed by the mass balance exercise highlighted (mini-catchments A, B and E).

A more detailed image shown in Figure 6.3 illustrates the land use in the area for which the nitrogen mass balance was calculated. Figure 6.3 shows that the majority of land within the nitrogen budget area was used for growing winter wheat during 2015 and a mixture of spring beans, winter barley and sugar beet during 2016. The data used to generate this image was obtained from The Salle Farms Co. Gatekeeper record. White areas Figure 6.3 are locations for which no data were available.

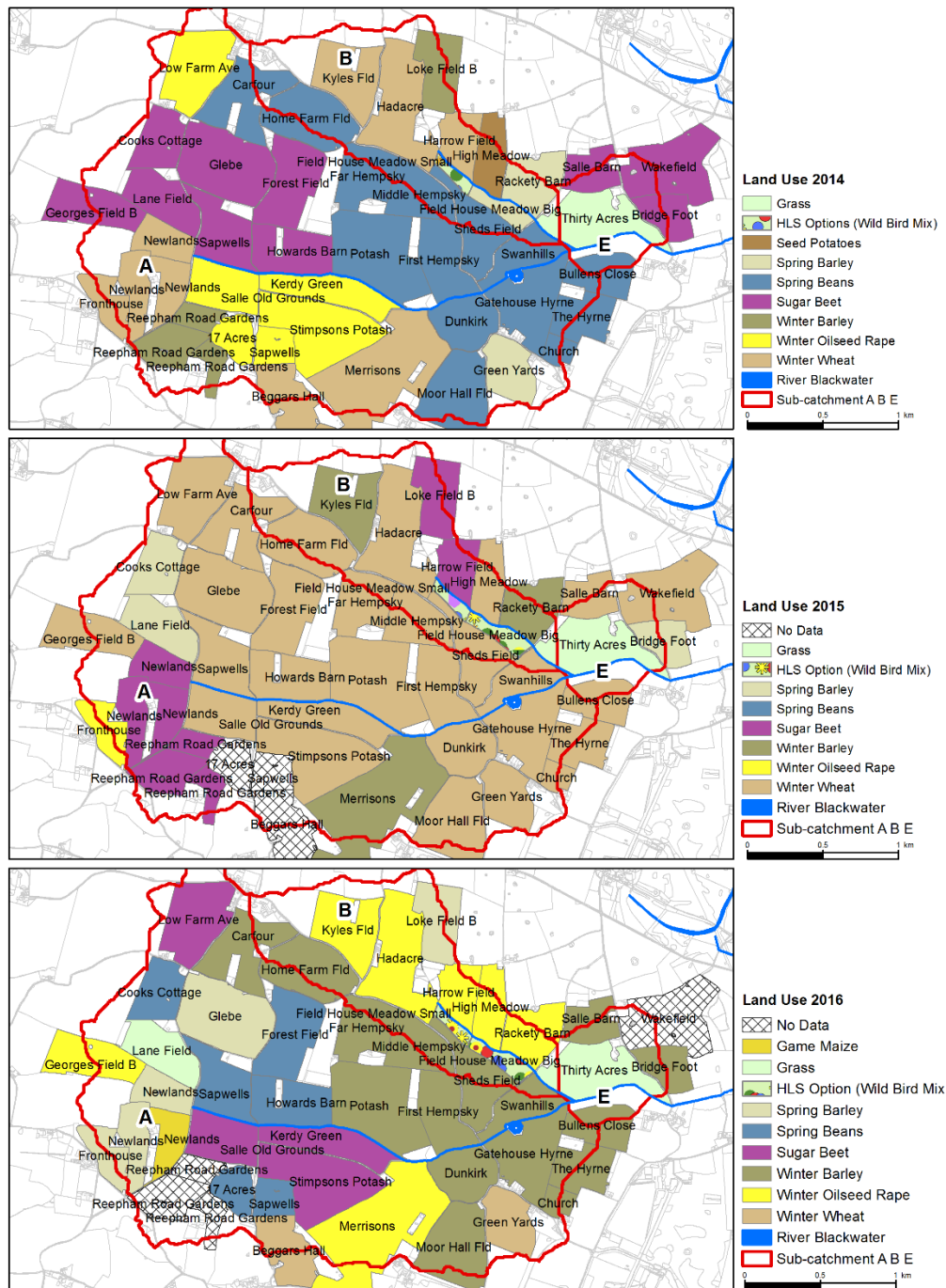


Figure 6.3 Land use in the area covered by the nitrogen budget calculation (mini-catchments A, B and E) in 2014, 2015 and 2016.

Prior to the study period, in 2014, the dominant crop types were sugar beet, spring beans and winter oilseed rape. Detailed information of cropping regimes and land use is key in any nutrient budget for an agricultural setting. As explained by Watson *et al.* (2002), nutrient budgets typically only include cultivated land, meaning that inputs and outputs are potentially underestimated. In this case, proportionally only a small amount of land is uncultivated (and hence excluded from this budget, Figure 6.3), therefore any underestimation generated through excluding this land were minimal. The time covered in this nutrient budget is 426 days, between 01/08/2015 – 30/09/2017 encompassing one farm year, with the land use covering the bottom two panels of Figure 6.3. This period is the longest for which nitrogen input to the study catchment data were available which coincided with the sampling period discussed in Chapters 4 and 5.

6.2.2 Nitrogen Export Coefficients

This nutrient mass balance approach takes into account uptake of nitrogen by crops. Although nutrient export coefficients (the fraction of nitrogen applied as fertiliser that remains following removal by the crop through uptake) are key components of nutrient budgets such as this, the purpose of this chapter is not to construct a new export coefficient model or to derive bespoke export coefficients for the different crop types shown in Figure 6.3. Nevertheless, some basic background on how nutrient exports are produced and used is necessary. At its core, a nutrient export model is designed to forecast nutrient loading at a given site within the surface drainage network of a catchment. This is based on the export of nutrients from all sources upstream within the catchment (Zhang and Hiscock, 2011). To construct a nutrient export model, spatial distribution of land use, fertilisers applied to each land use type, livestock and human population, and total nutrient inputs to the catchment data are collated and combined with existing export coefficients from the literature and field experiments examining the rate of export of nutrients to surface drainage (Johnes *et al.*, 1996).

The export coefficients used in this chapter are from Zhang and Hiscock (2011), who took six land use change scenarios centred around two public supply borehole capture zones on the unconfined Sherwood Sandstone aquifer, UK. The aim of this study was to predict the evolution of nitrate concentrations within the aquifer under these different land use scenarios up to 2025. Groundwater and mass transport modelling in conjunction with an export coefficient model facilitated the comparison of these different scenarios.

Specific export coefficients can be generated for individual crop types. These are based on a combination of the inherent nutrient retention and export capacity of a given crop type, and the land management practice itself (e.g. tillage regime, fertiliser application type and timing etc) (Zhang and Hiscock, 2011). The export coefficients for different crop types presented in Zhang and Hiscock (2011), were primarily derived from field data reported in existing studies carried out in the same, or similar (in terms of soil type, topography and nutrient management practices) areas (Germon, 1989; Shepherd and Lord, 1996; Lord and Mitchell, 1998; Webb *et al.*, 2000.; Haygarth *et al.*, 2003; Silgram *et al.*, 2003; Lovett *et al.*, 2006)

Crops grown during the period covered by the nitrogen budget include sugar beet, winter barley malt, spring beans, winter oilseed rape, winter barley and wheat. Table 6.1 summarises the crops with their corresponding export coefficients. In three fields, no crop data were available, but nitrogen application rates were known, in these cases, the nitrogen export coefficient of wheat (0.23) was applied, as it represents the median of the export coefficients shown in Table 6.1

Table 6.1 Crops grown in the study site during the timeframe covered by the nutrient budget and their corresponding nitrogen export coefficients from Zhang and Hiscock (2011). The export coefficients represent the percentage of nitrogen remaining following crop uptake.

Crop	Export coefficient
Sugar beet	0.17
Winter barley	0.20
Spring beans	0.48
Winter oilseed rape	0.42
Wheat	0.23

6.2.3 Nitrogen inputs to the study area

Detailed fertiliser application records were available at the field scale for all fields within the area covered by the nitrogen budget from the Salle Farms Co. Gatekeeper software record, provided by Lister Noble. A number of products were applied to the fields in mini-catchments A, B and E, each containing differing fractions of nitrogen. Table 6.2 shows all of the known nitrogen-bearing products used over the period covered by the nitrogen mass balance and their respective nitrogen fractions. All other applications made to the fields within the study site were pesticides and herbicides, containing trace amounts, or no nitrogen and so were not included in the nitrogen inputs summary data. Atmospheric nitrogen (ammonium and nitrate) deposition across the study catchment was low, totalling 6950 ± 1248 kg N (based on average precipitation nitrate and ammonium concentrations between 1986 and 2007, reported in DEFRA, 2008) from nitrate and ammonium deposition, representing ~5 – 8 % of all nitrogen inputs. As such, these sources of nitrogen have not been included in the nitrogen mass balance.

Table 6.2 Nitrogen product applied to fields with corresponding percentage nitrogen

Nitrogen bearing product	Percentage nitrogen	Manufacturer
Turkey manure	2.18 – 3.89	-
Nuram 35 + 7SO ₃	35	Yara UK
Nuram 25 + 14 SO ₄	25	Yara UK
YaraBela Extran	33.5	Yara UK
OMEX NITRIFLO -XS	20	Omex
OMEX NITRIFLO -S	26	Omex
Yara Sulphur Plus	29	Yara UK
Yara Sulphan	24	Yara UK
Oilseed extra	20	Omex
Koch Advanced Nitrogen	46	Koch
Origin Enhanced N	46	Origin
Yara New Extran	24	Yara UK

One major source of uncertainty in the nitrogen inputs to the study catchment is the turkey manure applications. A large amount of turkey manure was applied to several fields within the study catchment, though the percentage of total nitrogen contained within the manure was low. Analysis of turkey manure samples from three sources was undertaken by NRM laboratories (<http://www.nrm.uk.com/>), with available N fractions of 2.18%, 2.39% and 3.89% reported (the vast majority of which was ammonium-N). In the mass balance shown in Section 6.3, a turkey manure nitrogen percentage of $2.82 \pm 0.74\%$ (the mean nitrogen percentage \pm sum of squares error) was used. Table 6.3 shows the values for turkey manure ammonium-N and uric acid-N from the three separate analyses.

Table 6.3 Calculation of uncertainty of turkey manure available nitrogen content from three analyses of turkey manure samples by NRM Laboratories in April, May and September 2012 using sum of squares error.

Ammonium-N (%)	Uric acid-N (%)	Mean ammonium-N (%)	Mean uric acid-N (%)	Std. dev. Ammonium-N (%)	Std. dev. Uric acid-N (%)
2.104	0.076				
2.756	1.130	2.81	0.62	0.52	0.53
1.732	0.662				

The sum of squares error for turkey manure nitrogen content was calculated as follows:

$$S_x = \sqrt{(S_a)^2 + (S_b)^2}$$

Where S_x is the overall uncertainty for the turkey manure available nitrogen percentage and S_a and S_b are the standard deviations for ammonium-N and uric acid-N in the turkey manure, respectively.

Loss of nitrogen through volatilisation of ammonia following application of turkey manure also represents significant uncertainty, associated with the potential mass of nitrogen available for leaching. Ammonia volatilisation is reported to account for 15 – 45% of nitrogen loss from poultry manure applications to soils in Europe (Jarvis and Pain, 1990; Moss *et al.* 1995; Chambers *et al.* 1997). Marshall *et al.* (1998) reported

much higher losses at 79%: over one week, roughly 25% of the nitrogen applied in poultry manure is lost on the first day of application, 17% is lost on the second day, 15% is lost on the third day and a further 22% of nitrogen is lost over days 4-7. Environmental conditions can drastically affect the amount of ammonia volatilisation, for example if the manure is applied during hot, dry conditions, the potential for volatilisation is much higher whereas if the manure is applied just prior to a heavy rainfall event, volatilisation losses are much lower but losses of nitrogen to runoff are increased. For these reasons, a loss of 79% N to volatilisation as reported in Marshall *et al.* (1998) is feasible. Common agricultural practice is to apply organic manures as close to the time of peak uptake rates within a crop growth cycle as possible to minimise losses.

Meisinger and Jokela (2000) explained that there are four main categories which govern volatilisation rates:

- The physicochemical characteristics of the manure, including ammonium-N, total N and dry matter content are key in governing losses of N to volatilisation, in particular ammonium-N. Drier manures tend to experience less volatilisation. Meisinger and Jokela (2000) draw comparisons between volatilisation and evaporation, where drier manures exhibit less loss of water and ammonium in comparison to dairy slurries (which typically have lower dry matter content).
- The management of application methods is one of the main factors controlling volatilisation and can be separated into losses during spreading and between spreading and incorporation into the soil zone. Volatilisation during spreading is typically minimal (around 1%), with the exception of irrigation of slurry, where 13% loss of total ammoniacal nitrogen was reported by Sharpe and Harper (1997). This does not apply to the methods at Salle however, where dry poultry manure is applied to the soil and ploughed in within 24h (Lister Noble, pers. comms.). The majority of losses of nitrogen to volatilisation occur after application, providing the manure is not incorporated into the soil quickly. The longer the manure remains at the surface, the higher the rates of volatilisation.
- Soil conditions including soil moisture content can also affect ammonia volatilisation. Soil moisture is important as soil water is the vector through which dissolved ammonia gas reaches the surface, and so more waterlogged soils would experience higher rates of ammonia volatilisation.

- Environmental factors such as wind speed and temperature influence ammonia volatilisation in the same way as they affect water evaporation as they govern the energy driving soil-air gas exchange. Therefore, higher temperatures and wind speeds increase the loss of nitrogen from poultry manure applications to volatilisation.

These factors explained by Meisinger and Jokela (2000) all contribute to the variable rates of ammonia volatilisation from poultry manure reported in the literature (15 – 45%, references in Table 6.5). The Ontario Ministry of Agriculture and Rural Affairs (2003) reported a quick reference guide for estimating volatilisation rates, shown in Table 6.4. Poultry manure applications were conducted on 12/09/2015 and 04/08/2015, when average temperatures were 17.0 and 19.6°C, respectively and total precipitation during the days where the turkey manure was applied was 3.6 and 0.0 mm, respectively. Based on Table 6.4, the rates of volatilisation for the poultry manure applied at the study site were 50%, the upper end of the range cited in the literature. Table 6.4 only takes into account the temperature and precipitation conditions (it is not shown what level of precipitation constitutes ‘wet’ and ‘dry’ in Table 6.4, though 0.0 and 3.6 mm precipitation are assumed to be ‘dry’) and so it is possible that the other factors mentioned in Meisinger and Jokela (2000) contributed to different, possibly lower rates of volatilisation. It is for this reason simulations of the mass balance have been conducted at 15% and 45% volatilisation rates.

Table 6.4 Rates of ammonia volatilisation from poultry manure under varying precipitation and temperature scenarios. The green shaded cell shows the volatilisation under the conditions when the turkey manure was applied to the study site presented in this chapter. Adapted from Ontario ministry of agriculture, food and rural affairs (2003)

Days before incorporation	Average	Cool (<10 °C)		Warm (>10 °C)	
		Wet	Dry	Wet	Dry
1	25	10	15	25	50
2	30	13	19	31	57
3	35	15	22	38	65
4	40	17	26	44	73
5	45	20	30	50	80
Not incorporated	66	40	50	75	100
Injected	0	0	0	0	0

Given the large uncertainty in the amount of nitrogen applied to the surface through turkey manure that is available for leaching, and loss of nitrogen through ammonia volatilisation, the nitrogen mass balance is separated into ‘low’ and ‘high’ scenarios, where the low scenario takes the lower end of the range of fraction of total nitrogen within turkey manure (2.07%), and assuming high losses of nitrogen to volatilisation (45%). The high nitrogen turkey manure scenario takes 3.55% nitrogen of the manure, and low losses to volatilisation (15%). The other ammonium nitrate fertilisers (shown in Table 6.2) are applied in liquid form and are incorporated immediately, therefore no volatilisation of ammonium is assumed (*pers comms.* Yara UK).

6.2.4 Riverine nitrogen flux

The riverine nitrogen flux represents the amount of nitrogen leaving the catchment, as measured at the kiosk in mini-catchment E, the most downstream location which incorporates flux from mini-catchments A and B as well. For the time period of 01/08/2015 – 30/09/2016, the total riverine nitrogen flux for the combined mini-catchments A, B and E was 18454 kg. Total riverine nitrogen flux was calculated using high resolution stream water nitrate- nitrogen concentration measurements in the kiosk at mini-catchment E. Concentrations combined with flow data (also collected by the kiosk at mini-catchment E) allowed for the calculation of the cumulative mass of nitrogen leaving the study area (mini-catchments A, B and E) via the stream every 30 minutes during the time period covered by the mass balance. An example of the calculation is as follows:

$$(\text{Stream flow (m}^3 \text{ s}^{-1}) \times 1000) \times \text{Concentration of nitrogen in the stream water (mg N L}^{-1}) \times 60 \times 30$$

6.3 Results of the nitrogen mass balance

The nitrogen mass balance calculation for the study catchment between 01/08/2015 and 30/09/2016 is shown in Table 6.5 (with a schematic diagram shown in Figure 6.4). Table 6.5 shows that 21 – 27% of the nitrogen leached from the soil zone in study catchment is unaccounted for and is assumed to be the result of denitrification in the soil zone and benthic stream sediments, with a potential minor contribution from dissimilatory nitrate reduction to ammonia (DNRA), also in the benthic sediments (Chapters 4 and 5, respectively). This equates to denitrification rates of 0.016 – 0.022 kg N ha⁻¹ d⁻¹ (see Table 6.5 for calculation)

Table 6.5 Results of the nitrogen mass balance for mini-catchments A, B and E (totalling 714.07 ha) with calculations.

Mass balance component	Value	Calculation
(a) Area covered by mass balance	714.07 ha	-
(b) Time covered by mass balance	426 days	-
(c) Total N input	99522 – 112885 kg	Fert. app. rate × field area × percentage of N in fert.
(d) Rate of volatilisation	15 -45%*	-
(e) Losses of N to volatilisation (as ammonium)	4808 – 8411 kg	N applied as TM** - (N applied as TM × (d))
(f) Amount of N removed in crop uptake	53722 – 70556 kg	(c) × (1 – crop export coefficient)
(g) Incorporation of N into SOM	12417 -13933 kg	(c) × 0.11 – 0.14***
(h) Riverine N load	18454 kg	As explained in Section 6.3
(i) Amount of N in soil leachate	23456 – 25103 kg	N available for crop uptake**** (c) - (f)
(j) Amount of N in soil leachate removed by denitrification	5002 – 6650 kg	(i) – (h)
(k) Proportion of the N in soil leachate unaccounted for	21 – 27%	$(1 - \mathbf{(h)} / \mathbf{(i)}) \times 100$
(l) Rate of denitrification	0.016 – 0.022 kg N ha ⁻¹ d ⁻¹	(j) / (a) / (b)

* Jarvis and Pain (1990); Moss *et al.* (1995); Chambers *et al.* (1997)

** Turkey Manure

***Rates of storage of nitrogen in SOM set to 11-14% of total N applied as reported in Sebilo *et al.* (2013)

**** Where turkey manure was applied, the nitrogen available for crop uptake was calculated as the nitrogen remaining following ammonia volatilisation. Where no turkey manure was applied, in the majority of cases, N available for crop uptake is the N applied as fertiliser.

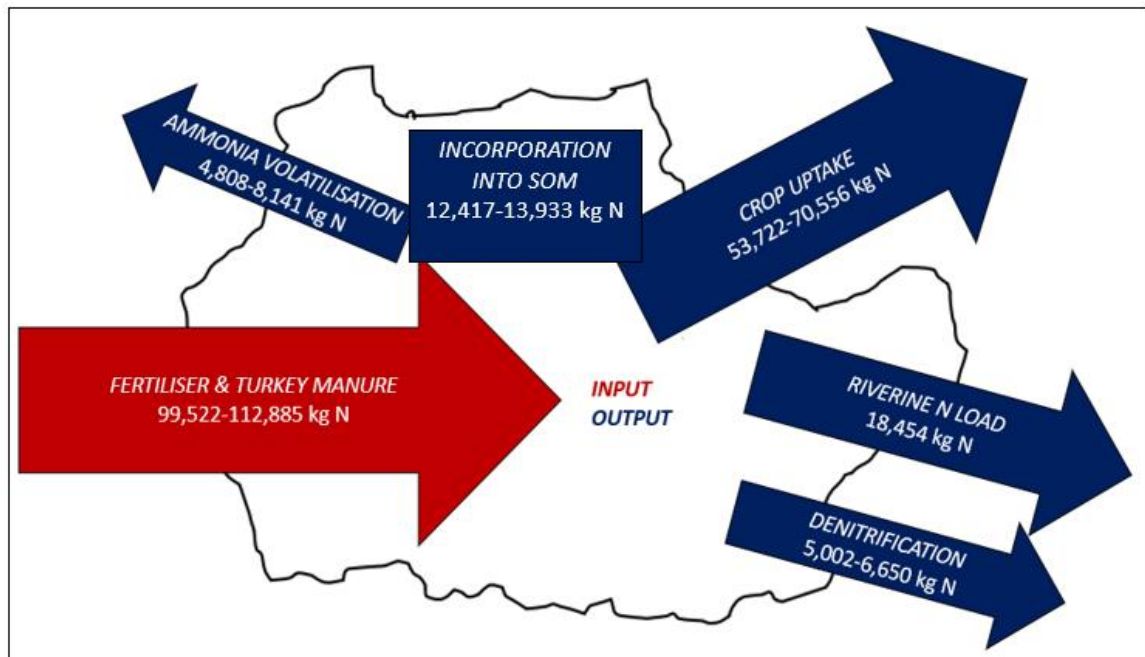


Figure 6.4 Schematic diagram of the nitrogen mass balance study area showing the inputs of nitrogen from fertiliser and turkey manure, and the removal pathways based on calculations shown in Table 6.5.

6.4 Discussion

6.4.1 Assumptions and uncertainties in the mass balance

There are a number of assumptions made regarding the nitrogen mass balance presented in Table 6.5. The first assumption is that nitrogen stored in soil organic matter (SOM) accounts for approximately 11-14% of total nitrogen applied. This is based on calculations presented in Sebilo *et al.* (2013) and not measured directly, therefore some difference in the rate of nitrogen incorporation in SOM between the system presented in Sebilo *et al.* (2013) and within the Blackwater subcatchment is presumed to exist and the 11-14% incorporation of fertiliser-derived nitrogen is therefore used as an estimation.

The second major assumption is that the system is in steady state and relates to the first assumption. The purpose of the mass balance calculation was to determine what happens to the fertiliser-N that is applied to the study catchment. To do so, a 'snapshot' of the catchment was taken and was treated as if there were no carry over of nitrogen from the previous year, with the amount of nitrogen beginning at zero. Many mass balance calculations aim to determine whether a soil has a deficit of nitrogen or a surplus and therefore whether it is a source or sink of nitrogen. For example, Lord *et al.* (2002), who constructed a spatially distributed UK-wide nitrogen mass balance for the year 1995 using annual statistics, found that the average soil nitrogen surplus was 115 kg ha^{-1} , between arable land, agricultural grassland and pig and poultry systems. For arable land, the nitrogen surplus across the UK was 51 kg ha^{-1} , substantially less than in agricultural grassland (140 kg N ha^{-1}) and more than in livestock systems (14 kg N ha^{-1}). Lord *et al.* (2002) commented that leaching of nitrogen from the soil zone can be substantial due to mineralisation of soil nitrogen and leaching is therefore correlated with nitrogen surplus, though zero soil nitrogen surplus or nitrogen deficit did not result in zero leaching in their calculations. This demonstrates that mineralisation of soil nitrogen is an important component of a mass balance in arable and grassland systems, such as the system presented in this chapter. Further work to improve this mass balance would therefore involve quantification of soil nitrogen mineralisation and fixation by legumes. Furthermore, tillage regime can affect nitrogen losses, through oxidation of soil nitrogen and potential subsequent loss of nitrogen by denitrification.

Additional uncertainties exist where the crop export coefficients were used, riverine nitrogen load was quantified, and atmospheric depositions omitted from the total nitrogen budget. As stated previously in this chapter, calculation of bespoke crop export coefficients was not an objective within this research. As such, export coefficients previously calculated by Zhang and Hiscock (2011) have been used. As with any calculated or measured export coefficient, some uncertainty must arise, though this is not reported in Zhang and Hiscock (2011). Therefore, to account for this an arbitrary uncertainty factor of $\pm 10\%$ of the values shown in Table 6.1 has been applied to the scenarios in the mass balance presented in Table 6.5, though the actual uncertainty may be greater. The quantification of riverine nitrogen loading was achieved through high resolution automated measurements of stream water dissolved nitrogen. Since there were occasions where this kiosk was not operational during the time covered by the mass

balance due to failures of maintenance, gaps in the data have been interpolated. Therefore, some uncertainty inherently exists with this component of the mass balance, though it is assumed to be minimal as the drop-outs in data were short-lived during the study period. Finally, atmospheric deposition of nitrogen has been omitted from this mass balance as it was considered to be a very minor contribution of nitrogen in comparison to fertiliser applications. As such, though a fraction of the nitrogen inputs to the study catchment, atmospheric deposition represents a further uncertainty in this mass balance.

6.4.2 Denitrification in the study catchment

The rate of denitrification calculated at the study site was $0.016 - 0.022 \text{ kg N ha}^{-1} \text{ d}^{-1}$, or $5.8 - 8.0 \text{ kg N ha}^{-1} \text{ a}^{-1}$. Barton *et al.* (1999) compiled a review of denitrification rates measured in forest and agricultural soils, reporting a mean denitrification rate of $13 \text{ kg N ha}^{-1} \text{ a}^{-1}$, slightly above the range calculated in Table 6.5 suggesting the results of this mass balance are reasonable, though fall at the low end of denitrification rates. Barton *et al.* (1999) commented that the highest rates of denitrification were reported in systems characterised by nitrogen fertilisation and irrigation. This is because irrigation increases the anoxic conditions within the soil (though waterlogging), stimulating denitrification. Furthermore, agricultural soils in which leguminous crops are grown were associated with higher rates of denitrification as nitrogen is fixed within the soil, resulting in a larger pool of reactive nitrogen. In Figure 6.3 it is shown that during 2015, the study site was primarily used for growing spring beans and so it is assumed that the loss of nitrogen through denitrification was proportionately higher between the start of the time covered by the mass balance and the establishment of the next cropping season in 2016, though some carryover soil nitrogen fixed by the spring beans and mineralisation of soil nitrogen into the next cropping season is likely as discussed in Section 6.4.1.

The purpose of this mass balance was not to establish whether a soil nitrogen surplus or deficit was present at the study site, though this information is valuable as it provides an indication of the sustainability of the soil and can inform management practices (Watson and Atkinson, 1999). To do so would involve quantification of soil nitrogen storage and mineralisation rates. Instead, given the evidence for denitrification presented in Chapters 4 and 5, the mass balance presented in this chapter aims to estimate the magnitude of

denitrification and discuss its implication in terms of nitrogen loss from an ecological and farm business perspective.

In Table 6.5 it is shown that 22 – 24% of the nitrogen applied as fertiliser leaves the soil zone as soil leachate, and that of this 22 – 24% leaving the soil zone, 21 – 27% is removed via denitrification. The clear management solution to this loss of nitrogen would be to store the nitrogen that leaves the soil zone as leachate in cover crops and reincorporate it as cover crop residue for use by the following crops. A typical approach to minimising soil nitrogen losses is to establish cover crops between cropping seasons, typically over winter. The main benefit of cover crops is that they remove moisture and nitrogen from the soil during periods when commercial crops are not established to take it up, preventing it from leaching into surface water and groundwater. Furthermore, soil organic matter content is increased with cover crop establishment and soil erosion is minimised (Strock *et al.*, 2004). These benefits not only improve soil nitrogen retention but also are beneficial to soil denitrification as soil organic matter acts as a key source of carbon for denitrification (Zhongjun *et al.*, 2017). Jackson *et al.* (1993) reported reduced soil nitrogen concentrations following winter cover crop establishment and increased soil nitrogen after incorporation of cover crop residue in relation to a fallow control field. Justes *et al.* (1999) also reported increased soil mineral nitrogen concentrations following cover crop reincorporation, indicating storage of soil nitrogen within the plant material.

In Chapter 4, strong isotopic and hydrochemical evidence for denitrification is presented as field drain data, acting as a proxy for the soil zone while in Chapter 5, some evidence for denitrification (through the same parameters as presented in Chapter 4). Based on discussions in Chapters 4 and 5, the nitrogen removed by denitrification calculated in this chapter (Table 6.5) is suggested to be primarily from the soil zone, with some contribution to denitrification occurring in the benthic sediments. There was no evidence for denitrification in groundwater shown in Chapter 5 so management approaches to minimising stream water nitrate should be focused on the soil zone, such as the establishment of cover crops to retain soil nitrogen and organic matter throughout periods where no crop is usually established. It should be noted that cover crops alone cannot solely influence denitrification in a system through denitrification. In Chapter 4 it was shown that two fields (Swanhills and Gatehouse, representing sampling sites 3 and 4, respectively), both with cover crops established showed different levels of nitrate isotopic fractionation, where the field with the higher soil clay content (Gatehouse)

actually showed less enrichment in $^{15}\text{N}_{\text{NO}_3}$ and $^{18}\text{O}_{\text{NO}_3}$. It was discussed that the cultivation regime could have had a potentially significant impact on rates of denitrification in Gatehouse, where nitrogen isotopes were less enriched, suggesting lower rates of denitrification (relative to Swanhills). Gatehouse was under a reduced tillage regime and Swanhills was under a direct drill regime. The influence of these two tillage regimes on crop residue incorporation and soil moisture and temperature was suggested to be the cause of the differences in isotope fraction in the field drains samples. Therefore, establishment of cover crops can be a powerful technique to retain nitrogen within the soil, but tillage regime should also be considered in the context of the cycling of the nitrogen that is retained, within the consideration of soil type. Farm management approaches should hence consider a holistic approach to soil nitrogen conservation in terms of its sources, how effectively it is taken up by crops, any losses to volatilisation, internal soil nitrogen cycling and ultimately its potential to leave the soil as leachate.

6.4.3 Catchment conceptual model

Figure 6.5 shows a conceptual model for the shallow deposits within the Blackwater sub-catchment of the Wensum, comprised of mini-catchments A, B and E. Figure 6.5 draws together all of the isotopic evidence for denitrification presented in Chapters 4 and 5, showing that denitrification is occurring in the soil zone and in the stream. Hyporheic zone samples did not show isotopic evidence of denitrification beneath the stream bed, however deeper in the till, at 12 m, groundwater samples with enriched (relative to the hyporheic zone samples) $\delta^{15}\text{N}_{\text{NO}_3}$ support the evidence presented by Feast *et al.* (1998) that denitrification is occurring in the subsurface. The 27 – 42% of the nitrogen leached from the soil zone that is denitrified (as presented in this chapter) is likely occurring mainly in the soil zone and to some extent in the stream.

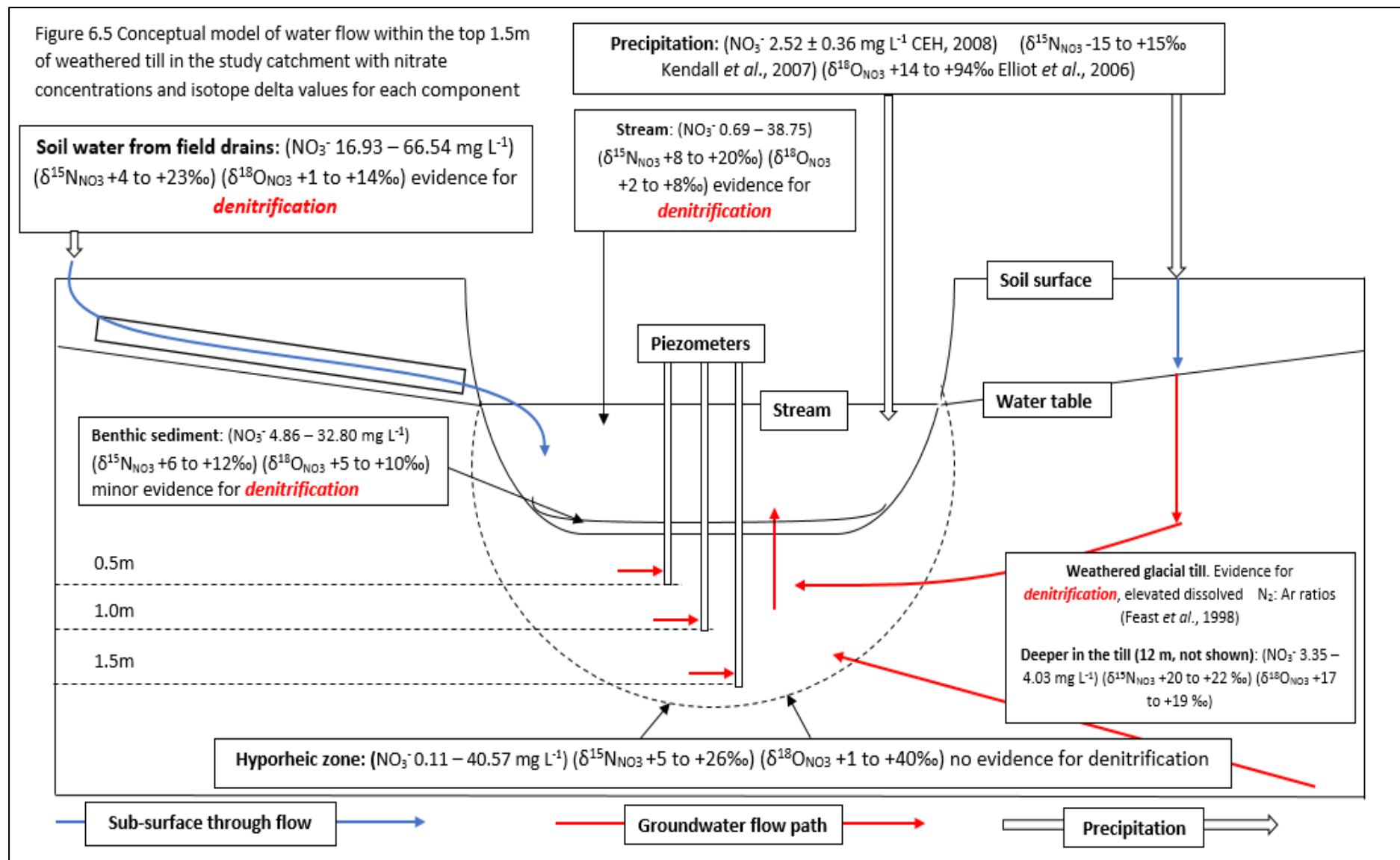


Figure 6.5 Conceptual model of water flow within the top 1.5 m of weathered till in the study catchment showing nitrate concentrations and isotope delta values for each component

6.5 Summary

In this chapter, a nitrogen mass balance for the 714.07 ha, comprised of mini-catchments A, B and E of the Blackwater sub-catchment over a period of 426 days was presented.

The nitrogen mass balance involved all nitrogen inputs from fertiliser and turkey manure applications, though did not include atmospheric deposition, which was considered a minor component. Also excluded from the mass balance was soil nitrogen mineralisation and nitrogen fixation by legumes. These factors are potentially important to the mass balance and should therefore be included in future developments of this mass balance.

Overall, of the 99522 – 112885 kg N applied to the study system, it was calculated that 22345 – 25103 kg N was leached from the soil zone (following crop uptake) and volatilisation and 5002 – 6650 kg of this leached nitrogen was then denitrified.

The riverine nitrogen load for the time covered by the study period was 18454 kg, therefore denitrification accounted for 22 – 27% of the soil leachate, resulting in a denitrification rate for the 714.07 ha of 0.016 – 0.022 kg N ha⁻¹ d⁻¹. The upper end of the range reported in the literature (0 – 0.65 kg N ha⁻¹ d⁻¹) is associated with irrigated agricultural systems where soil moisture is much higher than that of the Blackwater sub-catchment, hence the denitrification rates reported in this chapter are likely to be at the lower end.

Chapter 7 Conclusions, policy implications and recommendations for further work

7.1 Conclusions

The main conclusions from this research are that:

- Denitrification is occurring within the soil zone, with its rate mediated by soil type
- Stream water nitrate isotope data suggest that denitrification is occurring within the stream, likely in the benthic sediments
- Hyporheic zone nitrate isotope data do not indicate that denitrification is occurring directly beneath the stream bed

The primary objective of the research presented in this thesis was to ascertain if and where denitrification was occurring within an agriculturally-impacted catchment. This research aim has been achieved through the use of the denitrifier method (Sigman *et al.*, 2001; Casciotti *et al.*, 2002), where $\delta^{15}\text{N}_{\text{NO}_3}$ and $\delta^{18}\text{O}_{\text{NO}_3}$ values of field drain, stream water, benthic sediment pore water, groundwater and hyporheic zone water were used to identify the presence or absence of denitrification in the surface water and groundwater. Alongside nitrate stable isotope data, hydrochemical data were used to support the inferences made based on the measured isotopic fractionation of nitrate within the study catchment. Furthermore, water isotope data ($\delta^2\text{H}_{\text{H}_2\text{O}}$ and $\delta^{18}\text{O}_{\text{H}_2\text{O}}$ values) allowed examination of the transfer of water across the groundwater – surface water interface, providing an insight into the hydrological connectivity within the study catchment, a key consideration when examining denitrification in aquatic environments. Soil denitrification was placed within the context of soil type and wider agricultural practices, allowing discussion regarding management approaches.

Denitrification was examined along a continuum from the soil zone, to the stream, within the stream benthic sediments and finally at three depths within the hyporheic zone (0.5, 1.0 and 1.5 m). In the soil zone, there was strong evidence for denitrification, where dual fractionation of $^{15}\text{N}_{\text{NO}_3}$ and $^{18}\text{O}_{\text{NO}_3}$ in an N:O ratio of 0.62 in the field drain samples was observed. This ratio is close to the theoretical 0.5 ratio associated with denitrification and

within the range reported in the literature (0.35 – 0.76, Bottcher *et al.*, 1999; Aravena and Robertson, 1998; Mengis *et al.*, 1999; Cey *et al.*, 1999; Panno *et al.*, 2006; Wexler *et al.*, 2014; Fukada *et al.*, 2003). Furthermore, decreasing field drain nitrate concentrations were concurrent with increasing $\delta^{15}\text{N}_{\text{NO}_3}$ and $\delta^{18}\text{O}_{\text{NO}_3}$ values. The field drain samples represented three different fields with differing soil clay content, with higher soil moisture content shown at Site 4 and that Site 3, no soil moisture data were available for Sites 1 and 2. Overall, increasing soil clay content was associated with higher $\delta^{15}\text{N}_{\text{NO}_3}$ and $\delta^{18}\text{O}_{\text{NO}_3}$ values and lower nitrate concentrations, suggesting that soil clay content was contributing to denitrification through its influence on soil moisture content and hence oxygen availability. In Gatehouse field, the clay content and soil moisture was higher than in Swanhills, yet the $\delta^{15}\text{N}_{\text{NO}_3}$ and $\delta^{18}\text{O}_{\text{NO}_3}$ values were less enriched, contrary to the expectation that high clay content equates to greater enrichment of nitrate isotopes through denitrification. This was suggested to be the result of the difference in tillage regimes between the two fields. In Gatehouse, a reduced tillage regime was established. In reduced tillage systems, crop residues are incorporated into the soil following harvest using a disc or tine instead of a conventional plough, where void spaces in the soil are maintained as the roots are retained, increasing infiltration rates and reducing soil water residence time. In Swanhills field, where $\delta^{15}\text{N}_{\text{NO}_3}$ and $\delta^{18}\text{O}_{\text{NO}_3}$ values were higher, yet clay content was slightly lower, a direct-drill regime was established. Under direct-drill, new seeds are sown directly into the undisturbed soil. Overall, increased infiltration rates associated with reduced-till indicate less favourable conditions for denitrification and likely explain the more enriched $\delta^{15}\text{N}_{\text{NO}_3}$ and $\delta^{18}\text{O}_{\text{NO}_3}$ values yet lower clay content of the direct-drilled field (Swanhills). This suggests that while soil texture (and hence moisture) is a key component in governing soil denitrification rates, tillage regime can also have an effect. From these observations it was concluded that denitrification was prominent within the soil zone, with rates being influenced by soil physical characteristics, while tillage regime was suggested to have the capacity to override the influence of soil structure to an extent.

A main research objective of this study was to produce an integrated field-scale assessment of soil zone denitrification. This has been achieved by using field drain leachate as an analogue for whole-field denitrification. Providing such integrated results is of use to land managers as it allows for the examination of denitrification potential on a field-by-field basis, considering differences in soil type, topography, and irrigation,

cropping and tillage regimes. A clear difference between individual fields in terms of soil zone denitrification has been presented in an accessible format, allowing for the discussion of why these differences might have occurred and from this, better management strategies can be developed. This represents a significant contribution to how end-users might approach managing their land on a higher spatial resolution than for example catchment scale. An extensive search of the literature suggests that the work presented in Chapter 4 of this thesis effectively addresses a knowledge gap regarding integrated field-scale nitrogen cycling.

In the stream, dual fractionation of nitrate isotopes was also observed, at an N:O ratio of 0.88, above the range reported in the literature. There was no associated reduction in nitrate concentration with increasing $\delta^{15}\text{N}_{\text{NO}_3}$ and $\delta^{18}\text{O}_{\text{NO}_3}$ values. The explanation for the apparent isotopic evidence for denitrification in the stream water but lack of simultaneous nitrate concentration reduction is complex. Since denitrification is more likely to occur within the benthic sediments than in the stream (because stream water is in direct contact with the atmosphere and is hence typically oxygen saturated), isotopic fractionation would be expected to be low, as rates of denitrification are limited by diffusion of nitrate from the overlying water column into the sediment, which does not result in significant isotopic fractionation. This is not consistent with the stream water nitrate isotope data. Examining the water isotope data ($\delta^2\text{H}_{\text{H}_2\text{O}}$ and $\delta^{18}\text{O}_{\text{H}_2\text{O}}$ values) suggests that the exchange of water across the groundwater - surface water interface may occur at different rates along the study reach. If this is the case, then the sites along the study reach where incorporation of stream water into the subsurface is relatively high, rates of benthic denitrification may not be limited by diffusion of nitrate into the sediment.

The ratio of N:O fractionation was still higher than the range reported in the literature associated with denitrification however. Atmospheric nitrate contains highly fractionated ^{18}O , and so its incorporation through precipitation, even in small amounts may be enough to increase the ratio of N:O isotopic fractionation above the expected range. Stream nitrite and ammonium concentrations were low, and so for nitrification to maintain stream nitrate concentrations, oxidation of ammonium to nitrite and successive oxidation of nitrite to nitrate must be rapid.

A second explanation for the trends observed in the stream data is the presence of dissimilatory nitrate reduction to ammonium (DNRA), also coupled with subsequent nitrification. This is because in - stream DNRA has been shown to produce high N:O isotopic fractionation ratios (0.88 – 1.02, Gentry et al., 2008) and requires similar conditions shown in the study stream, though DNRA is typically favoured over denitrification when nitrate is limited and organic carbon is in abundance. In the stream, dissolved organic carbon (DOC) concentrations were low and nitrate concentrations were not limiting, contrary to the conditions required by DNRA. Incorporation of atmospheric nitrate with high $\delta^{18}\text{O}_{\text{NO}_3}$ values is likely to be driving the high N:O fraction ratio in the stream water, and rapid nitrification of ammonium in the benthic sediments was probably occurring to provide the dual fractionation of nitrate isotope ratios, though DNRA cannot be entirely dismissed.

Much of the discussion of in - stream denitrification relates to the benthic sediments. Diffuse Equilibrium in Thin Films (DET) probes were deployed into the sediments at the most downstream sampling site (i.e. the location of the most downstream field drain and piezometers sampled). Isotopic analysis of sediment pore waters along a 2.5 – 15.0 cm profile was carried out and although the data were few in number, dual fractionation of nitrate isotopes is tentatively suggested, though this should be treated with caution as the correlation between $\delta^{15}\text{N}_{\text{NO}_3}$ and $\delta^{18}\text{O}_{\text{NO}_3}$ values is weak ($r^2 = 0.14$). A slope of 0.32 was calculated for the sediment pore water $\delta^{15}\text{N}_{\text{NO}_3}$ and $\delta^{18}\text{O}_{\text{NO}_3}$ values, close to the low end of the range reported in the literature associated with denitrification. This is consistent with the discussion of stream water nitrate isotope data where the isotope signal is likely the result of benthic denitrification as opposed to within the water column. From the stream water and benthic sediment pore nitrate isotope and nitrate concentration data it was concluded that denitrification was likely to be occurring in the benthic sediments, facilitated by zones of preferential exchange of water and nutrients across the surface water – groundwater boundary. Furthermore, nitrification coupled to denitrification was suggested to be occurring, given the lack of concurrent reduction of stream water nitrate concentration with enrichment of $\delta^{15}\text{N}_{\text{NO}_3}$ and $\delta^{18}\text{O}_{\text{NO}_3}$ values. Therefore, it was concluded that the nitrate isotope composition in the stream water could be the result of benthic denitrification coupled with nitrification which would maintain stream nitrate concentrations, thus negating the reduction in nitrate concentration associated with increasing $\delta^{15}\text{N}_{\text{NO}_3}$ and $\delta^{18}\text{O}_{\text{NO}_3}$ values. This is suggested by the $\delta^{15}\text{N}_{\text{NO}_3}$ and $\delta^{18}\text{O}_{\text{NO}_3}$

values in the stream water which fell within the range typically associated with nitrification of fertiliser ammonium and soil organic matter. The isotopic effects of denitrification and nitrification act in opposite directions (i.e. where denitrification enriches the remaining pool of nitrate in ^{15}N and ^{18}O and nitrification produces isotopically light nitrate). For denitrification or DNRA to have been the only process influencing stream water nitrate isotope values, the $\delta^{15}\text{N}_{\text{NO}_3}$ and $\delta^{18}\text{O}_{\text{NO}_3}$ values must have been higher than observed, therefore it is suggested that nitrification of fertiliser ammonium and soil organic matter in the stream was both maintaining nitrate concentrations, thus negating the expected inverse relationship between nitrate concentration and isotopic enrichment, but also acted to curtail enrichments of the dissolved nitrate.

The hyporheic zone is typically regarded as containing ideal conditions for denitrification, where incorporation of organic matter from the overlying surface water provides a source of carbon (and hence an electron donor) for denitrification of nitrate contained in the groundwater. No isotopic evidence for denitrification was observed in the hyporheic zone (0.5 1.0 and 1.5 m beneath the stream bed) however, though nitrate concentrations were low. Feast *et al.* (1998) showed that denitrification was occurring in the weathered glacial till of Norfolk through elevated dissolved $\text{N}_2:\text{Ar}$ ratios. The low nitrate concentrations yet lack of isotopic evidence for denitrification in the piezometer samples presented in this thesis is therefore assumed to be because the shallow groundwater is already denitrified before it arrives in the piezometers. Mixing with other sources of water within the catchment and potential diffusion of nitrate into the matrix therefore must result in the absence of dual fractionation of nitrate isotopes.

The hydraulic gradient across the sites at which the piezometer nests were installed covered both upwelling and downwelling. It is generally assumed that at downwelling sites, dissolved oxygen and carbon species are delivered to the hyporheic sediments and at upwelling sites, nitrate rich groundwater is delivered to the surface. This variation in conditions should influence the denitrification potential of hyporheic sediments, however there was no significant difference in nitrate, dissolved oxygen or dissolved organic carbon concentration measured in the hyporheic zone samples collected across all sites. It was therefore concluded that the direction of groundwater flow across the groundwater-surface water interface was not a key determining factor in hyporheic zone denitrification in this study system. The majority of studies examine denitrification in hyporheic

sediments at shallow depths, with deeper (>0.5m) sediments being significantly underrepresented in the literature. The piezometers used in this study to assess hyporheic zone denitrification were installed to 0.5, 1.0 and 1.5m beneath the stream bed, occupying a much greater range of potential groundwater flow patterns. Therefore, the results in Chapter 5 contribute to this knowledge gap and are the main novel contribution of this part of the thesis.

A nitrogen mass balance for the study catchment was presented in Chapter 6, in which the rate of denitrification for three mini-catchments within the Blackwater subcatchment (totalling 714.07 ha) was calculated. Denitrification rates in the Blackwater sub-catchment were calculated as $0.023 - 0.043 \text{ kg N ha}^{-1} \text{ d}^{-1}$, with the range in the data arising from uncertainty in turkey manure nitrogen content and rates of ammonia volatilisation. It was estimated that 27% - 42% of the nitrogen leached from the soil zone following crop uptake and volatilisation was removed from the system by denitrification. Based on discussions in Chapters 4 and 5, this denitrification occurs in the soil zone and stream, with the soil zone likely contributing the majority of denitrification, as soil conditions are less variable than those in the benthic sediments, and the isotopic and hydrochemical evidence is stronger in the field drain samples than in the stream and sediment samples.

7.2 Policy implications

The UK currently adheres to the European Union Water Framework Directive (WFD) (WFD/2000/60 EC), which requires that surface waters and groundwaters maintain 'good' ecological and chemical status. This is achieved by the adoption of river basin management plans, which aim to reduce the impacts of pollutants (including nitrogen). At the river basin and catchment scales, the measures available to reduce the impact of pollutants on surface water and groundwater quality are typically better identified and executed than at larger scales, since the hydrologic data and demographic information, and extent of agricultural activity can easily be quantified within a catchment (CEC, 2000). The WFD takes two key approaches in the prevention of water resource pollution: addressing pollution at the source and setting environmental targets. Nitrate pollution from agriculture is difficult to tackle at the source as it is typically diffuse in nature

where no single source is present (Bouraoui and Grizzetti, 2014). One example of a directive relevant to diffuse pollution is the Nitrates Directive (91/676/EEC), in which safe drinking water in terms of nitrate concentration is the goal.

Given the evidence for denitrification presented in Chapters 4, 5 and 6 of this thesis, it is clear that denitrification is occurring in the soil zone rather than in the hyporheic zone, and that the soil zone has great potential for denitrification. Therefore, policy makers and farmers should focus on managing soil conditions, as opposed to hyporheic zone conditions in this instance. This is favourable as a range of approaches has already been established to enhance soil nitrogen cycling potential. From an ecological perspective, enhancing soil denitrification reduces the risk of eutrophication of surface water bodies from soil runoff and of contamination of potable groundwater sources. This is detrimental from a farm business perspective however, as denitrification represents a loss of fertiliser or soil nitrogen which could otherwise be retained and used for subsequent crops. In this respect, directing management efforts towards practices such as establishing cover crops achieves both goals: less nitrate reaches adjacent aquatic ecosystems and groundwater, and less soil nitrogen is lost through denitrification. It was discussed in Chapter 4 how tillage regime can also influence soil denitrification potential, where a direct-drill method resulted in more enriched field drain nitrate isotope values than in a soil where clay content was higher but reduced-tillage was established. This demonstrates the potential for tillage regime to preserve soil nitrate and in combination with cover cropping, may ensure the sustainability of many farming systems. Policy makers should encourage the uptake of such approaches as they are practically achievable, and their benefits are easily quantified.

The hyporheic zone should not be ignored entirely however, as there is a wealth of evidence in the literature demonstrating its efficacy in nitrogen cycling in agricultural settings (e.g. Welsh *et al.*, 2016; Zarnetske *et al.*, 2011b). Managing hyporheic zone denitrification potential in an agricultural setting is difficult as it typically involves altering river geomorphology by introducing meanders to generate riffle pool sequences (encouraging down welling of stream water into the subsurface). Agricultural streams are usually straight as this is the most efficient use of the land surface area. In comparison, managing soil zone denitrification is straightforward by e.g. establishing cover crops, an approach for which a farm will already have the machinery and infrastructure. Where river restoration projects are already occurring however, the functionality of the

hyporheic zone could be taken into account as improving natural remediation of nitrogen-enriched waters would be consistent with the purpose of a river restoration project: to improve the capacity of the river to deliver ecological services.

7.3 Recommendations for further work

This thesis presents a spatial distribution approach to examining denitrification within a catchment, focusing on the groundwater – surface water continuum. Within this research, $\delta^{15}\text{N}_{\text{NO}_3}$ and $\delta^{18}\text{O}_{\text{NO}_3}$ values were placed in the context of soil physical structure. Though not extensively examined, this is a novel approach, and which warrants further research as it would improve the understanding of field scale denitrification, particularly in areas where soil type is highly variable. The application of Diffuse Equilibrium in Thin Films (DET) probes to pore water nitrate isotopic composition was introduced, a method that is currently in its infancy with few existing studies taking this approach. Therefore, the following recommendations for further work aim to build on these methods.

The work presented in this thesis successfully identified denitrification in discrete zones along a groundwater – surface water continuum. The magnitude of denitrification was also estimated. Further work to refine these findings would include analysis of precipitation nitrate and water isotopes to quantify the contribution of precipitation to the isotopic signal of the soil water, stream and groundwater samples through a mass balance calculation. Further application of the denitrifier method on assessing stream sediment pore water nitrate isotopic characteristics would also be of interest as the use of DET probes in this research is limited, with the intention to carry out a much larger sampling campaign. Given the isotopic evidence for denitrification in the stream water samples, further investigation of benthic sediment processes would provide a much clearer understanding of coupled stream-benthic zone nitrogen cycling, a potentially important region of denitrification. The nitrogen mass balance calculation presented in Chapter 6 is a useful tool for examining the fate of the nitrogen applied to the catchment. Analysis of legume root leaf and stem nitrogen content, however, would provide a better understanding of soil nitrogen fixation alongside measurement of soil organic matter nitrogen content. Since soil nitrogen was not included in the mass balance, its quantification would improve the calculations as a whole.

It was discussed that tillage regime had an influence on soil denitrification, though was not the main purpose of this study. A more in-depth investigation utilising the denitrifier method into soil water denitrification in the context of soil type and tillage regime would be of interest. Connecting field drain $\delta^{15}\text{N}_{\text{NO}_3}$ and $\delta^{18}\text{O}_{\text{NO}_3}$ values to soil texture and tillage regime is a novel application of dual stable isotope research which was discussed in Chapter 4. This would provide isotopic and hydrochemical information on the influence of tillage regime and, for example, presence/absence of cover crops on soil nitrogen cycling processes. To achieve this, porous pots could be installed into fields with different soil types and tillage regimes and sampled using a vacuum pump. Overall, this thesis presents a novel examination of denitrification in different vertical zones within an agriculturally-impacted catchment. To build upon the results presented here generate the capacity for predictive inferences on the fate of nitrogen fertiliser applications would be of great ecological and economic interest to policy makers and land managers alike.

References

- Aber, J. D., Magill, A., McNulty, S. G., Boone, R. D., Nadelhoffer, K. J., Downs, M. and Hallett, R., 1995. Forest biogeochemistry and primary production altered by nitrogen saturation. *Water Air and Soil Pollution*, **85**, 1665-1670.
- Aleem M. I. H., Hoch G. E., and Varner J. E., 1965. Water as the source of oxidant and reductant in bacterial chemosynthesis. *Biochemistry*, **54**, 869–873.
- Alkhatib, M., Lehmann, M.F., and del Giorgio, P.A., 2012. The nitrogen isotope effect of benthic remineralization-nitrification-denitrification coupling in an estuarine environment. *Biogeosciences*, **9**, 1633-1646.
- Andrews, J.E., Brimblecombe, P., Jickells, T.D., and Liss, P.S., 1996. An introduction to environmental chemistry. Blackwell Science, Oxford.
- Aravena, R., and Robertson, W.D., 1998. Use of Multiple Isotope Tracers to Evaluate Denitrification in Ground Water: Study of Nitrate from a Large-Flux Septic System Plume. *Groundwater*, **36**, 975-982
- Bacon P.E. and Freney J.R., 1989. Nitrogen loss from different tillage systems and the effect on cereal grain yield. *Fertiliser Research*, **20**, 59–66.
- Baggs, E. M., 2008. A review of stable isotope techniques for N₂O source partitioning in soils: recent progress, remaining challenges and future considerations. *Rapid Communications in Mass Spectrometry*, **22**, 1664-1672.
- Barton, L., McLay, C.D.A., Schiper, L.A., and Smith, C.T., 1999. Annual denitrification rates in agricultural and forest soils: a review. *Australian Journal of Soil Research*, **37**, 1073 - 1097.
- Bateman, A.S., and Kelly, S.D., 2007. Fertiliser nitrogen isotope signatures. *Isotopes in Environmental and Health Studies*, **3**, 237 – 247.
- Kendall, C., and McDonnell, J.C., 1998. Isotope Tracers In Catchment Hydrology. Elsevier, Amsterdam.
- Boulton, A. J., Findlay, S., Marmonier, P., Stanley, E. H. and Valett, H. M., 1998. The functional significance of the hyporheic zone in streams and rivers. *Annual Review of Ecology and Systematics*, **29**, 59-81.
- Bot, A., and Benites, J., 2005. The importance of soil organic matter: key to drought-resistant soil and sustained food production. Food and Agriculture Organisation of the United States, Rome.
- Böttcher, J., Strebel, O, Voerkelius, S., and Schmidt, H.L., 1990. Using isotope fractionation of nitrate-nitrogen and nitrate-oxygen for evaluation of microbial denitrification in a sandy aquifer. *Journal of Hydrology*, **114**, 413-424.
- Boulton, A. J., Findlay, S., Marmonier, P., Stanley, E. H. and Valett, H. M. 1998. The functional significance of the hyporheic zone in streams and rivers. *Annual Review of Ecology and Systematics*, **29**, 59-81.
- Bouraoiu, F., and Grizzetti, B., 2014. Modelling mitigation options to reduce diffuse nitrogen water pollution from agriculture. *Science of the Total Environment*, **468**, 1267-1277.
- Briggs, M. A., Day-lewis, F. D., Zarnetske, J. P. and Harvey, J. W., 2015. A physical explanation for the development of redox microzones in hyporheic flow. *Geophysical Research Letters*, **42**, 4402-4410.

- Briody, A.C., Cardenas, M.B., Shuai, P., Knappett, S.K., and Bennett, P.C., 2016. Groundwater flow, nutrient, and stable isotope dynamics in the parafluvial-synergetic zone of the regulated Lower Colorado River (Texas, USA) over the course of a small flood. *Hydrogeology Journal*, **24**, 923-935.
- Bristow, L.A., 2009. Tracing nitrogen flows across the southern North Sea: A stable isotope approach. PhD thesis, University of East Anglia, UK.
- Brunke, M. and Gonser, T., 1997. The ecological significance of exchange processes between rivers and groundwater. *Freshwater Biology*, **37**, 1-33.
- Buchwald, C. and Casciotti, K. L., 2010. Oxygen isotopic fractionation and exchange during bacterial nitrite oxidation. *Limnology and Oceanography*, **55**, 1064-1074.
- Bugler, P.R., Kehew, A.E., and Nelson, R.A., 1989. Dissimilatory nitrate reduction in a wastewater contaminated aquifer. *Ground Water*, **25**, 664-671.
- Burgin, A.J., and Hamilton, S.K., 2007. Have we overemphasized the role of denitrification in aquatic ecosystems? A review of nitrate removal pathways. *Frontiers in Ecology and the Environment*, **5**, 89 – 96.
- Byrne, P., Binley, A., Heathwaite, A.L., Ulla, S., Heppell, C.M., Lansdown, K., Zhang, H., Trimmer, M., and Keenan, P., 2014. Control of river stage on the reactive chemistry of the hyporheic zone. *Hydrological Processes*, **28**, 4766-4779.
- Cambell, D., H., Kendall, C., Chang, C., C.Y., Silva, S., R. and Tonnessen, K., A., 2002. Pathways for nitrate release from an alpine watershed: Determination using $\delta^{15}\text{N}$ and $\delta^{18}\text{O}$. *Water Resources Research*, **38**: DOI: 10.1029/2001WR000292.
- Casciotti, K.L., 2009. Inverse kinetic isotope fractionation during bacterial nitrite oxidation. *Geochimica et Cosmochimica Acta*, **73**, 2061-2076.
- Casciotti, K.L., Sigman, D.M., and Ward, B.B., 2003. Linking diversity and stable isotope fractionation in ammonia-oxidising bacteria. *Geomicrobiology Journal*, **20**, 335-353.
- Casciotti, K.L., Sigman, D.M., Hastings, M.G., Bolker, J.K., and Hilkert, A., 2002. Measurement of the oxygen isotopic composition of nitrate in seawater and freshwater using the denitrifier method. *Analytical Chemistry*, **74**, 4905 – 4912.
- Centre for Ecology and Hydrology, 2009. National River Flow Archive. Natural Environment Research Council.
- Castellano, M.J., Lewis, D.B., Kaye, J.P., 2013. Response of soil nitrogen retention to the interactive effects of soil texture, hydrology, and organic matter. *Journal of Geophysical Research: Biogeosciences*, **118**: DOI 10.1002/jgrg.20015.
- Centre for Ecology and Hydrology, 2009. National River Flow Archive. Natural Environment Research Council.
- Centre for Ecology and Hydrology, 2008. UK Acid Deposition Network: Data Summary 2007. AEAT/ENV/R/2706 Issue 1.
- CEC. Establishing a framework for community action in the field of water policy. Brussels: Commission of the European Communities, 2000.
- Cey, E.E., Rudolph, D.L., Aravena, R., and Parkin, G., 1999. Role of riparian zone in controlling the distribution and fate of agricultural nitrogen near a small stream in Southern Ontario. *Journal of Contaminant Hydrology*, **37**, 46-67.
- Chadwick, O.A., and Chorover, J., 2001. The chemistry of pedogenic thresholds. *Geoderma*, **100**, 321-353.

- Chambers, B.J., Smith, K.A., and Van Der Weerden, T.J., Ammonia emissions following the land spreading of solid manures. In *Gaseous Nitrogen Emissions from Grasslands*. (Eds) Jarvis, S.C., and Pain, B.F., pp 275 – 280. CAB International. Oxon, UK.
- Claret, C. and Fontvieille, D., 1997. Characteristics of biofilm assemblages in two contrasted hydrodynamic and trophic contexts. *Microbial Ecology*, **34**, 49-57.
- Clayton, H., McTaggart, I.P., Parker, J., Swan, L., and Smith, K.A., 1997. Nitrous oxide emissions from fertilised grassland: A 2-year study of the effects of N fertiliser form and environmental conditions. *Biology and Fertility of Soils*, **25**, 252-260.
- Cooper, R.J., 2015. Advancing methods for apportioning the source of sediment in rivers: Combining spectroscopy and stable isotopes with Bayesian mixing models. PhD thesis, University of East Anglia, UK.
- Council of European Communities, 2000. Directive of the European Parliament and of the Council establishing a framework for the Community action in the field of water policy (2000/60/EC).
- Council of European Communities, 1991. Directive Concerning the Protection of Waters against Pollution Caused by Nitrates from Agricultural Sources (91/676/EEC).
- Craig, H., 1961. Isotopic variations in meteoric waters. *Science*, **133**, 1702 – 1703.
- Davidsson, T.E., and Stahl, M., 2000. The influence of organic carbon on nitrogen transformations in five wetland soils. *Soil Science Society of America Journal*, **64**, 1129-1136.
- De Klein, C.A.M., and Van Logtestijn, R.S.P., 1994. Denitrification in the top soil of managed grasslands in The Netherlands in relation to soil type and fertilizer level. *Plant and Soil*, **163**, 33-34.
- Delwiche, C.C., and Steyn, P.L., 1970. Nitrogen isotope fractionation in soils and microbial reactions. *Environmental Science and Technology*, **4**, 929-935.
- Department of Environment, Food and Rural Affairs: Water Quality Division, 2008. Implementation of the Nitrates Directive (91/676/EEC): Description of the methodology applied in identifying waters and designating Nitrates Vulnerable Zones in England, 2008. Department for Environment, Food and Rural Affairs.
- Dreyfus, B. L. and Dommergues, Y. R., 1981. Nitrogen-fixing nodules induced by rhizobium on the stem of the tropical legume sesbania-rostrata. *FEMS Microbiology Letters*, **10**, 313-317.
- Drtil, M., Németh, P., Kucman, K., Bodík, I., and Kašperek, V., 1995. Acidobasic balances in the course of heterotrophic denitrification. *Water Research*, **29**, 1353-1360.
- Durka W., Schulze E. D., Gebauer G., and Voerkelius S., 1994). Effects of forest decline on uptake and leaching of deposited nitrate determined from ¹⁵N and ¹⁸O measurements. *Nature*, **372**, 765–767.
- Edwards, A. M. C., 1973. The variation of dissolved constituents with discharge in some Norfolk rivers. *Journal of Hydrology*, **18**, 219-242.
- Elliot, E.M., Kendall, C., Wankel, D., Burns, D.A., Boyer, E.W., Harlin, K., Bain, D.J., and Butler, T.J., 2006. Nitrogen isotopes as indicators of NO_x source contributions to atmospheric nitrate deposition across the Midwestern and Northern United States. *Environmental Science and Technology*, **41**, 7661 – 7667.
- Environment Agency, 2009a. What's in your backyard? urban wastewater treatment. Environment Agency, <http://maps.environment-agency.gov.uk/wiyby> Last accessed 11/2009.

- Environment Agency, 2009b. HiFlows-UK. Environment Agency <http://www.environment-agency.gov.uk/hiflows/91727.aspx> Last accessed 10/2009.
- Environment Agency, 2007. Tracer tests for investigating flow and transport in the hyporheic zone. Science report SCV030155/8.
- ENTEC, 2007. Phase 3 Project Report for the Yare and North Norfolk Groundwater Resource Investigation Area. Wensum and Tud Reporting Area, Volume 1: Characterisation of Catchment Behaviour. Peterborough, Environment Agency.
- Erisman J.W., de Vries W., Kros H., Oenema O., van der Eerden L., van Zeijts H. and Smeulders S., 2001. An outlook for a national integrated nitrogen policy. *Environmental Science and Policy*, **4**, 87–95.
- Essington, M.E., 2004. 'Soil Water Chemistry' in Essington, M.E., Soil and Water Chemistry, an Integrated Approach. CRC Press, Florida, US. pp. 183-251.
- Erisman, J. W., Sutton, M. A., Galloway, J., Klimont, Z. and Winiwarter, W., 2008. How a century of ammonia synthesis changed the world. *Nature Geoscience*, **1**, 636-639.
- Farr, G.J., Patton, A.M., Boon, D., James, D.R., Williams, B., and Schofield, D.I., 2017. Mapping shallow urban groundwater temperatures, a case study from Cardiff, UK. *Quarterly Journal of Engineering Geology and Hydrogeology*, **50**, 187-198.
- Feast, N.A., Hiscock, K.M., Dennis, P.F., and Andrews, J.N., 1998. Nitrogen isotope hydrochemistry and denitrification within the Chalk aquifer system of north Norfolk, UK. *Journal of Hydrology*, **211**, 233-252.
- Feigin, A., Shearer, G., Kohl, D.H., and Commoner, B., 1947. The amount and nitrogen-15 content of nitrate in soil profiles from two central Illinois fields in a corn-soybean rotation. *Soil Science Society of America Proceedings*, **38**, 465-471.
- Fogel, M.L., and Cifuentes, L.A., 1993. Isotope fractionation during primary production. In: Engel, M.H., and Macko, S.A. (Eds). *Organic Geochemistry*, Plenum Press New York, pp 73-98.
- Fowler, D., Coyle, M., Skiba, U., Sutton, M. A., Cape, J. N., Reis, S., Sheppard, L. J., Jenkins, A., Grizzetti, B., Galloway, J. N., Vitousek, P., Leach, A., Bouwman, A. F., Butterbach-Bahl, K., Dentener, F., Stevenson, D., Amann, M. and Voss, M., 2013. The global nitrogen cycle in the twenty-first century. *Philosophical Transactions of the Royal Society B-Biological Sciences*, 368.
- Fukada, T., Hiscock, K. M., Dennis, P. F. and Grischek, T. 2003. A dual isotope approach to identify denitrification in groundwater at a river-bank infiltration site. *Water Research*, **37**, 3070-3078.
- Galloway, J. N., Dentener, F. J., Capone, D. G., Boyer, E. W., Howarth, R. W., Seitzinger, S. P., Asner, G. P., Cleveland, C. C., Green, P. A., Holland, E. A., Karl, D. M., Michaels, A. F., Porter, J. H., Townsend, A. R. and Vorosmarty, C. J., 2004. Nitrogen cycles: past, present, and future. *Biogeochemistry*, **70**, 153-226.
- Galloway, J. N., Aber, J. D., Erisman, J. W., Seitzinger, S. P., Howarth, R. W., Cowling, E. B. and Cosby, B. J., 2003. The nitrogen cascade. *Bioscience*, **53**, 341-356.
- Galloway, J.N., Schlesinger, W.H., Levy, H. II, Michaels, A., and Schnoor, J.L., 1995. Nitrogen fixation: atmospheric enhancement–environmental response. *Global Biogeochemical Cycles*, **9**, 235–252.
- Gat J. R., 1996. Oxygen and hydrogen isotopes in the hydrological cycle. *Annual Review of Earth and Planetary Sciences*, **24**, 225–262.

- Gentry, L. E., David, M. B., Below, F. E., Royer, T. V. and McIsaac, G. F., 2009. Nitrogen Mass Balance of a Tile-drained Agricultural Watershed in East-Central Illinois. *Journal of Environmental Quality*, **38**, 1841-1847.
- George, M.A., 1998. High precision stable isotope imaging of groundwater flow dynamics in the chalk aquifer systems of Cambridgeshire and Norfolk. PhD thesis, University of East Anglia, UK.
- Germon, J.C. (Ed.), 1989. Management Systems to Reproduce Impact of Nitrates. Elsevier Science, Amsterdam.
- Granger, J., Sigman, D.M., Lehmann, M.F., and Tortell, P.D., 2008. Nitrogen and oxygen isotope fractionation during dissimilatory reduction of nitrate to ammonium by denitrifying bacteria. *Limnology and Oceanography*, **53**, 2533 – 2545.
- Green P.A., Vörösmarty C.J., Meybeck M., Galloway J.N., Peterson B.J. and Boyer E.W., 2004. Pre-industrial and contemporary fluxes of nitrogen through rivers: a global assessment based on typology. *Biogeochemistry*, **68**, 71–105.
- Grimm, N. B., 1987. Nitrogen dynamics during succession in a desert stream. *Ecology*, **68**, 1157-1170.
- Groffman, P. M., Butterbach-Bahl, K., Fulweiler, R. W., Gold, A. J., Morse, J. L., Stander, E. K., Tague, C., Tonitto, C. and Vidon, P., 2009. Challenges to incorporating spatially and temporally explicit phenomena (hotspots and hot moments) in denitrification models. *Biogeochemistry*, **93**, 49-77.
- Hama – Aziz, Z.Q., Assessment of the application of a cover crop and conservation tillage on soil and water properties and on dissolved nitrous oxide in an arable system, Ph.D. thesis, University of East Anglia, UK.
- Harvey, J.W., Böhlke, J.K., Voytek, M.A., Scott, D., and Tobias, C.R., 2013. Hyporheic zone denitrification: controls on effective reaction depth and contribution to whole-stream mass balance. *AGU Publications*, doi: 10.1002/wrcr.20492.
- Haygarth, P., Johnes, P., Butterfield, D., Foy, B., and Withers, P., 2003. Land Use for Achieving ‘Good Ecological Status’ of Water Bodies in England and Wales: A Theoretical Exploration for Nitrogen and Phosphorus. The Institute of Grassland and Environmental Research, Okehampton.
- Heppell, C., Heathwaite, A.L., Binley, A., Byrne, P., Ullah, S., Lansdown, K., Keenan, P., Trimmer, M., and Zhang, H., 2014. Interpreting spatial patterns in redox and coupled water-nitrogen fluxes in the streambed of a gaining river reach. *Biogeochemistry*, **117**, 491-509.
- Heppell, C. M., Binley, A., Trimmer, M., Darch, T., Jones, A., Malone, E., Collins, A. L., Johnes, P. J., Freer, J. E. and Lloyd, C. E. M., 2017. Hydrological controls on DOC: nitrate resource stoichiometry in a lowland, agricultural catchment, southern UK. *Hydrology and Earth System Sciences*, **21**, 4785-4802.
- Hill, A.R., Devito, K.J., Campagnolo, S., and Sanmugas, K., 2000. Subsurface denitrification in a forest riparian zone: Interactions between hydrology and supplies of nitrate and organic carbon. *Biogeochemistry*, **51**, 193-223.
- Hill, A.R., 1996. Nitrate removal in stream riparian zones. *Journal of Environmental Quality*, **25**, 743-755.
- Hill, R. D., Rinker, R. G. and Wilson, H. D. 1980. Atmospheric nitrogen-fixation by lightning. *Journal of the Atmospheric Sciences*, **37**, 179-192.
- Hiscock, K.M., and Bense, V.F., 2014. Environmental isotope hydrogeology. In *Hydrogeology: Principles and Practice* (2nd Edition). Wiley Blackwell.

- Hiscock, K. M., Dennis, P. F., Saynor, P. R. and Thomas, M. O., 1996. Hydrochemical and stable isotope evidence for the extent and nature of the effective Chalk aquifer of north Norfolk, UK. *Journal of Hydrology*, **180**, 79-107.
- Hiscock, K. M. 1993. The influence of pre-devensian glacial deposits on the hydrogeochemistry of the chalk aquifer system of north Norfolk, UK. *Journal of Hydrology*, **144**, 335-369.
- Hobbie, E.A., and Buimette, A.P., 2009. Controls on nitrogen isotope patterns in soils. *Biogeochemistry*, **95**, 355-371.
- Hoefs, J., 2004. *Stable Isotope Geochemistry*, Berlin, Springer-Verlag.
- Hoering, T.C., and Ford, H.T., 1960. The isotope effect in the fixation of nitrogen by *Azobacter*. *Journal of the American Chemistry Society*, **82**, 376-378.
- Hofstra, N., and Bouwman, A.F., 2005. Denitrification in agricultural soils: summarizing published data and estimating global annual rates. *Nutrient Cycling in Agroecosystems*, **72**, 267-278.
- Holmes, R. M., Jones, J. B., Fisher, S. G. and Grimm, N. B., 1996. Denitrification in a nitrogen-limited stream ecosystem. *Biogeochemistry*, **33**, 125-146.
- Horibe Y., Shigehara K., and Takakuwa Y., 1973. Isotopic separation factors of carbon-dioxide-water system and isotopic composition of atmospheric oxygen. *Journal of Geophysical Research*, **78**, 2625-2629.
- Howarth R.W., Billen G, Swaney D., Townsend A., Jaworski N., Lajtha K., Downing J.A., Elmgren R., Caraco N., Jordan T., Berendse F., Freney J., Kudeyarov V., Murdoch P. and Zhao-Liang, Z., 1996. Regional nitrogen budgets and riverine N and P fluxes for the drainages to the North Atlantic Ocean: Natural and human influences. *Biogeochemistry*, **35** 75-139.
- Huang, P.M., 2004. Soil mineral-organic matter-microorganism interactions: Fundamentals and impacts. *Advances in Agronomy*, **82**, 391-472.
- Hübner, H., 1986. Isotope effects of nitrogen in the soil and biosphere. In: Fritz, p., and Fontes, J.C. (Eds). *Handbook of Environmental Isotope Geochemistry*, vol. 2b, The Terrestrial Environment, Elsevier, pp. 361-425.
- Isaksen, I. S. A., Granier, C., Myhre, G., Berntsen, T. K., Dalsoren, S. B., Gauss, M., Klimont, Z., Benestad, R., Bousquet, P., Collins, W., Cox, T., Eyring, V., Fowler, D., Fuzzi, S., Joeckel, P., Laj, P., Lohmann, U., Maione, M., Monks, P., Prevo, A. S. H., Raes, F., Richter, A., Rognerud, B., Schulz, M., Shindell, D., Stevenson, D. S., Storelvmo, T., Wang, W. C., Van weele, M., Wild, M. and Wuebbles, D., 2009. Atmospheric composition change: Climate-Chemistry interactions. *Atmospheric Environment*, **43**, 5138-5192.
- Jackson, L.E., Wyland, L.J., and Stilvers, L.J., 1993. Winter cover crops to minimize nitrate losses in intensive lettuce production. *Journal of Agricultural Science*, **121**, 55-62.
- Jarvis, S.C., 1999. Accounting for nutrients in grassland: challenges and needs. In: *Accounting for nutrients: A challenge for grassland farmers in the 21st century*. Ed Corral, A.J., BGS Occasional Symposium 33, British Grassland Society, Reading. pp 3 – 12.
- Jarvis, S.C., and pain, B.F., 1990. Ammonia volatilisation from agricultural land. *The Fertiliser Society Proceedings*. No 298, pp 1 – 35. The Fertiliser Society, London.
- Johnes, P. J. 1996. Evaluation and management of the impact of land use change on the nitrogen and phosphorus load delivered to surface waters: The export coefficient modelling approach. *Journal of Hydrology*, **183**, 323-349.

- Justes, E., Mary, B., and Nicolardot, B., 1999. Comparing the effectiveness of radish cover crop, oilseed rape volunteers and oilseed rape residues incorporation for reducing nitrate leaching. *Nutrient Cycling in Agroecosystems*, **55**, 207 – 220.
- Kellman, L., and Hillarie-Marcel, C., 1998. Nitrate cycling in streams: using natural abundances of NO₃—δ¹⁵N to measure in-situ denitrification. *Biogeochemistry*, **43**, 273-292.
- Kellner, E., and Hubbart, J., 2015. Agricultural and forested land use impacts on floodplain shallow groundwater temperature regime. *Hydrological Processes*, **30**, 625-636.
- Kelso, B.H.L., Smith, R.V., Laughlin, R.J., and Lennox, S.D. 1997. Dissimilatory nitrate reduction in anaerobic sediments leading to river nitrate accumulation. *Applied Environmental Microbiology*, **63**, 4697-4685.
- Kendall, C., Elliott, E. M. and Wankel, S. D., 2007. Tracing Anthropogenic Inputs of Nitrogen to Ecosystems. In Lajtha, K. and Michener, R. (Eds.) *Stable Isotopes in Ecology and Environmental Science* (2nd Edition). Blackwell.
- Khan SA, Mulvaney RL, Ellsworth TR, Boast CW (2007) The myth of nitrogen fertilization for soil carbon sequestration. *Journal of Environmental Quality* **36**,1821–1832.
- Kool, D.M., Dolfing, J., Wrage, N., and Van Groenigen, J.W., 2011. Nitrifier denitrification as a distinct and significant source of nitrous oxide from soil. *Soil Biology and Biochemistry*, **43**, 174-178.
- Kopacek, J., Cosby, B. J., Evans, C. D., Hruska, J., Moldan, F., Oulehle, F., Santruckova, H., Tahovska, K. and Wright, R. F. 2013. Nitrogen, organic carbon and sulphur cycling in terrestrial ecosystems: linking nitrogen saturation to carbon limitation of soil microbial processes. *Biogeochemistry*, **115**, 33-51.
- Krause, S., Heathwaite, L., Binley, A., and Kennan, P., 2009. Nitrate concentration changes at the groundwater-surface water interface of a small Cumbrian river. *Hydrological Processes*, **23**, 2195-2211.
- Liu, Y., Liu, C., Nelson, W.C., Shi, L., Xu, F., Liu, Y., Yan, A., Zhong, L., Thompson, C., Fredrickson, J.K., and Zachara, J.M., 2017. Effect of water chemistry and hydrodynamics on nitrogen transformation activity and microbial community functional potential in hyporheic zone sediment columns. *Environmental Science and Technology*, **51**, 4877-4886.
- Lawes, J.B., Gilbert, J.H., and Warrington, R., 1882. On the amount and composition of the rain and drainage waters collected at Rothamsted. *Royal Agricultural Society of England Series 2*, **17**, 241 – 279.
- Leichtfried, M. 1991. POM in bed sediments of a gravel stream (Ritrodat-Lunz study area, Austria). *SIL Proceedings*, **24**, 1921 – 1925.
- Leininger, S., Urich, T., Schloter, M., Schwark, L., Qi, J., Nicol, W., Prosser, J.I., Schuster, S.C., and Schleper, C., 2006. Archaea predominate among ammonia-oxidising prokaryotes in soils. *Nature*, **442**, 806-806.
- Létolle, R., 1980. Nitrogen-15 in the natural environment. In: *Handbook of Environmental Isotope Geochemistry*, Vol 1 (Eds Fritz, P., and Fontes, J.C.), pp 407-433. Elsevier, Amsterdam.
- Lewicka-Szczebak, D., Well, R., Bol, R., Gregory, A.S., Matthews, G.P., Misselbrook, T., Whalley, W.R., and Cardenas, L.M., 2014. Isotope fractionation factors controlling isotopocule signatures of soil- emitted N₂O produced by denitrification processes of various rates. *Rapid Communications in Mass Spectrometry*, **29**, 269-282.
- Lewis, M. A., 2014. Borehole drilling and sampling in the Wensum Demonstration Test Catchment. British Geological Survey Commissioned Report, CR/11/162. 52pp.

- Lott, D. A. and Stewart, M. T. 2016. Base flow separation: A comparison of analytical and mass balance methods. *Journal of Hydrology*, **535**, 525-533.
- Lord, E.I., Anthony, S.G., and Goodlass, G., 2002. Agricultural nitrogen balance and water quality in the UK. *Soil Use and Management*, **18**, 33 – 369.
- Lord, E.I., and Mitchell, R.D., 1998. Effect of nitrogen inputs to cereals on nitrate leaching from sandy soils. *Soil Use and Management*, **14**, 78 – 83.
- Loveland, P., and Webb, J., 2003. Is there a critical level of organic matter in the agricultural soils of temperate regions: a review. *Soil and Tillage Research*, **70**, 1-18.
- Lovett, A.A., Hiscock., K., Dockerty, T., Saich, A., Sandhu, C., Johnson, P., Sünnerberg, G., and Appleton, K., 2006. Science Report – Assessing Land-Use Scenarios to Improve Groundwater Quality: A Slea Catchment Study. Environment Agency, Bristol.
- Macko, S.A., and Estep, M.L.F., 1984. Microbial alteration of stable nitrogen and carbon isotopic compositions of organic matter. *Organic Chemistry*, **6**, 787-790.
- Marshall, S.B., Wood, C.W., Braun, L.C., Cabrer, M.L., Mullen, M.D., and Guertal, E.A., 1998. Ammonia volatilisation from tall fescue pastures fertilised with broiler litter. *Journal of Environmental Quality*, **27**, 1125 – 1129.
- Mariotti, A., Germon, J.C., Hubert, P., Kaiser, P., Letolle, R., Tardieux, A., and Tardieux, P., 1981. Experimental determination of nitrogen kinetic isotope fractionation: some principles; illustration for the denitrification and nitrification processes. *Plant and Soil*, **62**, 413-430.
- Mariotti, A., Pierre, D., Vedy, J. C., Bruckert, S. and Guillemot, J. 1980. The abundance of natural nitrogen 15 in the organic matter of soils along an altitudinal gradient (Chablais, Haute Savoie, France). *Catena*, **7**, 293-300.
- Marsh, T. J. and Hannaford, J. (Eds.), 2008. UK Hydrometric Register, Centre for Ecology and Hydrology.
- McClain, M. E., Boyer, E. W., Dent, C. L., Gergel, S. E., Grimm, N. B., Groffman, P. M., Hart, S. C., Harvey, J. W., Johnston, C. A., Mayorga, E., McDowell, W. H. and Pinay, G. 2003. Biogeochemical hot spots and hot moments at the interface of terrestrial and aquatic ecosystems. *Ecosystems*, **6**, 301-312.
- McCrackin, M. L., Harrison, J. A. and Compton, J. E., 2015. Future Riverine Nitrogen Export to Coastal Regions in the United States: Prospects for Improving Water Quality. *Journal of Environmental Quality*, **44**, 345-355.
- Megonigal, J., Hines, M., and Visscher, P., 2004. Anaerobic metabolism: linkages to trace gases and aerobic processes. In: Schlesinger, W.H. (Ed). Biogeochemistry. Oxford, UK: Elsevier – Pergamon.
- Meijide, A., Cardenas, L.M., Bol, R., Bergstermann, A., Goulding, K., Well, R., Vallejo, A., and Schofield, D., 2010. Dual isotope and isotopomer measurements for the understanding of N₂O production and consumption during denitrification in an arable soil. *European Journal of Soil Science*, **61**, 364-374.
- Meisinger, J.J. and Randall, G.W., 1991. Estimating nitrogen budgets for soil-crop systems. In: Follett, R.F., Keeney, D.R., and Cruse, R.M., (eds). Managing Nitrogen for Groundwater Quality and Farm Profitability, pp 85–124. ASA, Madison, WI.
- Mengis, M., Schiff, S.L., Harris, M., English, M.C., Aravena, R., Elgood, R.J., and Maclean, A., 1999. Multiple geochemical and isotopic approaches for assessing groundwater NO₃⁻ elimination in riparian zones. *Ground Water*, **37**, 448 – 457.

- Menyailo, O.V., and Hungate, B.A., 2006. Stable isotope discrimination during soil denitrification: Production and consumption of nitrous oxide. *Global Biogeochemical Cycles*, **20**: Doi:10.1029/2005GB002527.
- Messinga, A.J., Ziadi, N., Plénet, D., Parent, L.-E., and Morel, C., 2010. Long-term changes in soil phosphorus status related to P budgets under maize monoculture and mineral P fertilization. *Soil use and Management*, **26**, 354-346.
- Met Office (2009). East Anglia 1961 – 1990 climate averages. Met Office, http://www.metoffice.gov.uk/climate/uk/averages/19611990/areal/east_anglia. Last accessed 11/2017
- Millennium Ecosystem Assessment, 2005. Ecosystems and Human Well-Being: findings of the Condition and Trends Working Group. Volume 1: Current State and Trends, Millennium
- Ming, T., Shen, S. and Caillo, S., 2016. Fighting global warming by greenhouse gas removal: destroying atmospheric nitrous oxide thanks to synergies between two breakthrough technologies. *Environmental Science and Pollution Research*, **23**, 1-20.
- Mosier A.R., Doran J.W. and Freney J.R., 2002. Managing soil denitrification. *Journal of Soil and Water Conservation*. **57**, 505–513.
- Morrice, J. A., Valett, H. M., Dahm, C. N. and Campana, M. E., 1997. Alluvial characteristics, groundwater–surface water exchange and hydrological retention in headwater streams. *Hydrological Processes*, **11**, 253-267.
- Moseley, R., Woodward, C. M., Day, J. B. W. & Langston, M. J. (1976) Hydrogeological map of northern East Anglia sheet 1. Institute of Geological Sciences.
- Moss, D.P., Chambers, B.J., and Van Der Weerden, T.J., 1995. Measurement of ammonia emissions from land application of organic manures. *Aspects of Applied Biology*, **43**, 221 – 228.
- Morrice, J. A., Valett, H. M., Dahm, C. N. and Campana, M. E., 1997. Alluvial characteristics, groundwater–surface water exchange and hydrological retention in headwater streams. *Hydrological Processes*, **11**, 253-267.
- Morris, N., 2009. The adoption of conservation tillage in the United Kingdom. *Journal of the Royal Agricultural Society of England*, **170**, 64-70.
- Mulholland PJ, Helton AM, Poole GC, Hall Jr RO, Hamilton SK, Peterson BJ, et al. Stream denitrification across biomes and its response to anthropogenic nitrate loading. *Nature* 2008;452:202–6
- Mulvaney RL, Khan SA, Ellsworth TR (2009) Synthetic nitrogen fertilizers deplete soil nitrogen: A global dilemma for sustainable cereal production. *Journal of Environmental Quality*, **38**, 2295–2314.
- Oberg, G., 1998. Chloride and organic chlorine in soil. *Environmental Science and Technology*, **26**, 137-144.
- Oenema, O., and Hienen, M., 1999. Uncertainties in nutrient budgets due to biases and error. In: Nutrient disequilibria in agro-ecosystems, concepts and case studies, eds Smaling, E.M.A., Oenema, O., Fresco, L.. CAB International, Wallingford, UK. pp 72 – 95.
- Ontario Ministry of Agriculture and Rural Affairs, 2003. The value and application of manure on forages Factsheet.
- Ostrom, N. E., Knoke, K. E., Hedin, L. O., Robertson, G. P. and Smucker, A. J. M., 1998. Temporal trends in nitrogen isotope values of nitrate leaching from an agricultural soil. *Chemical Geology*, **146**, 219-227.

- Pain, B., F., Phillips, V.R., Clarkson, C.R., and Klarenbeek, J.V., 1989. Loss of nitrogen through ammonia volatilisation during and following the application of pig or cattle slurry to grassland. *Science of Food and Agriculture*. DOI: 10.1002/jsfa.2740470102.
- Palta, M. M., Ehrenfeld, J. G., Giménez, D., Groffman, P. M. and Subroy, V. 2016., Soil texture and water retention as spatial predictors of denitrification in urban wetlands. *Soil Biology and Biochemistry*, **101**, 237-250.
- Palta, M.M., Ehrenfeld, J.G., Groffman, P.M., 2014. “Hotspots” and “Hot Moments” of denitrification in urban brownfield wetlands. *Ecosystems*, **17**, 1121 - 1137.
- Panno, S.V., Hackley, K.C., Kelly, W.R., and Hwang, H-H., 2006. Isotopic evidence of nitrate sources and denitrification in the Mississippi River, Illinois. *Journal of Environmental Quality*, **35**, 495 – 504.
- Powell, K.L., Taylor, R.G., Cronin, A.A., Barrett, M.H., Pedley, S., Sellwood, J., Trowsdale, S.A., and Lerner, D.N., 2003. Microbial contamination of two urban sandstone aquifers in the UK. *Water Research*, **37**, 339-352.
- Pretty, J. N., Mason, C. F., Nedwell, D. B., Hine, R. E., Leaf, S. and Dils, R. 2003. Environmental costs of freshwater eutrophication in England and Wales. *Environmental Science and Technology*, **37**, 201-208.
- Puckett, L.J., Cowdery, T.K., Lorenz, D.L., and Stoner, J.D., 1999. Estimation of nitrate contamination of an agro-ecosystem outwash using a nitrogen mass balance budget. *Journal of Environmental Quality*, **28**, 2015-2025.
- Rabalais, N. N., 2002. Nitrogen in aquatic ecosystems. *Ambio*, **31**, 102-112.
- Rahimi, M., Essaid, H.I., and Wilson, J.T., 2015. The role of dynamic surface water-groundwater exchange on streambed denitrification in a first-order, low relief agricultural watershed. *Water Resources Research*, **51**, 9514-9538.
- Ray, C., and Member, P.E., 1999. Management of nitrate problems for domestic wells in irrigated alluvial aquifers. *Journal of Irrigation and Drain Engineering*, **127**, 49 – 53.
- Razali, N.M., and Wah, Y.B., 2011. Power comparisons of Shapiro-Wilk, Kolmogorov-Smirnov, Lilliefors and Anderson-Darling tests. *Journal of Statistical Modeling and Analytics*, **2**, 21-33.
- Rivett, M.O., Smith, J.W.N., Buss, S.R., and Morgan, P., 2007. Nitrate occurrence and attenuation in the major aquifers of England and Wales. *Quarterly Journal of Engineering Geology and Hydrology*, **40**, 335-352.
- Rivett, M. O., Smith, J. W. N., Buss, S. R. and Morgan, P. 2007. Nitrate occurrence and attenuation in the major aquifers of England and Wales. *Quarterly Journal of Engineering Geology and Hydrogeology*, **40**, 335-352.
- Robertson, W.D., Russel, B.M., and Cherry, J.A., 1996. Attenuation of nitrate in aquitard sediments in southern Ontario. *Journal of Hydrology*, **180**, 267-281.
- Scholes, R., Hassan, R. M., Ash, N. and Assessment, M. E., 2005. Ecosystems and Human Well-being: Findings of the Condition and Trends Working Group of the Millennium Ecosystem Assessment, Island Press.
- Sear DA, Newson M, Old JC, Hill C., 2006. Geomorphological appraisal of the River Wensum Special Area of Conservation. English Nature Research Reports, No 685.
- Sebilo, M., Billen, G., Grably, M., and Mariotti, A., 2003. Isotopic composition of nitrate-nitrogen as a marker of riparian and benthic denitrification at the scale of the whole Seine river system. *Biogeochemistry*, **63**, 35-51.

- Sebilo, M., Billen, G., Mayer, B., Billiou, D., Grably, M., Garnier, J., and Mariotti, A., 2006. Assessing nitrification and denitrification in the Seine river and estuary using chemical and isotopic techniques. *Ecosystems*, **9**, 564-577.
- Sebilo, M., Mayer, B., Nicolardot, B., Pinay, G., and Mariotti, A., 2013. Long-term fate of nitrogen fertilizer in agricultural soils. *PNAS*, **110**, 18185 – 18189.
- Seitzinger S.P., Styles R.V., Boyer E., Alexander R.B., Billen G., Howarth R., Mayer B. and Van Breemen N. 2002. Nitrogen retention in rivers: model development and application to watersheds in the eastern US. *Biogeochemistry*, **57**, 199–237.
- Shapiro, S.S., and Wilk, M.B., 1965. An analysis of variance test for normality (complete samples) *Biometrika*, **52**, 591-611.
- Shearer, G., and Kohl, D.H., 1986. N₂-fixation in field settings – estimations based on natural ¹⁵N abundance. *Australian Journal of Plant Physiology*, **13**, 699-756.
- Shepherd, M.A., and Lord, E.I., 1996. Nitrate leaching from a sandy soil: the effect of previous crop and post-harvest soil management in an arable rotation. *Journal of Agricultural Science*, **127**, 215 – 229.
- Sigman, D. M., Granger, J., Difiore, P. J., Lehmann, M. M., HO, R., Cane, G. and van Geen, A., 2005. Coupled nitrogen and oxygen isotope measurements of nitrate along the eastern North Pacific margin. *Global Biogeochemical Cycles*, **19**: Doi:10.1029/2005GB002458.
- Sigman, D. M., Casciotti, K. L., Andreani, M., Barford, C., M., G. and Bohlke, J. K., 2001. A bacterial method for the nitrogen isotopic analysis of nitrate in seawater and freshwater. *Analytical Chemistry*, **73**, 4145-4153.
- Silgram, M., Williams, A., Waring, R., Neumann, I., Hughes, A., Gaus, I., Mansour, and M., 2003. Assessment of the Effectiveness of the Nitrate Sensitive Areas Scheme in Reducing Nitrate Concentrations in Groundwater. R&D Technical Report P2-267/2/TR. Environment Agency, Bristol.
- Smil, V., 1999. Detonator of the population explosion. *Nature*, **400**, 415-415.
- Smith, J. W. N., Surridge, B. W. J., Haxton, T. H. and Lerner, D. N., 2009. Pollutant attenuation at the groundwater-surface water interface: A classification scheme and statistical analysis using national-scale nitrate data. *Journal of Hydrology*, **369**, 392-402.
- Snider, D.M., Wagner-Riddle, C., and Spoelstra, J., 2017. Stable isotopes reveal rapid cycling of soil nitrogen after manure application. *Journal of Environmental Quality*, **46**, 261-271.
- Snider, D., Thompson, K., Wagner-Riddle, C., Spoelstra, and Dunfield, K., 2015. Molecular and stable isotope ratios at natural abundance give complementary inferences about N₂O production pathways in an agricultural soil following a rainfall event. *Soil Biology and Biochemistry*, **88**, 197-213.
- Stolt, M.H., and Lindbo, D.L., 2010. Soil Organic Matter. In: Stoops, G., Marcellino, V., and Mees, F. Interpretation of Micromorphological Features of Soils and Regoliths. Elsevier, Amsterdam. pp 369 – 396.
- Stopes, C., Lord, E.I., Phillips, L., and Woodward, L., 2002. Nitrate leaching from organic farms and conventional farms following best practice. *Soil Use and Management*, **18**, 256-263.
- Stow, C.A., Walker, J.T., Cardoch, L., Spence, P., and Geron, C., 2005. N₂O emissions from streams in the Neuse River Watershed. North Carolina. *Environmental Science and Technology*, **29**, 6999-7004.

- Strebel, O., Duynisveld, W.H.M., and Böttcher, J., 1989. Nitrate pollution of groundwater in Western Europe. *Agriculture, Ecosystems and Environment*, **26**, 189-214.
- Sutton, M. A., Oenema, O., Erisman, J. W., Leip, A., Van Grinsven, H. and Winiwarter, W., 2011. Too much of a good thing. *Nature*, **472**, 159-161.
- Sulzman, E.W., 2007. Stable isotope chemistry and measurement, a primer. In Lajtha, K., and Michener, R. (Eds.) *Stable Isotopes in Ecology and Environmental Science* (2nd Edition). Blackwell.
- Swart, P.K., Evans, S., Capo, T., and Altabet, M.A., 2014. The fractionation of nitrogen and oxygen isotopes in macroalgae during the assimilation of nitrate. *Biogeosciences Discuss*, **11**, 6909 – 6903.
- Tiedje J.M., 1988. Ecology of denitrification and dissimilatory nitrate reduction to ammonium. In: Zehnder A.J.B. (ed.), *Biology of Anaerobic Microorganisms*. Wiley and Sons, New York, pp. 179–244.
- Toynton, R., 1979. Waste disposal hydrogeology with special reference to the Chalk of East Anglia. PhD Thesis. School of Environmental Sciences, University of East Anglia UK.
- Trimmer, M., Grey, J., Heppell, C.M., Hildrew, A.G., Lansdown, K., Stahl, H., and Yvon-Durocher, G., 2012. River bed carbon and nitrogen cycling: State of play and some new directions. *Science of the Total Environment*, **434**, 143 – 158.
- Triska, F. J., Duff, J. H. and Avanzino, R. J., 1990. Influence of exchange flow between the channel and hyporheic zone on nitrate production in a small mountain stream. *Canadian Journal of Fisheries and Aquatic Sciences*, **47**, 2099-2111.
- Valett, H. M., Fisher, S. G., Grimm, N. B. and Camill, P. 1994. Vertical hydrologic exchange and ecological stability of a desert stream ecosystem. *Ecology*, **75**, 548-560.
- Vervier, P., Dobson, M., and Pinay, G., 1993. Role of interaction zones between surface and groundwaters in DOC transport and processing: considerations for river restoration. *Freshwater Biology*, **29**, 275 – 284.
- Ward, M. H., Dekok, T. M., Levallois, P., Brender, J., Gulis, G., Nolan, B. T. and Vanderslice, J., 2005. Workgroup report: Drinking-water nitrate and health-recent findings and research needs. *Environmental Health Perspectives*, **113**, 1607-1614.
- Watson, C. A., Bengtsson, H., Ebbesvik, M., Loes, A. K., Myrbeck, A., Salomon, E., Schroder, J. and Stockdale, E. A. 2002. A review of farm-scale nutrient budgets for organic farms as a tool for management of soil fertility. *Soil Use and Management*, **18**, 264-273.
- Watson, C. A. and Atkinson, D. 1999. Using nitrogen budgets to indicate nitrogen use efficiency and losses from whole farm systems: a comparison of three methodological approaches. *Nutrient Cycling in Agroecosystems*, **53**, 259-267.
- Webb, J., Sylvester-Bradley, R., and Seenet, F.M., 2000. The fertiliser nitrogen requirement of cereals grown on sandy soils. *Journal of the Science of Food and Agriculture*, **80**, 263 – 274.
- Welsh, M.K., McMillan, S.K., and Vidon, P.G., 2016. Denitrification along the stream-riparian continuum in restored and unrestored agricultural streams. *Journal of Environmental Quality*, **46**, 1010-1019.
- Westhoff, M.C., Gooseff, M.N., Bogaard, T.A., and Savenije, H.H.G., 2011. Quantifying hyporheic exchange at high spatial resolution using natural temperature variations along a 1st-order stream. *Water Resources Research*, **47**. DOI:10.1029/2010wr009767.

- Wexler, S.K., Goodale, C.L., McGuire, K.J., Bailey, S.W., and Groffman, P.M., 2014. Isotopic signals of summer denitrification in a northern hardwood forest catchment. *Proceedings of the National Academy of Sciences of the United States of America*, **111**, 16413 – 16418.
- Wexler, S. K., Hiscock, K. M. and Dennis, P. F. 2011. Catchment-Scale Quantification of Hyporheic Denitrification Using an Isotopic and Solute Flux Approach. *Environmental Science and Technology*, **45**, 3967-3973.
- Wexler, S., 2010. An investigation into the sources, cycling and attenuation of nitrate in an agricultural lowland catchment using stable isotopes of nitrogen and oxygen in nitrate. PhD thesis. School of Environmental Sciences, University of East Anglia, UK.
- Wier, K.L., Doran, J.W., Power, J.F., and Walters, D.T., 1992. Denitrification and the dinitrogen/nitrous oxide ratio as affected by soil water, available carbon, and nitrate. *Soil Science Society of America Journal*, **57**, 66-71.
- Williams, D.D., 1989. Towards a biological and chemical definition of the hyporheic zone in two Canadian rivers. *Freshwater Biology*, **22**, 189 – 208.
- Wiodarczyk, T., Stępniewski, W., and Brzezińska, M., 2005. Nitrous oxide production and consumption in Calcaric Regosols as related to soil redox and texture. *International Agrophysics*, **19**, 314-326.
- Wolfe, A. H. and Patz, J. A., 2002. Reactive nitrogen and human health: Acute and long-term implications. *Ambio*, **31**, 120-125.
- Wondzell SM. Effect of morphology and discharge on hyporheic exchange flows in two small streams in the Cascade Mountains of Oregon, USA. *Hydrological Process*, 2006;**20**: 267–87.
- Wunderlich, A., Meckenstock, R., and Einsiedl, F., 2012. Effect of different carbon substrates on nitrate stable isotope fractionation during microbial denitrification. *Environmental Science and Technology*, **46**, 4681 – 4868.
- Xing, G.X., Cao, Y.C., Shi, S.L., Sun, G.Q., Du, L.J., and Zhu, J.G. 2002. Denitrification in underground saturated soil in a rice paddy region. *Soil Biology and Biochemistry*, **34**, 1593-1598.
- Yusoff, I., Hiscock, K.M., and Conway, D., 2002. Simulation of the impacts of climate change on groundwater resources in Eastern England. In Hiscock, K.M., Rivett, M.O., and Davidson, R.M. (Eds.) *Sustainable Groundwater Development*, London, Geological Society Special Publications #193.
- Zarnetske, J.P., 2014. The stream subsurface: Nitrogen cycling and the cleansing function of hyporheic zones. *Pacific Northwest Science Findings*, **166**, 1-4.
- Zarnetske, J.P., Haggerty, R., Wondzell, S.M., and Baker, M.A., 2011a. Labile dissolved organic carbon supply limits hyporheic denitrification. *Journal of Geophysical Research: Biogeosciences*, **116**, doi: 10.1029/2011JG001730.
- Zarnetske, J.P., Haggerty, R., Wondzell, S.M., and Baker, M.A., 2011. Dynamics of nitrate production and removal as a function of residence time in the hyporheic zone. *Journal of Geophysical Research: Biogeosciences*, **116**, G01025, doi:10.1029/2010JG001356.
- Zhang, H., and Hiscock, K.M., 2011. Modelling the effect of forest cover in mitigating nitrate contamination of groundwater. A case study of the Sherwood Sandstone aquifer in the East Midlands, UK. *Journal of Hydrology*, **399**, 212-225.
- Zhang, J., Müller, C., and Cai, Z., 2015. Heterotrophic nitrification of organic N and its contribution to nitrous oxide emissions in soils. *Soil Biology and Biochemistry*, **84**, 199-209.
- Zhongjun, J.I.A., Kuzyakov, Y., Myrold, D., and Tiedje, J., 2017. Soil organic carbon in a changing world. *Pedosphere*, **27**, 789 – 791.

Zumft, W. G., 1997. Cell biology and molecular basis of denitrification. *Microbiology and Molecular Biology Reviews*, **61**, 533-616.

Appendix 1 - Field measurements

Temperature, pH, Dissolved Oxygen (DO) and Electrical Conductivity (EC) measurements for all samples collected where data are available. (S) and (D) represent stream and drain samples, respectively. 0.5, 1.0 and 1.5 are depths below the stream bed to which the piezometers are installed (m). Numbers outside brackets correspond to the sampling site (1 – 5).

Date sampled	Sample ID	Temp °C	DO (mg L ⁻¹)	pH	EC (µS cm ⁻¹)
6.11.2015	1 (D)				534
6.11.2015	2 (1.5)				508
6.11.2015	2 (1)				492
6.11.2015	2 (0.5)				478
6.11.2015	2 (D)				499
6.11.2015	3 (1.5)				481
6.11.2015	3 (1)				405
6.11.2015	3 (D)				503
6.11.2015	4 (1)				586
6.11.2015	4 (0.5)				631
19.11.2015	1 (0.5)				368
19.11.2015	1 (S)				458
19.11.2015	1 (D)				454
19.11.2015	2 (1.5)				415
19.11.2015	2 (1)				455
19.11.2015	2 (0.5)				439
19.11.2015	2 (S)				483
19.11.2015	2 (D)				491
19.11.2015	3 (1.5)				398
19.11.2015	3 (1)				377
19.11.2015	3 (0.5)				399
19.11.2015	3 (S)				485
19.11.2015	3 (D)				518
19.11.2015	4 (1.5)				459
19.11.2015	4 (1)				350
19.11.2015	4 (0.5)				362
19.11.2015	4 (S)				589
19.11.2015	5 (1.5)				397
19.11.2015	5 (1)				417
19.11.2015	5 (0.5)				298
26.11.2015	1 (1.5)	7	5.43	8.07	332
26.11.2015	1 (1)	8	5.07	7.4	709
26.11.2015	1 (0.5)	9	5.7	7.76	1062
26.11.2015	1 (S)	8	6.78	7.92	915
26.11.2015	1 (D)	7	5.59	7.34	586
26.11.2015	2 (1.5)	10	4.87	7.44	649

26.11.2015	2 (1)	11	5.44	7.33	1262
26.11.2015	2 (0.5)	9.5	4.4	7.39	809
26.11.2015	2 (S)	8.5	6.6	7.97	1273
26.11.2015	2 (D)	9	5.54	7.21	672
Date sampled	Sample ID	Temp °C	DO (mg L ⁻¹)	pH	EC (µS cm ⁻¹)
26.11.2015	3 (1.5)	10	6.12	7.87	948
26.11.2015	3 (1)	6.75	6.25	8.05	1314
26.11.2015	3 (0.5)				
26.11.2015	3 (S)	6	6.43	7.93	1305
26.11.2015	3 (D)	6.5	5.74	7.32	677
26.11.2015	4 (1.5)	9	6.69	7.79	1205
26.11.2015	4 (1)	6	4.8	7.43	1171
26.11.2015	4 (0.5)	7.5	6.31	7.36	1438
26.11.2015	4 (S)				692
26.11.2015	5 (1.5)				463
26.11.2015	5 (1)				445
26.11.2015	5 (0.5)				430
26.11.2015	5 (D)				371
7.12.2015	1 (1.5)	14	4.96	7.69	1334
7.12.2015	1 (1)	11.5	5	7.54	391
7.12.2015	1 (0.5)	13	5.5	8.06	412
7.12.2015	1 (S)	10.5	5.74	8.17	902
7.12.2015	1 (D)	10	5.66	7.63	552
7.12.2015	2 (1.5)	11.5	3.83	8.12	799
7.12.2015	2 (1)	11	2.93	7.23	950
7.12.2015	2 (0.5)	11.5	4.82	7.95	409
7.12.2015	2 (S)	10.5	5.7	8.12	577
7.12.2015	2 (D)	10	5.63	7.71	822
7.12.2015	3 (1.5)	11.5	4.82	7.95	409
7.12.2015	3 (1)	11.5	5.33	7.77	452
7.12.2015	3 (0.5)	11.5	5.44	7.4	310
7.12.2015	3 (S)	10.5	5.67	8.04	808
7.12.2015	3 (D)	10.5	5.18	7.85	630
7.12.2015	4 (1.5)	11	5.26	7.58	419
7.12.2015	4 (1)	10	4.53	7.34	798
7.12.2015	4 (0.5)	10.5	5.29	7.36	615
7.12.2015	4 (S)	10.5	5.72	8.08	816
7.12.2015	5 (1.5)	11.5	3.74	7.52	568
7.12.2015	5 (1)	11.5	4.36	7.52	622
7.12.2015	5 (0.5)	12.5	4.05	7.43	599
7.12.2015	5 (S)	11	5.64	8.07	914
8.1.2016	1 (1.5)	9	5.41	8.06	429
8.1.2016	1 (0.5)	8.5	5.8	7.64	343
8.1.2016	1 (S)	7	6.01	7.64	764
8.1.2016	1 (D)	7	5.45	7.57	491

8.1.2016	2 (1.5)	9	4.58	7.85	515
8.1.2016	2 (1)	8.5	4.77	7.52	338
8.1.2016	2 (0.5)	8	5.18	7.56	658
8.1.2016	2 (S)	7.5	5.93	7.54	714
Date sampled	Sample ID	Temp °C	DO (mg L ⁻¹)	pH	EC (µS cm ⁻¹)
8.1.2016	2 (D)	8	5.32	7.56	458
8.1.2016	3 (1.5)	9	6.22	7.6	392
8.1.2016	3 (1)	8.5	6.18	7.64	498
8.1.2016	3 (0.5)	8.5	5.76	7.91	612
8.1.2016	3 (S)	7	6.12	7.46	729
8.1.2016	3 (D)	7.5	6.2	7.42	565
8.1.2016	4 (1.5)	9	4.81	7.82	731
8.1.2016	4 (S)	7.5	5.95	6.92	755
8.1.2016	5 (1.5)	9	4.43	7.42	624
8.1.2016	5 (1)	9	4.12	7.59	559
8.1.2016	5 (0.5)	7.5	4.93	7.41	620
8.1.2016	5 (S)	7.5	5.85	7.4	779
20.01.2016	1 (1.5)	9.5	5.85	7.06	405
20.01.2016	1 (1)	8.5	5.81	7.58	588
20.01.2016	1 (0.5)	8	6.03	7.21	346
20.01.2016	1 (S)	6.5	6.56	8.02	767
20.01.2016	1 (D)	8	6.1	7.62	463
20.01.2016	2 (1.5)	5.5	4.09	6.9	780
20.01.2016	2 (1)	8			514
20.01.2016	2 (0.5)		4.32	7.09	655
20.01.2016	2 (S)	6.5	6.58	7.42	756
20.01.2016	2 (D)	5.5	5.69	7.37	515
20.01.2016	3 (1.5)	8	6.18	7.4	308
20.01.2016	3 (1)	8	6.24	6.93	728
20.01.2016	3 (0.5)	7			481
20.01.2016	3 (S)	5.5	6.81	7.89	781
20.01.2016	3 (D)	7.5	6.12	7.52	590
20.01.2016	4 (1.5)	8	5.98	7.35	1882
20.01.2016	4 (1)	7	5.22	7.12	340
20.01.2016	4 (0.5)	7.5	5.95	7.24	530
20.01.2016	4 (S)	5.5	7.56	7.81	510
20.01.2016	4 (D)	7	5.38	7.46	623
20.01.2016	5 (1.5)	8.5	5.29	7.19	348
20.01.2016	5 (1)	8	4.64	7.11	349
20.01.2016	5 (0.5)	7.5	5.16	7.15	373
20.01.2016	5 (S)	6	6.31	7.76	518
20.01.2016	5 (D)	7	6.21	7.64	705
5.2.2016	1 (0.5)		6.29	7.21	929
5.2.2016	1 (S)		6.46	7.05	
5.2.2016	1 (D)		6.27	6.84	484

5.2.2016	2 (1.5)		5.08	6.91	581
5.2.2016	2 (0.5)		5.99	7	
5.2.2016	2 (S)		6.29	7.56	
5.2.2016	2 (D)		6.46	7.92	566
Date sampled	Sample ID	Temp °C	DO (mg L ⁻¹)	pH	EC (µS cm ⁻¹)
5.2.2016	3 (1.5)			7.11	437
5.2.2016	3 (0.5)			8.12	522
5.2.2016	3 (S)		6.3	7.49	668
5.2.2016	3 (D)		6.6	7.33	574
5.2.2016	4 (0.5)			7.41	587
5.2.2016	4 (S)		6.4	7.52	
5.2.2016	4 (D)		5.47	7.09	536
5.2.2016	5 (1.5)		4.8	7.22	623
5.2.2016	5 (1)		5.38	6.99	534
5.2.2016	5 (0.5)		5.38	7.15	524
5.2.2016	5 (S)		6.87	7.77	516
5.2.2016	5 (D)		6.74	8.01	472
7.3.2016	1 (1.5)	7.5		6.97	692
7.3.2016	1 (1)	7.5		7.17	612
7.3.2016	1 (0.5)	6.5		6.84	553
7.3.2016	1 (S)	5.5		7.66	687
7.3.2016	1 (D)	6		7.43	494
7.3.2016	2 (1.5)	7		7.22	658
7.3.2016	2 (0.5)	6		7	745
7.3.2016	2 (S)	6		7.57	707
7.3.2016	2 (D)	6.5		7.25	564
7.3.2016	3 (1.5)	7		7.18	421
7.3.2016	3 (1)	6.5		7.05	460
7.3.2016	3 (0.5)	6		6.76	422
7.3.2016	3 (S)	5.5		7.55	688
7.3.2016	3 (D)	7		7.53	557
7.3.2016	4 (1.5)	7		7.74	732
7.3.2016	4 (0.5)	7		6.7	610
7.3.2016	4 (S)	6		7.64	524
7.3.2016	4 (D)	6.5		7.33	550
7.3.2016	5 (1.5)	7.5		7.17	571
7.3.2016	5 (1)	7		6.73	842
7.3.2016	5 (0.5)	7		7.22	574
7.3.2016	5 (S)	5.5		7.59	777
7.3.2016	5 (D)	6.5		7.34	382
22.4.16	1 (S)		8.15	8.16	1111
22.4.16	1(D)		6.27	7.57	715
22.4.16	2(1.5)		5.63	7.57	595
22.4.16	2(0.5)		3.37	7.31	585
22.4.16	2(S)		8.26	8.14	1036

22.4.16	2(D)		5.46	7	694
22.4.16	3(1.5)			7.51	
22.4.16	3(1)		5.81	7.3	486
22.4.16	3(0.5)			6.89	497
Date sampled	Sample ID	Temp °C	DO (mg L ⁻¹)	pH	EC (µS cm ⁻¹)
22.4.16	3(S)		7.55	8.14	1183
22.4.16	3(D)		7.56	6.75	619
22.4.16	4(1.5)				473
22.4.16	4(0.5)				468
22.4.16	4(S)		4.95	7.97	1046
22.4.16	4(D)		4.97	7.03	686
22.4.16	5(1.5)		4.33	7.53	796
22.4.16	5(1)		3.75	7.52	769
22.4.16	5(0.5)		4.65	7.48	833
22.4.16	5(S)		7.9	8.02	1045
22.4.16	5(D)		6.47	7.88	599
27.5.2016	1(0.5)	13			502
27.5.2016	1(S)	13	5.32	7.53	708
27.5.2016	2(1.5)	13.5	4.19	7.5	532
27.5.2016	2(1)	13	4.53	7.44	468
27.5.2016	2(0.5)	13	3.38		680
27.5.2016	2(S)	12	4.97	7.76	679
27.5.2016	2(D)	11.5	5.4	7.81	721
27.5.2016	3(1.5)	14	3.16	7.53	603
27.5.2016	3(1)	14		7.01	519
27.5.2016	3(0.5)	14		7.5	625
27.5.2016	3(D)	12	5.2	7.33	922
27.5.2016	4(1.5)	13.5	3.78	7.61	595
27.5.2016	4(1)	15	2.5	6.43	1333
27.5.2016	4(0.5)	15.5	4.25	6.25	1665
27.5.2016	4(S)	13.5	5.1	7.57	677
27.5.2016	4(D)	13	4.09	7.66	764
27.5.2016	5(1.5)	16.5	3.15	7.59	538
27.5.2016	5(1)	14	3.13	7.61	515
27.5.2016	5(0.5)	14	3	7	540
27.5.2016	5(S)	12.5	5.15	7.57	664
27.5.2016	5(D)	12	5.34	7.81	770
17.6.2016	1(1.5)	17			607
17.6.2016	1(1)				425
17.6.2016	1(0.5)				349
17.6.2016	1(S)	14.5	6.22	7.53	784
17.6.2016	1(D)	14	6.16	7.55	742
17.6.2016	2(1.5)	14	4.68	7.53	669
17.6.2016	2(1)	14.5	4.49	6.93	785
17.6.2016	2(0.5)	14	3.43	7.96	632

17.6.2016	2(S)	13.5	5.67	7.52	650
17.6.2016	2(D)	14.5	5.38	7.51	759
17.6.2016	3(1.5)	14		7.48	443
17.6.2016	3(1)	14			
Date sampled	Sample ID	Temp °C	DO (mg L ⁻¹)	pH	EC (µS cm ⁻¹)
17.6.2016	3(0.5)	14.5		7.46	323
17.6.2016	3(S)	13	6.2	7.38	780
17.6.2016	3(D)	13	6.3	7.09	827
17.6.2016	4(1.5)	14	4.94	7.28	700
17.6.2016	4(1)	14	3.77	7.36	1017
17.6.2016	4(S)	14.5	5.82	7.45	789
17.6.2016	4(D)	14.5	4.17	6.83	580
17.6.2016	5(1.5)	14.5	3.49	6.6	1245
17.6.2016	5(1)	14	4.71	7.21	539
17.6.2016	5(S)	13.5	5.74	7.76	737
17.6.2016	5(D)	12	6.11	8.03	735
1.7.2016	1(1.5)	15.5			447
1.7.2016	1(1)	17			614
1.7.2016	1(0.5)	16			612
1.7.2016	1(D)	15			775
1.7.2016	1(S)	14.5			
1.7.2016	2(1.5)	15			693
1.7.2016	2(1)	16			643
1.7.2016	2(0.5)	16			772
1.7.2016	2(D)	14			807
1.7.2016	2(S)	15			
1.7.2016	3(1.5)	15			499
1.7.2016	3(1)	14			590
1.7.2016	3(0.5)	16			609
1.7.2016	3(D)	13.5			915
1.7.2016	3(S)	14.5			
1.7.2016	4(1.5)	15			693
1.7.2016	4(1)	16.5			699
1.7.2016	4(0.5)	16.5			671
1.7.2016	4(D)	14.5			753
1.7.2016	4(S)	15			
1.7.2016	5(1.5)	15			584
1.7.2016	5(1)	15			555
1.7.2016	5(S)	15			
12.8.2016	1(1.5)	17			567
12.8.2016	1(1)	17.5			530
12.8.2016	1(0.5)	17			527
12.8.2016	1(S)	16.5			
12.8.2016	2(1.5)	17			701
12.8.2016	2(1)	17.5			605

12.8.2016	2(0.5)	17.5			686
12.8.2016	2(D)	16			293
12.8.2016	2(S)	16			
12.8.2016	3(1.5)	19			493
Date sampled	Sample ID	Temp °C	DO (mg L ⁻¹)	pH	EC (µS cm ⁻¹)
12.8.2016	3(1)	18			529
12.8.2016	3(0.5)	21			502
12.8.2016	3(D)	16			858
12.8.2016	4(1.5)	19			713
12.8.2016	4(1)	17			794
12.8.2016	4(0.5)	22			489
12.8.2016	4(D)	16			675
12.8.2016	4(S)	19			
12.8.2016	5(1.5)	17.5			533
12.8.2016	5(1)	19			511
12.8.2016	5(D)	16			743
12.8.2016	5(S)	17			
09.09.2016	1(1.5)	17			
09.09.2016	1(1)	17	4.66	7.24	564
09.09.2016	1(0.5)	16.5	5.36		587
09.09.2016	1(S)	15	4.98	7.48	738
09.09.2016	2(1.5)	15	5.55	7.04	729
09.09.2016	2(1)	16.5	8.41	6.78	858
09.09.2016	2(0.5)	16.5	4.62	6.97	713
09.09.2016	2(D)	16	6.73	7.11	772
09.09.2016	2(S)	15.5	4.28	7.22	760
09.09.2016	3(1.5)	17.5			
09.09.2016	3(1)	18			
09.09.2016	3(0.5)	17.5			657
09.09.2016	3(S)	15	6.34	7.27	722
09.09.2016	4(1.5)	16.5	6.25	6.75	1613
09.09.2016	4(1)	16	2.83	6.22	865
09.09.2016	4(D)	15.5	5.41	6.61	573
09.09.2016	4(S)	15	6.34	7.44	766
09.09.2016	5(1.5)	16.5	2.25	7.13	607
09.09.2016	5(1)	17	1.49	7.18	609
09.09.2016	5(0.5)	19	3.07	7.14	586
09.09.2016	5(D)	16	7.33	7.34	743
09.09.2016	5(S)	15.5	5.63	7.34	732
03.11.2016	1(0.5)		7.78	6.49	466
03.11.2016	1(S)		8.62	7.14	628
03.11.2016	3(D)		7.6	7.1	456
03.11.2016	4(1)		8.44	6.89	650
03.11.2016	4(S)		7.72	6.79	588
03.11.2016	4(D)		5.56	6.94	716

03.11.2016	5(1.5)		5.83	6.42	517
03.11.2016	5(1)		6.53	6.51	479
03.11.2016	5(0.5)		6.22	6.62	495
03.11.2016	5(S)		8.63	6.98	639
Date sampled	Sample ID	Temp °C	DO (mg L ⁻¹)	pH	EC (µS cm ⁻¹)
25.11.2016	1(1)	11			
25.11.2016	1(0.5)	11			
25.11.2016	1(S)	8	9.3	7.61	403
25.11.2016	1(D)	9	7.95	6.86	438
25.11.2016	2(S)	7.5	8.38	7.28	388
25.11.2016	3(S)	7	8.12	7.19	627
25.11.2016	3(D)	9.5	7.77	6.51	416
25.11.2016	4(1.5)	11			
25.11.2016	4(1)	10.5	6.82	6.48	579
25.11.2016	4(0.5)	10.5	7.1	6.49	664
25.11.2016	4(D)	10			491
25.11.2016	4(S)	8	7.71	7.1	329
25.11.2016	5(1.5)	9.5	4	6.62	513
25.11.2016	5(1)	9.5	5.04	6.68	497
25.11.2016	5(0.5)	9.5	5.38	6.95	514
25.11.2016	5(S)	7	9.01	7.64	655
09.12.2016	1(1)	11.5			
09.12.2016	1(0.5)	13			
09.12.2016	1(S)	10		7.64	643
09.12.2016	1(D)	9		7.32	730
09.12.2016	2(S)	10		7.81	633
09.12.2016	3(1.5)	11.5			
09.12.2016	3(S)	10.5		7.4	377
09.12.2016	3(D)	9		6.9	456
09.12.2016	4(1.5)	11			
09.12.2016	4(1)	11		6.78	686
09.12.2016	4(0.5)	10			
09.12.2016	4(S)	10.5		7.28	655
09.12.2016	4(D)	9		6.39	436
09.12.2016	5(1.5)	11.5		6.95	598
09.12.2016	5(1)	11		6.9	492
09.12.2016	5(0.5)	11		7.01	521
09.12.2016	5(S)	10		7.55	653
09.12.2016	5(D)	10		7.44	489
20.1.2017	1(0.5)	6.5	6.85	7.04	567
20.1.2017	1(S)	3	6.47	7.55	397
20.1.2017	1(D)	5		6.86	667
20.1.2017	2(S)	3	7.01	7.52	420
20.1.2017	2(D)	5	5.39	7.22	558
20.1.2017	3(S)	3	6.66	7.23	786

20.1.2017	3(D)	6	5.38	6.72	618
20.1.2017	4(S)	3	7.09	7.24	809
20.1.2017	4(D)	6	5	6.71	423
20.1.2017	5(1.5)	7	7.39	7.02	599
Date sampled	Sample ID	Temp °C	DO (mg L ⁻¹)	pH	EC (µS cm ⁻¹)
20.1.2017	5(1)	7	3.92	6.8	546
20.1.2017	5(0.5)	6	3.84	6.63	567
20.1.2017	5(S)	3	7.06	7.52	753
20.1.2017	5(D)	5	5.5	7.44	571
03.04.2016	BH	11.5	1.58	6.63	671
17.07.2016	BH	11.5	1.66	6.68	557
16.12.2016	BH	12	4.31	7.19	525
03.02.2017	BH	12	4.22	7.22	648
17.03.2017	BH	11	1.54	6.80	576

Appendix 2 – Stable isotope data

Nitrate and water stable isotope data in all samples for which data are available. (S) and (D) represent stream and drain samples, respectively. 0.5, 1.0 and 1.5 are the depths beneath the stream bed to which the piezometers were installed (m). BH is the borehole data (12 m beneath the surface). The numbers outside the brackets show which site the samples were collected from (1 – 5)

Date sampled	Sample ID	$\delta^{15}\text{N}_{\text{NO}_3}$ (‰)	$\delta^{18}\text{O}_{\text{NO}_3}$ (‰)	$\delta^{18}\text{O}_{\text{H}_2\text{O}}$ (‰)	$\delta^2\text{H}_{\text{H}_2\text{O}}$ (‰)
6.11.2015	2 (1)			-7.15	-45.23
6.11.2015	3 (1.5)			-7.29	-46.75
6.11.2015	4 (1)			-6.97	-45.10
19.11.2015	1 (S)	10.64	3.82	-6.80	-43.93
19.11.2015	1 (D)	16.05	6.60		
19.11.2015	2 (1.5)	8.45	16.95	-6.80	-43.41
19.11.2015	2 (0.5)	9.84	24.43	-7.19	-45.33
19.11.2015	2 (S)	10.72	4.01	-6.99	-44.62
19.11.2015	2 (D)	9.51	3.57		
19.11.2015	3 (1.5)	9.62	25.70		
19.11.2015	3 (1)	10.35	15.98	-7.13	-46.43
19.11.2015	3 (S)	10.72	4.02		
19.11.2015	3 (D)	10.02	4.20		
19.11.2015	4 (1.5)	9.19	23.13	-7.00	-44.88
19.11.2015	4 (1)	11.25	10.39	-6.85	-44.65
19.11.2015	4 (0.5)	10.49	17.05		
19.11.2015	4 (S)	10.72	3.93	-6.66	-43.46
19.11.2015	5 (1.5)	9.13	28.51		
19.11.2015	5 (1)	10.39	10.88	-7.40	-46.82
19.11.2015	5 (0.5)	9.82	31.95		
19.11.2015	5 (S)	10.40	4.04		
26.11.2015	1 (1.5)	10.66	10.43	-6.82	-44.88
26.11.2015	1 (1)	11.60	8.24	-7.32	-46.30
26.11.2015	1 (0.5)	8.65	17.26		
26.11.2015	1 (S)	9.75	2.96	-6.64	-42.79
26.11.2015	1 (D)	12.79	4.83		
26.11.2015	2 (1.5)	8.22	25.19	-7.09	-45.33
26.11.2015	2 (1)	10.78	5.46	-7.00	-44.70
26.11.2015	2 (0.5)	8.33	21.23	-6.98	-44.96
26.11.2015	2 (S)	9.54	2.80	-6.55	-42.67
26.11.2015	2 (D)	7.66	1.69		
26.11.2015	3 (1.5)	10.27	4.40		
26.11.2015	3 (1)	9.76	18.81		
26.11.2015	3 (S)	11.02	3.94		
26.11.2015	3 (D)	9.04	3.60		

26.11.2015	4 (1.5)	9.05	22.24	-6.92	-45.80
26.11.2015	4 (1)	9.74	4.77	-7.08	-45.01
26.11.2015	4 (0.5)	9.62	10.67		
26.11.2015	4 (S)	9.44	2.74	-6.80	-43.19
26.11.2015	5 (1.5)	10.41	13.42		
26.11.2015	5 (1)	9.26	7.27	-7.45	-47.40
Date sampled	Sample ID	$\delta^{15}\text{N}_{\text{NO}_3}$ (‰)	$\delta^{18}\text{O}_{\text{NO}_3}$ (‰)	$\delta^{18}\text{O}_{\text{H}_2\text{O}}$ (‰)	$\delta^2\text{H}_{\text{H}_2\text{O}}$ (‰)
26.11.2015	5 (0.5)	9.12	26.59	-7.39	-47.59
26.11.2015	5 (S)	9.40	2.77		
7.12.2015	1 (1.5)	9.68	32.08		
7.12.2015	1 (1)	9.40	20.38	-7.27	-45.72
7.12.2015	1 (0.5)	10.16	21.88	-7.29	-46.08
7.12.2015	1 (S)	10.77	4.34	-6.76	-43.19
7.12.2015	1 (D)	13.83	5.65		
7.12.2015	2 (1.5)	9.06	32.97	-7.12	-45.22
7.12.2015	2 (1)	11.95	10.62	-7.23	-45.31
7.12.2015	2 (0.5)	11.43	5.64	-6.94	-44.17
7.12.2015	2 (S)	10.54	3.96	-6.68	-43.26
7.12.2015	2 (D)	9.00	3.34		
7.12.2015	3 (1.5)	9.52	13.51	-7.16	-45.74
7.12.2015	3 (1)	9.92	31.33		
7.12.2015	3 (0.5)	10.36	26.45	-7.07	-45.56
7.12.2015	3 (S)	10.48	4.15		
7.12.2015	3 (D)	7.48	2.62		
7.12.2015	4 (1.5)	8.43	32.03	-6.70	-44.56
7.12.2015	4 (1)	10.66	10.01	-7.15	-45.55
7.12.2015	4 (0.5)	9.90	21.47	-6.98	-44.32
7.12.2015	4 (S)	10.42	4.10	-6.70	-43.43
7.12.2015	5 (1.5)	9.88	18.97	-7.27	-46.77
7.12.2015	5 (1)	9.62	27.41		
7.12.2015	5 (0.5)	9.85	30.52	-7.35	-46.93
7.12.2015	5 (S)	9.75	3.55	-6.91	-44.78
8.1.2016	1 (1.5)	10.31	4.16		
8.1.2016	1 (0.5)	9.52	14.47	-7.32	-47.22
8.1.2016	1 (S)	9.21	2.07		
8.1.2016	1 (D)	14.12	6.03		
8.1.2016	2 (1.5)	8.68	23.12		
8.1.2016	2 (1)	9.86	13.87		
8.1.2016	2 (0.5)	11.04	9.40		
8.1.2016	2 (S)	9.05	1.98		
8.1.2016	2 (D)	8.53	2.54		
8.1.2016	3 (1.5)	10.10	13.27	-7.11	-46.12
8.1.2016	3 (1)	10.50	13.64	-7.45	-47.29
8.1.2016	3 (0.5)	9.10	15.78	-7.03	-45.98
8.1.2016	3 (S)	9.17	2.38		

8.1.2016	3 (D)	7.81	2.28		
8.1.2016	4 (1.5)	8.50	20.77	-7.10	-45.75
8.1.2016	4 (S)	9.19	2.49		
8.1.2016	5 (1.5)	9.41	19.48	-7.45	-47.10
8.1.2016	5 (1)	8.88	16.58	-7.37	-47.15
8.1.2016	5 (0.5)	10.56	7.79	-7.51	-48.02
8.1.2016	5 (S)	8.63	1.99		
Date sampled	Sample ID	$\delta^{15}\text{N}_{\text{NO}_3}$ (‰)	$\delta^{18}\text{O}_{\text{NO}_3}$ (‰)	$\delta^{18}\text{O}_{\text{H}_2\text{O}}$ (‰)	$\delta^2\text{H}_{\text{H}_2\text{O}}$ (‰)
20.01.2016	1 (1.5)	12.21	7.88		
20.01.2016	1 (0.5)	10.00	25.47	-7.05	-46.09
20.01.2016	1 (S)	10.37	3.58	-6.90	-44.36
20.01.2016	1 (D)	15.74	7.86		
20.01.2016	2 (1.5)	10.06	20.75	-7.26	-45.78
20.01.2016	2 (1)	11.01	31.17		
20.01.2016	2 (0.5)	11.31	19.96		
20.01.2016	2 (S)	10.13	3.15	-6.97	-44.14
20.01.2016	2 (D)	9.63	3.55		
20.01.2016	3 (1.5)	9.21	24.72		
20.01.2016	3 (1)	9.74	25.15		
20.01.2016	3 (0.5)	9.81	29.73		
20.01.2016	3 (S)	9.72	2.80	-6.94	-44.90
20.01.2016	3 (D)	7.43	2.77		
20.01.2016	4 (1.5)	9.02	23.89		
20.01.2016	4 (1)	10.31	6.69	-7.28	-46.13
20.01.2016	4 (0.5)	11.10	3.60	-7.39	-47.92
20.01.2016	4 (S)	10.39	3.94	-6.94	-44.40
20.01.2016	4 (D)	5.29	3.35		
20.01.2016	5 (1.5)	9.54	20.75		
20.01.2016	5 (1)	9.15	24.27	-7.38	-47.10
20.01.2016	5 (0.5)	9.46	25.39	-7.43	-46.83
20.01.2016	5 (S)	9.82	3.83		
20.01.2016	5 (D)	8.29	3.38		
5.2.2016	1 (0.5)	8.29	32.27		
5.2.2016	1 (S)	10.61	3.84	-7.05	-44.27
5.2.2016	1 (D)	15.44	7.23		
5.2.2016	2 (1.5)	9.73	19.97		
5.2.2016	2 (0.5)	15.00	9.78	-7.13	-44.86
5.2.2016	2 (S)	11.95	4.33	-6.83	-44.04
5.2.2016	2 (D)	10.84	4.11		
5.2.2016	3 (1.5)	9.81	29.44		
5.2.2016	3 (0.5)	9.37	20.41		
5.2.2016	3 (S)	11.23	3.79	-6.77	-44.21
5.2.2016	3 (D)	7.37	1.79		
5.2.2016	4 (S)	11.32	3.67	-6.92	-44.24
5.2.2016	4 (D)	4.85	1.62		

5.2.2016	5 (1.5)	8.82	19.81	-7.46	-46.97
5.2.2016	5 (1)	6.82	24.20	-7.46	-46.77
5.2.2016	5 (0.5)	7.21	24.80	-7.35	-47.51
5.2.2016	5 (S)	9.95	3.28		
5.2.2016	5 (D)	9.03	3.01		
7.3.2016	1 (1.5)	9.45	11.22	-7.22	-46.42
7.3.2016	1 (1)	9.24	22.74	-7.36	-46.91
7.3.2016	1 (0.5)	10.32	13.86		
Date sampled	Sample ID	$\delta^{15}\text{N}_{\text{NO}_3}$ (‰)	$\delta^{18}\text{O}_{\text{NO}_3}$ (‰)	$\delta^{18}\text{O}_{\text{H}_2\text{O}}$ (‰)	$\delta^2\text{H}_{\text{H}_2\text{O}}$ (‰)
7.3.2016	1 (S)	10.31	4.29	-7.07	-44.56
7.3.2016	1 (D)	9.12	11.98		
7.3.2016	2 (1.5)	10.61	25.43	-7.06	-45.56
7.3.2016	2 (0.5)	11.40	6.57	-6.91	-44.80
7.3.2016	2 (S)	10.40	4.66	-7.09	-44.70
7.3.2016	2 (D)	8.76	7.49		
7.3.2016	3 (1.5)	9.16	20.17		
7.3.2016	3 (1)	9.67	28.18		
7.3.2016	3 (0.5)	10.31	23.56		
7.3.2016	3 (S)	9.77	4.70	-7.11	-44.41
7.3.2016	3 (D)	5.77	4.55		
7.3.2016	4 (1.5)	9.92	14.60		
7.3.2016	4 (0.5)	8.59	15.16	-6.95	-44.82
7.3.2016	4 (S)	9.66	4.54	-6.91	-44.62
7.3.2016	4 (D)	4.08	2.30		
7.3.2016	5 (1.5)	9.77	12.80	-7.42	-46.50
7.3.2016	5 (1)	9.03	24.00	-7.36	-47.67
7.3.2016	5 (0.5)	9.64	14.84		
7.3.2016	5 (S)	9.35	4.09		
7.3.2016	5 (D)	7.68	4.53		
22.4.16	1 (1)			-6.92	-43.63
22.4.16	1 (S)	10.95	4.35		
22.4.16	1(D)	13.55	11.00		
22.4.16	2(1.5)	10.48	16.09	-7.07	-45.38
22.4.16	2(0.5)	14.53	8.56		
22.4.16	2(S)	11.88	5.35	-6.66	-42.98
22.4.16	2(D)	10.74	8.52		
22.4.16	3(1.5)	10.68	23.54	-7.23	-46.35
22.4.16	3(1)	16.36	0.98		
22.4.16	3(0.5)	8.60	21.74		
22.4.16	3(S)	10.97	4.42		
22.4.16	3(D)	6.43	1.70		
22.4.16	4(1.5)	16.23	23.79		
22.4.16	4(S)	10.93	5.08	-6.83	-43.69
22.4.16	4(D)	4.48	1.45		
22.4.16	5(1.5)	9.66	23.86		

22.4.16	5(1)	9.14	25.55	-7.33	-47.04
22.4.16	5(0.5)	9.28	23.41	-7.24	-46.63
22.4.16	5(S)	9.42	4.20		
22.4.16	5(D)	8.36	3.50		
27.5.2016	1(0.5)	6.59	17.99		
27.5.2016	1(S)	12.49	6.92	-6.80	-44.07
27.5.2016	2(1.5)	6.30	1.83	-6.86	-43.58
27.5.2016	2(1)	6.95	28.97		
27.5.2016	2(0.5)	7.36	26.96	-7.04	-44.95
Date sampled	Sample ID	$\delta^{15}\text{N}_{\text{NO}_3}$ (‰)	$\delta^{18}\text{O}_{\text{NO}_3}$ (‰)	$\delta^{18}\text{O}_{\text{H}_2\text{O}}$ (‰)	$\delta^2\text{H}_{\text{H}_2\text{O}}$ (‰)
27.5.2016	2(S)	9.66	4.39	-7.01	-45.20
27.5.2016	2(D)	4.50	1.35		
27.5.2016	3(1.5)	8.03	33.56	-6.79	-44.58
27.5.2016	3(1)	5.37	24.88		
27.5.2016	3(0.5)	6.59	23.35		
27.5.2016	3(D)	6.46	1.65		
27.5.2016	4(1.5)			-6.88	-45.12
27.5.2016	4(1)	7.76	27.36		
27.5.2016	4(S)	10.00	4.98	-6.77	-43.95
27.5.2016	4(D)	4.99	1.78		
27.5.2016	5(1.5)			-7.20	-46.79
27.5.2016	5(1)	7.22	25.93		
27.5.2016	5(0.5)	6.80	25.94		
27.5.2016	5(S)	7.76	3.59		
27.5.2016	5(D)	11.96	7.07		
17.6.2016	1(1)	6.59	17.99		
17.6.2016	1(0.5)	26.44	19.25		
17.6.2016	1(S)	11.56	8.42	-6.78	-43.77
17.6.2016	1(D)	9.74	24.42		
17.6.2016	2(1.5)	8.25	27.00		
17.6.2016	2(1)	11.68	27.23		
17.6.2016	2(0.5)	7.36	26.96	-7.03	-45.30
17.6.2016	2(S)	11.33	7.92	-6.79	-43.92
17.6.2016	2(D)	7.88	31.32		
17.6.2016	3(1)	10.85	27.92		
17.6.2016	3(0.5)	7.19	3.64		
17.6.2016	3(D)	7.39	2.22		
17.6.2016	4(1.5)	12.96	7.23		
17.6.2016	4(1)	13.33	7.04		
17.6.2016	4(0.5)	6.83	27.58		
17.6.2016	4(S)	11.61	7.72	-6.87	-43.58
17.6.2016	4(D)	6.24	2.64	-7.08	-45.42
17.6.2016	5(1.5)	12.01	7.48		
17.6.2016	5(S)	10.25	7.00		
17.6.2016	5(D)	12.53	6.42		

1.7.2016	1(1.5)	9.36	13.00		
1.7.2016	1(1)	4.69	25.00	-7.23	-46.29
1.7.2016	1(0.5)	6.53	22.69	-7.16	-45.72
1.7.2016	1(D)	19.19	12.60		
1.7.2016	1(S)	12.50	7.85	-6.84	-44.01
1.7.2016	2(1.5)	5.47	22.05	-7.19	-45.32
1.7.2016	2(1)	8.55	21.53	-7.31	-45.68
1.7.2016	2(0.5)	20.17	13.86	-7.00	-45.06
1.7.2016	2(D)	12.46	7.78		
1.7.2016	2(S)	12.25	7.59		
Date sampled	Sample ID	$\delta^{15}\text{N}_{\text{NO}_3}$ (‰)	$\delta^{18}\text{O}_{\text{NO}_3}$ (‰)	$\delta^{18}\text{O}_{\text{H}_2\text{O}}$ (‰)	$\delta^2\text{H}_{\text{H}_2\text{O}}$ (‰)
1.7.2016	3(1.5)	10.59	12.23		
1.7.2016	3(1)	12.32	7.19		
1.7.2016	3(0.5)	13.04	8.70	-7.08	-46.20
1.7.2016	3(D)	6.88	2.24		
1.7.2016	3(S)	12.55	7.87	-6.90	-43.70
1.7.2016	4(1.5)	8.95	15.83	-7.08	-45.82
1.7.2016	4(1)	10.51	15.83	-7.19	-46.18
1.7.2016	4(0.5)	6.29	22.56		
1.7.2016	4(D)	4.82	1.57		
1.7.2016	4(S)	12.22	7.88	-6.92	-44.21
1.7.2016	5(1.5)	4.89	23.60	-7.33	-46.81
1.7.2016	5(1)	11.36	25.47	-7.46	-47.15
1.7.2016	5(S)	10.56	5.93		
12.8.2016	1(1.5)	8.87	24.69	-7.13	-45.49
12.8.2016	1(1)	10.98	26.27	-7.46	-46.78
12.8.2016	1(S)	12.44	5.85	-6.90	-44.53
12.8.2016	2(1.5)			-7.25	-45.98
12.8.2016	2(0.5)			-7.18	-46.01
12.8.2016	2(D)	15.84	8.51		
12.8.2016	2(S)	14.04	5.64	-6.95	-44.18
12.8.2016	3(1.5)	8.85	29.72	-6.68	-44.39
12.8.2016	3(1)	5.48	23.01	-7.39	-47.25
12.8.2016	3(D)	8.53	1.69		
12.8.2016	4(1.5)	8.53	19.66	-6.90	-44.63
12.8.2016	4(1)			-7.11	-45.15
12.8.2016	4(0.5)			-6.67	-43.96
12.8.2016	4(D)	6.74	3.73		
12.8.2016	4(S)	9.87	3.78	-6.92	-44.94
12.8.2016	5(1.5)	8.50	40.12	-7.33	-46.45
12.8.2016	5(1)	11.64	23.03	-7.31	-47.29
12.8.2016	5(S)	11.88	6.31		
09.09.2016	1(1)	8.32	32.39	-7.08	-45.57
09.09.2016	1(0.5)	7.76	33.04		
09.09.2016	1(S)	10.83	5.07	-7.01	-45.11

09.09.2016	2(1.5)	8.26	35.71		
09.09.2016	2(1)	6.93	2.02	-7.19	-45.73
09.09.2016	2(0.5)	7.63	28.06		
09.09.2016	2(D)	16.41	8.78		
09.09.2016	2(S)	11.82	4.81	-7.01	-44.84
09.09.2016	3(0.5)	4.82	22.99		
09.09.2016	3(S)	13.52	6.56	-7.04	-44.80
09.09.2016	4(1.5)	9.16	20.51		
09.09.2016	4(D)	6.06	3.80		
09.09.2016	4(S)	8.21	3.03	-7.03	-44.77
09.09.2016	5(1.5)	10.00	24.19		
Date sampled	Sample ID	$\delta^{15}\text{N}_{\text{NO}_3}$ (‰)	$\delta^{18}\text{O}_{\text{NO}_3}$ (‰)	$\delta^{18}\text{O}_{\text{H}_2\text{O}}$ (‰)	$\delta^2\text{H}_{\text{H}_2\text{O}}$ (‰)
09.09.2016	5(D)	15.63	4.97		
09.09.2016	5(S)	8.24	4.35		
03.11.2016	1(0.5)	6.26	38.68		
03.11.2016	1(S)	14.66	7.51	-6.82	-43.65
03.11.2016	3(S)	13.95	8.17		
03.11.2016	4(0.5)	8.69	29.00		
03.11.2016	4(1)	9.38	3.92	-7.00	-44.29
03.11.2016	4(1.5)				
03.11.2016	4(D)	4.23	2.03		
03.11.2016	5(1.5)			-7.46	-46.72
03.11.2016	5(1)	7.35	27.00	-7.52	-47.91
03.11.2016	5(0.5)				
03.11.2016	5(S)	8.29	3.58		
25.11.2016	1(1)			-7.31	-46.58
25.11.2016	1(0.5)	10.00	10.09	-7.18	-46.07
25.11.2016	1(S)	9.22	3.11		
25.11.2016	1(D)	17.93	11.08		
25.11.2016	2(S)	9.29	3.20	-6.75	-43.07
25.11.2016	3(S)	9.42	3.84		
25.11.2016	3(D)	6.40	1.90		
25.11.2016	4(1)			-7.19	-45.82
25.11.2016	4(0.5)	8.43	4.55	-6.78	-42.80
25.11.2016	4(D)	5.22	2.78		
25.11.2016	4(S)	9.40	3.62		
25.11.2016	5(1.5)	16.37	5.54		
25.11.2016	5(1)	10.40	5.66	-7.44	-46.86
25.11.2016	5(0.5)			-7.34	-46.87
25.11.2016	5(S)	9.53	3.71		
09.12.2016	1(0.5)			-6.76	-44.81
09.12.2016	1(S)	12.68	6.14		
09.12.2016	1(D)	22.67	13.74		
09.12.2016	2(S)	12.80	6.06		
09.12.2016	3(1.5)	8.50	30.59	-7.42	-46.87

09.12.2016	3(S)	12.67	6.47	-6.80	-43.79
09.12.2016	3(D)	6.50	1.62		
09.12.2016	4(1)	6.60	26.12		
09.12.2016	4(0.5)	7.15	24.01		
09.12.2016	4(S)	11.35	5.34		
09.12.2016	4(D)	4.95	2.46		
09.12.2016	5(1)	9.13	-0.01		
09.12.2016	5(S)	9.40	3.92		
09.12.2016	5(D)	10.09	5.01	-7.49	-47.68
20.1.2017	1(0.5)	8.29	26.80		
20.1.2017	1(S)			-6.88	-43.39
20.1.2017	1(D)	19.72	12.05		
Date sampled	Sample ID	$\delta^{15}\text{N}_{\text{NO}_3}$ (‰)	$\delta^{18}\text{O}_{\text{NO}_3}$ (‰)	$\delta^{18}\text{O}_{\text{H}_2\text{O}}$ (‰)	$\delta^2\text{H}_{\text{H}_2\text{O}}$ (‰)
20.1.2017	2(S)			-6.72	-43.55
20.1.2017	2(D)	14.33	8.75		
20.1.2017	3(S)	10.32	4.54		
20.1.2017	4(S)	9.79	3.49		
20.1.2017	4(D)	4.83	2.57		
20.1.2017	5(1.5)			-7.36	-46.93
20.1.2017	5(0.5)			-7.52	-47.56
20.1.2017	5(S)	9.09	3.28		
20.1.2017	5(D)	9.58	4.93		
03.04.2016	BH	21.99	18.53		
17.07.2016	BH	20.64	17.97		
16.12.2016	BH	20.18	16.93		
03.03.2017	BH	19.89	17.85		
17.03.2017	BH	21.57	17.72		

Appendix 3 – Major ion data

Major ion concentrations in all samples collected. (S) and (D) represent stream and drain samples, respectively. 0.5, 1.0 and 1.5 show the piezometer depths beneath the stream bed (m). BH refers to the borehole, installed to 12 m below the surface. Numbers outside the brackets show from which site the sample was collected (1 – 5). All concentrations in mg L⁻¹.

Date sampled	Sample ID	NO ₃ ⁻	SO ₄ ²⁻	Cl ⁻	NO ₂ ⁻	NH ₄ ⁺	HCO ₃ ⁻	Ca ²⁺	K ⁺	Mg ²⁺	Na ⁺
6.11.2015	1 (1)	2.05	17.11	35.48	0.02	0.08	250	75.02	6.99	7.31	22.79
6.11.2015	1 (S)	1.61	11.82	42.01	0.01	1.58	174	60.61	4.28	5.03	16.15
6.11.2015	1 (D)	39.32	34.27	63.79	0.03	1.61	112	71.05	4.96	6.25	17.15
6.11.2015	2 (1.5)	12.43	67.69	58.19	0.06		90	68.06	5.55	5.19	18.90
6.11.2015	2 (1)	24.53	29.70	60.00	0.01		113	63.86	5.97	5.32	18.70
6.11.2015	2 (0.5)	2.35	40.30	41.85	0.01	1.24	162	66.63	5.32	5.47	17.68
6.11.2015	2 (S)	12.83	29.89	57.55	0.01	1.93	102	57.75	4.41	4.74	15.30
6.11.2015	2 (D)	2.45	24.75	45.36	0.04	1.29	191	85.83	3.16	2.00	10.15
6.11.2015	3 (1.5)	17.07	35.70	52.52	0.05	0.02					
6.11.2015	3 (1)	13.60	17.89	34.53	0.02		143	53.74	5.50	4.00	17.92
6.11.2015	3 (S)	2.96	15.38	47.50	0.04	2.79	193	69.22	4.98	5.13	16.80
6.11.2015	3 (D)	1.23	9.68	43.87	0.05	1.95					
6.11.2015	4 (1)	21.87	72.13	73.41	0.04	0.01	122	67.43	5.52	9.98	17.65
6.11.2015	4 (0.5)	20.11	28.55	53.85	0.01		238	93.32	6.00	9.58	17.76
6.11.2015	4 (S)	3.12	53.69	44.71	0.04	1.11	122	65.82	4.86	4.80	14.20
19.11.2015	1 (0.5)	3.86	13.83	30.48	0.05	0.01	156	64.29	1.77	1.04	5.01
19.11.2015	1 (S)	32.63	13.92	48.84	0.01	1.07	142	68.62	0.68	2.55	10.94
19.11.2015	1 (D)	21.02	14.45	28.31	0.04	2.39	150	85.12	0.35	1.09	17.93
19.11.2015	2 (1.5)	0.50	53.28	28.70	0.04	0.01	129	74.97	0.91	1.16	6.47
19.11.2015	2 (1)	10.13	28.18	42.25	0.06	6.15	163	71.89	1.47	2.31	10.33
19.11.2015	2 (0.5)	0.28	25.51	28.94	0.01	1.43					
19.11.2015	2 (S)	31.00	23.80	45.28	0.06	2.30	161	83.81	0.30	0.61	3.48
19.11.2015	2 (D)	28.84	22.08	42.04	0.06	8.88	181	91.96	0.30	1.32	7.44
19.11.2015	3 (1.5)	0.43	37.04	21.09	0.05	1.41	154	74.31	1.17	0.83	6.59
19.11.2015	3 (1)	0.97	28.81	27.23	0.06	1.11	155	64.56	1.54	0.90	5.80
19.11.2015	3 (0.5)	0.35	7.27	45.41	0.01	2.37					
19.11.2015	3 (S)	31.80	12.35	43.53	0.02	1.54	179	85.10	0.37	0.66	3.81
19.11.2015	3 (D)	33.52	9.92	59.75	0.03	2.14	151	79.02	0.66	2.22	9.89
19.11.2015	4 (1.5)	0.65	70.86	39.64	0.03	0.03	132	69.22	1.66	3.05	9.88
19.11.2015	4 (1)	1.68	27.60	29.45	0.02	0.02	44	30.15	1.81	3.59	7.81
19.11.2015	4 (0.5)	2.03	14.90	31.28	0.02	1.33					
19.11.2015	4 (S)	29.53	52.29	46.76	0.04	1.01	192	99.44	0.75	2.53	10.78
19.11.2015	5 (1.5)	0.16	42.01	18.88	0.00	1.06	179	68.44	0.58	1.09	4.74
19.11.2015	5 (1)	0.69	31.85	21.30	0.04	1.10	189	79.22	0.49	0.70	3.42
19.11.2015	5 (0.5)	0.11	11.84	18.86	0.02		122	56.20	0.47	0.79	3.64
19.11.2015	5 (S)	28.84	11.21	41.69	0.01	0.05	109	57.64	0.96	2.93	12.48
26.11.2015	1 (1.5)	3.42	30.58	78.46	0.02	0.04	73	30.87	45.11	4.32	25.23

26.11.2015	1 (1)	3.35	37.60	75.49	0.03	2.30	118	50.30	40.13	4.38	21.36
26.11.2015	1 (0.5)	3.84	7.05	192.97	0.06	1.93	213	74.95	145.70	5.76	26.73
26.11.2015	1 (S)	33.48	12.49	123.86	0.06	1.22	134	76.65	63.57	3.62	16.72
26.11.2015	1 (D)	26.96	13.06	67.98	0.02	1.75	182	84.59	10.91	3.75	17.01
Date sampled	Sample ID	NO ₃ ⁻	SO ₄ ²⁻	Cl ⁻	NO ₂ ⁻	NH ₄ ⁺	HCO ₃ ⁻	Ca ²⁺	K ⁺	Mg ²⁺	Na ⁺
26.11.2015	2 (1.5)	0.57	30.62	112.44	0.03	0.02	146	60.70	41.54	3.72	20.42
26.11.2015	2 (1)	5.79	30.59	152.76	0.01	0.05	162	85.86	46.27	3.65	21.89
26.11.2015	2 (0.5)	0.52	39.51	108.56	0.02	1.20	121	66.11	55.34	3.73	19.51
26.11.2015	2 (S)	38.75	32.41	72.15	0.01	1.83	192	91.57	19.56	3.53	24.39
26.11.2015	2 (D)	42.76	29.17	80.61	0.04	1.18	128	91.57	30.19	3.53	24.39
26.11.2015	3 (1.5)	9.90	39.87	204.82	0.03		121	87.22	71.41	2.84	22.48
26.11.2015	3 (1)	1.85	31.03	320.78	0.02	0.03	113	91.77	156.05	2.41	22.82
26.11.2015	3 (0.5)	3.31	21.01	48.06	0.03	2.13					
26.11.2015	3 (S)	33.48	17.69	129.78	0.06	1.90	133	79.42	63.64	3.97	18.07
26.11.2015	3 (D)	53.92	17.72	111.27	0.02	2.49	98	64.76	56.30	2.98	14.16
26.11.2015	4 (1.5)	1.38	40.76	235.50	0.00	0.03	115	86.23	131.68	6.14	26.28
26.11.2015	4 (1)	3.14	32.98	120.35	0.05	0.05	258	88.29	93.43	8.79	20.54
26.11.2015	4 (0.5)	2.55	52.79	312.58	0.01	1.20	151	72.94	230.23	6.92	21.89
26.11.2015	4 (S)	33.48	29.11	113.54	0.06	0.96	120	69.42	45.22	3.76	13.43
26.11.2015	5 (1.5)	2.12	33.31	22.04	0.03		208	74.41	2.80	3.94	15.61
26.11.2015	5 (1)	1.14	33.17	18.98	0.01	0.08	203	72.27	4.18	3.88	12.93
26.11.2015	5 (0.5)	0.19	11.93	22.81	0.02	1.21	212	70.57	4.02	3.82	13.00
26.11.2015	5 (S)	33.48	12.03	43.61	0.02	0.88	197	82.11	2.58	4.32	16.32
26.11.2015	5 (D)	2.82	15.97	30.88	0.05	0.86	141	58.13	0.52	2.99	13.46
7.12.2015	1 (1.5)	3.12	10.13	285.10	0.05	2.15	215	61.07	232.10	2.53	15.03
7.12.2015	1 (1)	2.56	16.96	45.55	0.03	1.82	132	58.37	6.56	1.01	5.76
7.12.2015	1 (0.5)	1.24	13.37	30.13	0.02	1.39	228	68.04	3.17	1.49	6.87
7.12.2015	1 (S)	32.63	22.40	64.27	0.01	0.02	123	65.07	25.44	3.63	15.17
7.12.2015	1 (D)	22.96	39.19	59.05	0.00	0.01	142	87.84	2.92	3.76	15.92
7.12.2015	2 (1.5)	2.02	35.30	28.85	0.07	1.62	195	71.55	2.62	3.89	17.71
7.12.2015	2 (1)	1.50	22.50	43.51	0.03	1.48	214	79.35	11.56	3.04	15.38
7.12.2015	2 (0.5)	10.83	27.74	95.84	0.03	1.83	183	74.83	61.25	3.93	18.07
7.12.2015	2 (S)	29.90	25.02	44.52	0.00	0.04	119	64.27	3.36	3.66	14.72
7.12.2015	2 (D)	34.12	26.23	44.31	0.02	0.01	199	83.96	17.24	3.27	17.09
7.12.2015	3 (1.5)	1.38	20.69	32.79	0.02	2.14	131	47.53	5.94	2.25	16.60
7.12.2015	3 (1)	1.70	18.11	48.38	0.03	2.19	156	55.12	18.57	2.94	17.62
7.12.2015	3 (0.5)	2.25	20.15	144.15	0.02	1.82	104	67.37	62.90	3.76	20.87
7.12.2015	3 (S)	31.80	29.23	45.74	0.00	0.04					
7.12.2015	3 (D)	44.29	47.85	50.98	0.01		111	74.79	4.02	4.39	18.78
7.12.2015	4 (1.5)	1.02	26.55	104.75	0.03	1.62	205	79.51	61.75	5.56	19.41
7.12.2015	4 (1)	1.57	46.94	38.69		1.56	205	77.24	7.82	7.63	16.59
7.12.2015	4 (0.5)	0.68					296	76.14	5.85	4.58	12.32
7.12.2015	4 (S)	32.63	27.80	46.54		0.08	123	67.78	4.21	3.75	15.27
7.12.2015	5 (1.5)	0.54	11.48	108.33	0.01	1.22	121	57.84	44.27	1.14	7.74
7.12.2015	5 (1)	0.34	11.29	27.67	0.01	1.29	156	50.91	8.98	2.95	11.88
7.12.2015	5 (0.5)	0.21	14.06	25.46	0.01	0.09	216	72.43	7.20	3.00	12.03

7.12.2015	5 (S)	32.63	32.98	38.87	0.05	0.03	174	67.10	32.01	3.77	16.53
8.1.2016	1 (1.5)	15.78	19.02	92.92	0.66	1.21	267	99.93	66.12	3.68	15.27
8.1.2016	1 (0.5)	2.25	12.89	39.86	0.02	1.22	165	55.35	17.18	3.44	13.73
8.1.2016	1 (S)	24.80	16.88	45.14	0.02	0.02	168	69.38	17.75	3.52	13.89
Date sampled	Sample ID	NO ₃ ⁻	SO ₄ ²⁻	Cl ⁻	NO ₂ ⁻	NH ₄ ⁺	HCO ₃ ⁻	Ca ²⁺	K ⁺	Mg ²⁺	Na ⁺
8.1.2016	1 (D)	14.94	17.26	22.11	0.01	0.02	233	76.30	6.09	4.91	15.95
8.1.2016	2 (1.5)	0.39	27.55	34.55	0.01	1.49	224	75.53	12.78	3.86	17.44
8.1.2016	2 (1)	0.94	19.29	45.16	0.04	1.39	201	73.04	15.22	3.18	14.74
8.1.2016	2 (0.5)	1.21	23.74	30.86	0.01	1.80	199	68.17	5.25	3.80	16.65
8.1.2016	2 (S)	27.15	22.10	37.20	0.01		134	64.26	3.55	3.44	13.45
8.1.2016	2 (D)	23.35	21.15	32.07	0.03		169	71.35	3.41	3.19	14.12
8.1.2016	3 (1.5)	1.63	12.67	39.48	0.03	1.76	146	50.32	11.12	2.70	16.07
8.1.2016	3 (1)	1.09	24.50	41.19	0.04	1.52	200	74.57	12.25	3.04	14.34
8.1.2016	3 (0.5)	1.59	13.57	95.95	0.04	1.07	143	57.82	63.69	2.53	14.30
8.1.2016	3 (S)	24.85	19.49	35.20	0.02		158	67.70	5.37	3.49	14.07
8.1.2016	3 (D)	36.02	45.78	48.58	0.01	0.03	156	83.73	3.40	4.49	20.06
8.1.2016	4 (1.5)	1.23	29.97	114.45	0.01	1.78	196	70.41	60.00	4.41	16.34
8.1.2016	4 (S)	24.22	18.73	39.95	0.02	0.05	165	68.69	10.52	3.58	14.72
8.1.2016	5 (1.5)	0.24	12.52	33.76	0.01	0.08	207	69.70	14.93	3.10	11.72
8.1.2016	5 (1)	0.72	9.99	151.81	0.01	0.09	138	52.20	131.40	3.12	13.55
8.1.2016	5 (0.5)	1.90	16.81	38.36	0.03	1.27	248	83.93	18.42	3.33	12.42
8.1.2016	5 (S)	28.69	23.22	54.54	0.02		203	86.85	21.30	3.64	15.19
20.01.2016	1 (1.5)	4.84	20.74	91.89	0.84	2.09	118	59.95	42.96	3.27	14.25
20.01.2016	1 (1)	3.80	14.83	34.72	0.01	1.56	214	64.99	9.52	5.33	19.99
20.01.2016	1 (0.5)	0.80	9.92	55.50	0.04	0.08	215	69.77	26.45	4.38	18.59
20.01.2016	1 (S)	30.17	26.49	47.41	0.02		150	76.12	4.66	3.55	15.01
20.01.2016	1 (D)	13.05	26.75	35.74	0.01	0.05	169	70.11	6.66	3.33	14.44
20.01.2016	2 (1.5)	0.30	29.76	54.78	0.00	1.24	268	91.95	32.08	3.92	18.25
20.01.2016	2 (1)	0.97	27.62	30.76	0.01	1.62					
20.01.2016	2 (0.5)	0.34	28.60	31.19	0.02	1.61	189	68.83	3.89	3.49	16.09
20.01.2016	2 (S)	26.01	22.76	38.11	0.02	0.04	163	74.29	1.00	3.55	14.86
20.01.2016	2 (D)	28.93	33.70	62.27	0.01	0.04	107	67.91	17.65	2.92	14.80
20.01.2016	3 (1.5)	0.59	23.86	56.01	0.03	0.09	216	80.35	26.12	3.05	16.85
20.01.2016	3 (1)	0.17	24.99	137.64	0.01	1.11	135	65.97	75.80	1.52	10.22
20.01.2016	3 (0.5)	0.52	16.69	36.33	0.02	0.10	213	80.50	2.41	2.51	13.79
20.01.2016	3 (S)	28.93	27.40	47.98	0.01	0.05	149	74.50	5.76	3.63	16.00
20.01.2016	3 (D)	34.92	42.40	46.00	0.01	0.03	188	90.54	4.03	4.33	20.36
20.01.2016	4 (1.5)	1.11	29.01	412.97	0.01	1.63	159	68.80	392.19	5.72	23.13
20.01.2016	4 (1)	1.24	45.16	34.99	0.05	1.44	108	50.66	0.75	0.43	1.75
20.01.2016	4 (0.5)	17.44	24.14	88.84	1.00	1.71	116	66.00	20.84	1.13	6.28
20.01.2016	4 (S)	27.58	20.17	46.90	0.03	0.07	198	84.96	2.37	0.69	3.82
20.01.2016	4 (D)	54.95	20.17	31.79	0.01	0.04	105	63.09	3.91	2.91	10.62
20.01.2016	5 (1.5)	0.40	12.37	47.55	0.01	0.09	108	45.88	15.00	1.40	5.85
20.01.2016	5 (1)	0.31	10.12	49.97	0.01	0.09	111	51.15	8.99	0.53	2.65
20.01.2016	5 (0.5)	1.87	15.12	49.87	0.02	1.31	122	49.49	13.64	0.99	4.49
20.01.2016	5 (S)	26.68	25.56	74.95	0.03	0.04	116	60.88	24.44	1.98	9.62

20.01.2016	5 (D)	38.34	28.03	44.33	0.07	1.57	288	134.26	8.20	1.27	5.45
5.2.2016	1 (0.5)	0.59	7.56	188.38	0.05		150	65.82	126.37	3.69	15.74
5.2.2016	1 (S)	26.51	28.11	51.81	0.02	0.05	118	63.97	7.81	4.36	15.75
5.2.2016	1 (D)	13.21	34.86	50.58	0.02	0.04	133	65.01	13.51	3.96	15.19
Date sampled	Sample ID	NO ₃ ⁻	SO ₄ ²⁻	Cl ⁻	NO ₂ ⁻	NH ₄ ⁺	HCO ₃ ⁻	Ca ²⁺	K ⁺	Mg ²⁺	Na ⁺
5.2.2016	2 (1.5)	0.22	34.22	35.34	0.04	1.70	264	93.36	8.15	4.25	17.51
5.2.2016	2 (0.5)	2.73	21.81	40.30	0.05	2.13					
5.2.2016	2 (S)	25.76	26.12	100.44	0.03	0.05	109	66.04	49.29	4.16	16.76
5.2.2016	2 (D)	25.64	29.15	46.47	0.01	0.03	197	83.81	9.78	4.66	17.73
5.2.2016	3 (1.5)	0.51	23.44	35.63	0.02	1.64	176	64.48	4.03	3.32	16.63
5.2.2016	3 (0.5)	0.86	18.96	43.91	0.06	1.47	222	84.96	4.16	3.31	14.25
5.2.2016	3 (S)	27.33	32.75	97.36	0.04	0.04	155	65.85	44.46	4.32	17.92
5.2.2016	3 (D)	42.77	57.59	63.25	0.00	0.02	119	76.79	9.19	4.89	20.19
5.2.2016	4 (0.5)	0.59	21.90	38.20	0.02	1.43					
5.2.2016	4 (S)	26.57	30.47	53.30	0.01	0.08	121	66.37	8.34	4.22	16.46
5.2.2016	4 (D)	69.05	26.70	40.85	0.01		148	85.60	0.18	1.23	7.17
5.2.2016	5 (1.5)	0.41	12.44	119.28	1.11		111	67.97	41.47	0.85	5.29
5.2.2016	5 (1)	0.33	8.64	93.16	0.03		133	56.44	42.99	1.44	6.56
5.2.2016	5 (0.5)	0.41	14.97	44.24	0.02	1.22	221	74.15	22.25	4.01	12.57
5.2.2016	5 (S)	27.97	31.27	60.68	0.03	0.08	144	58.03	16.27	4.37	16.58
5.2.2016	5 (D)	38.30	33.52	45.03	0.04	1.86	109	57.17	16.92	4.71	14.58
7.3.2016	1 (1.5)	2.16	11.80	129.81	0.01	1.36	136	62.84	53.58	4.93	22.55
7.3.2016	1 (1)	1.09	12.96	34.38	0.01	1.51	280	82.93	8.72	6.34	20.74
7.3.2016	1 (0.5)	1.38	6.82	50.04	0.05		221	73.21	17.08	4.43	17.38
7.3.2016	1 (S)	29.51	27.97	40.98	0.05		107	60.16	3.55	3.87	13.62
7.3.2016	1 (D)	22.67	29.43	29.66	0.05	1.36	192	75.80	5.86	4.49	13.99
7.3.2016	2 (1.5)	0.44	34.16	38.73	0.02	1.44	251	91.28	5.36	4.93	17.80
7.3.2016	2 (0.5)	5.63	29.40	76.01	0.06	1.59	265	98.91	40.23	4.83	18.01
7.3.2016	2 (S)	27.98	27.66	49.39	0.06		145	71.52	11.29	4.17	14.46
7.3.2016	2 (D)	22.03	29.27	32.77	0.06		214	40.88	45.75	4.86	43.22
7.3.2016	3 (1.5)	0.74	20.25	34.40	0.04	1.33	177	63.07	4.85	3.41	16.22
7.3.2016	3 (1)	0.40	20.18	41.45	0.02	1.23	164	67.94	4.60	2.16	12.61
7.3.2016	3 (0.5)	0.85	11.22	120.26	0.02	1.02	145	69.94	68.69	2.33	13.22
7.3.2016	3 (S)	28.19	27.44	41.36	0.03		126	64.86	2.31	3.62	15.97
7.3.2016	3 (D)	42.58	48.70	53.52	0.05	1.63	126	77.43	8.60	4.37	18.09
7.3.2016	4 (1.5)	2.30	31.74	53.04	0.02	1.47	193	77.40	3.88	6.15	19.55
7.3.2016	4 (0.5)	0.84	25.18	103.11	0.03		131	65.85	51.27	2.08	7.29
7.3.2016	4 (S)	29.01	28.47	41.88	0.04		202	75.06	2.68	3.60	15.52
7.3.2016	4 (D)	63.64	27.96	44.39	0.03	1.69	144	78.28	10.97	4.11	14.47
7.3.2016	5 (1.5)	1.30	10.96	36.99	0.03		242	85.27	7.56	3.51	12.51
7.3.2016	5 (1)	0.40	6.11	129.11	0.02		149	67.56	80.72	3.09	13.03
7.3.2016	5 (0.5)	0.33	14.17	23.48	0.03		228	74.46	4.67	3.66	13.42
7.3.2016	5 (S)	27.95	27.39	66.25	0.06						
7.3.2016	5 (D)	28.99	22.64	28.54	0.01	2.34	117	50.53	6.47	3.85	12.87
22.4.16	1 (1)	8.02	12.38	27.92	0.04						
22.4.16	1 (S)	28.77	27.90	58.77	0.06		260	118.13	0.64	3.87	17.58

22.4.16	1(D)	21.01	38.12	41.41	0.03		317	131.29	0.92	3.61	15.31
22.4.16	2(1.5)	0.59	30.22	32.95	0.06		285	102.36	2.38	4.04	17.68
22.4.16	2(0.5)	3.16	22.92	42.90	0.03		258	92.85	4.67	4.23	20.72
22.4.16	2(S)	28.45	27.77	56.31	0.05		233	109.93	0.55	3.56	15.95
Date sampled	Sample ID	NO ₃ ⁻	SO ₄ ²⁻	Cl ⁻	NO ₂ ⁻	NH ₄ ⁺	HCO ₃ ⁻	Ca ²⁺	K ⁺	Mg ²⁺	Na ⁺
22.4.16	2(D)	14.76	27.22	36.35	0.05		337	128.34	0.56	3.16	16.18
22.4.16	3(1.5)	2.31	16.74	61.45	0.03		169	83.74	1.32	2.80	10.81
22.4.16	3(1)	2.25	20.23	54.86	0.06		179	74.57	2.18	2.13	12.58
22.4.16	3(0.5)	0.81	26.04	64.34	0.04		166	73.90	4.08	2.74	9.15
22.4.16	3(S)	27.59	32.67	65.78	0.06		228	111.40	1.13	3.98	19.42
22.4.16	3(D)	42.18	59.13	66.54	0.00						
22.4.16	4(1.5)	2.21	31.13	61.78	0.04		125	64.19	2.10	6.09	17.33
22.4.16	4(0.5)										
22.4.16	4(S)	22.94	22.07	39.77	0.04		284	111.32	0.75	3.79	17.24
22.4.16	4(D)	66.54	30.45	72.62	0.00		165	101.30	11.78	4.11	18.69
22.4.16	5(1.5)	0.28	8.67	25.17	0.01		245	82.87	1.15	3.10	11.43
22.4.16	5(1)	5.90	3.98	30.37	0.04		189	68.17	1.46	2.38	11.77
22.4.16	5(0.5)	0.31	14.98	28.26	0.03		387	125.52	1.14	4.00	19.71
22.4.16	5(S)	31.29	33.28	57.01	0.01		394	157.08	1.38	4.87	23.62
22.4.16	5(D)	31.83	27.48	37.95	0.02		237	98.13	6.75	4.36	14.77
27.5.2016	1(0.5)	0.86	38.40	72.30	0.01						
27.5.2016	1(S)	3.08	24.01	49.24	0.06		414	152.87	0.72	4.10	17.90
27.5.2016	2(1.5)	1.67	24.60	49.14	0.01		254	98.53	2.65	3.09	20.23
27.5.2016	2(1)	2.57	32.48	38.02	0.03		207	82.14	2.58	2.47	19.53
27.5.2016	2(0.5)	2.30	14.21	40.20	0.06		350	118.55	2.22	4.32	20.48
27.5.2016	2(S)	2.65	31.11	41.37	0.01		419	152.93	0.49	4.11	18.01
27.5.2016	2(D)	4.00	9.36	46.56	0.02		400	123.55	0.77	3.83	16.70
27.5.2016	3(1.5)	1.26	18.31	47.84	0.06						
27.5.2016	3(1)	0.67	12.54	47.96	0.02		217	82.71	1.62	1.90	20.40
27.5.2016	3(0.5)	3.55	12.62	29.65	0.02		335	105.66	2.64	3.01	24.58
27.5.2016	3(D)	44.29	51.18	72.94	0.06		346	159.20	9.31	4.48	23.26
27.5.2016	4(1.5)	1.16	29.81	54.70	0.00		287	106.50	3.71	6.59	22.51
27.5.2016	4(1)	0.38	45.33	239.69	0.06		210	131.30	124.62	8.61	18.61
27.5.2016	4(0.5)	8.86	37.26	40.20	0.04		509	43.69	281.80	2.69	18.98
27.5.2016	4(S)	13.93	25.83	44.24	0.05		402	148.63	1.37	4.21	19.17
27.5.2016	4(D)	53.92	26.34	49.71	0.06		305	133.40	1.27	4.24	18.87
27.5.2016	5(1.5)	1.28	11.84	23.77	0.06		339	110.28	2.13	3.43	15.39
27.5.2016	5(1)	0.15	3.83	22.76	0.04		327	103.49	1.27	3.14	14.52
27.5.2016	5(0.5)	0.31	11.46	28.01	0.05		332	109.05	3.26	3.51	15.53
27.5.2016	5(S)	20.00	36.17	51.17	0.01		317	129.26	1.90	4.16	21.16
27.5.2016	5(D)	15.50	27.24	34.14	0.05		396	141.42	5.27	4.59	16.71
17.6.2016	1(1.5)	1.92	20.88	37.31	0.06		309	93.74	8.11	4.11	16.03
17.6.2016	1(1)	2.34	19.53	35.81	0.05		189	61.36	2.75	2.92	12.72
17.6.2016	1(0.5)	2.63	3.77	34.93	0.03		142	55.28	2.29	1.83	8.34
17.6.2016	1(S)	38.33	31.16	66.48	0.04		328	151.60	1.25	3.79	15.01
17.6.2016	1(D)	7.79	45.23	42.21	0.02		342	140.87	1.90	3.75	12.15

17.6.2016	2(1.5)	2.19	33.88	40.71	0.03		322	121.43	5.13	4.07	15.66
17.6.2016	2(1)	2.17	12.97	106.01	0.00		227	98.40	48.92	3.04	14.83
17.6.2016	2(0.5)	2.01	17.29	45.84	0.01		314	114.19	4.59	4.24	15.90
17.6.2016	2(S)	0.69	6.46	149.86	0.04		110	91.43	0.32	2.25	9.96
Date sampled	Sample ID	NO ₃ ⁻	SO ₄ ²⁻	Cl ⁻	NO ₂ ⁻	NH ₄ ⁺	HCO ₃ ⁻	Ca ²⁺	K ⁺	Mg ²⁺	Na ⁺
17.6.2016	2(D)	12.71	30.71	40.77	0.03		372	141.84	1.44	3.96	15.55
17.6.2016	3(1.5)	1.74	15.27	50.07	0.04		257	92.29	12.71	4.92	15.16
17.6.2016	3(1)	3.88	16.01	52.11	0.01		185	84.23	2.06	2.02	11.45
17.6.2016	3(0.5)	1.85	14.95	60.05	0.01		218	89.93	13.24	2.72	13.56
17.6.2016	3(S)							168.87	1.98	4.53	13.80
17.6.2016	3(D)	36.25	46.17	64.66	0.04		316	146.94	4.60	4.31	18.27
17.6.2016	4(1.5)	2.28	29.52	65.91	0.04		268	107.31	15.35	6.73	14.68
17.6.2016	4(1)	5.54	44.09	147.96	0.06		300	135.04	80.52	8.54	15.69
17.6.2016	4(0.5)	1.95	7.56	44.58	0.02		125	55.96	2.38	3.02	9.62
17.6.2016	4(S)	30.72	30.24	67.15	0.03		268	129.32	4.52	3.38	13.78
17.6.2016	4(D)	51.65	26.54	54.00	0.03		160	94.32	3.82	3.12	11.63
17.6.2016	5(1.5)	1.75	6.59	242.31	0.01		222	101.67	186.41	3.32	13.92
17.6.2016	5(1)	0.50	25.99	87.42	0.03		146	92.97	5.60	2.92	9.93
17.6.2016	5(0.5)										
17.6.2016	5(S)	26.84	32.14	55.77	0.02		128	83.62	1.07	2.22	9.95
17.6.2016	5(D)	16.97	29.84	39.37	0.02		351	130.93	9.01	4.66	14.68
1.7.2016	1(1.5)	5.21	10.48	40.87	0.03						
1.7.2016	1(1)	1.46	13.06	37.38	0.05		312	98.71	1.74	6.29	22.82
1.7.2016	1(0.5)	2.19	11.41	31.98	0.06		323	97.52	2.32	5.19	26.12
1.7.2016	1(D)	12.71	57.06	37.12	0.00		334	155.11	0.62	3.81	15.51
1.7.2016	1(S)	29.24	45.28	28.47	0.04		405	174.24	0.69	4.96	20.98
1.7.2016	2(1.5)	0.27	37.14	38.95	0.04		334	124.00	1.90	4.14	18.80
1.7.2016	2(1)	1.08	24.35	41.49	0.04		307	109.94	2.26	3.62	20.84
1.7.2016	2(0.5)	8.01	20.80	43.56	0.02		394	139.27	2.25	4.82	20.18
1.7.2016	2(D)	17.91	32.59	41.49	0.01		398	152.80	0.54	3.60	17.47
1.7.2016	2(S)	30.60	33.29	53.14	0.06		285	127.85	0.58	3.80	15.97
1.7.2016	3(1.5)	1.54	22.01	40.78	0.05		205	79.65	2.57	2.78	17.28
1.7.2016	3(1)	16.66	20.71	43.73	0.02		247	102.98	2.02	2.65	13.95
1.7.2016	3(0.5)	9.82	31.75	38.14	0.06		268	105.26	2.26	3.50	16.46
1.7.2016	3(D)	40.40	53.93	65.46	0.03		381	162.40	1.34	4.35	21.02
1.7.2016	3(S)	24.13	24.55	41.64	0.01		367	141.56	0.56	3.76	16.90
1.7.2016	4(1.5)	1.24	30.14	38.64	0.04		344	117.69	3.10	7.12	20.11
1.7.2016	4(1)	0.23	45.71	42.49	0.04		319	118.22	3.08	7.14	19.88
1.7.2016	4(0.5)	0.61	22.53	41.06	0.02		300	130.60	0.88	3.98	16.66
1.7.2016	4(D)	51.67	29.10	52.50	0.02		412	130.60	0.88	3.98	16.66
1.7.2016	4(S)	13.52	8.41	11.83	0.02		511	160.52	0.83	3.88	17.34
1.7.2016	5(1.5)	0.58	9.35	26.27	0.05		322	109.31	1.55	3.15	10.98
1.7.2016	5(1)	0.52	3.45	30.57	0.02		297	102.21	1.47	2.84	10.54
1.7.2016	5(S)	24.94	30.54	48.61	0.01		373	151.61	0.95	3.81	15.09
12.8.2016	1(1.5)	2.31	8.88	31.60	0.06		296	94.96	2.51	5.11	17.45
12.8.2016	1(1)	2.57	16.88	29.56	0.04		262	88.07	1.36	5.18	15.93

12.8.2016	1(0.5)	2.03	8.14	29.39	0.03		273	84.14	2.64	4.84	19.76
12.8.2016	1(S)	3.85	24.33	42.25	0.03		376	131.60	2.23	5.07	20.80
12.8.2016	2(1.5)		43.72	34.74	0.02		340	128.51	2.19	3.92	16.47
12.8.2016	2(1)	2.04	22.96	31.92	0.03		303	108.41	2.37	3.19	15.37
Date sampled	Sample ID	NO ₃ ⁻	SO ₄ ²⁻	Cl ⁻	NO ₂ ⁻	NH ₄ ⁺	HCO ₃ ⁻	Ca ²⁺	K ⁺	Mg ²⁺	Na ⁺
12.8.2016	2(0.5)	2.60	15.76	34.60	0.05		366	124.00	2.82	4.34	17.20
12.8.2016	2(D)	10.70	34.63	32.06	0.03		418	153.87	0.56	3.45	16.21
12.8.2016	2(S)	4.33	28.44	39.82	0.00		276	100.93	2.38	4.82	19.47
12.8.2016	3(1.5)	2.49	18.55	38.06	0.03		212	79.81	3.66	2.75	15.83
12.8.2016	3(1)	1.83	12.96	38.86	0.04		244	94.00	2.27	1.88	11.89
12.8.2016	3(0.5)	2.41	15.03	38.89	0.05		221	83.95	3.28	2.42	14.16
12.8.2016	3(D)	38.16	60.05	51.28	0.05		350	158.47	1.43	4.19	18.60
12.8.2016	4(1.5)	3.25	36.91	47.01	0.05		327	121.54	4.43	7.07	18.13
12.8.2016	4(1)		49.67	33.61	0.00		409	145.59	2.49	8.94	15.46
12.8.2016	4(0.5)		10.85	39.46	0.00		219	80.07	2.46	4.43	12.00
12.8.2016	4(D)	27.86	28.28	40.38	0.02		294	116.76	1.75	5.21	16.68
12.8.2016	4(S)	12.61	39.83	42.53	0.05		332	128.00	3.25	4.86	19.57
12.8.2016	5(1.5)	2.69	13.21	22.87	0.03		286	97.24	1.58	3.36	11.28
12.8.2016	5(1)	2.65	5.16	22.51	0.05		282	92.81	1.71	3.23	10.91
12.8.2016	5(D)	23.32	31.25	36.73	0.03		364	127.69	9.39	5.12	15.01
12.8.2016	5(S)	8.66	43.15	41.39	0.01		368	139.82	6.09	5.02	16.89
09.09.2016	1(1.5)	0.75	5.08	27.18	0.03						
09.09.2016	1(1)	0.18	10.18	28.35	0.06		352	106.81	3.19	6.36	19.72
09.09.2016	1(0.5)	0.40	9.44	21.25	0.04		312	95.94	3.52	4.35	15.85
09.09.2016	1(S)	3.50	15.26	33.23	0.03		257	84.69	2.54	5.13	19.18
09.09.2016	2(1.5)	0.90	33.67	29.59	0.02		361	127.90	3.03	3.90	16.50
09.09.2016	2(1)	40.57	59.88	47.39	0.00		344	154.82	2.92	4.12	18.24
09.09.2016	2(0.5)	2.66	12.06	28.36	0.00		388	124.22	4.12	4.35	18.65
09.09.2016	2(D)	9.15	32.31	29.19	0.05		413	148.58	1.10	3.55	16.47
09.09.2016	2(S)	2.65	20.03	36.26	0.04		411	138.25	3.98	4.88	19.16
09.09.2016	3(1.5)	0.61	15.38	36.11	0.02						
09.09.2016	3(1)	0.75	18.06	39.71	0.00		267	100.71	2.85	2.79	13.25
09.09.2016	3(0.5)	0.32	19.59	30.52	0.03		324	111.71	2.95	3.35	15.57
09.09.2016	3(S)	2.69	21.43	31.84	0.05		410	137.96	2.89	4.67	18.30
09.09.2016	4(1.5)	0.61	38.85	266.15	0.01		349	121.71	261.56	7.01	18.66
09.09.2016	4(1)	0.33	42.84	38.74	0.05		431	149.55	8.88	8.89	15.39
09.09.2016	4(D)	12.99	23.47	34.99	0.01		787	236.33	7.78	12.21	37.18
09.09.2016	4(S)	11.83	33.72	34.81	0.06		381	139.04	2.19	4.58	17.91
09.09.2016	5(1.5)	0.65	12.46	18.58	0.05						
09.09.2016	5(1)	0.71	3.25	19.60	0.01		326	105.01	1.70	2.95	10.58
09.09.2016	5(0.5)	0.27	6.41	19.42	0.05		342	109.45	2.66	3.49	11.21
09.09.2016	5(D)	10.31	33.47	35.15	0.05		368	129.02	12.99	5.09	16.74
09.09.2016	5(S)	14.69	34.22	30.61	0.02		363	135.13	1.63	4.11	15.30
03.11.2016	1(1)										
03.11.2016	1(0.5)	1.63	2.50	57.18	0.04		209	79.92	1.93	4.40	16.87
03.11.2016	1(S)	7.62	20.25	32.15	0.05		402	138.88	1.70	4.29	17.08

03.11.2016	3(S)	9.57	21.50	57.55	0.05						
03.11.2016	3(D)	0.73	0.96	1.12	0.06		555	159.63	1.95	4.20	18.56
03.11.2016	4(0.5)	1.60	6.65	61.71	0.01		193	83.46	2.27	4.72	11.20
03.11.2016	4(1)	11.83	26.38	63.79	0.03		349	143.87	1.82	4.25	16.78
Date sampled	Sample ID	NO ₃ ⁻	SO ₄ ²⁻	Cl ⁻	NO ₂ ⁻	NH ₄ ⁺	HCO ₃ ⁻	Ca ²⁺	K ⁺	Mg ²⁺	Na ⁺
03.11.2016	4(D)	30.21	20.01	54.41	0.05		298	123.48	1.50	5.40	16.42
03.11.2016	5(1.5)	1.25	6.65	43.62	0.05		287	107.72	1.25	3.07	10.50
03.11.2016	5(1)	2.94	1.90	48.63	0.01		269	103.23	1.35	2.87	10.59
03.11.2016	5(0.5)	2.99	9.71	19.44	0.01		330	109.08	1.30	3.35	10.71
03.11.2016	5(S)	16.70	28.15	58.35	0.06		332	138.56	1.50	4.00	16.02
25.11.2016	1(1)	3.89	35.43	41.88	0.05						
25.11.2016	1(0.5)	3.59	23.80	54.10	0.03						
25.11.2016	1(S)	31.75	17.23	56.32	0.03		110	54.30	0.22	1.67	6.95
25.11.2016	1(D)	8.66	26.90	26.94	0.04		170	80.58	0.08	2.18	8.79
25.11.2016	2(S)	34.09	20.75	42.29	0.05		105	55.23	0.99	1.74	7.50
25.11.2016	3(S)	36.83	30.01	35.05	0.04		117	63.50	0.60	3.60	15.72
25.11.2016	3(D)	18.20	14.76	24.54	0.01		174	65.40	0.66	3.31	14.18
25.11.2016	4(1.5)	3.19	97.57	75.12	0.06						
25.11.2016	4(1)	46.27	16.46	26.60	0.02		144	62.77	1.04	6.29	12.39
25.11.2016	4(0.5)	33.20	30.85	81.42	0.01		139	86.93	15.09	4.11	16.83
25.11.2016	4(D)	66.76	25.43	34.19	0.05		118	82.42	4.25	1.91	8.04
25.11.2016	4(S)	20.28	10.78	38.90	0.02		101	50.68	0.16	1.06	3.93
25.11.2016	5(1.5)	0.57	13.13	42.93	0.04		146	61.19	1.25	3.22	12.96
25.11.2016	5(1)	1.70	10.18	19.34	0.06		107	37.85	0.62	2.56	10.05
25.11.2016	5(0.5)	2.97	14.56	51.79	0.00		108	57.51	0.66	2.88	11.24
25.11.2016	5(S)	16.64	20.24	25.47	0.01		147	56.42	0.68	3.83	15.90
09.12.2016	1(1)	0.31	36.34	31.14	0.03						
09.12.2016	1(0.5)	0.83	24.82	26.44	0.02						
09.12.2016	1(S)	14.43	14.82	22.81	0.05		136	53.43	0.45	2.81	11.82
09.12.2016	1(D)	3.93	43.10	29.07	0.06		143	66.45	0.39	3.54	12.43
09.12.2016	2(S)	19.90	27.29	33.10	0.05		99	56.08	0.62	2.50	10.51
09.12.2016	3(1.5)	1.27	30.25	38.84	0.03		180	71.29	1.57	3.22	19.92
09.12.2016	3(S)	19.12	25.83	34.90	0.00		118	55.98	0.37	2.14	9.26
09.12.2016	3(D)	31.29	40.88	39.99	0.05		119	71.20	0.88	3.94	13.15
09.12.2016	4(1.5)	1.00	65.35	35.32	0.01						
09.12.2016	4(1)	0.34	43.57	35.26	0.01		150	64.52	1.24	6.63	13.98
09.12.2016	4(0.5)	0.36	30.21	40.78	0.02		241	87.13	1.07	6.81	19.11
09.12.2016	4(S)	19.97	32.10	38.24	0.01		51	46.72	0.43	2.23	9.68
09.12.2016	4(D)	60.86	23.56	31.97	0.05		102	62.81	0.66	3.15	15.37
09.12.2016	5(1.5)						245	58.71	12.12	3.03	12.02
09.12.2016	5(1)	0.17	8.65	30.80	0.04		177	65.02	0.51	2.86	10.75
09.12.2016	5(0.5)	0.46	17.78	20.69	0.05		127	47.53	0.56	2.76	10.33
09.12.2016	5(S)						228	54.72	0.97	3.62	15.56
09.12.2016	5(D)	21.55	28.17	28.42	0.01		190	81.41	4.86	3.26	11.22
20.1.2017	1(0.5)	0.80	11.36	45.70	0.04		158	51.30	23.47	3.89	15.30
20.1.2017	1(S)	36.62	32.08	58.62	0.02		66	49.93	2.42	1.47	6.54

20.1.2017	1(D)	6.98	34.57	62.63	0.02		192	135.46	5.22	2.75	10.66
20.1.2017	2(S)	34.10	31.33	62.98	0.02		62	52.60	0.48	3.24	11.83
20.1.2017	2(D)	8.91	27.48	51.59	0.01		303	135.46	12.12	0.97	7.36
20.1.2017	3(0.5)	1.07	14.16	54.09	0.04						
Date sampled	Sample ID	NO ₃ ⁻	SO ₄ ²⁻	Cl ⁻	NO ₂ ⁻	NH ₄ ⁺	HCO ₃ ⁻	Ca ²⁺	K ⁺	Mg ²⁺	Na ⁺
20.1.2017	3(S)	32.06	28.06	62.25	0.04		60	53.58	4.20	2.97	11.65
20.1.2017	3(D)	38.30	42.08	67.10	0.00		138	100.90	3.16	3.83	16.25
20.1.2017	4(S)	31.43	28.94	88.48	0.05		56	55.83	6.49	3.32	13.15
20.1.2017	4(D)	65.06	24.48	69.21	0.05		106	77.80	3.96	3.61	11.18
20.1.2017	5(1.5)	0.93	14.95	74.88	0.04		54	42.12	24.73	2.60	9.39
20.1.2017	5(1)	0.41	8.15	43.62	0.01		185	62.98	26.74	2.72	9.43
20.1.2017	5(0.5)	0.42	11.48	41.16	0.01		162	55.07	27.58	2.66	9.41
20.1.2017	5(S)	32.86	33.34	44.62	0.01		94	46.40	35.04	3.22	13.35
20.1.2017	5(D)	24.05	31.22	53.97	0.02		186	39.13	14.06	3.27	10.28
03.04.2016	BH	4.03	16.63	13.97			402	124.72	0.99	3.84	19.23
17.07.2016	BH	3.90	32.50	23.08			273	97.04	1.90	3.41	16.52
16.12.2016	BH	3.46	28.71	22.06			263	94.09	0.66	2.65	12.47
03.02.2016	BH	3.35	24.77	21.99			339	125.22	0.79	3.29	16.92
17.03.2017	BH	4.01	21.90	18.41			308	104.88	1.01	3.45	17.54

Appendix 4 – Mass balance data

Data used in the low and high nitrogen mass balance calculations for both the low and high nitrogen scenarios

High nitrogen scenario (low volatilisation, high turkey manure N)												
Field	Crop	Date	Product	Area (ha)	Rate (kg ha ⁻¹)	N fraction (%)	Export coefficient	Total N in (kg)	N lost to volatilisation (kg)	N available for crop uptake (kg)	Crop N uptake (kg)	Leached N (kg)
Low Farm Ave.	Sugar Beet	12/09/2015	Turkey Manure	17.75	7765.00	3.55%	0.17	4892.92	733.94	4158.98	3451.96	707.03
Salle Old Grounds	Sugar Beet	12/09/2015	Turkey Manure	6.00	7765.00	3.55%	0.17	1653.95	248.09	1405.85	1166.86	239.00
Merrisons	W OSR	04/08/2015	Turkey Manure	39.03	7765.00	3.55%	0.42	10758.91	1613.84	9145.08	5304.14	3840.93
Merrisons	W OSR	04/08/2015	Turkey Manure	15.42	7765.00	3.55%	0.42	4250.64	637.60	3613.04	2095.56	1517.48
Merrisons	W OSR	04/08/2015	Turkey Manure	20.64	7765.00	3.55%	0.42	5689.57	853.44	4836.14	2804.96	2031.18
Merrisons	W OSR	04/08/2015	Turkey Manure	17.44	7765.00	3.55%	0.42	4807.47	721.12	4086.35	2370.08	1716.27
Merrisons	W OSR	01/05/2016	Nuram 35 + 7So3	16.78	100.00	35.00%	0.17	587.30		587.30	487.46	99.84
Merrisons	W OSR	05/05/2016	Nuram 25 + 14So3	17.07	280.00	25.00%	0.17	1194.90		1194.90	991.77	203.13
Merrisons	W OSR	15/05/2016	33.5% Nitrogen	17.31	45.00	33.50%	0.17	260.95		260.95	216.59	44.36
Carfour	Winter Barley Malt	26/02/2016	Nuram 35 + 7So3	15.85	200.00	35.00%	0.2	1109.50		1109.50	887.60	221.90
Carfour	Winter Barley Malt	18/03/2016	Nuram 35 + 7So3	15.65	220.00	35.00%	0.2	1205.05		1205.05	964.04	241.01
Home Farm Fld	Winter Barley Malt	26/02/2016	Nuram 35 + 7So3	19.07	200.00	35.00%	0.2	1334.90		1334.90	1067.92	266.98
Home Farm Fld	Winter Barley Malt	18/03/2016	Nuram 35 + 7So3	19.62	220.00	35.00%	0.2	1510.74		1510.74	1208.59	302.15

West Chase	???	06/07/2016	33.5% Nitrogen	2.34	444.06	33.50%	0.2	348.10	348.10	278.48	69.62
Far Hempsky	Winter Barley Feed	27/02/2016	Nuram 35 + 7So3	12.54	200.00	35.00%	0.2	877.80	877.80	702.24	175.56
Far Hempsky	Winter Barley Feed	18/03/2016	Nuram 35 + 7So3	11.80	200.00	35.00%	0.2	826.00	826.00	660.80	165.20
Far Hempsky	Winter Barley Feed	06/04/2016	Nuram 35 + 7So3	12.54	200.00	35.00%	0.2	877.80	877.80	702.24	175.56
Middle Hempsky	Winter Barley Feed	27/02/2016	Nuram 35 + 7So3	11.35	200.00	35.00%	0.2	794.50	794.50	635.60	158.90
Middle Hempsky	Winter Barley Feed	18/03/2016	Nuram 35 + 7So3	10.80	200.00	35.00%	0.2	756.00	756.00	604.80	151.20
Middle Hempsky	Winter Barley Feed	06/04/2016	Nuram 35 + 7So3	11.35	200.00	35.00%	0.2	794.50	794.50	635.60	158.90
Lane Field	???	06/07/2016	33.5% Nitrogen	0.83	444.06	33.50%	0.2	123.47	123.47	98.78	24.69
Potash	Winter Barley Feed	27/02/2016	Nuram 35 + 7So3	24.20	200.00	35.00%	0.2	1694.00	1694.00	1355.20	338.80
Potash	Winter Barley Feed	18/03/2016	Nuram 35 + 7So3	24.40	200.00	35.00%	0.2	1708.00	1708.00	1366.40	341.60
Potash	Winter Barley Feed	06/04/2016	Nuram 35 + 7So3	24.34	200.00	35.00%	0.2	1703.80	1703.80	1363.04	340.76
First Hempsky	Winter Barley Feed	27/02/2016	Nuram 35 + 7So3	13.81	200.00	35.00%	0.2	966.70	966.70	773.36	193.34
First Hempsky	Winter Barley Feed	18/03/2016	Nuram 35 + 7So3	13.30	200.00	35.00%	0.2	931.00	931.00	744.80	186.20

First Hempshy	Winter Barley Feed	06/04/2016	Nuram 35 + 7So3	13.81	200.00	35.00%	0.2	966.70	966.70	773.36	193.34
Sheds Field	Winter Barley Feed	27/02/2016	Nuram 35 + 7So3	14.36	200.00	35.00%	0.2	1005.20	1005.20	804.16	201.04
Sheds Field	Winter Barley Feed	18/03/2016	Nuram 35 + 7So3	13.80	200.00	35.00%	0.2	966.00	966.00	772.80	193.20
Sheds Field	Winter Barley Feed	06/04/2016	Nuram 35 + 7So3	14.36	200.00	35.00%	0.2	1005.20	1005.20	804.16	201.04
Swanhill s	Winter Barley Feed	27/02/2016	Nuram 35 + 7So3	10.37	200.00	35.00%	0.2	725.90	725.90	580.72	145.18
Swanhill s	Winter Barley Feed	18/03/2016	Nuram 35 + 7So3	7.55	200.00	35.00%	0.2	528.50	528.50	422.80	105.70
Swanhill s	Winter Barley Feed	06/04/2016	Nuram 35 + 7So3	10.37	200.00	35.00%	0.2	725.90	725.90	580.72	145.18
Swanhill s	Winter Barley Feed	04/05/2016	Nuram 35 + 7So3	11.97	100.00	35.00%	0.17	418.95	418.95	347.73	71.22
Swanhill s	Winter Barley Feed	10/05/2016	Nuram 25 + 14So3	12.20	280.00	25.00%	0.17	854.00	854.00	708.82	145.18
Swanhill s	Winter Barley Feed	15/05/2016	33.5% Nitrogen	12.16	106.91	33.50%	0.17	435.50	435.50	361.47	74.04
Swanhill s	Winter Barley Feed	21/04/2016	Nuram 35 + 7So3	12.25	100.00	35.00%	0.17	428.75	428.75	355.86	72.89
Swanhill s	Winter Barley Feed	23/04/2016	Nuram 25 + 14So3	12.89	280.00	25.00%	0.17	902.30	902.30	748.91	153.39
Swanhill s	Winter Barley	15/05/2016	33.5% Nitrogen	12.49	45.00	33.50%	0.17	188.29	188.29	156.28	32.01

	y Feed											
Swanhill s	Wint er Barle y Feed	23/04/20 16	Nuram 35 + 7So3	23.1 6	100.0 0	35.00 %	0.17	810.60	810.60	672.8 0	137.80	
Swanhill s	Wint er Barle y Feed	25/04/20 16	Nuram 25 + 14So3	24.0 9	280.0 0	25.00 %	0.17	1686.3 0	1686.3 0	1399. 63	286.67	
Swanhill s	Wint er Barle y Feed	15/05/20 16	33.5% Nitroge n	23.5 8	45.00	33.50 %	0.17	355.47	355.47	295.0 4	60.43	
Swanhill s	Wint er Barle y Feed	26/02/20 16	Nuram 25 + 14So3	39.0 3	190.0 0	25.00 %	0.42	1853.9 3	1853.9 3	1075. 28	778.65	
Swanhill s	Wint er Barle y Feed	17/03/20 16	Nuram 35 + 7So3	38.7 2	250.0 0	35.00 %	0.42	3388.0 0	3388.0 0	1965. 04	1422.9 6	
Swanhill s	Wint er Barle y Feed	07/04/20 16	Nuram 35 + 7So3	39.0 3	190.0 0	35.00 %	0.42	2595.5 0	2595.5 0	1505. 39	1090.1 1	
Dunkirk	Wint er Barle y Feed	27/02/20 16	Nuram 35 + 7So3	12.3 0	200.0 0	35.00 %	0.2	861.00	861.00	688.8 0	172.20	
Dunkirk	Wint er Barle y Feed	18/03/20 16	Nuram 35 + 7So3	12.3 0	200.0 0	35.00 %	0.2	861.00	861.00	688.8 0	172.20	
Dunkirk	Wint er Barle y Feed	06/04/20 16	Nuram 35 + 7So3	13.0 9	200.0 0	35.00 %	0.2	916.30	916.30	733.0 4	183.26	
Gatehou se Hyrne	Wint er Barle y Feed	26/02/20 16	Nuram 35 + 7So3	16.5 5	200.0 0	35.00 %	0.2	1158.5 0	1158.5 0	926.8 0	231.70	
Gatehou se Hyrne	Wint er Barle y Feed	18/03/20 16	Nuram 35 + 7So3	15.6 0	200.0 0	35.00 %	0.2	1092.0 0	1092.0 0	873.6 0	218.40	
Gatehou se Hyrne	Wint er Barle y Feed	06/04/20 16	Nuram 35 + 7So3	16.5 5	200.0 0	35.00 %	0.2	1158.5 0	1158.5 0	926.8 0	231.70	

Moor Hall Fld	Winter Barley Feed	27/02/2016	Nuram 35 + 7So3	20.00	200.00	35.00%	0.2	1400.00	1400.00	1120.00	280.00
Moor Hall Fld	Winter Barley Feed	18/03/2016	Nuram 35 + 7So3	19.50	200.00	35.00%	0.2	1365.00	1365.00	1092.00	273.00
Moor Hall Fld	Winter Barley Feed	06/04/2016	Nuram 35 + 7So3	19.81	200.00	35.00%	0.2	1386.70	1386.70	1109.36	277.34
Green Yards	Feed Wheat	27/02/2016	Nuram 35 + 7So3	11.25	200.00	35.00%	0.23	787.50	787.50	606.38	181.13
Green Yards	Feed Wheat	01/04/2016	Nuram 35 + 7So3	11.25	230.00	35.00%	0.23	905.63	905.63	697.33	208.29
Green Yards	Feed Wheat	30/04/2016	33.5% Nitrogen	10.89	223.52	33.50%	0.23	815.42	815.42	627.87	187.55
Green Yards	Feed Wheat	26/02/2016	Nuram 35 + 7So3	10.47	200.00	35.00%	0.2	732.90	732.90	586.32	146.58
Green Yards	Feed Wheat	18/03/2016	Nuram 35 + 7So3	10.13	220.00	35.00%	0.2	780.01	780.01	624.01	156.00
The Hyrne	Winter Barley Malt	26/02/2016	Nuram 35 + 7So3	9.63	200.00	35.00%	0.2	674.10	674.10	539.28	134.82
The Hyrne	Winter Barley Malt	18/03/2016	Nuram 35 + 7So3	9.35	220.00	35.00%	0.2	719.95	719.95	575.96	143.99
Church	Winter Barley Malt	26/02/2016	Nuram 35 + 7So3	3.55	200.00	35.00%	0.2	248.50	248.50	198.80	49.70
Church	Winter Barley Malt	18/03/2016	Nuram 35 + 7So3	3.41	220.00	35.00%	0.2	262.57	262.57	210.06	52.51
Church	Winter Barley Malt	21/04/2016	Nuram 35 + 7So3	28.36	100.00	35.00%	0.17	992.60	992.60	823.86	168.74
Church	Winter Barley Malt	25/04/2016	Nuram 25 + 14So3	27.07	280.00	25.00%	0.17	1894.90	1894.90	1572.77	322.13

Church	Winter Barley Malt	15/05/2016	33.5% Nitrogen	28.85	45.00	33.50%	0.17	434.91	434.91	360.98	73.94
Church	Winter Barley Malt	26/02/2016	Nuram 25 + 14So3	15.42	190.00	25.00%	0.42	732.45	732.45	424.82	307.63
Church	Winter Barley Malt	16/03/2016	Nuram 35 + 7So3	14.18	250.00	35.00%	0.42	1240.75	1240.75	719.64	521.12
Church	Winter Barley Malt	07/04/2016	Nuram 35 + 7So3	15.42	190.00	35.00%	0.42	1025.43	1025.43	594.75	430.68
Church	Winter Barley Malt	26/02/2016	Nuram 25 + 14So3	20.64	190.00	25.00%	0.42	980.40	980.40	568.63	411.77
Church	Winter Barley Malt	17/03/2016	Nuram 35 + 7So3	20.04	250.00	35.00%	0.42	1753.50	1753.50	1017.03	736.47
Church	Winter Barley Malt	07/04/2016	Nuram 35 + 7So3	20.64	190.00	35.00%	0.42	1372.56	1372.56	796.08	576.48
Crabgate	W OSR	26/02/2016	Nuram 25 + 14So3	17.23	190.00	25.00%	0.42	818.43	818.43	474.69	343.74
Crabgate	W OSR	22/03/2016	Nuram 35 + 7So3	17.30	250.00	35.00%	0.42	1513.75	1513.75	877.98	635.78
Crabgate	W OSR	07/04/2016	Nuram 35 + 7So3	17.48	190.00	35.00%	0.42	1162.42	1162.42	674.20	488.22
Clarke (Loke)	Winter Barley	11/01/2016	OMEX NITROFL O-XS	14.17	165.00	33.40%	0.2	780.91	780.91	624.73	156.18
Clarke (Loke)	Winter Barley	11/01/2016	OMEX NITROFL O-S	14.17	150.00	33.40%	0.2	709.92	709.92	567.93	141.98
FH Meadow (big)	W OSR	23/02/2016	Yara Sulphur Plus	4.39	250.00	29.00%	0.42	318.28	318.28	184.60	133.68
FH Meadow (big)	W OSR	07/04/2016	Yara Sulphan	4.39	167.00	24.00%	0.42	175.95	175.95	102.05	73.90
FH Meadow (big)	W OSR	21/05/2016	Oilseed extra	4.39	150.55	20.00%	0.42	132.18	132.18	76.67	55.52

Harrow	W OSR	24/02/20 16	Yara Sulphur Plus	8.71	250.0 0	29.00 %	0.42	631.48	631.48	366.2 6	265.22
Harrow	W OSR	06/04/20 16	Yara Sulphan	8.71	167.0 0	24.00 %	0.42	349.10	349.10	202.4 8	146.62
Harrow	W OSR	08/04/20 16	Koch Advance d Nitroge n	8.71	148.0 0	46.00 %	0.42	592.98	592.98	343.9 3	249.05
Harrow	W OSR	21/05/20 16	Oilseed Extra	8.71	150.5 5	20.00 %	0.42	262.26	262.26	152.1 1	110.15
High Meadow	W OSR	23/02/20 16	Yara Sulphur Plus	8.94	250.0 0	29.00 %	0.42	648.15	648.15	375.9 3	272.22
High Meadow	W OSR	06/04/20 16	Yara Sulphan	8.94	167.0 0	24.00 %	0.42	358.32	358.32	207.8 2	150.49
High Meadow	W OSR	08/04/20 16	Koch Advance d Nitroge n	8.94	148.0 0	46.00 %	0.42	608.64	608.64	353.0 1	255.63
High Meadow	W OSR	08/04/20 16	Origin Enhance d N	8.94	148.0 0	46.00 %	0.42	608.64	608.64	353.0 1	255.63
High Meadow	W OSR	21/05/20 16	Oilseed Extra	8.94	150.5 5	20.00 %	0.42	269.19	269.19	156.1 3	113.06
Rackety Barn	W OSR	23/02/20 16	Yara Sulphur Plus	10.5 3	250.0 0	29.00 %	0.42	763.43	763.43	442.7 9	320.64
Rackety Barn	W OSR	06/04/20 16	Yara Sulphan	10.5 3	167.0 0	24.00 %	0.42	422.04	422.04	244.7 8	177.26
Rackety Barn	W OSR	08/04/20 16	Origin Enhance d N	10.5 3	148.0 0	46.00 %	0.42	716.88	716.88	415.7 9	301.09
Field House (small)	Whea t	27/02/20 16	Yara Sulphur Plus	6.89	200.0 0	29.00 %	0.23	399.62	399.62	307.7 1	91.91
Field House (small)	Whea t	20/04/20 16	Origin Enhance d N	6.89	220.0 0	46.00 %	0.23	697.27	697.27	536.9 0	160.37
Field House (small)	Whea t	19/05/20 16	Yara New Extran	6.89	120.0 0	33.50 %	0.23	276.98	276.98	213.2 7	63.70
Thirty Acres	???	06/07/20 16	33.5% Nitroge n	0.69	444.0 6	33.50 %	0.23	102.64	102.64	79.04	23.61
Thirty Acres	???	26/02/20 16	Nuram 35 + 7So3	10.4 7	200.0 0	35.00 %	0.2	732.90	732.90	586.3 2	146.58
Thirty Acres	???	18/03/20 16	Nuram 35 + 7So3	10.1 3	220.0 0	35.00 %	0.2	780.01	780.01	624.0 1	156.00

The low nitrate scenario shares the same data as the high scenario, with the only differences being the initial nitrogen content of the turkey manure and the amount of loss of nitrogen due to ammonia volatilisation, shown below

Low nitrogen scenario (high volatilisation, low turkey manure N)												
Field	Crop	Date	Product	Area (ha)	Rate (kg ha ⁻¹)	N fraction (%)	Export coefficient	Total N in (kg)	N lost to volatilisation (kg)	N available for crop uptake (kg)	Crop N uptake (kg)	Leached N (kg)
Low Farm Ave.	Sugar Beet	12/09/2015	Turkey Manure	17.75	7765.00	2.07%	0.17	2853.06	1283.87	1569.18	1302.42	266.76
Salle Old Grounds	Sugar Beet	12/09/2015	Turkey Manure	6.00	7765.00	2.07%	0.17	964.41	433.99	530.43	440.25	90.17
Merrisons	W OSR	04/08/2015	Turkey Manure	39.03	7765.00	2.07%	0.42	6273.51	2823.08	3450.43	2001.25	1449.18
Merrisons	W OSR	04/08/2015	Turkey Manure	15.42	7765.00	2.07%	0.42	2478.54	1115.34	1363.20	790.65	572.54
Merrisons	W OSR	04/08/2015	Turkey Manure	20.64	7765.00	2.07%	0.42	3317.58	1492.91	1824.67	1058.31	766.36
Merrisons	W OSR	04/08/2015	Turkey Manure	17.44	7765.00	2.07%	0.42	2803.23	1261.45	1541.77	894.23	647.55